The Dissertation Committee for David Finley Sanders Certifies that this is the approved version of the following dissertation:

The Effect of Synthesis Route and *ortho*-Position Functional Group on Thermally Rearranged Polymer Transport Properties

Committee:

Benny D. Freeman, Co-Supervisor

Donald R. Paul, Co-Supervisor

James E. McGrath

Isaac C. Sanchez

Christopher J. Ellison

The Effect of Synthesis Route and *ortho*-Position Functional Group on Thermally Rearranged Polymer Thermal and Transport Properties

by

David Finley Sanders, B.S.Ch.E.

Dissertation

Presented to the Faculty of the Graduate School of

The University of Texas at Austin

in Partial Fulfillment

of the Requirements

for the Degree of

Doctor of Philosophy

The University of Texas at Austin

May 2013

Dedication

To my mother and father, my sister, my wife, my daughter, and my dog Rufus.

Acknowledgements

I would like to acknowledge my thesis advisors, Dr. Benny Freeman and Dr. Don Paul, for their support and guidance throughout my Ph.D. program. Dr. Freeman has been particularly influential in the development of my experimental design process and professional skills. His trust and management style allowed me to present on my work to a wide variety of audiences during my time as a Ph.D. student. These opportunities have been invaluable in improving my ability to shape results and content to varying audiences. His advice has also taught me to always check the practical limits of an experiment before interpreting results and moving on to the next steps. Dr. Paul has frequently taught me the value of having a deep knowledge of the literature and drawing empirical conclusions from data to guide future research. Both of my advisors have been friendly and open to my ideas throughout my research, and I feel very fortunate to have studied under their guidance.

I have also had the opportunity to work with many bright colleagues during my time in graduate school. I have particularly enjoyed collaborating with the other students studying TR polymers: Zachary Smith, Claudio Ribeiro, Qiang Liu, Kevin Stevens, Kris Gleason, and Katrina Czenkusch. I am also grateful to the rest of the Freeman group: Dan Miller, Grant Offord, Tom Murphy, Kevin Tung, Lisa He, Ni Yan, Peach Kasemset, Joe Cook, and Hee Jeung Oh, who always provided great conversation on a variety of topics. While their research projects were significantly different than my own, they also provided valuable suggestions and advice throughout my work that have contributed to my success.

During my time as an undergraduate researcher, I was fortunate enough to work under two great researchers and teachers, Scott Matteucci and Ho Bum Park. I am very thankful for the time they took to mentor and teach me basic lab techniques for membrane characterization. The techniques they taught me have helped me continuously in the lab. I was also fortunate enough to work with Hao Ju, Richard Li, Roy Raharjo, Bryan McCloskey, Brandon Rowe, Keith Ashcraft, Alyson Sagle, Victor Kusuma, and Liz Van Wagner. All of these former members of the Freeman group have always been friendly and helpful.

I would also like to thank the graduate students who joined me every Monday to play basketball at the Pickle Research Center Gym over the years: Hao Ju, Roy Raharjo, Richard Li, Tom Murphy, Grant Offord, Kevin Tung, Zach Smith, Gina Smith, Peach Kasemset, Qiang Liu, Ni Yan, Albert Lee, Fabrice Tanguy, Jovan Kamcev, Jaesung Park, and the structural engineering students we played against. This was a valuable time for me to unwind, and I built many relationships that have continued past graduation.

Finally, I would like to acknowledge the support of my mother and father, who encouraged me to enter graduate school and have supported my efforts during my studies. I would also like to thank my wife, my dog, and my one year old daughter for suffering through my time away from home, the many hours of work discussions, and for always supporting me.

The Effect of Synthesis Route and *ortho*-Position Functional Group on Thermally Rearranged Polymer Thermal and Transport Properties

David Finley Sanders, Ph.D.

The University of Texas at Austin, 2013

Supervisor: Benny D. Freeman and Donald R. Paul

This dissertation discusses the effect of synthesis route and *ortho*-position group on the thermal and transport properties of thermally rearranged polymers. Thermally rearranged polymers are polybenzoxazoles formed via the solid state rearrangement of *ortho*-functional polyimides. In this study, polymers were derived from 3,3'-dihydroxy-4,4'-diamino-biphenyl and 2,2'-bis-(3,4-dicarboxyphenyl) hexafluoropropane dianhydride (HAB-6FDA). These HAB-6FDA polymers were synthesized using chemical and thermal imidization, and hydroxyl, acetate, propanoate, or pivalate *ortho*-position groups were considered. In these polymers, gas permeability increases as a function of conversion for all samples. The polyimide synthesis route does not affect the thermal or transport properties. However, the precursor *ortho*-position group strongly influences the thermal and transport properties of TR polymers. Additionally, it was determined that an increase in gas diffusivity was the primary cause of increased permeability as a function of thermal rearrangement.

Table of Contents

List of Tables

List of Figures

Chapter 1: Introduction[1]

The gas separation membrane market has grown significantly since its beginnings in the 1970's (approximately), and continued growth is expected in the coming years as technology improves and applications expand [1]. Previously, several review articles and monographs have chronicled overall progress in the field as well as specific progress in applications and materials science [1-9]. The background discussion for this thesis summarizes current commercial membrane materials, emerging membrane materials, membrane terminology and equations, and major membrane materials challenges. A more detailed discussion of applications can be found in the previously mentioned reviews.

1.1 Membrane History

The first recorded description of semi-permeable membranes was in 1748 when Jean Antoine (Abbé) Nollet reported that a pig bladder (*i.e.*, a natural membrane) was more permeable to water than to ethanol [10-12]. Later, in 1831, a related observation regarding gas transport through balloons prepared from natural rubber, which is largely *cis*-poly(isoprene), was made by John Kearsley Mitchell [13]. After filling a series of these balloons with hydrogen and letting them rise to the ceiling of his lecture room, the balloons descended from the ceiling over time. Mitchell hypothesized that the hydrogen was somehow passing through the walls of these rubber balloons [13]. Further experiments showed that various gases passed through the same material at different

[1] Portions of this section were adapted from Sanders, D.F., Smith, Z.P., Guo, R., Robeson, L.M., McGrath, J.E., Paul, D.R., and Freeman, B.D., Energy efficient polymeric gas separation membranes for a sustainable future: A review. Polymer, submitted; Copyright Elsevier. D. F. wrote sections of the paper and compiled and edited the document. Z. P. Smith, R. Guo, and L. M. Robeson authored portions of the document and provided input. B. D. Freeman, J. E. McGrath, and D. R. Paul supervised the writing of this document, provided technical expertise, and edited the manuscript.

rates, a critically important concept that foreshadowed the commercial development of polymeric gas separation membranes in the late 1970's [3].

Adolph Fick's laws of diffusion, derived in analogy with Fourier's law of heat conduction and Ohm's law of electrical conduction, provided the fundamental mathematical framework for mass transfer across nonporous membranes [14], and Sir Thomas Graham published a seminal paper in 1866 setting forth the basic principles underpinning the solution-diffusion model, which is understood to govern gas transport in all nonporous polymeric gas separation membranes [15]. In this model, gas is transported through a nonporous polymer film or membrane by dissolving into the face of the membrane exposed to high gas pressure, diffusing through the polymer, and desorbing from the face of the membrane exposed to low pressure [16]. The middle step, diffusion through the polymer, is the rate-limiting step for gas permeation in all polymer membranes used today. The rate-limiting step in diffusion is the local scale segmental dynamics of the polymer chains that lead to the opening and closing of transient gaps (*i.e.*, free volume elements) in the polymer; the gas molecules execute Brownian motion (*i.e.*, diffusion) through these free volume elements. Thus, the local segmental motions of polymer chains and the packing of polymer chains are two critically important variables in gating the diffusion of small gas molecules through polymers.

1.2 NATURAL GAS PURIFICATION

This research focuses on the development of new membrane materials for CO_2 removal from natural gas. Natural gas is often a complex mixture of methane, carbon dioxide, ethane, higher hydrocarbons, hydrogen sulfide, inert gases, and trace components of many other compounds, such as BTEX aromatics (benzene, toluene, ethylbenzene, and xylenes) [2]. The actual composition of natural gas varies depending

on the well, and delivery of gas to the U.S. national pipeline grid requires that all natural gas be treated, at least to some degree. This treatment is designed to prevent pipeline corrosion as well as adjust the heating value and dew point of the fuel to a standard level. U.S. pipeline specifications require that natural gas contains less than 2% CO_2, 4 ppm H_2S, and 7 lb/MMscf water [17]. Moreover, it must have a heating value of 950-1050 Btu/scf and a dew point of -20°C or less [7].

Removal of CO_2 and H_2S (*i.e.*, acid gases) from natural gas is a growing area for membrane technology. In 2008, it was estimated that the worldwide market for natural gas separation equipment was approximately $5 billion/yr, and membrane technology accounted for approximately 5% of this market, but this market share is expected to grow if membrane technology continues to improve [2]. Membrane separation competes most directly with amine absorption, which has existed since the 1930's and is commonly used for acid gas separations [18]. The capital costs, energy consumption, plant footprint, and maintenance costs of amine absorption have encouraged the development of membrane systems and membrane/absorption hybrid systems for natural gas purification [19]. The first membranes for natural gas purification were developed in the early to mid-1980's. W.R. Grace (now part of UOP) and Separex (now part of UOP) developed spiral-wound membranes, and Cynara (now part of Cameron) developed hollow-fiber membranes based on cellulose acetate [2]. These cellulose acetate membranes are still widely in use today, but polyimides and other materials have gained some traction in this field over the past 15 – 20 years [2]. These membranes can be configured a variety of ways, but the number of membrane modules, compressors, and the configuration of these systems often depends on the desired flowrate [2, 7, 20]. The development of new membrane materials could greatly increase the attractiveness of membranes in this separation, offering a lower energy alternative to the commonly used amine absorption technology.

1.3 DISSERTATION GOALS

In 2007, Park et al. presented a novel class of membranes for the separation of CO_2 from natural gas known as TR polymers [21]. TR polymers are polybenzoxazoles prepared by solid state thermal rearrangement of polyimides with ortho-position functional groups to obtain a polymer membrane. Polybenzoxazole gas separation properties previously remained unexplored due to their lack of solubility in common solvents. Park's research, which circumvented the insolubility of these polymers by preparing soluble precursors that could be processed to form membranes and then subsequently thermally rearranged to insoluble polybenzoxazoles, opened the door to a wide range of studies on this family of gas separation materials.

Altering functional groups on the backbone of a polymer chain can alter the transport properties, but these changes are not always consistent across families of polymers [3]. Park's work explored various TR structures and showed that the gas separation performance does indeed vary from one structure to another. This research focuses on the fundamental properties of gas transport in TR polymers, including the changes in diffusivity and solubility as a function of TR conversion. This dissertation also discusses the effect of TR polymer synthesis route and the effect of *ortho*-position functional group on TR polymer transport properties. The results of this study will help to better understand the unique characteristics of these polymers and develop an ideal synthesis method for gas separation applications which can be paired with the large number of structure/property studies in the literature. Four major subjects will be discussed in this dissertation: the thermal properties of TR polymers as a function of synthesis route and *ortho*-position, permeability and selectivity of TR polymers as a function of synthesis route and *ortho*-position functional group, fractional free volume of

TR polymers as a function of *ortho*-position functional group and conversion, and TR polymer pure gas diffusivity and solubility as a function of thermal rearrangement.

1.4 REFERENCES

1. Baker, R.W., *Future directions of membrane gas separation technology.* Industrial & Engineering Chemistry Research, 2002. **41**(6): p. 1393-1411.

2. Baker, R.W. and Lokhandwala, K., *Natural gas processing with membranes: An overview.* Industrial & Engineering Chemistry Research, 2008. **47**(7): p. 2109-2121.

3. Koros, W.J. and Fleming, G.K., *Membrane-based gas separation.* Journal of Membrane Science, 1993. **83**(1): p. 1-80.

4. Lonsdale, H.K., *The growth of membrane technology.* Journal of Membrane Science, 1982. **10**(2-3): p. 81-181.

5. Stern, S.A., *Polymers for gas separations: the next decade.* Journal of Membrane Science, 1994. **94**: p. 1-65.

6. Ghosal, K. and Freeman, B.D., *Gas separation using polymer membranes: An overview.* Polymers for Advanced Technologies, 1994. **5**: p. 673-697.

7. Baker, R.W., *Membrane technology and applications*. 2nd ed. 2004, Chichester: John Wiley & Sons.

8. Kesting, R.E. and Fritzsche, A.K., *Polymeric gas separation membranes*. 1993, New York, NY, USA: John Wiley & Sons.

9. Yampolskii, Y., *Polymeric Gas Separation Membranes.* Macromolecules, 2012. **45**: p. 3298-3311.

10. Mason, E.A., *From pig bladders and cracked jars to polysulfones: an historical perspective on membrane transport.* Journal of Membrane Science, 1991. **60**: p. 125-145.

11. Böddeker, K.W., *Commentary: Tracing membrane science.* Journal of Membrane Science, 1995. **100**: p. 65-68.

12. Nollet, J.A., *Investigations on the causes for the ebullition of liquids.* Journal of Membrane Science, 1995. **100**: p. 1-3.

13. Mitchell, J.K., *On the penetrativeness of fluids.* Journal of Membrane Science, 1995. **100**: p. 11-16.

14. Fick, A., *On liquid diffusion.* Journal of Membrane Science, 1995. **100**: p. 33-38.

15. Graham, T., *On the absorption and dialytic separation of gases by colloid septa Part I. - Action of a septum of caoutchouc.* Journal of Membrane Science, 1995. **100**: p. 27-31.

16. Wijmans, J.G. and Baker, R.W., *The solution-diffusion model - a review.* Journal of Membrane Science, 1995. **107**(1-2): p. 1-21.

17. Kohl, A. and Nielsen, R., *Gas purification*. 5th ed. 1997, Houston, TX: Gulf Publishing Company.

18. Bottoms, R.R., Process for separating acidic gases. US Patent 1,834,016. 1931.

19. Cooley, T.E. and Coady, A.B., Removal of H_2S and/or CO_2 from a light hydrocarbon stream by use of gas permeable membrane. US Patent 4,130,403. 1978.

20. Spillman, R.W., *Economics of gas separation membranes.* Chemical Engineering Progress, 1989. **85**(1): p. 41–62.

21. Park, H.B., Jung, C.H., Lee, Y.M., Hill, A.J., Pas, S.J., Mudie, S.T., Van Wagner, E., Freeman, B.D., and Cookson, D.J., *Polymers with cavities tuned for fast selective transport of small molecules and ions.* Science, 2007. **318**(5848): p. 254-258.

Chapter 2: Background[2]

This chapter provides background information for understanding the results of the thesis and framing these results within the current state of membrane literature. A short review of equations and terminology in membranes is provided, followed by a discussion of common materials-related challenges faced in membrane research. In addition, the benefits and shortcomings of both commercially available and emerging membrane materials are discussed to show other relevant membrane materials in addition to TR polymers. Finally, a short discussion is provided on the effect of synthesis route and ortho-position functional group in polyimides and TR polymers.

2.1 Equations and Terminology

The equations and terminology discussed below illustrate basic concepts used to describe gas transport in polymers and evaluate membrane material performance. Detailed derivations and discussion of these equations are available elsewhere [1-5]. Membrane performance is often characterized by gas throughput and separation efficiency and these properties are most commonly expressed by permeability and selectivity coefficients.

[2]Adapted from Sanders, D.F., Smith, Z.P., Guo, R., Robeson, L.M., McGrath, J.E., Paul, D.R., and Freeman, B.D., Energy efficient polymeric gas separation membranes for a sustainable future: A review. Polymer, submitted. D. F. wrote sections of the paper and compiled and edited the document. Z. P. Smith, R. Guo, and L. M. Robeson authored portions of the document and provided input. B. D. Freeman, J. E. McGrath, and D. R. Paul supervised the writing of this document, provided technical expertise, and edited the manuscript.

2.1.1 Permeability Coefficient

For a pure gas permeating through a polymer film or membrane, gas permeability, P_A, is defined as the trans-membrane pressure difference, p_2-p_1, and thickness normalized steady-state gas flux, N_A [6]:

$$P_A = \frac{N_A l}{(p_{2,A} - p_{1,A})} \tag{2.1}$$

where l is the membrane thickness, p_2 is the upstream pressure, and p_1 is the downstream pressure. Unlike flux, which depends upon l and Δp, P_A is typically viewed, to a first approximation, as being a material property that is much less dependent than flux on membrane thickness and Δp. For gas mixtures permeating through polymers, Δp is taken to be the partial pressure difference of the component of interest, and for non-ideal gases, Δp can be replaced by the fugacity difference across a membrane or film [7].

Typically permeability coefficients are expressed in Barrer, where [1]:

$$1 \text{ Barrer} = \frac{10^{-10} \text{ cm}^3 (\text{STP}) \text{ cm}}{\text{cm}^2 \text{ s cmHg}} \tag{2.2}$$

Each polymer has a different permeability coefficient for each gas, and the faster permeation of some gases relative to others provides the basis for the use of polymers to separate gas mixtures. The range over which permeability can vary in different polymers is enormous. For example, oxygen permeability in poly(acrylonitrile) (PAN), a high barrier polymer, is 2.8×10^{-4} Barrer [8]. At the other end of the scale, a polymer based upon an indan-containing poly(diphenylactylene) derivative has an oxygen permeability of 18,700 Barrer, which is believed to be the highest oxygen permeability among nonporous polymers [9]. Thus, oxygen permeability values span nearly 8 orders of magnitude in these two examples, and there are polymers, such as dry poly(vinyl alcohol), that are more than an order of magnitude less permeable than PAN [10]. This

enormous range of gas permeabilities in polymers illustrates the extraordinary sensitivity of gas permeability to polymer material structure.

Using the solution-diffusion model, the gas permeability coefficient can be written as the product of a gas solubility coefficient, S_a, and a concentration-averaged, effective diffusion coefficient, D_a [11]:

$$P_a = D_a S_a \tag{2.3}$$

The diffusion coefficient is commonly expressed in cm^2/sec, and solubility is often expressed in cm^3(STP)/(cm^3 polymer atm) or cm^3(STP)/(cm^3 polymer cmHg) .

Penetrant size has a significant effect on diffusion coefficients, with larger gases generally having lower diffusion coefficients [11]. In polymers of interest for gas separations, gas diffusion coefficients can range from approximately 10^{-4} cm^2/s for helium diffusion in poly(1-trimethylsilyl-1-propyne), PTMSP, which is among the most permeable polymers known, to approximately $3x10^{-9}$ cm^2/s for CH_4 in polycarbonate [11, 12]. Diffusion coefficients are also sensitive to polymer chain flexibility and the free volume in the polymer, which gauges the amount of packing defects, gaps between polymer chains and other structural features that give rise to openings within a polymer large enough to permit penetrant diffusion.

The solubility coefficient in Equation 2.4 is defined as the ratio of the concentration of gas in a polymer, *C*, to the pressure of gas, *p*, contiguous to the polymer [1]:

$$S_A = \frac{C}{p} \tag{2.4}$$

Solubility depends mainly on gas molecule condensability (as characterized, for example, by gas critical temperature, Lennard-Jones potential well depth, normal boiling point, enthalpy of vaporization, *etc.*) and, to a lesser extent, on gas-polymer interactions

[11]. Polymer morphological features, such as crystallinity and liquid crystallinity, can also influence gas solubility in polymers [13-16].

2.1.2 Selectivity

A common parameter characterizing the ability of a polymer to separate two gases (*e.g.*, A and B) is the ideal selectivity, $\alpha_{A/B}$ [17]:

$$\alpha_{A/B} = \frac{P_A}{P_B} \tag{2.5}$$

By combining Equations 2.4 and 2.5, permeability selectivity can be written as a product of solubility and diffusivity selectivity:

$$\alpha_{A/B} = \frac{D_A}{D_B}\frac{S_B}{S_B} \tag{2.6}$$

Like permeability, the ideal selectivity is often treated as a material property of a polymer.

Another measure of the ability of a membrane to separate a particular gas mixture is the separation factor, α^*, where x_A is the concentration of gas *A* in the feed and y_A is the concentration of gas *A* in the permeate [17]:

$$\alpha^*_{A/B} = \frac{y_A / y_B}{x_A / x_B} \tag{2.7}$$

This value is less commonly reported in the membrane materials literature because it depends more sensitively on the operating conditions (*e.g.*, upstream and downstream pressure and feed gas composition) than $\alpha_{A/B}$. Thus, the separation factor is not a material property of the polymer being used as the membrane. However, when the upstream pressure is much greater than the downstream pressure, the separation factor becomes equal to the ideal selectivity. This relationship can be shown by recognizing that the mole fraction of component A produced in the permeate, y_A, is related to the flux of A and B as follows:

$$y_A = \frac{N_A}{N_A + N_B} \tag{2.8}$$

An analogous relation may be written for component B. Substituting Equation 2.8 into Equation 2.7 and using the definition of permeability in Equation 2.1 to solve for flux, the following expression is obtained:

$$\alpha^*_{A/B} = \alpha_{A/B} \frac{p_2 - p_1\left(\frac{y_A}{y_B}\right)}{p_2 - p_1\left(\frac{y_A}{y_B}\right)} \tag{2.9}$$

Therefore, when the upstream pressure, p_2, is much greater than the downstream pressure, p_1, $\alpha^*_{A/B} = \alpha_{A/B}$. However, in a mixed gas environment, the observed selectivity may differ from pure gas selectivity due to plasticization and competitive effects, which will be discussed later.

2.1.3 Fractional Free Volume

Free volume is among the most important structural variables influencing gas transport properties in polymers. The Cohen-Turnbull model predicts that diffusion coefficients increase strongly as free volume increases [18]. This relationship is shown in Equation 2.10 where A is a constant related to a geometric factor, molecular diameter, and gas kinetic velocity, v^* is related to the size of the gas molecule, γ is an overlap factor between 0.5 and 1, and FFV is the fractional free volume of the polymer [11, 18-20].

$$D = A\exp(-\frac{\gamma v^*}{FFV}) \tag{2.10}$$

In gas separation polymers, free volume is often quantified using the concept of fractional free volume (FFV), which is defined as the void space between polymer chains that is available to assist in molecular transport [21]. Free volume can be generated by

inefficiencies in polymer chain packing in the solid state and by molecular motion of polymer chain segments, which effectively open gaps in the polymer matrix on a transient basis that allow penetrant molecules to diffuse through the polymer [22].

Fractional free volume is calculated as the difference between the experimental specific volume (*i.e.*, reciprocal of polymer density) and the theoretical volume occupied by the polymer chains [23, 24]:

$$FFV = \frac{V - V_0}{V} \tag{2.11}$$

where V is the measured experimental specific volume of the polymer in cm^3/g, and V_0 is the theoretical occupied volume of the polymer chains in cm^3/g. V_0 is typically estimated using group contribution theory described by Bondi, where V_W is the van der Waal's volume of groups comprising the polymer chain [23-25]:

$$V_O = 1.3\sum V_W \tag{2.12}$$

As seen in Figure 2.1a, which presents an example of a relationship between fractional free volume and diffusion coefficients in a systematic series of polysulfones of varying chemical structure, there is often a good correlation between FFV and diffusion coefficients. Due to uncertainties associated with estimating occupied volume increments with various families of polymers, correlations of FFV with gas diffusion coefficients often work best when restricted to polymers with similar backbone structures [26]. Because gas solubility typically depends weakly on free volume, gas permeability coefficients often correlate well with FFV, and many studies report strong correlations of permeability with FFV as seen in Figure 2.1b [27].

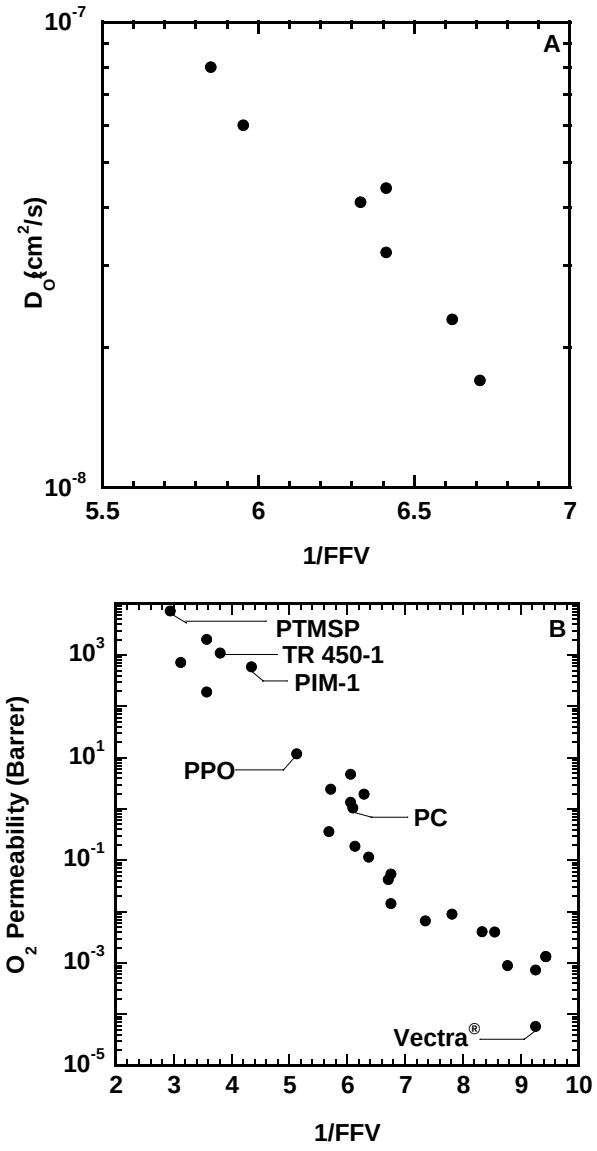

Figure 2.1 (a) Oxygen diffusion coefficient in polysulfones of varying fractional free volume [19]. (b) Oxygen permeability for many families of polymers including poly(1-trimethylsilyl-1-propyne (PTMSP), 6F containing thermally rearranged polymer (TR 450-1), polymer of intrinsic microporosity (PIM-1), polycarbonate (PC), poly(2,6-dimethyl-1,4-phenylene oxide) (PPO), Vectra® (a commercial polyester liquid crystalline polymer), and various polymers from [28-30].

2.2 CHALLENGES IN MEMBANE SCIENCE AND LIMITS OF TECHNOLOGY

2.2.1 Permeability/Selectivity Tradeoff (The Upper Bound)

The polymer used to make a membrane is crucial to separation performance. Thus, structure/property studies related to membrane separation have been a significant area of research since the early 1980's [2-4, 31, 32]. The key factors in membrane transport performance are flux, permeability, and selectivity. Inherent in this relationship, which is based on the solution-diffusion model, are both diffusion and solubility coefficient selectivities, which were introduced previously.

The flux is governed by the choice of the polymer (permeability) and its achievable dense layer thickness. The selectivity is also determined by the choice of polymer and the ability to achieve "pinhole-free" membranes. As thickness is a process fabrication parameter, permeability and selectivity of the polymer are key material properties for polymer studies.

Considerable numbers of structure-property studies have identified polymer structural components that yield high permeability, and a number of these studies have defined structural characteristics desirable for gas separation [31, 32]. Specifically, polymers offering the best combinations of α_{ij} and P_i are generally glassy and have rigid structures that exhibit poor chain packing [32]. In essence, these polymers offer the size distribution of free volume elements required for approaching molecular sieving characteristics.

Since the advent of commercial membrane gas separation systems, structure-property data on polymeric membranes has significantly increased in the literature. It became apparent that a balance (trade-off relationship) existed between selectivity and permeability [33-36]. A concept emerged in the literature called the "upper bound" where log-log plots of selectivity versus permeability of the more permeable gas

demonstrated that virtually all the data points were below a well-defined line [31, 37]. An example is shown in Figure 2.2. This relationship was found to be valid for gas pairs chosen from the common gases of He, H_2, O_2, N_2, CO_2, and CH_4. The "upper bound" line has the following form [31, 32]:

$$P_A = k\alpha_{A/B}^{n} \tag{13}$$

where P_A is the permeability of the more permeable gas, n is the slope of the upper bound line, and k is a constant for a specific gas pair termed the front factor. The value of the upper bound slope was shown to correlate with kinetic diameters determined from zeolite data, which gave a better fit than other gas diameter data in the literature [31, 38]. An empirical analysis demonstrated a linear relationship between *1/n* and the difference in the gas diameters ($d_j - d_i$) [31]. An example of the upper bound relationship for CO_2/CH_4 from the 1991 publication is shown in Figure 2.2 [31].

The upper bound analysis is based on homogeneous membranes utilizing data from studies where the permeability and selectivity data were determined on the same films using the same measurement methods. Data from different studies or different film preparation methods would not be accurate enough to provide reliable data for the analysis. Surface modified films, laminates of different films, phase separated polymer blends, polymers containing particulates (such as zeolites) and phase separated block copolymers would not be relevant for this analysis as specific combinations could be fabricated whereby the upper bound can be surpassed based on heterogeneous membrane models [39]. Specifically, a film laminate of a low permeability polymer with a high permeability polymer (both comprising values on or near the upper bound relationship) can yield laminate film values well above the upper bound based on the series resistance model.

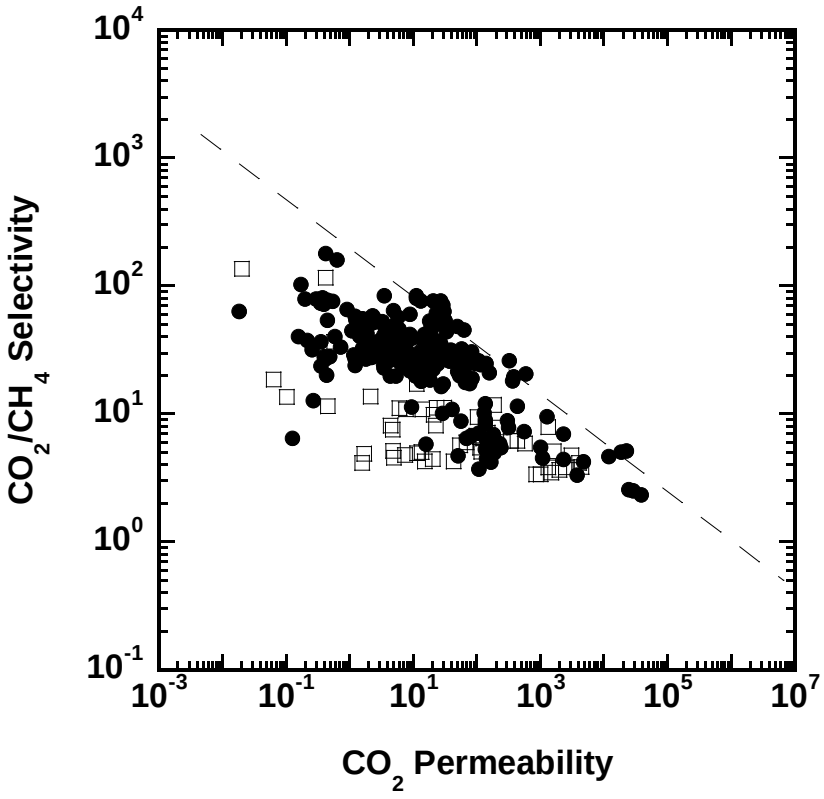

Figure 2.2 Experimental Data for CO_2/CH_4 separation demonstrating an empirical upper bound for glassy (●) and rubbery (□) polymers from 1991. Adapted from [31]; copyright Elsevier.

The upper bound relationship is an empirical correlation based on experimental data, but a theoretical analysis by Freeman [40] yielded good agreement with the observed empirical results. This theory allowed for the prediction of both the upper bound slope and the front factor. Freeman identified the upper bound slope predicted from activation energy theory as:

$$\lambda_{AB} = -\frac{1}{n} = \left(\frac{d_B}{d_A}\right)^2 - 1 = \left(\frac{d_B + d_A}{d_A^2}\right)\left(d_B - d_A\right) \tag{2.14}$$

The value of $(d_B + d_A)/d_A^2$ has modest variation compared to $d_B - d_A$ and, therefore, gave reasonable agreement between theory and experimental observations. The value of the front factor, *k*, required a more complex analysis, yielding the following relationship:

$$\beta_{A/B} = k^{-1/n} = \frac{S_A}{S_B} S_A^{\lambda_{A/B}} \exp\left\{-\lambda_{A/B}\left[b - f\left(\frac{1-a}{RT}\right)\right]\right\} \tag{2.15}$$

where S_A and S_B represent the gas solubilities. The linear free energy relationship between the activation energy of diffusion, E_{di} and D_{0i} [40-42]:

$$\ln D_{0_A} = a\frac{E_{d_A}}{RT} - b \tag{2.16}$$

was employed to determine values of *a* and *b*, where *a* is 0.64 and *b* has values of 9.2 and 11.5 for rubbery and glassy polymers, respectively [25]. The parameter, *f*, was determined from the following expression relating activation energy of diffusion with the diameter of the penetrant molecule [40, 43]:

$$E_{d_A} = cd_A^2 - f \tag{2.17}$$

Values of *c* and *f* are adjustable and relate to a specific polymer. Freeman observed the best match between the empirical upper bound lines and the theory was attained with *f* =12,600 cal/mole [40]. The solubility constant for gases may be correlated with the gas critical temperature, T_c, boiling point, T_b, or Lennard-Jones temperature (ε/k) by the following equations [25]:

$$\begin{aligned} \ln S_A &= m + 0.025T_b \\ \ln S_A &= x + 0.016T_c \\ \ln S_A &= y + 0.023(\varepsilon_A / k) \end{aligned} \tag{2.18}$$

where *m*, *x* and *y* have unique values for each polymer. These relationships appear to work well for a wide variety of polymers (specifically aliphatic and aromatic polymers),

except for the polymer class of perfluorinated polymers where the slope values are different [32]. For this analysis, Freeman chose the Lennard-Jones solubility relationship with y = -9.84 cm^3(STP)/(cm^3 polymer cmHg) [40]. The comparison of the empirical upper bound results with the predicted results are shown in Figure 2.3 for comparison of the front factor k.

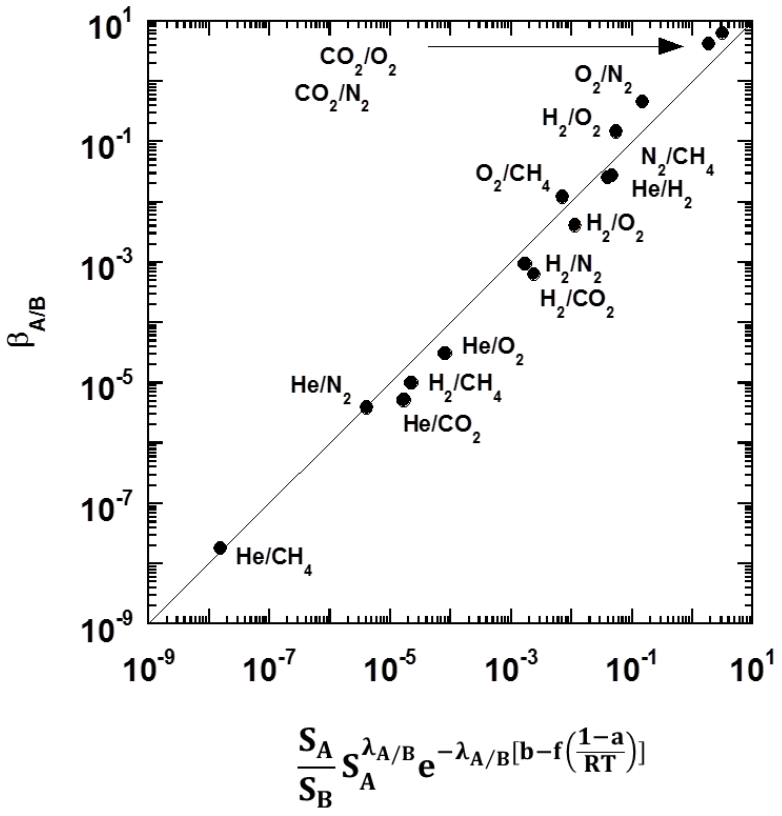

Figure 2.3 Comparison of the front factor k from the experimental data with the prediction values. The parameter f was set to 12,600 cal/mol. The units of $\beta_{A/B}$ are (cc(STP)-cm/cm^2-sec-cmHg)$^{-1/n}$ ($\beta_{A/B} = k^{-1/n}$) (note i = A and j = B relative to the discussion from reference [40]; Adapted from [44]; Copyright Elsevier).

The upper bound observation for gas separation has been also proposed for other transport processes including fuel cell membranes and water desalination using similar log-log plots [45-48]. For fuel cell membranes, an empirical upper bound was observed

with experimental data plotted as proton conductivity versus water sorption for proton exchange membranes. For water desalination, experimental water/salt selectivity versus water permeability was plotted and compared with theoretical considerations.

As more data on polymer gas separation characteristics beyond what was utilized in the 1991 analysis became available, a revised compilation was published [32]. As would be expected, some shifts in the upper bound resulted. However, most of these shifts were minor and involved changes in the front factor while the upper bound slope values remained virtually unchanged. Significant shifts in the front factor are primarily due to recent data on perfluorinated polymers that did not exist in 1991. The solubility relationship for perfluorinated polymers for gases is different than that for aliphatic and aromatic polymers as discussed above [49]. The gas pairs where significant shifts were noted for perfluorinated polymers primarily involved helium as the fast gas. Without the inclusion of the perfluorinated polymer data, the upper bound relationships noted in 1991 showed minor changes for all gas pairs of interest. The results of the recent data on O_2/N_2 separation compared with the initial 1991 publication are illustrated in Figure 2.4 showing a minor shift in the empirical upper bound resulting from intensive optimization of structure-property relationships. An illustration of the deviation of perfluorinated polymer data, involving He as the fast gas, from data obtained with other polymeric structures is given in Figure 2.5. This figure illustrates that perfluorinated polymers exhibit a unique upper bound relationship relative to their aliphatic and aromatic counterparts.

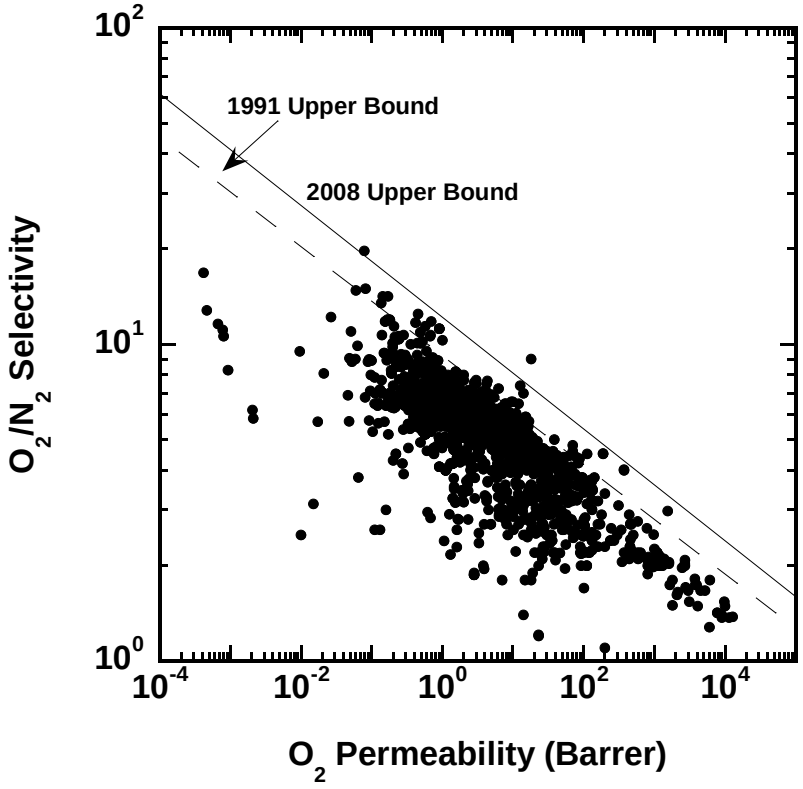

Figure 2.4 The upper bound correlation for O_2/N_2 separation. Adapted from [32]; copyright Elsevier.

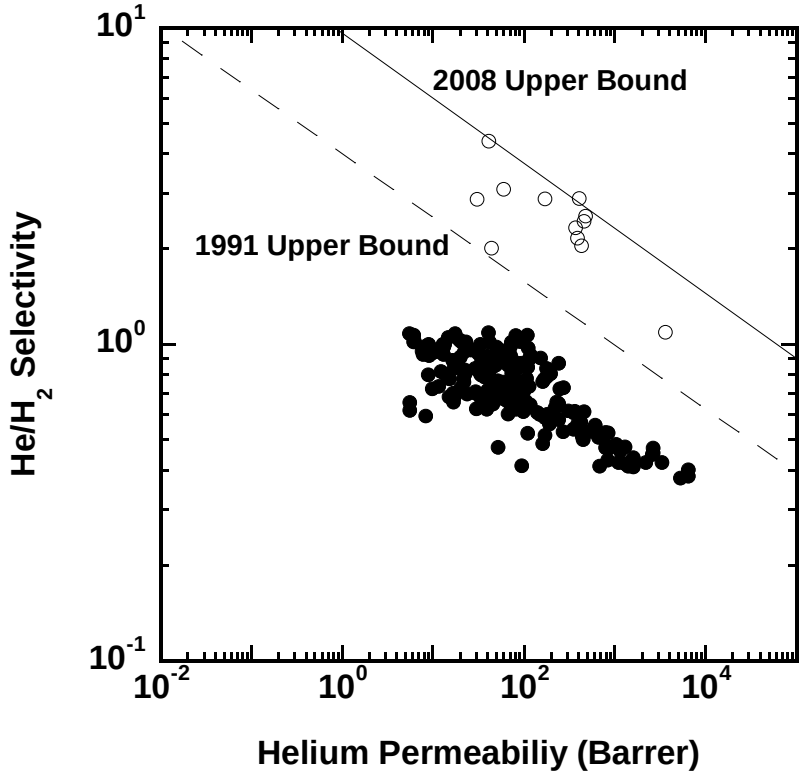

Figure 2.5 The upper bound correlation for He/H_2 membrane separation. Open circles are for perfluoropolymers and filled circles are hydrocarbons. Adapted from [32]; copyright Elsevier.

The permeability database from the recent upper bound paper [32] was also used to correlate gas permeability data in a different format. The data show that as the permeability of one gas (from the list of common gases) increases, the permeability for other gases also increases [44]. This result is a consequence of the diffusion coefficient of the gases being related to the free volume of the polymer. The solubility ratio of the gases is also predicted to be in a tight range for the myriad of polymers available [31]. The database covers over ten orders of magnitude in permeability values that form a linear log-log relationship for all gas pairs (chosen from He, H_2, O_2, N_2, CO_2 and CH_4). In this correlation, log P_i is plotted against log P_j yielding a linear relationship for all gas

pairs over the experimental permeability range. The value of i and j are chosen such that n>1 in the relationship:

$$P_J = k_c P_i^n \tag{2.19}$$

A representation of the above analysis is shown in Figure 2.6 for the gas pair CO_2/N_2. Alentiev and Yampolskii reported similar correlations [50].

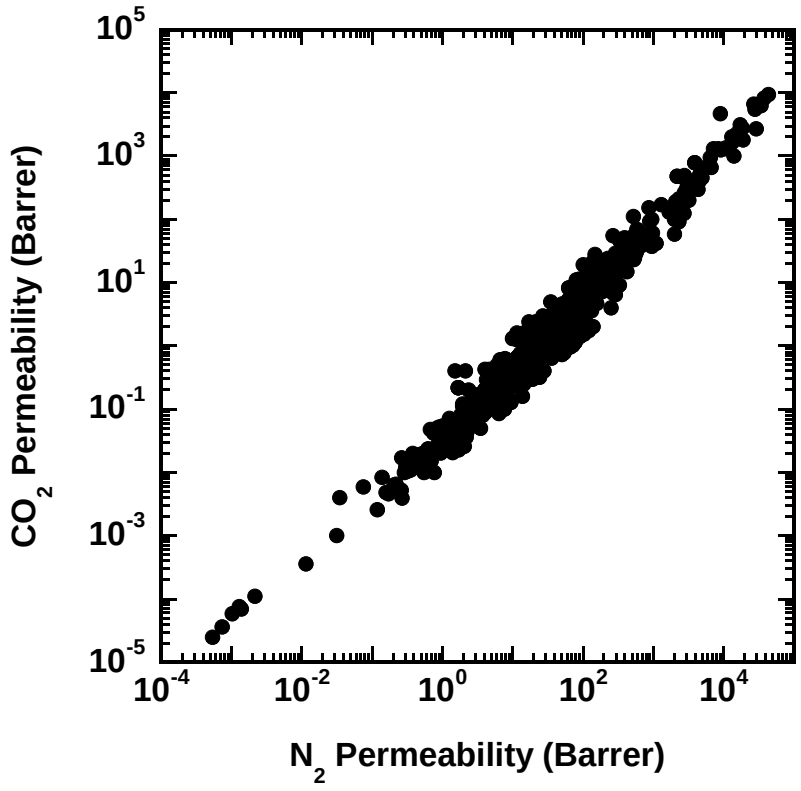

Figure 2.6 Permeability correlation for CO_2/N_2. Reprinted with permission from [44]; copyright Elsevier.

The value of k_c in Equation 2.19 is correlated with the Freeman theory developed for the upper bound relationship and gives an excellent fit of the experimental data with theoretical predictions. This analysis provides strong additional verification of the

validity of the theory and provides a means for determination of kinetic diameters for the common gases of interest that represent an improvement over the values employed previously based on the zeolite based data of Breck [38]. These updated gas diameter values are recorded in Table 2.1 along with the kinetic diameter values from Breck for comparison.

Table 2.1 Breck kinetic diameter and correlation diameters for common gases

Gas	Breck Kinetic Diameter Å [38]	Correlation Diameter Å [44]
He	2.6	2.644
H_2	2.89	2.875
CO_2	3.3	3.325
O_2	3.46	3.347
N_2	3.64	3.568
CH_4	3.8	3.817

The upper bound relationship is based on data in the temperature range of 25-35 ºC. In a recent publication [51], it was noted that the upper bound shifts with temperature and the Freeman theory was utilized to predict the shift for a number of gas pairs of interest.

Group contribution methods have been applied to ascertain the specific structural features of aromatic polymers that lead to optimizing permeability and separation. Two approaches from separate groups were published by Park and Paul [52] and by Robeson et al. in a similar time frame [53, 54]. While both approaches superficially appeared to be quite different, close observation show they were actually quite similar and allowed

for predicting both permeability and selectivity of aromatic polymers with good accuracy. The resulting group contribution predictions allowed for a quantitative determination of the effect of many structural variables including linking groups, *iso* versus *para* substitution, aromatic group substitutions, alkyl versus halide substitution and symmetry around the main chain. A much larger (and unpublished) analysis was employed in the industrial laboratory approach [53, 54] to circumvent the synthesis of large numbers of polymers for experimental analysis.

2.2.2 Physical Aging

While the permeability/selectivity tradeoff is a widely recognized challenge, there are other significant material challenges, such as physical aging, that affect a polymer's industrial viability. Many polymers used in gas separations are glassy materials [55, 56]. Glassy polymers are non-equilibrium materials having excess free volume due to kinetic constraints on polymer segmental motion that prevent such materials from coming completely to equilibrium properties (*e.g.*, specific volume) once they are below their glass transition temperature. However, even in the kinetically constrained glassy state, polymers undergo at least local scale segmental motions, and these motions act to gradually increase the density of the polymer (and, therefore, reduce its free volume) towards the thermodynamic equilibrium value [57]. Physical aging slows over time for two reasons: (1) as the excess free volume gradually decreases, the driving force for physical aging is diminished, and (2) as free volume is reduced, polymer chain mobility decreases, which decreases segmental motions available to assist in reorganizing the polymer chains. Physical aging reduces gas permeability and alters other physical properties of polymers (*e.g.*, specific volume, enthalpy, entropy, *etc.*) [58-65]. The observed decrease in permeability, usually accompanied by an increase in selectivity, is

seen as a reduction in membrane flux over time. Recently, it has become widely recognized that physical aging also depends on the thickness of the polymer under study, particularly when the thickness becomes of the order of less than 1 micron. Gas separation membranes are often believed to be on the order of approximately 0.1 microns thick, making the effects of thickness on aging a relevant field of study [59].

Equation 2.20 presents the most common framework used to describe physical aging [57, 59]

$$\frac{dV}{dt} = \frac{-(V - V_\infty)}{\tau} \tag{2.20}$$

where the rate of change in the specific volume, V, of a polymer with time depends on the departure of the polymer's specific volume from its equilibrium value, V_∞, and the characteristic timescale for relaxation of the specific volume towards equilibrium, τ. The characteristic relaxation time is related to the mobility of the polymer chains, and it is typically taken to be a function of the specific volume of the polymer and temperature [59]. Additionally, the dependence of physical aging on sample thickness is typically accounted for by allowing τ to vary with thickness, suggesting that molecular mobility of polymer chains near free interfaces may be greater, at least initially following the beginning of an aging experiment, than that of polymer chains in bulk polymer [59]. The fractional free volume is directly related to a polymer's specific volume, as discussed in Section 1. Therefore, as a polymer ages and fractional free volume decreases, gas permeability also decreases, albeit at slower and slower rates as time goes on, due to the self-retarding nature of physical aging. Because the losses in permeability and densification due to physical aging come from relaxation of the polymer matrix, they are thermally reversible, so losses in permeability (*i.e.*, increases in density) can be restored by heating the polymer above its T_g [66].

Because of the relationship between free volume and physical aging, the aging of high free volume polymers has been a point of interest in the literature. In particular, the aging of PTMSP, one of the most permeable polymers known, has been widely studied [67-72]. Many of these studies have documented a rapid loss in gas permeability as a function of time, but the permeability of PTMSP films is also affected by contaminants, such as vacuum pump oil, which has led to discrepancies in these measurements in the literature. In a study accounting for this contamination, PTMSP films with thicknesses of approximately 100 μm still showed significant physical aging [69]. Permeabilities of CH_4, O_2, and N_2 decreased by more than 20% over roughly 200 days. These films were first preconditioned in methanol, increasing the initial free volume, which increases the driving force for physical aging [69]. In contrast, Pfromm and Dorkenoo found no loss in permeability in an 85 μm PTSMP film that was not pretreated with methanol; however, thin films with thicknesses of 1 and 3 μm showed 76% and 38% losses in N_2 permeability, respectively [72]. These results show the complexity of physical aging and the importance of membrane preparation conditions in physical aging studies.

However, physical aging is not restricted to only high free volume glassy polymers; it occurs in any glassy material. For example, thin films of glassy polyimides, such as 6FDA-DAM, underwent an order of magnitude decrease in permeability over 1000 hours [63]. The rate of physical aging is often characterized by a parameter, r, which is defined as follows [69]:

$$r = -\left(\frac{d\ln V}{d\ln t}\right)_{P,T} \tag{2.21}$$

In Equation 2.21, the higher the value of *r*, the more rapid the physical aging in a material. A rough correlation between the rate of physical aging and the fractional free volume has been observed for a number of polymers; a basic form of this correlation is

presented in Figure 2.7, although the relationship is likely more complicated. That is, higher free volume glassy polymers tend to age more rapidly than lower free volume polymers, all other factors (*e.g.*, thickness) being equal.

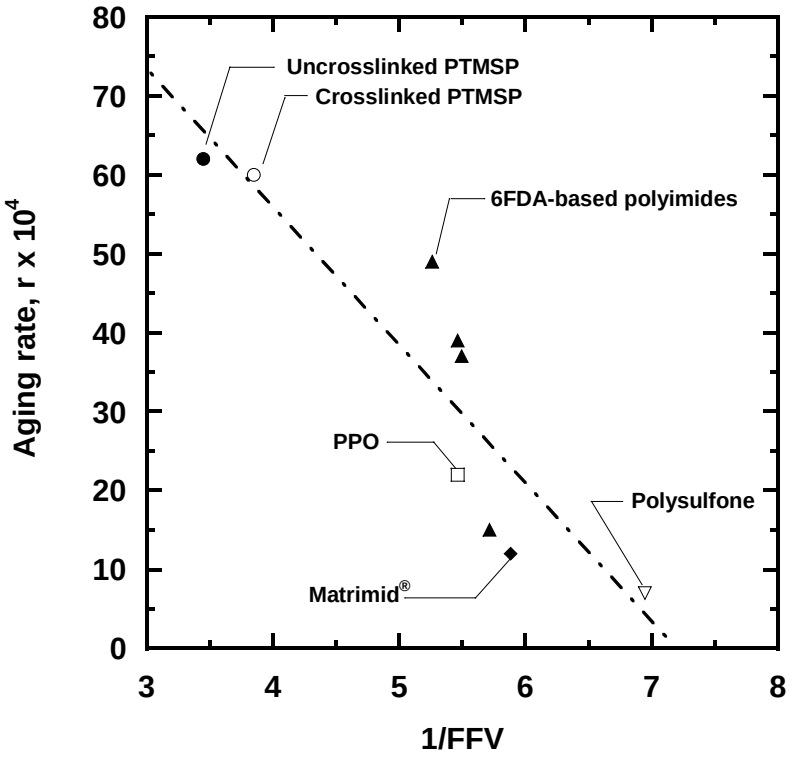

Figure 2.7 Effect of fractional free volume on the physical aging rate of selected polymers including crosslinked and uncrosslinked poly(1-trimethylsilyl-1-propyne (PTMSP), and poly(2,6-dimethyl-1,4-phenylene oxide) (PPO). Aging rate is defined in Eq 19. All films were approximately 400 nm thick. Adapted from Kelman *et al.* [69]; copyright Elsevier.

The dependence of thickness on physical aging has become a growing area of study. Physical aging rates increase substantially, as tracked both by gas transport and optical properties, as films approach sub-micron thicknesses [59-61, 64, 66, 73-84]. For example, in polysulfone, significant deviation from the aging behavior in bulk films is

seen once films become thinner than roughly 10 μm, while thicker films age at rates similar to bulk films [76].

The physical aging of ultrathin films has also been examined. The ultrathin regime encompasses polymer films thinner than 400 nm [59]. Figure 2.8 presents the impact of film thickness on oxygen permeability of Matrimid®, a commonly studied gas separation polymer. The differences in oxygen permeability as a function of thickness at short aging times is attributed to rapid physical aging in the first hour after quenching the samples from above to below T_g to start the aging experiment, but before the samples could be prepared for permeability testing [59]. Even within the ultrathin regime, thinner samples generally have higher rates of physical aging, as judged by the slope of the permeability versus log aging time results in Figure 2.8. Increased physical aging at such thicknesses is relevant because commercial membranes have effective thicknesses on the order of 100 nm. At this thickness or thinner, physical aging can lead to a rapid loss in transport properties that would not be expected based on bulk properties.

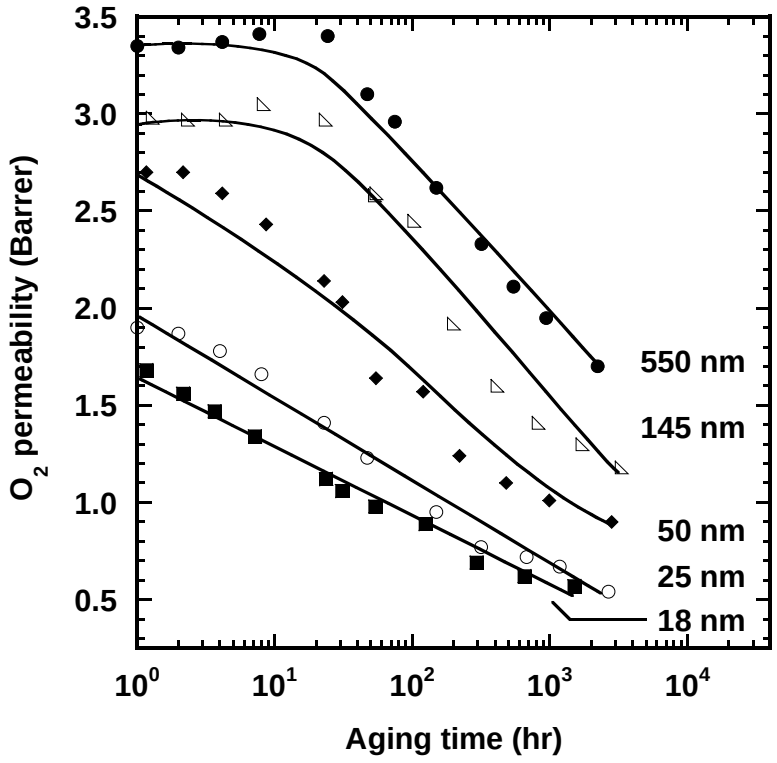

Figure 2.8 The effect of film thickness on Matrimid® with PDMS coating O_2 permeability in ultrathin films. Permeability measured at 35ºC and 2 bar. Adapted from Rowe *et al.* [59]; copyright Elsevier.

The thickness dependence of physical aging has interesting implications for gas separation membranes. Historically, the effective thickness of the dense layer of asymmetric gas separation membranes is estimated by measuring gas flux and back-calculating the thickness based on bulk permeability values. However, because the calculated thickness of these dense layers is in the ultrathin regime, the bulk permeability may not be an accurate indicator of the permeability through the thin, dense skin of the membrane. If so, then the true thickness of the separating layer of commercial gas separation polymers may, in fact, be substantially thinner than the often-quoted figure of approximately 100 nm.

2.2.3 Plasticization

As the concentration of gas inside a polymer increases, the polymer can swell, which increases free volume and chain motion, which increases gas diffusion coefficients and decreases diffusion selectivity. This phenomenon is known as plasticization. Plasticization often results in higher gas flux but lower mixed gas selectivities, particularly at high pressures [19, 85, 86]. One common signature of plasticization is an increase in permeability of a gas as the upstream partial pressure of that gas increases. However, strictly speaking, increases in permeability can be due to either increases in solubility, increases in diffusivity, or both, and plasticization is typically associated with increases in permeability driven by increases in gas diffusion coefficients as upstream pressure and, therefore, the concentration of gas dissolved in the polymer, increases [87]. Another common symptom of plasticization is an increase in permeability of all components in a mixture and a loss in selectivity as upstream total pressure (or partial pressure of one or more components) increases [88].

CO_2 is a common gas used in plasticization studies [73, 74, 89-97]. Among gases of importance in gas separation applications, CO_2 is often among the more soluble gases, and plasticization by CO_2 is widely known and studied in relation CO_2 removal from natural gas (*i.e.*, methane) [98]. Many polymers sorb enough CO_2 at accessible pressures to strongly plasticize, so it is a convenient penetrant for such studies.

For glassy polymers that plasticize, gas permeability generally decreases with increasing feed (*i.e.*, upstream) pressure until plasticization occurs, when gas permeability begins to increase with increasing pressure [91, 97, 99]. For CO_2 in glassy polymers, typical plasticization pressures are 10 to 35 bar for polymers relevant to gas separations, and it has been suggested that the CO_2 concentrations in such polymers are similar, ranging from 30 to 45 cm^3(STP)/cm^3 polymer, at the plasticization pressure [91].

Polymers that sorb less CO_2 are often thought to be less prone to plasticization than those sorbing more CO_2 at a given pressure, though this guideline should not be viewed as a universal rule. Figure 2.9 presents the relative change in permeability with feed pressure for four polymers commonly studied in the gas separation literature. The relative increase in permeability and plasticization pressure varies from polymer to polymer, highlighting the continuing need to explore plasticization in greater depth as new materials are developed.

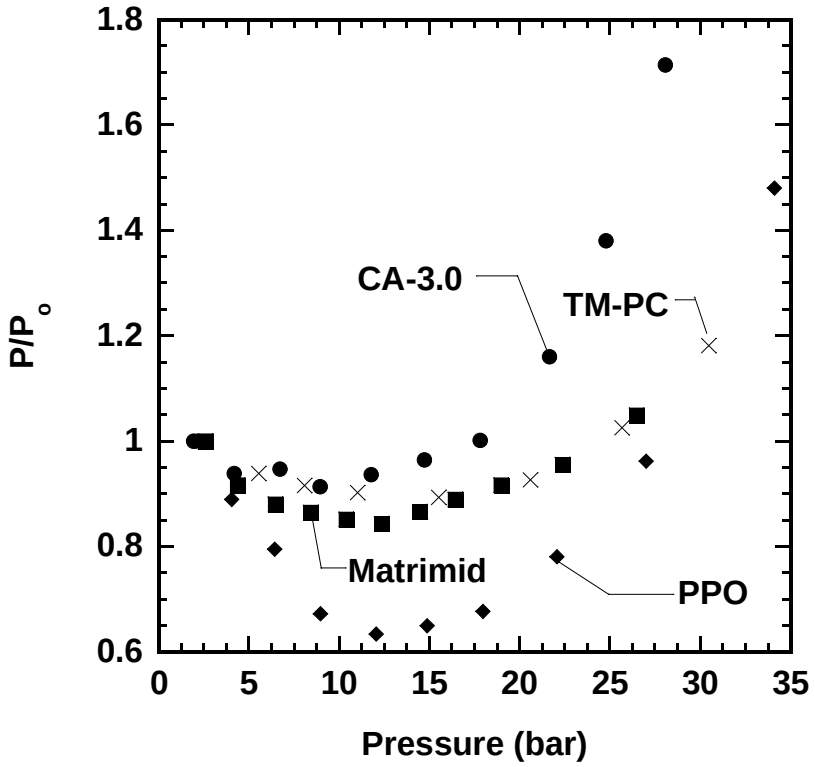

Figure 2.9 Relative permeability increase (where P_O is permeability at a feed pressure of roughly 1 bar) as a function of feed pressure for selected glassy polymer films. Cellulose triacetate (CA-3.0) at 24ºC (●), Matrimid® at 22ºC (■), tetramethyl bisphenol A polycarbonate (TM-PC) at 25ºC (X), and poly(2,6-dimethyl-1,4-phenylene oxide) (PPO) at 25ºC (♦) [91].

In addition to a rapid increase in permeability with increasing feed pressure, polymers undergoing plasticization may also display a slow increase in permeability over timescales far exceeding those required to achieve steady state. This behavior in Matrimid® polyimide is shown in Figure 2.10. Despite an expected time lag of seconds or minutes, depending on film thickness, CO_2 permeability continues to increase with time even after two hours. The effect of film thickness on these increases in permeability will also be discussed later [73]. This upward drift in permeability and related properties

has also been noted in other polymers. For example, CO_2 sorption in polyethersulfone at high pressures can continue to increase for more than six days without reaching equilibrium [100]. Cellulose acetate, which is widely known to plasticize in the presence of CO_2, has shown approximately a 40% increase in CO_2 permeability with time at constant feed pressure [101].

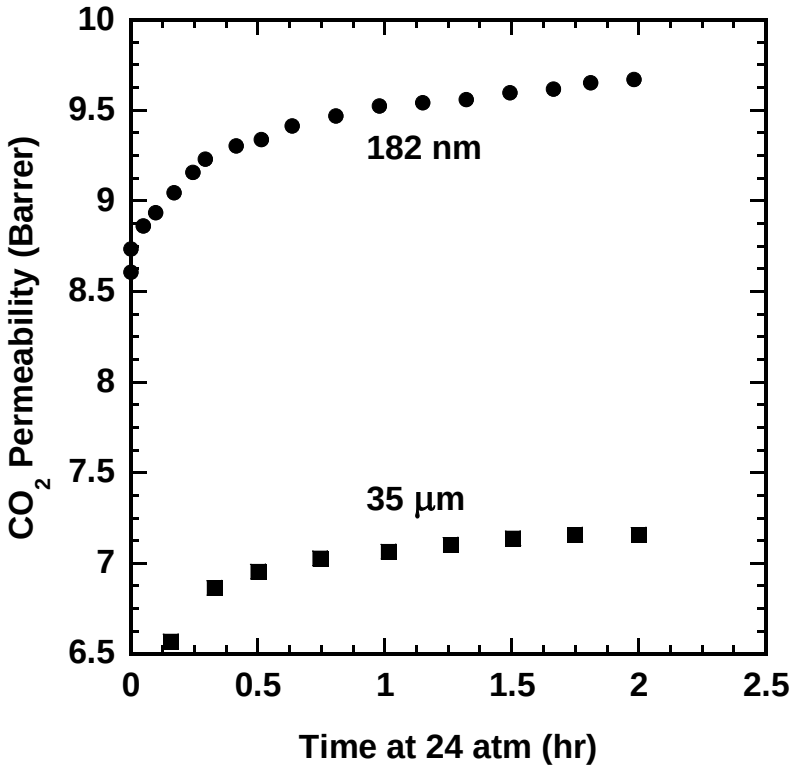

Figure 2.10 CO_2 Permeability through Matrimid® films as a function of time after the feed pressure was set to 24.3 bar. Films were previously held at 8.1 bar and 16.2 bar . 182 nm (●) and 35 μm (■) thick films were considered at 35ºC [73].

This change in permeability with time suggests that, when exposed to CO_2, the properties of these glassy, nonequilibrium materials may change over time, presumably due to CO_2 swelling-induced structural relaxation and solid state reorganization in the polymer [90, 101]. As polymers swell due to increased penetrant concentration, diffusion

coefficients can increase due to increasing free volume, increasing chain mobility, or both [91, 100]. These increases in D are often described as plasticization. In addition to changing diffusion coefficients, increased penetrant concentration at higher pressure can also influence permeability, solubility, selectivity, and mechanical properties.

Glassy polymers undergoing plasticization may also show hysteresis in permeation properties, with transport properties at a given pressure being different depending on whether permeability was measured during pressurization or depressurization, but this phenomenon alone does not definitively identify plasticization. This effect has been observed in many different polymers, but the degree of hysteresis often varies from polymer to polymer [98, 101-104]. Figure 2.11 presents an example of CO_2 permeability hysteresis in cellulose acetate. In this case, CO_2 permeability was first measured as a function of increasing feed gas pressure; then, the permeability was measured as the sample was held at the highest gas pressure considered; finally, gas permeability was measured as feed pressure was decreased [101]. Gas permeabilities measured as feed pressure was decreased are substantially higher than those measured while feed pressure was being increased. When the sample was continuously exposed to the highest feed pressure considered (*i.e.*, 30.4 bar), permeability gradually drifted upwards, reflecting a slow swelling of the polymer by the gas. This hysteresis is the result of conditioning this glassy polymer by the CO_2, where exposure to CO_2 presumably causes the polymer to dilate, increasing the free volume of the material; because the polymer is a nonequilibrium glass, changes in the free volume of the polymer due to such process history effects can be relatively long-lived [22]. This phenomenon of permeation hysteresis is, like physical aging, another manifestation of the nonequilibrium nature of glassy polymers used in most gas separation applications today.

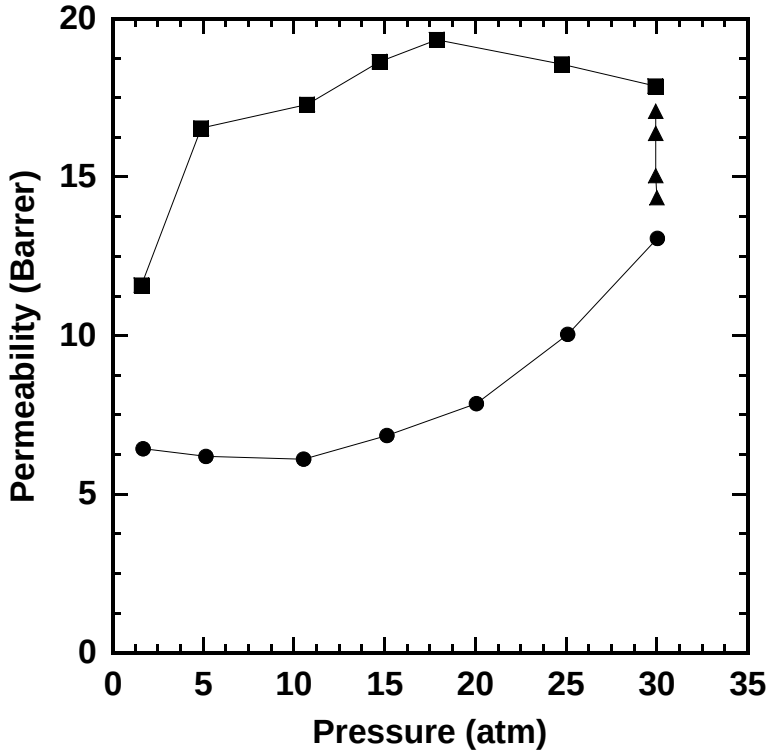

Figure 2.11 CO_2 Permeability as a function of feed pressure for cellulose acetate at 35ºC. (●) indicates permeability measurements made as feed pressure was increased, (▲) indicates measurements made while feed pressure was held constant at 30.4 bar, and (■) indicates permeability measurements made as feed pressure was decreased. Adapted from [101]; copyright Elsevier.

Increasing CO_2 permeability and plasticization of the polymer membrane can cause selectivity to decrease under mixed gas conditions in separations such as natural gas purification, which is typically represented as a CO_2/CH_4 separation [86, 88]. This decrease in selectivity is due to the CH_4 permeability increasing more with increasing pressure than that of CO_2, and it is typically thought to be a result of the free volume increases caused by CO_2-induced plasticization, similar to the way CO_2 plasticization has been shown to effect CO_2/ethane and CO_2/CH_4 selectivity in various polymers [105]. A more rapid increase in CH_4 than CO_2 permeability as free volume increases is predicted

by the Cohen-Turnbull theory, which predicts an exponential dependence of diffusion coefficient on the required size of a free volume element for the molecule to pass through as seen in Equation 2.10 [18]. This decreasing selectivity has been observed in cellulose acetate, Matrimid®, and many other materials [101, 106].

While this section has focused on plasticization caused by CO_2, plasticization can be caused by any component or even impurities in a feed stream [93, 107]. Penetrants that exhibit higher sorption in polymers are more likely to cause plasticization and conditioning effects. One practical example is the plasticization of membranes used for natural gas purification by higher hydrocarbon contaminants in the feed [108].

Recently, the plasticization behavior of films with thicknesses of about 200 nm was characterized. These results were compared to those obtained using films with thicknesses ranging from 20 to 50 μm, and the thin films showed a much larger increase in permeability at the same CO_2 concentration [73, 74]. These changes in permeability also occurred over a much shorter timescale in thin films. While much is still unknown about this behavior, the discrepancies between thick and thin films behavior have been attributed to the difference in relaxation time distribution between thick and thin films [73, 74]. Plasticization and physical aging occur in both thin and thick films; however, as demonstrated in Figure 2.12, these effects are much more prominent in thin films [73, 74]. In roughly the first 5 hours, the transport properties of the thin film are dominated by plasticization and permeability. However, at longer times, the transport properties are dictated by physical aging and permeability decreases. Because the timescale for plasticization is longer and the effects of physical aging less dramatic in thick films, the same behavior is not seen in the thick film. An understanding of plasticization in thin films and how it differs from widely studied thick films with thicknesses of 20-50 μm is interesting from a fundamental standpoint, but it also has practical ramifications because

commercial gas separation membranes have effective thicknesses in the hundreds of nanometers range [109].

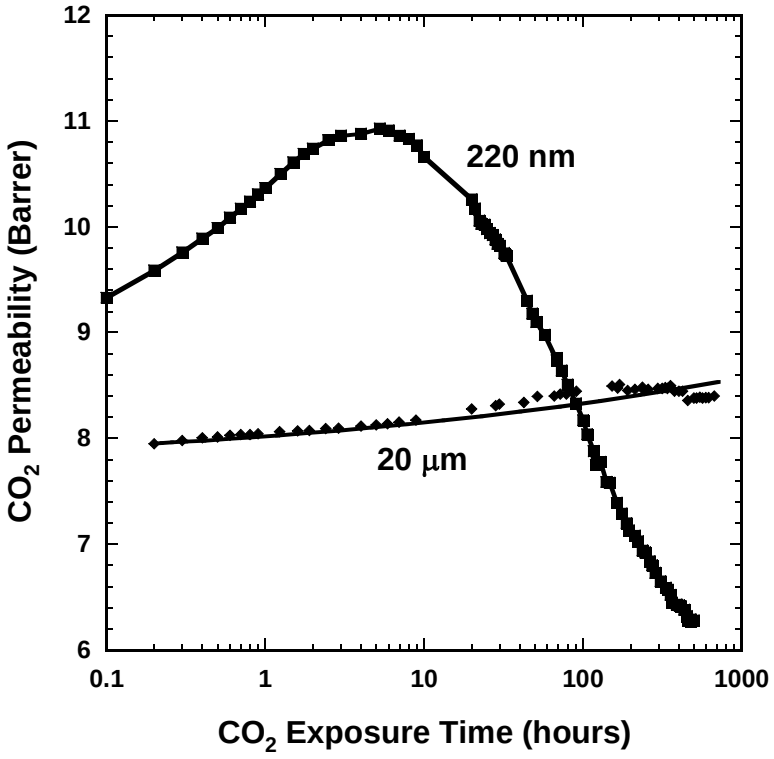

Figure 2.12 Simultaneous physical aging and plasticization in 200 nm and 20 μm Matrimid® films which were aged 200 hours at 35ºC while being exposed to CO_2 at 32.4 bar [73].

2.3 SELECTED COMMERCIALLY RELEVANT POLYMERS

Over the last 30 years, polymer membranes have developed into a feasible industrial process for gas separations. During this time, several polymers have been established as common gas separation membranes. This section will highlight commercially relevant polysulfones (PSF), cellulose acetates (CA-DS, where DS is the degree of acetylation of the cellulose), poly(phenylene oxides) – particularly poly(2,6-dimethyl-1,4-phenylene oxide) (PPO), aramids, and polyimides (PI). In particular, the polysulfone section will focus on Bisphenol A based polysulfones and other

modifications of these polymers, such as brominated bisphenol-A polysulfone (TB-BisA-PC) [110, 111]. The polyimides section will focus on Matrimid® and BPDA-ODA, while a later section will highlight new developments in polyimides. For comparison, Table 2.2 and Table 2.3 present pure gas permeabilities, pure gas selectivities, and free volume measured on thick films for these selected polymers.

Table 2.2 Permeability of common gases and fractional free volume of representative commercially used polymers.

Polymer	CO_2	H_2	O_2	N_2	CH_4	FFV
Matrimid®[a,g]	10	18	2.1	0.32	0.28	0.170
CA-2.45[b]	4.8	12	0.82	0.15	0.15	-
PSF[c,g]	5.6	14	1.4	0.25	0.25	0.144
PPO[d,g]	61	61	16.8	4.1	4.3	0.183
TB-BisA-PC[e,h]	4.2	-	1.4	0.18	0.13	0.092
Selected Aramid[f]	-	24.5	-	-	0.1	-

[a] O_2, N_2, CH_4 at 35ºC, 2 bar (all pressures in these notes refer to feed pressure) from [78]; CO_2 at 3.4 bar and 35ºC from [112]; H_2 at 4.1 bar and 35ºC from [113]
[b] cellulose acetate (2.45 degree of acetylation), 1 bar and 35ºC from [101]
[c] polysulfone, CO_2, CH_4 at 10 bar and 35ºC; O_2, N_2, H_2 at 1 bar and 35ºC from [114]
[d] poly(2,6-dimethylphenylene oxide), data from [115]
[e] CO_2, CH_4 at 20 bar and 35ºC; O_2, N_2 at 1 bar and 35ºC from [110]
[f] selected aramid at 90ºC from [116]
[g] FFV for Matrimid®, PSF, PPO bulk films from [117]
[h] FFV for TB-BisA-PC bulk film from [110]

Table 2.3 Common gas selectivities for commercially relevant polymers

Polymer	H_2/CH_4	H_2/N_2	CO_2/CH_4	CO_2/N_2	CO_2/H_2	O_2/N_2	N_2/CH_4
Matrimid®	64	56	36	31	0.56	6.6	1.1
CA-2.45	80	80	32	32	0.4	5.5	0.67
PSF	56	56	22.4	22.4	0.4	5.6	1
PPO	14	15	14	15	1	4.1	0.95
TB-BisA-PC	-	-	32	23	-	7.8	1.4
Selected Aramid	245	-	-	-	-	-	-

2.3.1 Polysulfones

Polysulfones are characterized by diphenylene sulfone repeat units (–Ar–SO_2–Ar'–), and are regarded as among the most chemically and thermally durable thermoplastic polymers available [118]. Repeating phenylene rings create backbone rigidity, steric hindrance to rotation within the molecule and an electronic attraction of resonating electron systems between adjacent molecules. These properties contribute to a high degree of molecular immobility, resulting in high rigidity (high T_g), high strength, good creep resistance, dimensional stability, and high heat deflection temperature [119]. The basic repeat units of several commercially available polysulfones (Vitrex® PES, Udel® PSF and Radel®R) are illustrated in Figure 2.13. A broad range of polysulfones can be prepared via nucleophilic aromatic (S_NAr) polycondensation of an aromatic dihydroxy compound with a bis-(halophenyl) sulfone. Detailed description of the synthesis of polysulfones can be found elsewhere [118].

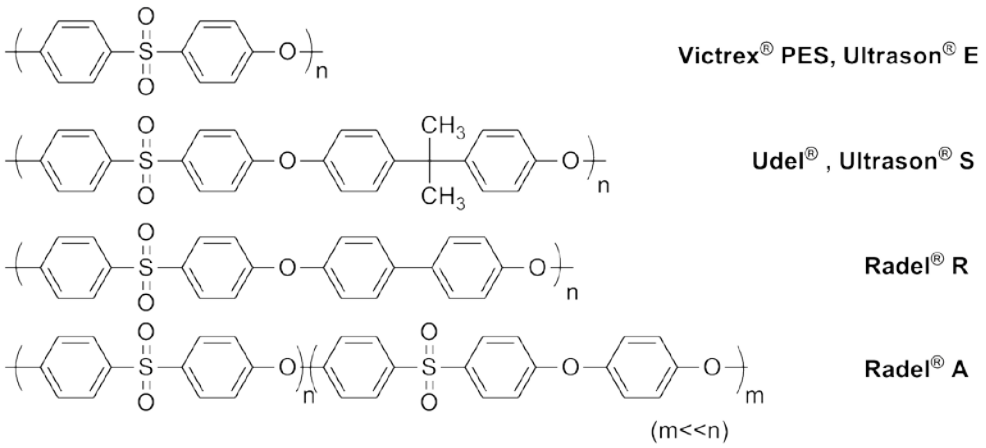

Figure 2.13 Chemical structures of several polysulfones

Polysulfones are an important commercial membrane material for gas separations due to their excellent mechanical properties, a wide operating temperature range, fairly good chemical resistance, and easy fabrication of membranes in a wide variety of configurations and modules [118]. The first large-scale membrane separation process, developed by Monsanto Co. in the late 1970s, utilized asymmetric hollow fiber membranes of bisphenol A polysulfone coated with a thin layer of silicone rubber [120]. The gas transport properties of commercial PSF and PSF variants, particularly the influence of various bridging moieties between the phenyl rings and the groups substituted on the phenyl rings on gas permeation properties, have been extensively studied [114, 121-128]. Symmetric bulky substitutions (e.g., methyl groups) on the phenyl rings significantly increase gas permeability, while asymmetric substitution of these same groups decreases gas permeability [129]. For example, replacing the isopropylidene bridging moiety with bulkier groups, like hexafluoro isopropylidene ($-C(CF_3)_2-$), makes the polymers much more permeable, mainly due to the enhanced free volume [121]. However, these large increases in CO_2 permeability can also affect the

susceptibility of gas transport properties to plasticization by gases such as CO_2. A combination of hexafluoro isopropylidene groups and symmetric substitution led to the appearance of plasticization effects when CO_2 pressure exceeded approximately 15.2 bar [128].

Polysulfone remains widely used for hydrogen and air separations [109]. Figure 2.14 and Figure 2.15 present the gas separation performance of representative commercial polymers from Table 2.2. Polysulfone has a higher H_2 permeability than cellulose acetate and a lower H_2 permeability than Matrimid®. However, CA, Matrimid®, and PSF are all similar distances from the upper bound in Figure 2.14, showing that they trade off permeability for selectivity as expected. As seen in Figure 2.15 for O_2/N_2 separations, PSF falls below Matrimid® and the tetrabromo-bisphenol A-polycarbonate in overall performance as judged by distance from the upper bound line. These polymers will be discussed in more detail in the following sections.

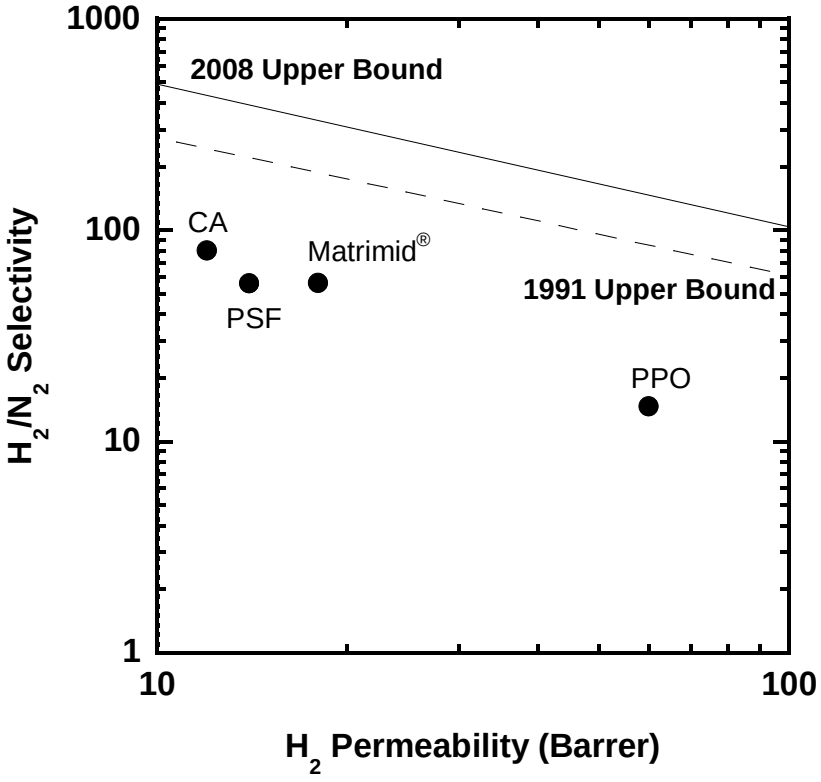

Figure 2.14 H_2/N_2 upper bound plot for representative common commercially relevant polymers in Table 2.2 [31, 32].

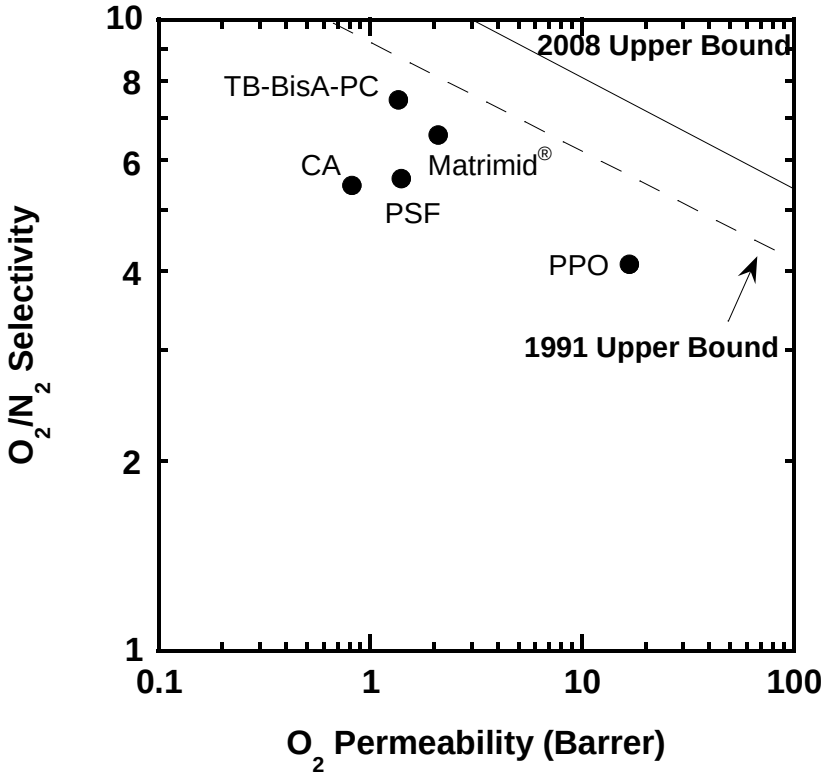

Figure 2.15 O_2/N_2 upper bound plot for representative common commercially relevant polymers in Table 2.2 [31, 32].

2.3.2 Cellulose Acetates

Cellulose acetate (CA) and its derivatives were among the first generation of commercial membranes used for natural gas separation [109, 130-132]. In addition to desirable transport properties, the development of the asymmetric membrane concept by Loeb and Sourirajan, which greatly reduced the surface area necessary to achieve high gas productivity, led to the commercialization of cellulose acetate membranes, initially for use in desalination applications [133]. CA continues to be used in gas separations for removal of acid gases (CO_2 and H_2S) from natural gas as well as the separation of CO_2 from mixtures with hydrocarbons in enhanced oil recovery operations [134].

CA polymers are produced by acetylation of cellulose with a source of acetate esters, typically acetic anhydride or acetic acid, and a catalyst such as sulfuric acid [135]. In general, the family of CA polymers includes a spectrum of materials of varying degrees of acetylation of the hydroxyl groups on cellulose and will be referred to as CA-DS, where DS refers to the degree of acetylation, or degree of substitution (DS). The degree of substitution refers to the number of –OH groups on each glucose unit that have been esterified by acetyl groups (*i.e.*, $0 \leq DS \leq 3$) [135]. Figure 2.16 shows the chemical structure of a cellulose repeat unit with all three hydroxyl groups esterified, commonly referred to as cellulose triacetate (CTA). Cellulose acetates with specific degrees of substitution are commonly produced by converting CA to CTA and hydrolyzing acetates until the desired degree of substitution is reached. CA polymers of varying DS are soluble in organic solvents because acetylation greatly reduces hydrogen bonding and membranes may then be manufactured using the phase inversion process [136].

Although cellulose acetate has been used for nearly 30 years commercially, pure gas permeability and selectivity values position this polymer well below Robeson's upper bound [31, 32]. As seen in Table 2.2, cellulose acetate with a DS of 2.45 has a pure gas CO_2 permeability of 4.8 Barrer, which is less than half that of Matrimid®. This permeability value is a function of the degree of acetylation in these polymers, and varying the degree of acetylation from 1.75 to 2.85 increases CO_2 permeability from 1.84 to 6.56 Barrer [101]. This increase is due to the replacement of polar hydroxyl groups with bulky acetate groups, which decreases polymer density and creates a higher free volume structure [101]. However, as seen in Figure 2.17, with a fairly high DS of 2.85, the CO_2/CH_4 selectivity is 33, significantly below 175, which is the selectivity value of the 2008 upper bound at a permeability of 6.56 Barrer.

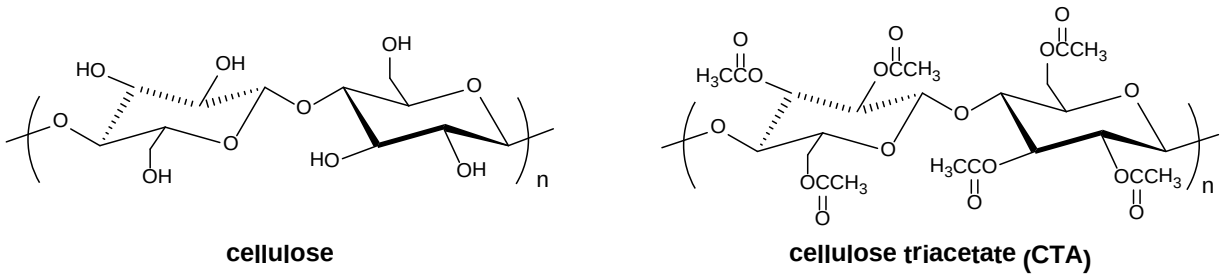

Figure 2.16 Chemical structures of cellulose and cellulose triacetate (CTA).

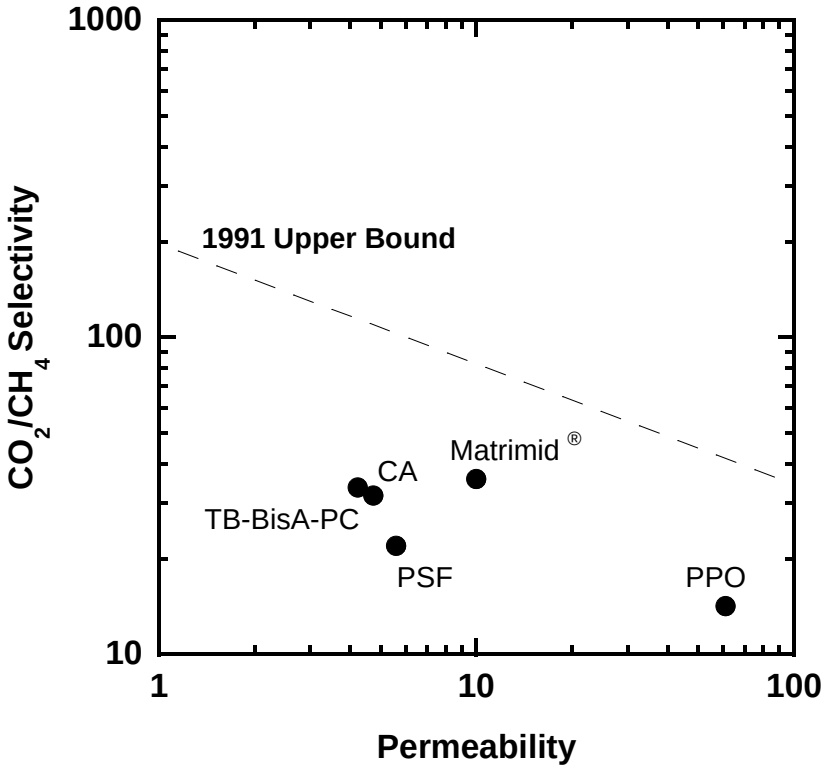

Figure 2.17 CO_2/CH_4 upper bound plot for representative common commercial polymers. The data are from the same sources as those in Table 2.2 [31, 32].

CA membranes are relatively inexpensive in part because cellulose (the raw material) is an abundant and renewable resource [137]. The technology to produce

membranes from cellulose acetate is also relatively well developed [138]. There are, however, several inherent limitations of CA membranes, which restrict its use in membrane gas separations. One limitation of cellulose acetate is that it plasticizes in the presence of CO_2. Plasticization causes the CO_2/CH_4 selectivity of cellulose acetate to decrease in mixed gas environments. For example, the CO_2/CH_4 selectivity decreased from 35 to 31 as CO_2 partial pressure increased from roughly 4.1 bar to 12.7 bar in a 30% CO_2 mixture [88]. This decrease in selectivity would reduce methane recovery in natural gas separations, but it is also accompanied by an increase in CO_2 permeability, which would reduce the membrane area required for removing CO_2 from a given amount of natural gas. These changes, which vary with feed gas concentration, mean that the separation performance of cellulose acetate depends on feed composition and feed pressure [139].

2.3.3 PPO

Poly(2,6-dimethyl-1,4-phenylene oxide) (PPO) is a high performance engineering thermoplastic with good mechanical properties and thermo-oxidative stability because of a low barrier to rotation and resonance stabilization of the aromatic ether bond (–Ar–O–Ar'–) [140, 141]. PPO was the first member of the family of poly(phenylene oxides) to be commercialized. The material was discovered by Hay [142] over 50 years ago and was commercialized by General Electric [143] (now SABIC Plastics) and AKZO [144]. PPO can be synthesized from substituted phenols via oxidative coupling polymerization which involves the room temperature oxidative C–O coupling of 2,6-dimethylphenol in the presence of stoichiometric amounts of oxygen. This process is catalyzed by CuCl and an amine ligand such as pyridine as shown in Figure 2.18. Care must be taken during the oxidative coupling of 2,6-dimethylphenol to avoid undesired C–C coupling that gives rise

to small dimeric molecules rather than high molecular weight polymers [118]. The C-O/C-C coupling selectivity and the molecular weight of polymers in oxidative coupling are both strongly dependent on the chemical structure of the phenol monomer, i.e., the substituents and the position of substitution [118]. Other synthetic methods, such as aromatic nucleophilic substitution (S_NAr), electrophilic aromatic substitution using Friedel-Crafts catalysts, Ullman polycondensation, etc., have also been developed to synthesize high molecular weight PPOs [118]. Compared with those methods, catalytic oxidative polymerization is considered a much cleaner process because the reaction can be conducted at moderate temperatures, halogen-free monomers can be utilized, and the only by-product is water.

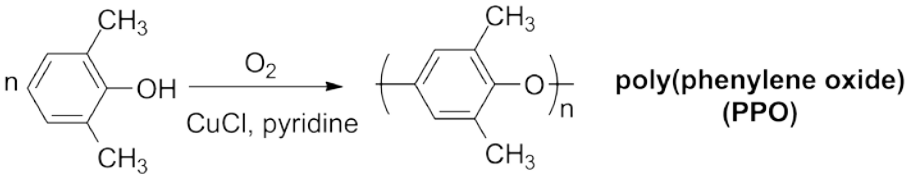

Figure 2.18 Synthesis of PPO via oxidative coupling polymerization.

PPO was the first commercialized aromatic polyether and is still being used in many industrial applications including gas separations [145]. As shown in previous upper bound plots, PPO displays relatively high permeabilities to light gases with moderate overall selectivities, which stems from its chemical and conformational structure of the aromatic ether bond. The kinked ether linkage and the absence of polar groups suppress efficient chain packing and densification, resulting in a relatively large fractional free volume in PPO, as seen in Table 2.3. The high free volume and the ease of rotation of the phenyl rings about the ether linkages contribute to high diffusivity and permeability, while the moderate gas selectivity comes in part from the absence of polar

moieties on the polymer backbone [146]. Therefore, most research on PPO has focused on their chemical modification with various functional groups to improve selectivity [125, 147-154]. For example, Monsanto developed a crosslinked PPO membrane which was first brominated PPO and then crosslinked [152]. This material was typically spun into hollow fibers which are coated with silicone rubber to repair defects [155]. The transport properties can be manipulated by altering the bromine content and degree of substitution [153, 154]. PPO has also been modified in various other ways to enhance gas transport properties, and it is often blended with impact polystyrene for commercial use [148-151]. In all cases, the membrane properties strongly depend on the extent of chemical modification and the location of substitution, *i.e.*, on the ring or on the methyl groups. Although the properties can be improved via chemical modification, there is still a need to develop an economic and efficient way to conduct such modifications in a controllable manner.

2.3.4 Aramids

Aromatic polyamides, or aramids, are generally produced from step polymerization or the polycondensation reaction of aromatic diamines with aromatic diacid chlorides. Examples of aramids include poly(*p*-phenylene terephthalamide) (*i.e.*, Kevlar®) and poly(*m*-phenylene isophthalamide) (*i.e.*, Nomex®) [156]. Figure 2.19 shows the chemical structures of isomeric phenylenediamines and aromatic diacid chlorides in commercial *meta*- and *para*-aramids.

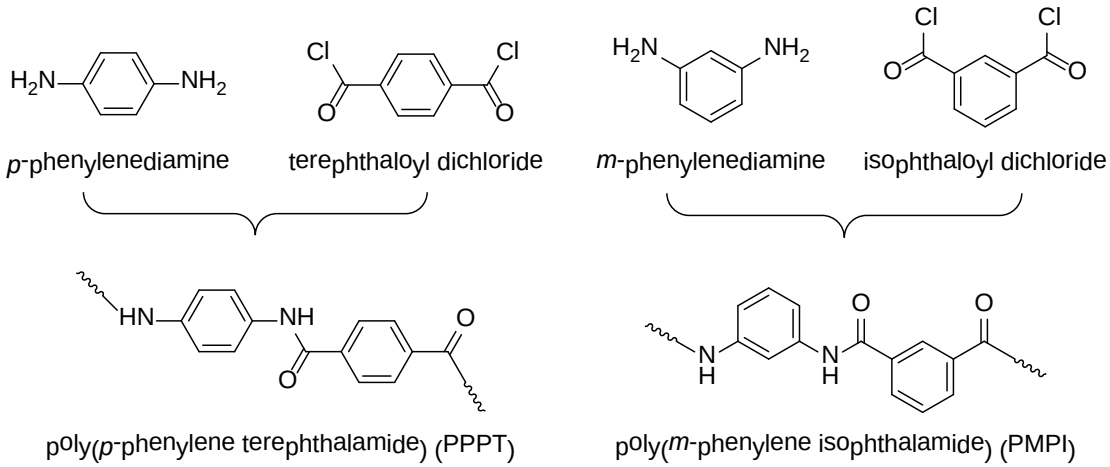

Figure 2.19 Chemical structures of phenylenediamines and aromatic diacid chlorides in commercial meta (PMPI) and para-aramids (PPPT).

These polymers are commercially synthesized via low-temperature polycondensation, typically in a solution of diacid dichloride and phenylenediamine with a tertiary base present to scavenge the liberated hydrogen chloride [157]. The resulting polymer solutions from these polymerizations are often used directly to spin fibers [158, 159]. The polycondensation reaction can also be conducted in a two-phase system, via so-called interfacial polymerization [160]. Interfacial polymerization usually produces polymers with a broad molecular weight distribution that are unsuitable for use as fibers [160]. However, crosslinked aramids synthesized via interfacial polymerization of trimesoyl chloride (TMC) with *m*-phenylene diamine (MPD) on a microporous polysulfone support have been commercially applied for many years as reverse osmosis (RO) membranes [161, 162].

The wholly aromatic structures of the aramid polymers give them excellent thermal and mechanical properties, which make them useful in technologies such as gas separations [159]. Aramids have been traditionally considered to be very efficient barrier materials; traditional aramids, such as PPPT and PMDI, have extremely low gas

permeabilities due to the high packing density (high cohesive energy) of the polymer chains [159]. Therefore, research efforts have been directed toward reducing the interchain hydrogen bonding, thus increasing the free volume via chemical modifications, to yield materials with better solubility (processibility) and improved gas permeability. Using this idea, aromatic polyamides with bulky substitutions on aromatic rings have been designed and synthesized to improve transport properties [163-167].

Publications from DuPont in 1990 and 2001 discuss fiber spinning and properties of high performance aramids. Theses aramids have the general structure shown in Figure 2.20 and, as of 1990, were used to purify a hydrogen feed stream at Conoco's Ponca City Refinery [116, 156, 168]. Such materials are now more widely used in a variety of hydrogen separation applications.

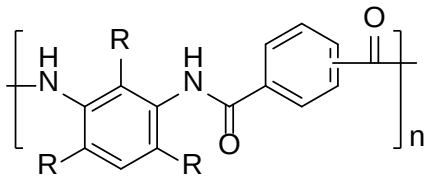

Figure 2.20 General structure of aramids reported by Eikner et al. [156].

These polymers have H_2 permeabilities ranging from 4 to 40 Barrer and selectivities ranging from 75 to 600 for H_2/CH_4 for a 50/50 mixture of H_2/CH_4 at 90ºC [116]. The transport properties are superior to those of the commercial polysulfone UDEL-3500, and aramids also had higher yield stress and modulus than those polysulfones [116]. Despite their limited number of solvents, aramids can be prepared into spin dopes using a combination of organic and inorganic additives such as polyvinylpyrrolidone, polyvinylpyridine, LiCl, $MgCl_2$ and others [116].

2.3.5 Polycarbonates

Polycarbonates are polyesters of carbonic acid (especially derived from phosgene or diphenyl carbonate) that are tough engineering thermoplastics. A commonly used commercial polycarbonate is based on bisphenol A (4,4'-isopropylidene diphenol). Conventionally, polycarbonate was produced via an interfacial phase-transfer catalyzed aqueous caustic process where alkali salts of bisphenol A (or its tetra-substituted variants) in aqueous solution are phosgenated in the presence of an inert solvent (cf., Figure 2.21) [169]. Phosgene-free solution or melt processes have been developed to produce polycarbonates via transesterification of diphenyl carbonate with bisphenol A. The melt transesterification process has found special commercial viability in recent years, largely due to its ability to eliminate the need for toxic phosgene [170].

A common modification to polycarbonates is the substitution of aromatic hydrogens with various functional groups as shown in Figure 2.21. One of the bisphenol A polycarbonates of interest for gas separation applications is tetrabromo bisphenol A polycarbonate (TB-BisA-PC), where the four hydrogen atoms are symmetrically replaced by Br atoms in the benzene ring (X = Br in Figure 2.21) [110]. This material is believed to be a key material in gas separation membranes marketed by Innovative Gas Systems, formerly Generon [171, 172]. At the time it was reported, the O_2/N_2 selectivity of 7.5 made TB-BisA-PC one of the most selective polymers available for air separations, and this high selectivity was coupled with a relatively good O_2 permeability of 1.83 Barrer [110]. Among the tetra-substituted polycarbonates reported in the literature, TB-BisA-PC has the highest T_g and density, and, as expected, the lowest free volume, diffusion coefficient, and gas permeability coefficients [110, 111]. These properties are a consequence of the introduction of stronger cohesive forces owing to polar halogens that may result in more dense packing and reduced rates local segmental motions believed to

be important in gas diffusion in polymers [110]. This enhanced chain packing contributes to increased O_2/N_2 selectivity in this polymer, making it more attractive for use as an air separation membrane.

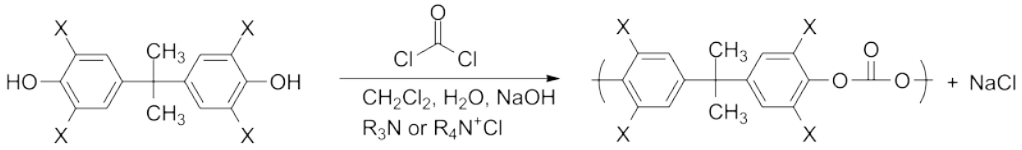

Figure 2.21 Interfacial polymerization of polycarbonates. Where X = CH_3 is tetramethylbisphenol A PC (TM-BisA-PC), X = Cl is tetrachlorobisphenol A PC (TC-BisA-PC), X = Br is tetrabromobisphenol A PC (TB-BisA-PC)

TB-BisA-PC is most likely a polyestercarbonate copolymer, which contains both ester linkages and carbonate linkages in the backbone of the polymer [173]. These polymers are generally prepared via a hybrid process of reacting the tetrabromo bisphenol A with a dicarboxylic acid or dicarboxylic acid halide and phosgene [173].

2.3.6 Polyimides

In general, aromatic polyimides have high gas permeability and high intrinsic selectivity combined with desirable physical properties, which make them attractive membrane materials. As of 2002, polyimides were reportedly used by Air Liquide, Praxair, Parker-Hannifin, and Ube for various gas separation applications [109]. Aromatic polyimides are typically the polycondensation products of aromatic dianhydride and aromatic diamine monomers. In a classic method of polyimide synthesis, a tetracarboxylic acid dianhydride is added to a solution of diamine in a polar aprotic solvent at relatively low temperatures (15-75 °C). The resulting poly(amic acid) is cyclodehydrated to the corresponding polyimide by extended heating at elevated

temperatures (*i.e.*, bulk solid-state thermal imidization or solution imidization), or by treatment with chemical dehydrating agents (*i.e.*, chemical imidization) [174].

Matrimid® is a commercial aromatic polyimide, consisting of 3,3'-4,4'-benzophenone tetracarboxylic dianhydride (BTDA) and diaminophenylindane (DAPI) [175-177]. DAPI (5(6)-amino-1-(4-aminophenyl)-1,3,3-trimethylindane) has an isomeric phenyl indane; therefore the polyimide formed is a mixture of 6-amino and 5-amino isomers, which are fully imidized during the manufacturing process [177]. The repeat unit structure of Matrimid® polyimide is shown in Figure 2.22. The DAPI monomer has a bent phenylindane ring structure, which is centered about the carbon bridging the indane structure and the phenyl ring. Four bulky groups (*i.e.*, three methyl groups and one phenyl group) stretch out of the plane, which stiffen the polymer backbone (its T_g is greater than 300 °C), and disrupt efficient chain packing. As a result of its isomeric composition and bulky nature, Matrimid® polyimide, along with 6F-containing polyimides, was one of the first aromatic polyimides truly soluble in common organic solvents [175, 178].

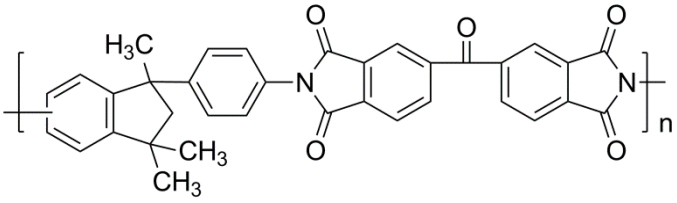

Figure 2.22 Chemical structure of Matrimid® polyimide.

Matrimid® was originally developed for use in the microelectronics industry [176], but it is also used in gas separation membranes [78, 90, 179, 180]. In addition, its mechanical strength and high T_g suit it better for more rigorous working environments, especially at high temperatures [181]. Furthermore, the good solubility of Matrimid® in

common organic solvents allows it to be solution processed, which is a requirement for fabrication into a gas separation membrane [181].

Matrimid® has the best combination of CO_2 permeability and CO_2/CH_4 selectivity among the commercially relevant polymers listed in Table 2.3, as judged by distance from the 1991 upper bound. With a pure gas CO_2 permeability of 10 Barrer and a CO_2/CH_4 selectivity of 36, Matrimid® has a higher pure gas permeability and selectivity than polysulfone, TB-BisA-polycarbonate or cellulose acetate [112]. However, like cellulose acetate, Matrimid® plasticizes exposed to gas streams with highly condensable components such as CO_2 [90, 91]. Plasticization results in increased CO_2 and CH_4 permeabilities and a significant loss in CO_2/CH_4 selectivities. Matrimid® CO_2/CH_4 selectivity decreases by approximately 45% in a 55/45 mol% CO_2/CH_4 mixture as the total feed pressure increases from 5 to 50 bar [90]. This decrease in separation efficiency highlights the importance of characterizing mixed gas separation performance (rather than relying solely on pure gas permeation properties to judge a material's performance) and the need for high performance polymers that maintain their separation characteristics in the presence of plasticizing components.

Research efforts have been directed to modify the morphology of Matrimid® membranes via either thermal treatment ("annealing") [90, 182, 183] or chemical crosslinking [89, 184, 185] to reduce or suppress plasticization, but these approaches often result in lower gas permeability. Although Matrimid® is significantly more expensive than many other commercial polymers, such as polysulfone, the economic production of membranes with Matrimid® separating layers is facilitated by advances in

composite spinning technology, where a thin Matrimid® separating layer can be applied to a support material prepared from a more economical materials [186].

Another polyimide relevant to gas separations is BPDA-ODA, or Upilex® (Type R), which was developed by UBE Industries by polymerizing biphenyl tetracarboxylic dianhydride (BPDA) and 4,4'-oxydianiline (ODA) (cf., Figure 2.23) [187]. The commercialization of Upilex® is largely due to the successful development of BPDA, which can be readily produced by oxidative coupling of inexpensive phthalic acid esters with a palladium catalyst [188, 189]. Instead of using the conventional two-step process of solid-state thermal imidization of poly(amic acid) intermediates, the industrial synthesis of BPDA-ODA is based on a one-step high temperature solution polymerization in a phenolic solvent [187]. Solution polymerization of diamine and dianhydride at high temperature is accompanied by imidization. High quality films and fibers can be produced from the polyimide-containing solution. However, it should be noted that the final treatment of solution-cast films at high temperature (300 °C) completes the closure of imide rings that are not fully imidized during solution polymerization, similar to the process of high temperature thermal imidization in solid-state. The polyimides produced by such a process have an almost completely imidized structure and provide superior properties than those prepared by solid-state imidization of poly(amic acid)s. For example, long term oxidative and hydrolytic stabilities and retention of electrical properties are substantially better [190].

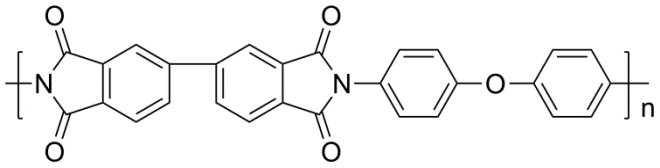

Figure 2.23 Chemical structure of BPDA-ODA polyimide.

UBE has supplied gas separation systems since 1985 using polyimides similar to the Upilex® polyimides. Due to their high thermal resistance (T_g of ~285 °C), BPDA-ODA membranes can be operated at temperatures up to 100 °C [191]. The transport properties, particularly the sorption and diffusion of CO_2 and water vapor, of BPDA-ODA membranes have been reported in the literature [192, 193]. BPDA-ODA shows a relatively low T_g and free volume, and it has relatively low water sorption compared to other common polyimides [193]. Because of this low water solubility, permeability, solubility and diffusivity are independent of water activity. Plasticization also does not occur in the presence of CO_2 up to approximately 30.4 bar [192].

In 2010, Honeywell UOP patented a blend of polyethersulfone and polyimides for natural gas and air separations [194]. This blend, which is roughly 90% by weight polyimide, based on 3,3'-4,4'-diphenylsulfone tetracarboxylic dianhydride (DSDA) and 3,3'-5,5'-tetramethyl-4,4'-methylene dianiline (TMMDA), and 10% polyethersulfone. This blend has a pure gas CO_2 permeability of 18.5 Barrer and a CO_2/CH_4 selectivity of 24.8. These transport properties place the blend well below the 2008 upper bound and show that there is commercial interest in a polymer with higher permeability and slightly lower selectivity than Matrimid® or cellulose acetate.

2.4 EMERGING MEMBRANE MATERIALS

In recent years, membrane science has developed new classes of materials and continued to improve existing families of gas separation membranes. The new classes of materials that will be highlighted in this review include thermally rearranged (TR) polymers, polymers of intrinsic microporosity (PIMs), polymerized room temperature ionic liquids (poly(RTIL)s), and perfluoropolymers. This section will also continue to discuss polyimides, as modification of polyimides continues to be an active area of study for producing high performance polymers. Mixed matrix membranes, which are often prepared by physically blending carbon or inorganics into a membrane matrix, are beyond the scope of this review, but additional information can be found elsewhere [195, 196].

2.4.1 Thermally Rearranged (TR) Polymers

Recently, Park *et al.* [28] reported a new family of polymeric membranes which were termed thermally rearranged (TR) polymers, for CO_2/CH_4 separations. These materials exhibit high CO_2 permeability, good CO_2/CH_4 permselectivity and excellent resistance to CO_2 induced plasticization. For example, the widely studied TR-1 polymer, based on a fluorinated diamine and dianhydride, exhibits a CO_2 permeability of roughly 2000 Barrer and a CO_2/CH_4 selectivity of roughly 40, with no evidence of plasticization up to 15.2 bar. These TR polymers, which have polybenzoxazole (PBO) structures, are believed to be formed via molecular thermal rearrangement of aromatic polyimides containing hydroxyl groups *ortho* to the imide ring. The general scheme of thermal rearrangement of an *ortho*-functional polyimide is shown in Figure 2.24. Upon heating at high temperatures (generally > 400°C) in an inert atmosphere (such as N_2 or Ar), aromatic poly(hydroxyimide)s thermally rearrange to PBOs with quantitative loss of carbon dioxide. In addition to the extraordinary membrane performance resulting from

TR process, a noticeable advantage of the TR approach is that it circumvents the typical insolubility of PBOs by starting from a soluble precursor, which makes industrial processing such as hollow fiber spinning possible [197].

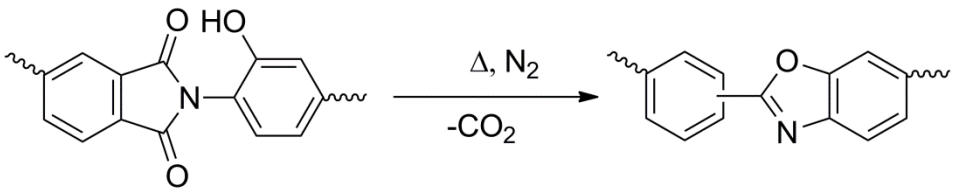

Figure 2.24 General scheme of thermal rearrangement (TR) of poly(hydroxyimide)s. End groups are not shown.

The exceptional combinations of permeability and selectivity in TR polymers have been attributed to an increase in fractional free volume and a narrowing of the free volume distribution [28]. Positron annihilation lifetime spectroscopy has been used to show that thermal rearrangement increases the average size of free volume elements and also makes the size distribution of these elements more uniform. The conversion of the initial polyimide to the PBO structure and the resulting increase in free volume leads to both an increase in solubility and diffusivity [198, 199]. However, diffusivity provides a much larger contribution than solubility to gas permeability increases. Thus, the rigid nature of the resulting PBO and large increase in fractional free volume after rearrangement are most likely critical to the large increases in permeability seen as a function of thermal rearrangement.

Following initial publications, additional studies have continued to explore the structure-property relationship of TR polymers [200-203]. However, most research efforts and some earlier fundamental studies on imide-to-benzoxazole conversion [204-206] require high temperature treatments (generally > 400 °C) to produce PBOs with

good separation properties, and thermal degradation may overlap with the TR process after long treatment times and result in poor mechanical properties of the TR membranes [198]. Therefore, high processing temperatures can reduce the mechanical properties of TR polymers. Reducing the TR temperature can be achieved by lowering the T_g of the precursors by using a flexible bisphenol A type dianhydride. Reductions in conversion temperature of up to 100 °C (from ~450 °C to ~350 °C) have been reported using this approach [207].

As next generation gas separation membranes, TR polymers have three major benefits: high combinations of permeability and selectivity, resistance to plasticization, and a high chemical resistance. As shown in Figure 2.25, TR polymers often show transport properties well above the 2008 CO_2/CH_4 upper bound, making these polymers among the best materials known for natural gas processing [32]. The permeability, selectivity, and position relative to the upper bound can vary significantly depending on the nature of the polymer backbone, allowing the transport properties of these polymers to be tuned for specific applications [28].

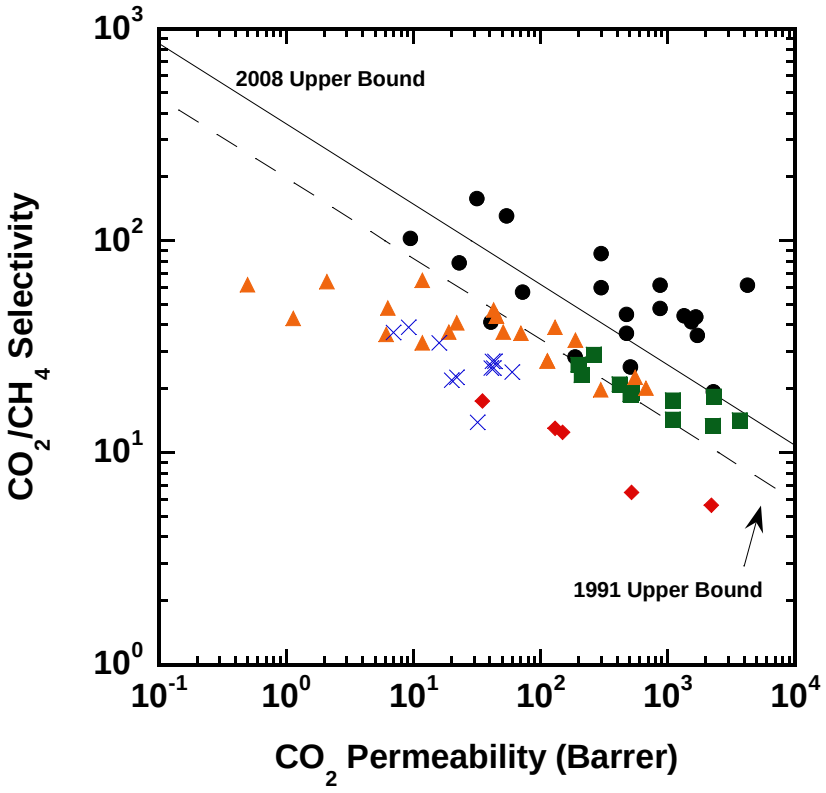

Figure 2.25 CO_2/CH_4 separation properties of various emerging polymer materials reported in the literature. TR polymers (●) from [28, 198]. PIMs (■) from [208-210]. Perfluoropolymers (♦) from [124, 211-213]. Polyimides (▲) from [64, 83, 214-217]. Poly(RTIL)s (X) from [218-220].

Polyimides with large *ortho*-functional groups other than hydroxyl groups (via either chemical imidization or chemical derivatization of poly(hydroxyimide)s) showed a much higher permeability after TR process than the TR polymers derived from its poly(hydroxyimide) analogs [198, 221-223]. An increase in gas permeability as the size of the *ortho*-functional group increased was obtained with some loss in selectivity [207]. This ortho-position group is lost during thermal rearrangement, resulting in a large increase in permeability as thermal rearrangement temperature increases. Thus, the

nature of the *ortho*-position group of the TR polymer precursor can be used to tailor permeability and selectivity in TR polymers.

TR polymers are promising candidates for high performance membrane materials for gas separations. Their practical applications can be significantly advanced if the conversion temperature can be reduced to a more energy-efficient level and commercially available monomers can be used. Additional studies are also necessary to continue examining effects of precursor structure and understand the effects of physical aging on TR polymer thin films.

2.4.2 Polymers of Intrinsic Microporosity (PIMs)

Among the many efforts to develop organic or organic–inorganic hybrid materials that mimic the structure of zeolites, one recent example is a family of non-network polymers featuring "intrinsic microporosity" (PIMs) introduced by Budd et al. [208, 224-227]. The microporous structure in PIMs is due to the highly rigid and contorted molecular structures, which prevent efficient packing of the macromolecules in the solid state. Two key features of PIMs are their kinked backbone (spiro-type structure) and highly restricted backbone rotational movements. The microporosity of PIMs is termed "intrinsic" as it arises solely from their molecular structures and does not derive from the thermal or processing history of the material. The synthesis of the most studied PIM-1 and PIM-7 materials and a molecular model of PIM-1 are shown in Figure 2.26 [226].

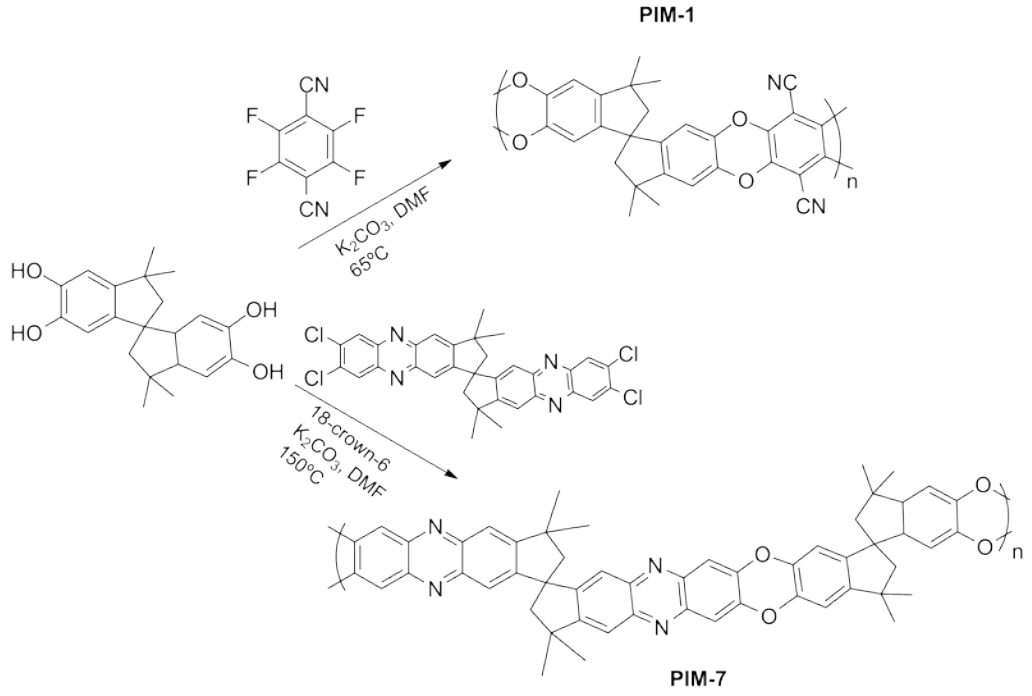

Figure 2.26 Synthesis and chemical structures of PIM-1 and PIM-7 [226].

The molecular scaffold used to synthesize PIMs is generally derived from an aromatic tetrol and an activated halogen-containing aromatic monomer, which are assembled via double nucleophilic aromatic substitution (S_NAr) reactions to form a dibenzodioxane. The efficiency of the double substitution reaction strongly depends on the reactivity of the aromatic halides. As shown, the spirocyclic feature of 5,5',6,6'-tetrahydroxy-3,3,3',3'-tetramethyl-1,1'-spirobisindane renders the kinked (contorted) conformation, and the formation of ladder-like dibenzodioxane structure results in rigid backbones, contributing to the intrinsic microporosity. Other PIMs (PIM-2 to PIM-6) were also prepared in a similar manner using different aromatic tetrols and polyfluorine-containing aromatic compounds. Although the aromatic tetrol in PIM-1 and PIM-7 is

commercially available, the activated aromatic halides, particularly the polyfluorine-containing aromatics, are limited in commercial availability and are relatively expensive. Despite the various chemical structures reported in the literature, PIM-1 and PIM-7 were the only two PIMs originally reported to form films sufficient for membrane tests. Moreover, low molecular weights (and low yields) have been issues in the synthesis of PIMs, which can make film formation difficult and contribute to poor mechanical properties. The first example of using PIMs as membrane materials was reported for PIM-1 in organo-selective pervaporation [225]. Membrane samples had a density in the range 1.06-1.09 g cm^{-3} and high specific surface areas (600-900 m^2 g^{-1}, by nitrogen BET). A promising combination of high flux and selectivity in pervaporative removal of phenols from aqueous solution was reported. Later, as shown in Figure 2.25 and Figure 2.27, gas separation properties were examined for PIM-1 and PIM-7; both of these materials showed transport properties above the 1991 Robeson upper bound and near the 2008 upper bound for both CO_2/CH_4 and O_2/N_2 separations [208]. More recently, some PIM-based systems, *i.e.*, PIM-polyimides, have been prepared via derivatizing the aromatic tetrol into bis(carboxylic anhydride) as the building monomer [209, 228, 229]. These new PIM-polyimides showed relatively similar properties to original PIMs, and they offered additional structures that could be cast into freestanding films. When compared with TR polymers for CO_2/CH_4 separations, PIMs, including PIM-polyimides, also exhibit high permeabilities but often lower selectivities. On average, the PIMs form a tighter cluster than the TR polymers, showing less variation in permeability and selectivity across the range of chemical structures examined than TR polymers. For

O_2/N_2 separations, as shown in Figure 2.27, PIMs also show generally lower selectivities at similar permeabilities when compared to TR polymers.

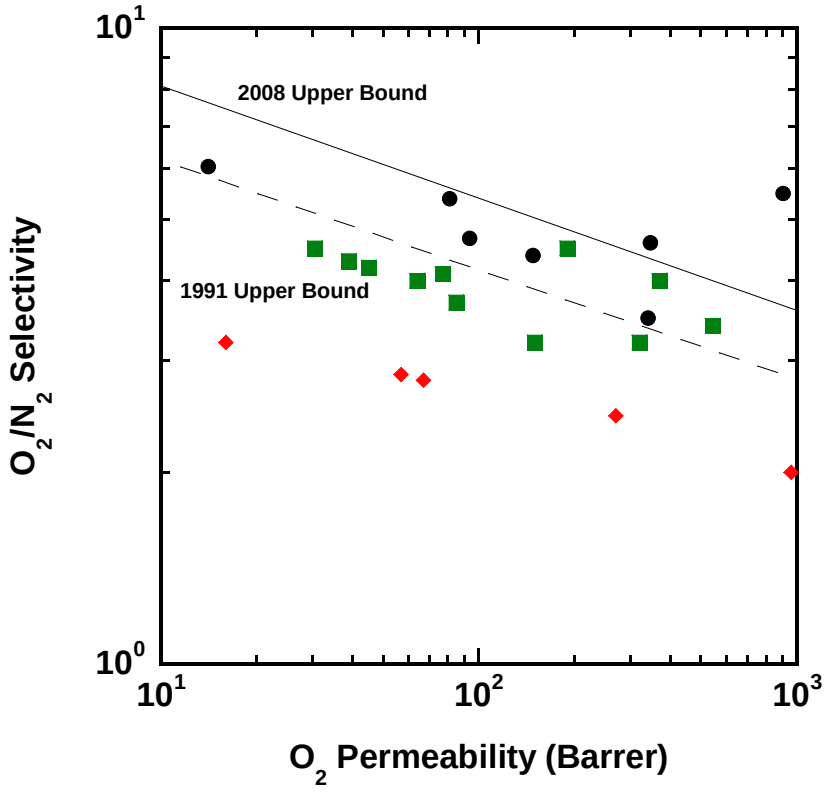

Figure 2.27 O_2/N_2 separation performance for emerging materials plotted on the 1991 and 2008 Robeson upper bound. TR polymers (●) from [198, 200]. PIMs (■) from [208-210]. Perfluoropolymers (♦)from [49, 159, 211, 212].

Despite the relatively low selectivities compared to TR polymers, PIMs show permeability/selectivity combinations that put them at the forefront of currently available membrane materials. In addition, these polymers do not need to be heat treated at the high temperatures necessary to form TR polymers. The removal of this heat treatment step means that PIMs can be solution cast directly into their final form. However, additional work is still necessary to further investigate mixed gas performance of PIMs,

assess the plasticization of these polymers at high CO_2 partial pressures, and study the effect of contaminants on gas permeation properties. Additionally, little information is currently available on physical aging at thicknesses of 1 micron or less, molecular weights, and mechanical behavior of PIMs.

2.4.3 Perfluoropolymers

Perfluoropolymers possess many unique properties that have made them suitable for numerous commercial applications, including automotive, aerospace, electronics, chemical, and medical industries [230]. The strong C–F bonds (485 kJ/mol) and the protective sheath of fluorine atoms around the carbon backbone result in the extremely high chemical resistance and thermo-oxidative stability for these polymers [231, 232]. Early generations of perfluoropolymers, such as polytetrafluoroethylene (PTFE), however, did not attract much interest for gas separation membranes, largely due to the low gas permeability and poor processability associated with the semicrystalline nature and lack of solubility in common solvents [230]. A major breakthrough in the use of perfluoropolymers for gas and vapor separation membranes was the development of a new family of amorphous glassy perfluoropolymers, *i.e.*, Teflon® AF, by DuPont in the late 1980s [233, 234]. Teflon® AF polymers are copolymers based on tetrafluoroethylene and 2,2-bis(trifluoromethyl)-4,5-difluoro-1,3-dioxole, and the chemical structure of these completely fluorinated (*i.e.*, perfluoro-) copolymers is shown in Figure 2.28. The bulky dioxole monomer disrupts chain packing in these materials so, unlike poly(tetrafluoroethylene), the commercial grades of Teflon® AF are wholly amorphous. Therefore, high gas permeability and much improved processability, related to their high solubility in perfluorinated solvents, are obtained for these polymers. Similarly, other amorphous perfluoropolymers were developed, such as Hyflon® AD (produced by

Solvay), and Cytop™ (by the Asahi Glass Company) [235-238]. The gas transport properties of these materials have been extensively studied [49, 231, 239-245].

As seen in Figure 2.25 and Figure 2.27, for gas separations such as CO_2/CH_4 and O_2/N_2, perfluoropolymers show gas separation properties well below the 2008 upper bound. However, one potential use for this class of polymers is the separation of nitrogen from natural gas. This separation, simplified to N_2 and CH_4, would be helpful to improve the heating quality of natural gas. Unfortunately, the physical properties, such as size and condensability, are similar for these two gases, making their separation difficult [11]. Figure 2.29 shows the N_2/CH_4 separation performance of perfluoropolymers and other modern membrane materials. Perfluoropolymers, along with TR polymers, exhibit performance near to the 2008 upper bound for this difficult separation [159, 211, 212]. This improved performance for N_2/CH_4 separations is attributed to fluorinated polymers having high light gas solubility relative to hydrocarbon solubility [49, 246]. The low solubility of hydrocarbons in perfluoropolymers has been implicated in improved plasticization resistance for hydrocarbon-based separation (*e.g.*, olefin/paraffin separations) [49]. The reason for the low solubilities of hydrocarbons in perfluoropolymers is not well-understood, and the details are discussed at length by Merkel et al. [49].

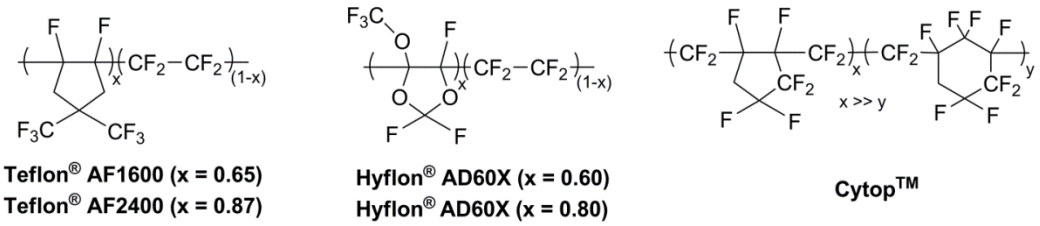

Figure 2.28 Chemical structure of commercial amorphous perfluoropolymers.

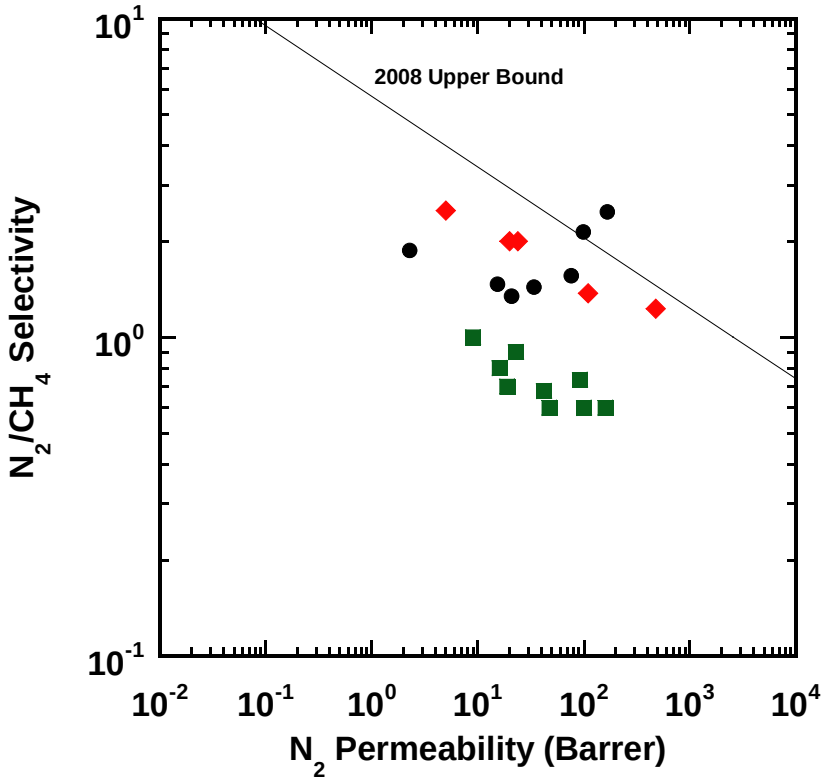

Figure 2.29 N_2/CH_4 upper bound performance for various emerging membrane materials. TR polymers (●) from [198, 200]. PIMs (■) from [208-210]. Perfluoropolymers (♦) from [49, 159, 211, 212].

2.4.4 Polyimides

Of the emerging polymers listed in this section, polyimides are among the most studied materials for gas separation polymers. Although aromatic polyimides are used as

gas separation membrane materials today, the polyimide family encompasses a large number of structural variants, and many studies on polyimide gas separation membranes indicate that the separation properties can be tailored by using different dianhydride and diamine monomers. Structure/property studies in the late 1980's showed that restricting both chain mobility and chain packing can simultaneously increase permeability and selectivity in polyimides [35, 36]. In particular, polyimides with a hexafluoro substituted carbon (*e.g.*, -$C(CF_3)_2$-) in the polyimide backbone have been the object of much research, as they tend to be considerably more gas-selective, particularly towards CO_2 relative to CH_4, than other glassy polymers with comparable permeabilities. The hexafluoro group in the dianhydride moieties (*e.g.*, hexafluoroisopropylidene diphthalic anhydride (6FDA)) increases the stiffness of the polymer chain, and it frustrates chain packing due to the steric hindrance from the CF_3 groups, which serve as molecular spacers and chain stiffeners in the polymer [247, 248]. The general structure of 6FDA-based polyimides is shown in Figure 2.30. These initial 6FDA-based polymers are labeled as "First Generation Polyimides" in Figure 2.31.

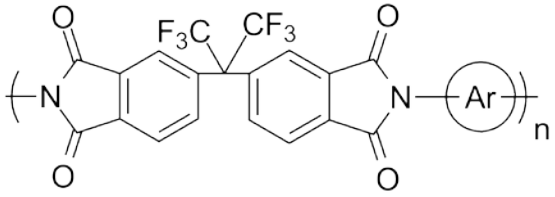

Figure 2.30 General structure of 6FDA-based aromatic polyimides (Ar represents the aromatic moieties in the diamine).

In addition to their relatively high cost, major drawbacks of 6FDA-based polyimides in gas separation are their tendency to plasticize and undergo physical aging [64, 83, 96]. There has been significant research to suppress plasticization and to retard the changes in the membrane performance caused by physical aging. In this regard,

crosslinking may be an effective method for improving membrane stability, specifically referring to these two properties [96, 249]. Various curing techniques have been reported to crosslink the polyimides, *i.e.*, thermal cure, UV irradiation, ion beam irradiation, or by reactions with added compounds [89, 95, 214, 250-254]. Examples of such cross-linked polymers are labeled as "Treated polyimides" in Figure 2.31, which highlights changes in polyimide transport properties as polyimide materials have advanced. In Figure 2.31, "First Generation Polyimides" are those studied in the 1980's, specifically high performance CF_3-containing materials, while the "Current Generation Polyimides" are modern polyimides. Both of these groups will be discussed more specifically in the following paragraphs.

Current generation polyimides populate much of the area near the 2008 Robeson CO_2/CH_4 upper bound. Of the 16 polymers highlighted as "close to the present upper bound" in Robeson's analysis, 7 are polyimides [32]. The majority of these polyimides contain 6FDA dianhydride and bulky diamines. For example, two of these polymers were made up of 6FDA and aromatic diamines containing three and four pendant methyl groups. These bulky diamines help disrupt chain packing and increase free volume. The 6FDA-durene polymer, with four methyl groups, has a CO_2 permeability of 678 Barrer and a CO_2/CH_4 selectivity of 20.2 [215]. The 6FDA-TMPD polymer, with three methyl groups, has a CO_2 permeability of 556 Barrer and a CO_2/CH_4 selectivity of 22.7 [217]. These polymers show relatively high selectivities at high CO_2 permeabilities, putting them near the upper bound for CO_2/CH_4 separations. Examples of these polymers are shown in Figure 2.31 as "Current Generation Polyimides."

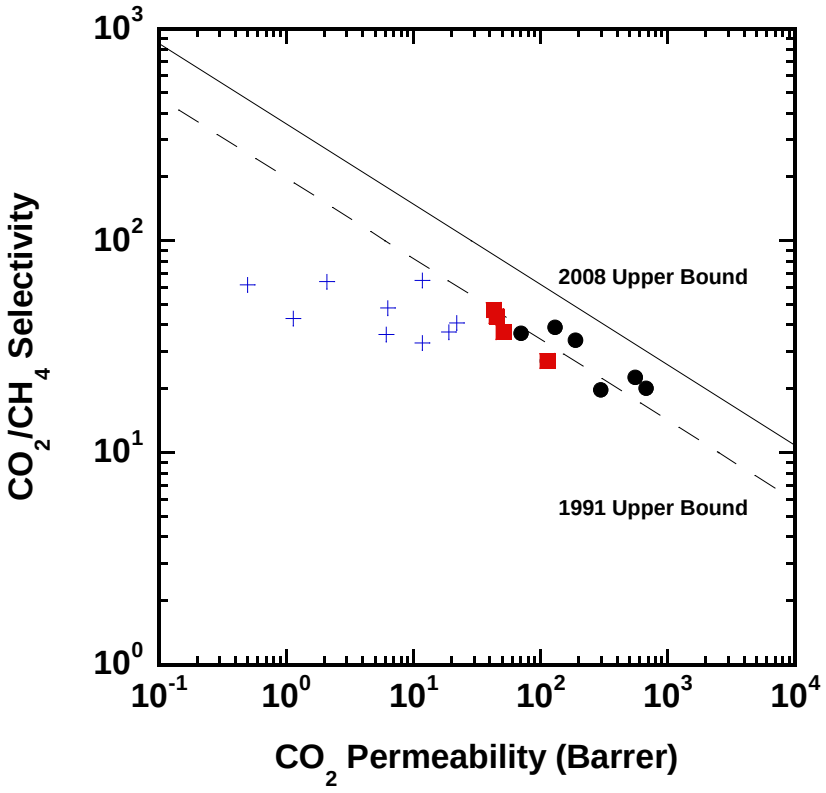

Figure 2.31 Robeson upper bound plot for CO_2/CH_4 separations. First generation polyimides (+) from [35]. Current generation polyimides (●) from [83, 215, 217]. Treated polyimides (■) from [64].

Recently, highly soluble polyimides with very high gas permeabilities have also been reported [83, 209, 215, 217, 228, 255-257]. These polyimides tend to have common characteristics in their backbone structure featuring bulky side groups and/or non-coplanar spatial configuration, which make them highly soluble and permeable due to lack of efficient chain packing (*i.e.*, high free volume). However, the synthesis of those polyimides is much more complicated than that of typical polyimides because it generally involves multiple steps of synthesis and purification to obtain monomers at high enough purity to produce high molecular weight polyimides. A recent review of the design of

polyimide-based membranes for CO_2 removal from natural gas can be found elsewhere [248].

2.4.5 Room Temperature Ionic Liquids

Room temperature ionic liquids (RTILs) are defined as organic/inorganic salts having a melting point lower than 100 °C and are typically non-volatile and inflammable liquids [258]. Because of their unique chemical and physical properties, RTILs have attracted attention for various applications [259]. The use of RTILs as solvents for CO_2 capture has been an active research area for these materials due to their low vapor pressure, which makes them environmentally friendly [260]. In addition to being used as absorbents in CO_2 capture, RTILs have been impregnated in porous materials to create supported ionic liquid membranes (SILMs). The ethylmethylimidazolium dicyanamide ([emim][dca]) polymer, shown in Figure 2.32, has a CO_2 permeability of roughly 600, a CO_2/N_2 selectivity of 20 and a CO_2/CH_4 selectivity of 11 [261]. The CO_2/N_2 permeabilities and selectivities were better than many common polymers as of 2004 [261-263]. The ionic liquids that have been examined most in SILMs have an organic cation and either an organic or an inorganic anion, in particular, the 1-*n*-alkyl-3-methylimidazolium cation with various anions [264]. The general structure of alkyl-imidazolium ionic liquids with some typical anions is presented in Figure 2.32. The CO_2 solubility of ionic liquids depends on the nature of their cations, anions, and substituents [261, 262, 265].

An upper bound has been created for these SILMs, and future improvements are primarily expected in selectivity rather than permeability [264]; however, significant increases in selectivity without losses in permeability would be necessary for these polymers to perform near the upper bound. For example, when compared to the most

recent 2008 upper bound, a polymer with a CO_2 permeability of 600 would need a CO_2/N_2 selectivity of roughly 43 to lie on the upper bound, meaning a SLIM with the CO_2 permeability of [emim][dca] would need double the selectivity to lie on the 2008 upper bound [32]. These materials are also often tested at low trans-membrane pressures, such as 0.2 bar, for [emim][dca] discussed earlier, due to the stability of the impregnated film at higher pressures, but it has been suggested that such films could pressure differences as high as 3 bar [261]. These stability concerns helped lead to the development of a polymerized form of these room temperature ionic liquids.

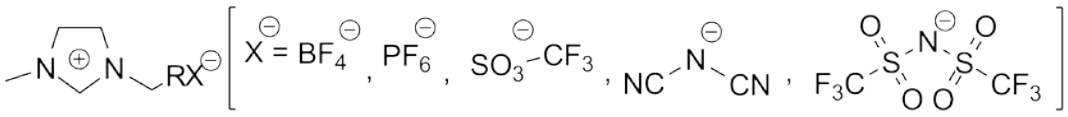

Figure 2.32 Chemical structures of alkyl-imidazolium type ionic liquids. The cation is ethylmethylimidazolium ([emim]) and the anions, from left to right, are tetrafluoroborate ([BF_4]), hexafluorophosphate ([PF_6]), dicyanamide [dca], and bis(trifluoromethanesulfonyl)amide [CF_3SO_3] [261, 262].

Polymeric ionic liquids, or poly(ionic liquid)s (poly(RTIL)s), exhibited higher CO_2 sorption capacity than the corresponding monomeric ionic liquids [220, 266-269]. The chemical structures of common types of poly(RTIL)s and their monomers are shown in Figure 2.33.

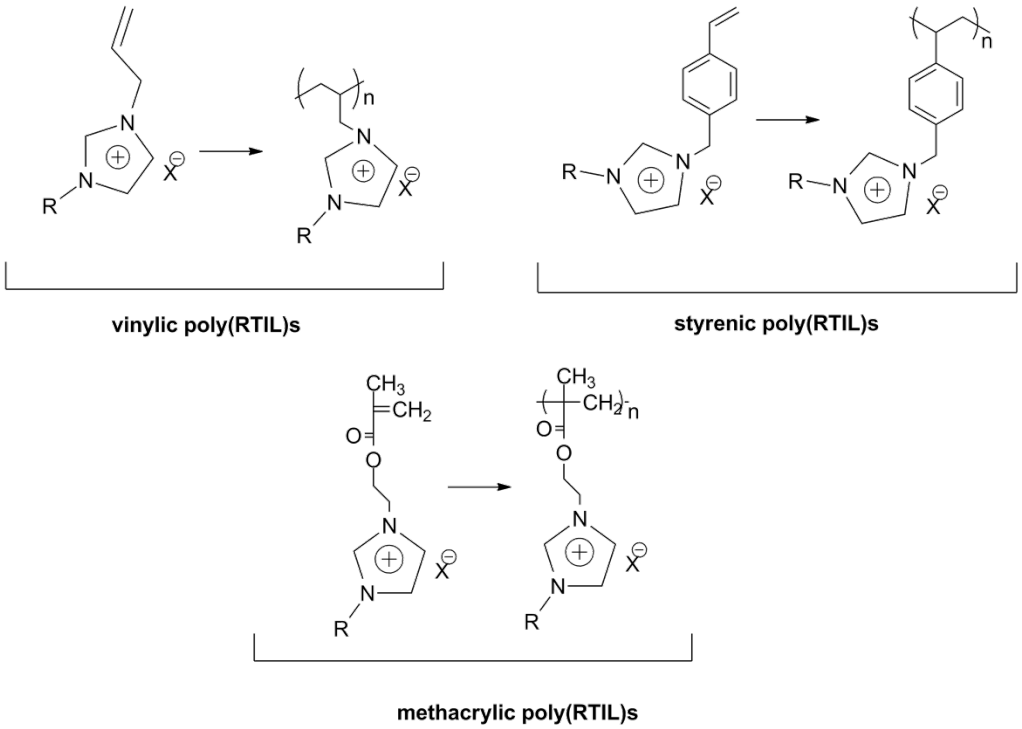

Figure 2.33 Chemical structure of poly(RTIL)s with polystyrene or polymethacrylate backbone. Where R = H or alkyl substitution, X = anion (BF_4^-, PF_6^-, $CF_3SO_3^-$, etc.)

These poly(RTIL)s are film forming, so they permit the preparation polymer films containing high concentrations of ionic liquid groups. The most studied poly(RTIL)s for CO_2 absorption/separation are alkyl-imidazolium type polymers featuring alkyl-imidazolium salts tethered to a polystyrene or polyacrylate backbone. Poly(RTIL)s with a poly(ethylene oxide) backbone have also been synthesized via post-modification of a PEO-like polymer with small molecule RTILs [269]. Poly(RTIL)s with short side chains of EO units were produced via direct reaction of ethylene oxide and RTILs followed by tethering to a polystyrene backbone [270, 271]. Generally, most of the imidazolium-type poly(RTIL)s with polystyrene or polyacrylate backbones have been synthesized from their corresponding vinyl RTIL monomers by conventional free radical

polymerization in bulk or in solution. Such cationic poly(RTIL)s bearing a large variety of counter anions (X−), such as tetrafluoroborate (BF4−) and hexafluorophosphate (PF6−), have been reported. In addition to linear poly(RTIL)s, crosslinked poly(RTIL)s were also synthesized via free radical polymerization of multi-functional acrylic or styrenic RTIL monomers. A comprehensive review of the synthesis of various polymeric ionic liquids can be found elsewhere [259].

Additional formulations of poly(RTIL)s have been made by combining poly(RTIL)s and RTILs. These composites are formed by polymerizing RTILs in the presence of non-polymerizable RTILs [218, 219, 272]. These materials show no phase separation after permeation experiments performed at 2 bar, and the strong interaction between polymerized and "free" RTILs is anticipated to hold the "free" RTILs in place better than the typical capillary forces in SILMs [218]. Including these "free" RTILs into the polymer matrix increases the gas permeability due to increased diffusion through the unbound RTILs [218, 219]. For example, one poly(RTIL) showed a factor of 4 increase in permeability and a 20% increase in CO_2/N_2 selectivity with the incorporation of 20% "free" RTIL [219]. However, Figure 2.34 shows various poly(RTIL) and composites on the 2008 Robeson upper bound for CO_2/N_2, a separation widely studied using these materials [219], and many of these RTIL-based polymers show permeabilities much lower than TR polymers or PIMs with similar selectivities. These poly(RTIL)s and composites currently in the literature seem to fall behind the state of the art for CO_2/N_2 separations including TR polymers and PIMs; however their performance still makes them competitive relative to many families of polymers.

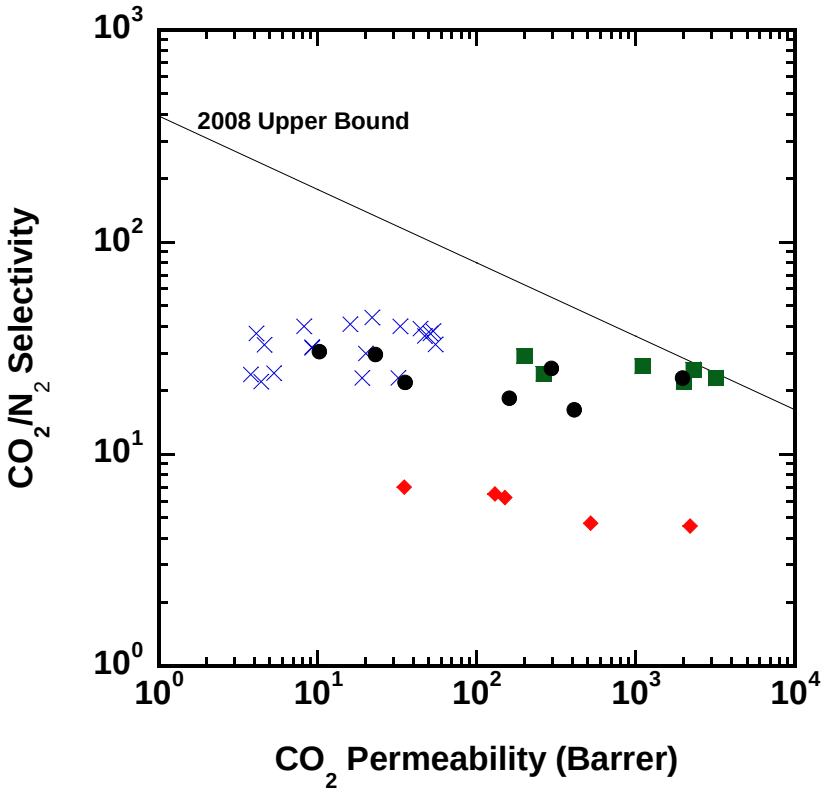

Figure 2.34 CO_2/N_2 separation properties of various emerging polymer materials. TR polymers (●) from[198, 200]. PIMs (■) from [208-210]. Perfluoropolymers (♦) from [49, 159, 211, 212]. Poly(RTIL)s (X) from [32, 219, 220, 270, 272-274].

2.5 Synthesis of Aromatic Polyimides – Precursors to TR Polymers

As mentioned previously, polybenzoxazoles can be formed by thermal rearrangement of ortho-functional polyimides. Polyimides for this purpose can be synthesized by reacting bis(aminophenol) compounds with an aromatic dianhydride through various synthesis routes. However, Park et al. investigated gas separation performance of only the solid state thermal imidization route [28].

Imidization is most commonly performed by thermal imidization of a poly(amic acid) intermediate, but this intermediate can also be chemically imidized to obtain the

desired polyimide [275, 276]. In addition to these routes, an ester-acid intermediate can also be prepared. This ester-acid is more hydrolytically stable than the poly(amic acid) intermediate and can be thermally imidized after reaction with a diamine. Polyimide synthesis routes have been shown to affect physical properties, as discussed in the next section, and it is possible that these synthesis routes will also affect TR transport properties due to their highly glassy, non-equilibrium nature.

As seen in Figure 2.24, these aromatic polyimides also contain functional groups *ortho* to the imide ring. In previous studies in the literature, this ortho-position group has largely been a hydroxyl group, except in the case of chemical imidization. The presence of acetic acid during chemical imidization causes the conversion of the *ortho*-position hydroxyl group into an acetate group [198]. This ortho-position group is lost during thermal rearrangement, and it is also possible that this ortho-position group loss influences the transport properties of the resulting TR polymer. This thesis explores the influence of synthesis route and *ortho*-position group on gas transport properties. Based on these studies, the *ortho*-position group has the largest influence on differences in transport properties of thermally and chemically imidized TR polymers.

2.6 Effect of Synthesis Route on Polyimide Properties

The effect of the polyimide synthesis route on the transport and physical properties of polymers has been studied in various ways in the literature [277, 278]. Xu and Matsumoto studied the pure gas permeability of CO_2 and CH_4 in the 6FDA-4,4'-ODA polyimide synthesized via chemical and thermal imidization [277]. The authors found that the chemically imidized sample had higher permeability and selectivity than the thermally imidized sample. However, the chemically imidized sample had an inherent viscosity of 2.37 dL/g compared to 0.442 dL/g for the thermally imidized sample,

proving that the two polymers had drastically different molecular weights, which may account for some of these differences.

Xu, Koros, and Paul also studied the effect of synthesis routes on polyimides. This study focused on the 6FDA-DAM-DABA polyimide synthesized through chemical and thermal imidization for pervaporation [278]. In this case, the samples had very similar molecular weights. Flux and selectivity were very similar for the 6FDA-DAM polyimides synthesized via each route, but differences based on the synthesis route appeared in copolymers. In this case, the thermally imidized copolymer showed higher flux but lower selectivity. This result was attributed to the formation of some isoimide and to the presence of residual poly(amic acid) in the chemically imidized copolymers.

These different synthesis routes have also resulted in physical property differences that have been investigated. Martinez-Richa et al. found that chemically imidized polymers exhibited a less ordered structure and, in this case, showed up to 15% isoimide [279]. Xie et al. showed that chemically imidized samples were generally more soluble and less thermally stable than thermally imidized samples [280]. This result was attributed to incomplete imidization.

The work of Xu and Matsumoto and Martinez-Richa et al. suggest that the synthesis route affects the transport and physical properties of polyimides. However, the work by Xu, Koros, and Paul suggest that there is no difference in pure polyimides synthesized using various routes. Thus, the behavior may vary from polymer to polymer.

Work published in 2010 by Han et al., done independently and concurrently with the work discussed in this dissertation, showed that different synthesis routes strongly influenced gas permeability in TR polymers [203]. The study was performed on a different polyimide than that used here, and it also showed that chemically imidized polymers had much higher permeabilities than polymers thermally imidized in solution.

The work of Han et al. also compared samples thermally imidized in the solid state from Park's work with chemically and thermally imidized polyimides [28]. Interestingly, the solid state thermal imidization showed similar properties to the chemically imidized sample, and both had much higher permeabilities than the samples thermally imidized in solution. However, the work of Han et al. did not decouple the effect of synthesis route from the chemical *ortho*-position change in these polymers.

2.7 REFERENCES

1. Ghosal, K. and Freeman, B.D., *Gas separation using polymer membranes: An overview.* Polymers for Advanced Technologies, 1994. **5**: p. 673-697.

2. Koros, W.J. and Fleming, G.K., *Membrane-based gas separation.* Journal of Membrane Science, 1993. **83**(1): p. 1-80.

3. Lonsdale, H.K., *The growth of membrane technology.* Journal of Membrane Science, 1982. **10**(2-3): p. 81-181.

4. Stern, S.A., *Polymers for gas separations: the next decade.* Journal of Membrane Science, 1994. **94**: p. 1-65.

5. Wijmans, J.G. and Baker, R.W., *The solution-diffusion model - a review.* Journal of Membrane Science, 1995. **107**(1-2): p. 1-21.

6. Matteucci, S.T., Yampolskii, Y.P., Freeman, B.D., and Pinnau, I., *Transport of gases and vapors in glassy and rubbery polymers,* in *Materials science of membranes for gas and vapor separation,* Y. Yampolskii, I. Pinnau, and B.D. Freeman, Editors. 2006, John Wiley & Sons: Chichester. p. 1-47.

7. Ribeiro, C.P., Freeman, B.D., and Paul, D.R., *Modeling of multicomponent mass transfer across polymer films using a thermodynamically consistent formulation of the Maxwell-Stefan equations in terms of volume fractions.* Polymer, 2011. **52**: p. 3970-3983.

8. Allen, S.M., Fujii, M., Stannett, V., Hopfenberg, H.B., and Williams, J.L., *The barrier properties of polyacrolonitrile.* Journal of Membrane Science, 1977. **2**(2): p. 153-163.

9. Hu, Y., Shiotsuki, M., Sanda, F., Freeman, B.D., and Masuda, T., *Synthesis and properties of indan-based polyacetylenes that feature the highest gas permeability among all the existing polymers.* Macromolecules, 2007. **41**: p. 8525-8532.

10. Dhoot, S.N., Freeman, B.D., and Stewart, M.E., *Barrier polymers,* in *Encyclopedia of polymer science and technology,* J. Kroschweitz, Editor 2003, John Wiley & Sons: New York. p. 198-263.

11. Matteucci, S., Yampolskii, Y., Pinnau, I., and Freeman, B.D., *Transport of gases and vapors in glassy and rubbery polymers,* in *Materials science of membranes*

for gas and vapor separation, Y. Yampolskii, I. Pinnau, and B.D. Freeman, Editors. 2006, John Wiley & Sons: Chichester. p. 2-46.

12. Srinivasan, R., Auvil, S.R., and Burban, P.M., *Elucidating the mechanism(s) of gas transport in poly[1-(trimethylsilyl)-1-propyne] (PTMSP) membranes.* Journal of Membrane Science, 1994. **86**: p. 67-86.

13. Weinkauf, D.H. and Paul, D.R., *Effects of structural order on barrier properties.* ACS Symposium Series. Barrier Polymers and Structures, 1990: p. 60-91.

14. Michaels, A.S. and Parker Jr., R.B., *Sorption and flow of gases in polyethylene.* Journal of Polymer Science, 1959. **41**: p. 53-71.

15. Michaels, A.S. and Bixler, H.J., *Solubility of gases in polyethylene [and rubbery polymers]*. Journal of Polymer Science, 1961. **50**: p. 393-412.

16. Michaels, A.S., Vieth, W.R., and Barrie, J.A., *Solution of gases in poly(ethylene terephthalate).* Journal of Applied Physics, 1963. **34**: p. 1-13.

17. Lin, H.Q. and Freeman, B.D., *Permeation and diffusion* in *Springer handbook for materials measurement methods*, H. Czichos, T. Saito, and L. Smith, Editors. 2011, Springer: Berlin. p. 426-444.

18. Cohen, M.H. and Turnbull, D., *Molecular transport in liquids and glasses.* The Journal of Physical Chemistry, 1959. **31**(5): p. 1164-1169.

19. Pixton, M.R. and Paul, D.R., *Relationships between structure and transport properties for polymers with aromatic backbones*, in *Polymeric gas separation membranes*, D.R. Paul and Y. Yampolskii, Editors. 1994, CRC Press: Boca Raton. p. 83-154.

20. Turnbull, D. and Cohen, M.H., *Free volume model of the amorphous phase: glass transition.* The Journal of Chemical Physics, 1961. **34**(1): p. 120-125.

21. Baker, R.W., *Membrane technology and applications*. 2nd ed. 2004, Chichester: John Wiley & Sons.

22. Fleming, G.K. and Koros, W.J., *Dilation of polymers by sorption of carbon dioxide at elevated pressures. 1. Silicone rubber and unoconditioned polycarbonate.* Macromolecules, 1986. **19**: p. 2285-2291.

23. Bondi, A., *van der Waals volumes and radii.* The Journal of Physical Chemistry, 1964. **68**(3): p. 441-451.

24. Bondi, A., *Physical properties of molecular crystals, liquids, and glasses*. 1968: Wiley.

25. van Krevelen, D.W., *Properties of polymers*. 1972, Amsterdam: Elsevier.

26. Weinkauf, D.H. and Paul, D.R., *Gas transport properties of thermotropic liquid-crystalline copolyesters. II. The effects of copolymer composition.* Journal of Polymer Science Part B-Polymer Physics, 1992. **30**: p. 837-849.

27. Lee, W.M., *Selection of barrier materials from molecular structure.* Polymer Engineering and Science, 1980. **20**(1): p. 65-69.

28. Park, H.B., Jung, C.H., Lee, Y.M., Hill, A.J., Pas, S.J., Mudie, S.T., Van Wagner, E., Freeman, B.D., and Cookson, D.J., *Polymers with cavities tuned for fast selective transport of small molecules and ions.* Science, 2007. **318**(5848): p. 254-258.

29. Hill, A.J., Tant, M.R., McGill, R.L., Shang, R.R., Stockl, D.L., Murray, D.L., and Cloyd, J.D., *Free volume distribution during consolidation and coalescence of latex films.* Journal of Coatings Technology, 2001. **73**(913): p. 115-124.

30. Thornton, A.W., Nairn, K.M., and Hill, A.J., *New relation between diffusion and free volume: 1. Predicting gas diffusion.* Journal of Membrane Science, 2009. **338**(1-2): p. 29-37.

31. Robeson, L.M., *Correlation of separation factor versus permeability for polymeric membranes.* Journal of Membrane Science, 1991. **62**(2): p. 165-185.

32. Robeson, L.M., *The upper bound revisited.* Journal of Membrane Science, 2008. **320**(1-2): p. 390-400.

33. Maeda, Y. and Paul, D.R., *Effect of antiplasticization on selectivity and productivity of gas separation membranes.* Journal of Membrane Science, 1987. **30**(1): p. 1-9.

34. Barbari, T.A., Koros, W.J., and Paul, D.R., *Polymeric membranes based on bisphenol A for gas separations.* Journal of Membrane Science, 1989. **42**(1-2): p. 69-86.

35. Stern, S.A., Mi, Y., and Yamamoto, H., *Structure/permeability relationships of polyimide membranes. Applications to the separation of gas mixtures.* Journal of Polymer Science: Part B: Polymer Physics, 1989. **27**: p. 1887-1909.

36. Kim, T.H., Koros, W.J., Husk, G.R., and O'Brien, K.C., *Relationship between gas separation properties and chemical structure in a series of aromatic polyimides.* Journal of Membrane Science, 1988. **37**(1): p. 45-62.

37. Robeson, L.M., Burgoyne, W.F., Langsam, M., Savoca, A.C., and Tien, C.F., *High performance polymers for membrane separation.* Polymer, 1994. **35**(23): p. 4970-4978.

38. Breck, D.W., *Zeolite molecular sieves*. 1974, New York, NY.

39. Robeson, L.M., *Polymer blends in membrane transport processes.* Industrial & Engineering Chemistry Research, 2010. **49**(23): p. 11859-11865.

40. Freeman, B.D., *Basis of permeability/selectivity tradeoff relations in polymeric gas separation membranes.* Macromolecules, 1999. **32**(2): p. 375-380.

41. Barrer, R.M., *Permeability in relation to viscosity and structure of rubber.* Transactions of the Faraday Society, 1942. **38**: p. 322-330.

42. Zheng, J., Qiu, J., Madeira, L.M., and Mendes, A., *Polymer structure and the compensation effect of the diffusion pre-exponential factor and activation energy of a permeating solute.* Journal of Physical Chemistry B, 2007. **111**: p. 2828-2835.

43. Meares, P., *The diffusion of gases through polyvinyl acetate.* Journal of the American Chemical Society, 1954. **76**: p. 3415-3422.

44. Robeson, L.M., Freeman, B.D., Paul, D.R., and Rowe, B.W., *An empirical correlation of gas permeability and permselectivity in polymers and its theoretical basis.* Journal of Membrane Science, 2009. **341**(1-2): p. 178-185.

45. Robeson, L.M., Hwu, H.H., and McGrath, J.E., *Upper bound relationship for proton exchange membranes: Empirical relationship and relevance of phase separated blends.* Journal of Membrane Science, 2007. **302**(1-2): p. 70-77.

46. Geise, G.M., Park, H.B., Sagle, A.C., Freeman, B.D., and McGrath, J.E., *Water permeability and water/salt selectivity tradeoff in polymers for desalination.* Journal of Membrane Science, 2011. **369**(1-2): p. 130-138.

47. Mehta, A. and Zydney, A.L., *Permeability and selectivity analysis for ultrafiltration membranes.* Journal of Membrane Science, 2005. **249**: p. 245-249.

48. Ribeiro, C.P., Freeman, B.D., Kalika, D.S., and Kalakkunnath, S., *Aromatic polyimide and polybenzoxazole membranes for the fractionation of aromatic/aliphatic hydrocarbons by pervaporation.* Journal of Membrane Science, 2012. **390-391**: p. 182-193.

49. Merkel, T.C., Pinnau, I., Prabhakar, R., and Freeman, B.D., *Gas and vapor transport properties of perfluoropolymers*, in *Materials science of membranes for gas and vapor separations*, Y. Yampolskii, I. Pinnau, and B.D. Freeman, Editors. 2006, John Wiley & Sons Ltd. p. 251-267.

50. Alentiev, A.Y. and Yampolskii, Y.P., *Free volume model and tradeoff relations of gas permeability and selectivity in glassy polymers.* Journal of Membrane Science, 2000. **165**(2): p. 201-216.

51. Rowe, B.W., Robeson, L.M., Freeman, B.D., and Paul, D.R., *Influence of temperature on the upper bound: Theoretical considerations and comparison with experimental results.* Journal of Membrane Science, 2010. **360**(1-2): p. 58-69.

52. Park, J.Y. and Paul, D.R., *Correlation and prediction of gas permeability in glassy polymer membrane materials via modified free volume based group contribution method.* Journal of Membrane Science, 1997. **125**(1): p. 23-39.

53. Laciak, D.V., Robeson, L.M., and Smith, C.D., *Group contribution modeling of gas transport inpolymeric membranes*, in *Polymer membranes for gas and vapor separation, ACS symposium series 733*, B.D. Freeman and I. Pinnau, Editors. 1999, American Chemical Society: Washington D.C.

54. Robeson, L.M., Smith, C.D., and Langsam, M., *A group contribution approach to predict permeability and permselectivity of aromatic polymers.* Journal of Membrane Science, 1997. **132**(1): p. 33-54.

55. Kesting, R.E. and Fritzsche, A.K., *Polymeric gas separation membranes*. 1993, New York, NY, USA: John Wiley & Sons.

56. Rowe, B.W., Freeman, B.D., and Paul, D.R., *Physical aging of membranes for gas separations*, in *Membrane engineering for the treatment of gases, volume 1: Gas-separation problems with membranes*, E. Drioli and G. Barbieri, Editors. 2011, Royal Society of Chemistry.

57. Struik, L.C.E., *Physical aging in amorphous polymers and other materials*. 1978, Amsterdam, The Netherlands: Elsevier.

58. Murphy, T.M., Offord, G.T., and Paul, D.R., *Fundamentals of membrane gas separation*, in *Membrane opperations. Innovative separations and transformations.*, E. Drioli and L. Giorno, Editors. 2009, Wiley-VCH: Weinheim, Germany. p. 63-82.

59. Rowe, B.W., Freeman, B.D., and Paul, D.R., *Physical aging of ultrathin glassy polymer films tracked by gas permeability.* Polymer, 2009. **50**: p. 5565-5575.

60. Rowe, B.W., Freeman, B.D., and Paul, D.R., *Influence of previous history on physical aging in thin glassy polymer films as gas separation membranes.* Polymer, 2010. **51**: p. 3784-3792.

61. Murphy, T.M., Langhe, D.S., Ponting, M., Baer, E., Freeman, B.D., and Paul, D.R., *Physical aging of layered glassy polymer films via gas permeability tracking.* Polymer, 2011. **52**: p. 6117-6125.

62. Rowe, B.W., Pas, S.J., Hill, A.J., Suzuki, R., Freeman, B.D., and Paul, D.R., *A variable energy positron annihilation life spectroscopy study of physical aging in thin glassy polymer films.* Polymer, 2009. **50**: p. 6149-6156.

63. Cui, L., Qiu, W., Paul, D.R., and Koros, W.J., *Physical aging of 6FDA-based polyimide membranes monitored by gas permeability.* Polymer, 2011. **52**: p. 3374-3380.

64. Kim, J.H., Koros, W.J., and Paul, D.R., *Physical aging of thin 6FDA-based polyimide membranes containing carboxyl acid groups. Part I. Transport properties.* Polymer, 2006. **47**: p. 3094-3103.

65. Hutchinson, J.M., *Physical aging of polymers.* Progress in Polymer Science, 1995. **20**(4): p. 703-760.

66. McCaig, M.S. and Paul, D.R., *Effect of film thickness on the changes in gas permeability of a glassy polyarylate due to physical aging. Part I. Experimental Observations.* Polymer, 2000. **41**: p. 629-637.

67. Nagai, K., Higuchi, A., and Nakagawa, T., *Gas permeability and stability of poly(1-trimethylsilyl-1-propyne-co-1-phenyl-1-propyne).* Journal of Polymer Science, Part B: Polymer Physics, 1995. **33**(2): p. 289-298.

68. Langsam, M. and Robeson, L.M., *Substituted propyne polymers - Part II. Effects of agining on the gas permeability properties of poly[1-(trimethylsilyl)propyne] for gas separation membranes.* Polymer Engineering and Science, 1989. **29**(1): p. 44-54.

69. Kelman, S.D., Rowe, B.W., Bielawski, C.W., Pas, S.J., Hill, A.J., Paul, D.R., and Freeman, B.D., *Crosslinking of poly[1-(trimethylsilyl)-1-propyne] and its effect on physical stability.* Journal of Membrane Science, 2008. **320**: p. 123-134.

70. Nagai, K. and Nakagawa, T., *Effects of aging on the gas permeability and solubility in poly(1-trimethylsilyl-1-propyne) membranes synthesized with various catalysts.* Journal of Membrane Science, 1995. **105**: p. 261-272.

71. Nagai, K., Freeman, B.D., and Hill, A.J., *Effect of pysical aging of poly(1-trimethylsilyl-1-propyne) films synthesized with $TaCl_5$ and $NbCl_5$ on gas permeability, fractional free volume, and positron annihilation lifetime spectroscopy parameters.* Journal of Polymer Science, Part B: Polymer Physics, 2000. **38**: p. 1222-1239.

72. Dorkenoo, K.D. and Pfromm, P.H., *Accelerated physical aging of thin poly[1-(trimethylsilyl)-1-propyne] films.* Macromolecules, 2000. **33**: p. 3747-3751.

73. Horn, N.R. and Paul, D.R., *Carbon dioxide plasticization and conditioning effects in thick vs. thin glassy polymer films.* Polymer, 2011. **52**: p. 1619-1627.

74. Horn, N.R. and Paul, D.R., *Carbon dioxide plasticization of thin glassy polymer films.* Polymer, 2011. **52**: p. 5587-5594.

75. Huang, Y. and Paul, D.R., *Experimental methods for tracking physical aging of thin glassy polymer films by gas permeation.* Journal of Membrane Science, 2004. **244**: p. 167-178.

76. Huang, Y. and Paul, D.R., *Physical aging of thin glassy polymer films monitored by gas permeability.* Polymer, 2004. **45**: p. 8377-8393.

77. Huang, Y. and Paul, D.R., *Physical aging of thin glassy polymer films monitored by optical properties.* Macromolecules, 2006. **39**(1554-1559).

78. Huang, Y. and Paul, D.R., *Effect of film thickness on the gas-permeation characteristics of glassy polymer membranes.* Industrial & Engineering Chemistry Research, 2007. **46**: p. 2343-2347.

79. Huang, Y. and Paul, D.R., *Effect of molecular weight and temperature on physical aging of thin glassy poly(2,6-dimethyl-1,4-phenylene oxide) films.* Journal of Polymer Science, Part B: Polymer Physics, 2007. **45**: p. 1390-1398.

80. Rowe, B.W., Freeman, B.D., and Paul, D.R., *Effect of sorbed water and temperature on the optical properties and density of thin glassy polymer films on a silicon substrate.* Macromolecules, 2007. **40**(8): p. 2806-2813.

81. McCaig, M.S. and Paul, D.R., *Effect of UV crosslinking and physical aging on the gas permeability of thin glassy polyarylate films.* Polymer, 1999. **40**: p. 7209-7225.

82. McCaig, M.S., Paul, D.R., and Barlow, J.W., *Effect of film thickness on the changes in gas permeability of a glassy polyarylate due to physical aging. Part II. Mathematical Model.* Polymer, 2000. **41**: p. 639-648.

83. Kim, J.H., Koros, W.J., and Paul, D.R., *Effects of CO_2 exposure and physical aging on the gas permeability of thin 6FDA-based polyimide membranes - Part 1. without crosslinking.* Journal of Membrane Science, 2006. **282**: p. 21-31.

84. Kim, J.H., Koros, W.J., and Paul, D.R., *Effects of CO_2 exposure and physical aging on the gas permeability of thin 6FDA-based polyimide membranes. Part 2. with crosslinking.* Journal of Membrane Science, 2006. **282**: p. 32-43.

85. Petropoulos, J.H., *Mechanisms and theories for sorption and diffusion of gases in polymers*, in *Polymeric gas separation membranes*, D.R. Paul and Y. Yampolskii, Editors. 1994, CRC Press: Boca Raton, Florida, USA. p. 17-82.

86. Wessling, M., Schoeman, S., van der Boomgaard, T., and Smolders, C.A., *Plasticization of gas separation membranes.* Gas Separation & Purification, 1991. **5**: p. 221-228.

87. Singh, A., Freeman, B.D., and Pinnau, I., *Pure and mixed gas acetone/nitrogen permeation properties of polydimethylsiloxane [PDMS]*. Journal of Polymer Science, Part B: Polymer Physics, 1998. **36**(2): p. 289-301.

88. Donohue, M.D., Minhas, B.S., and Lee, S.Y., *Permeation behavior of carbon dioxide-methane mixtures in cellulose acetate membranes.* Journal of Membrane Science, 1989. **42**: p. 197-214.

89. Bos, A., Pünt, I.G.M., Wessling, M., and Strathmann, H., *Suppression of CO2-plasticization by semiinterpenetrating polymer network formation.* Journal of Polymer Science Part B-Polymer Physics, 1998. **36**(9): p. 1547-1556.

90. Bos, A., Pünt, I.G.M., Wessling, M., and Strathmann, H., *Plasticization-resistant glassy polyimide membranes for CO_2/CH_4 separations.* Separation and Purification Technology, 1998. **14**: p. 27-39.

91. Bos, A., Pünt, I.G.M., Wessling, M., and Strathmann, H., *CO_2-induced plasticization phenomenon in glassy polymers.* Journal of Membrane Science, 1999. **155**: p. 67-78.

92. Chen, C., Qiu, W., Miller, S.J., and Koros, W.J., *Plasticization-resistant hollow fiber membranes for CO_2/CH_4 separation based on a thermally crosslinkable polyimide.* Journal of Membrane Science, 2011. **382**: p. 212-221.

93. Chern, R.T. and Provan, C.N., *Gas-induced plasticization and the permselectivity of poly(tetrabromophenolphthalein terephthalate) to a mixture of carbon dioxide and methane.* Macromolecules, 1991. **24**: p. 2203-2207.

94. Wind, J.D., Paul, D.R., and Koros, W.J., *Natural gas permeation in polyimide membranes.* Journal of Membrane Science, 2004. **228**(2): p. 227-236.

95. Wind, J.D., Staudt-Bickel, C., Paul, D.R., and Koros, W.J., *Solid-state covalent cross-linking of polyimide membranes for carbon dioxide plasticization reduction.* Macromolecules, 2003. **36**(6): p. 1882-1888.

96. Wind, J.D., Staudt-Bickel, C., Paul, D.R., and Koros, W.J., *The effects of crosslinking chemistry on CO_2 plasticization of polyimide gas separation membranes.* Industrial & Engineering Chemistry Research, 2002. **41**: p. 6139-6148.

97. Wind, J.D., Sirard, S.M., Paul, D.R., Green, P.F., Johnston, K.P., and Koros, W.J., *Carbon dioxide-induced plasticization of polyimide membranes: Pseudo-equilibrium relationships of diffusion, sorption, and swelling.* Macromolecules, 2003. **36**: p. 6433-6441.

98. Chiou, J.S. and Paul, D.R., *Effects of CO_2 exposure on gas transport properties of glassy polymers.* Journal of Membrane Science, 1987. **32**: p. 195-205.

99. Kanehashi, S., Nakagawa, T., Nagai, K., Duthie, X., Kentish, S., and Stevens, G., *Effects of carbon dioxide-induced plasticization on the gas transport properties of glassy polyimide membranes.* Journal of Membrane Science, 2007. **298**: p. 147-155.

100. Sanders, E.S., *Penetrant-induced plasticization and gas permeation in glassy polymers.* Journal of Membrane Science, 1988. **37**: p. 63-80.

101. Puleo, A.C., Paul, D.R., and Kelley, S.S., *The effect of degree of acetylation on gas sorption and transport behavior in cellulose-acetate.* Journal of Membrane Science, 1989. **47**(3): p. 301-332.

102. Jordan, S.M., Fleming, G.K., and Koros, W.J., *Permeability of carbon dioxide at elevated pressures in substituted polycarbonates.* Journal of Polymer Science Part B: Polymer Physics, 2003. **28**(12): p. 2305-2327.

103. Fleming, G.K. and Koros, W.J., *Dilation of substituted polycarbonates caused by high-pressure carbon dioxide sorption.* Journal of Polymer Science Part B: Polymer Physics, 2003. **28**(7): p. 1137-1152.

104. Fleming, G.K. and Koros, W.J., *Carbon dioxide conditioning effects on sorption and volume dilation behavior for bisphenol A-polycarbonate.* Macromolecules, 1990. **23**: p. 1353-1360.

105. Lin, H.Q., Freeman, B.D., Kalakkunnath, S., and Kalika, D.S., *Effect of copolymer composition, temperature, and carbon dioxide fugacity on pure- and mixed-gas permeability in poly(ethylene glycol)-based materials: Free volume interpretation.* Journal of Membrane Science, 2007. **291**: p. 131-139.

106. Visser, T., Masetto, N., and Wessling, M., *Materials dependence of mixed gas plasticization behavior in asymmetric membranes.* Journal of Membrane Science, 2007. **306**: p. 16-28.

107. Tanaka, K., Taguchi, A., Hao, J., Kita, H., and Okamoto, K., *Permeation and separation properties of polyimide membranes to olefins and paraffins.* Journal of Membrane Science, 1996. **121**: p. 197-207.

108. White, L.S., Blinka, T.A., Kloczewski, H.A., and Wang, I., *Properties of a polyimide gas separation membrane in natural gas streams.* Journal of Membrane Science, 1995. **103**: p. 73-82.

109. Baker, R.W., *Future directions of membrane gas separation technology.* Industrial & Engineering Chemistry Research, 2002. **41**(6): p. 1393-1411.

110. Muruganandam, N., Koros, W.J., and Paul, D.R., *Gas Sorption and Transport in Substituted Polycarbonates.* Journal of Polymer Science Part B-Polymer Physics, 1987. **25**(9): p. 1999-2026.

111. Muruganandam, N. and Paul, D.R., *Evaluation of substituted polycarbonates and a blend with polystyrene as gas separation membranes.* Journal of Membrane Science, 1987. **34**: p. 1987.

112. Vu, D.Q., Koros, W.J., and Miller, S.J., *Mixed matrix membranes using carbon molecular sieves - I. Preparation and experimental results.* Journal of Membrane Science, 2003. **211**(2): p. 311-334.

113. Zhang, Y., Musselman, I., Ferraris, J., and Balkus Jr., K.J., *Gas permeability properties of Matrimid® membranes containing metal-organic framework Cu-BPY-HFS.* Journal of Membrane Science, 2008. **313**: p. 170-181.

114. Aitken, C.L., Koros, W.J., and Paul, D.R., *Effect of Structural Symmetry on Gas-Transport Properties of Polysulfones.* Macromolecules, 1992. **25**(13): p. 3424-3434.

115. Koros, W.J., Fleming, G.K., Jordan, S.M., Kim, T.H., and Hoehn, H.H., *Polymeric membrane materials for solution-diffusion based permeation separations.* Progress in Polymer Science, 1988. **13**(4): p. 339-401.

116. Ekiner, O.M. and Vassilatos, G., *Polyaramide hollow fibers for hydrogen/methane separation - spinning and properties.* Journal of Membrane Science, 1990. **53**: p. 259-273.

117. Huang, Y., Wang, X., and Paul, D.R., *Physical aging of thin glassy polymer films: Free volume interpretation.* Journal of Membrane Science, 2006. **277**: p. 219-229.

118. Guo, R. and McGrath, J.E., *Aromatic polyethers, polyetherketones, polysulfides, and polysulfones,* in *Polymer science: A comprehensive reference,* K. Matyjaszewski and M. Möller, Editors. 2012, Elsevier BV: Amsterdam. p. 377-430.

119. McGrail, P.T., *Polyaromatics.* Polymer International, 1996. **41**(2): p. 103-121.

120. Henis, J.S. and Tripodi, M.K., Multicomponent membranes for gas separations. US. Patent 4,230,463. 1977.

121. Aitken, C.L., Koros, W.J., and Paul, D.R., *Gas-Transport Properties of Biphenol Polysulfones.* Macromolecules, 1992. **25**(14): p. 3651-3658.

122. Erb, A.J. and Paul, D.R., *Gas Sorption and Transport in Polysulfone.* Journal of Membrane Science, 1981. **8**(1): p. 11-22.

123. Ghosal, K., Chern, R.T., and Freeman, B.D., *Gas-Permeability of Radel-a Polysulfone.* Journal of Polymer Science Part B-Polymer Physics, 1993. **31**(7): p. 891-893.

124. McHattie, J.S., Koros, W.J., and Paul, D.R., *Gas-Transport Properties of Polysulfones .2. Effect of Bisphenol Connector Groups.* Polymer, 1991. **32**(14): p. 2618-2625.

125. Ghosal, K. and Chern, R.T., *Aryl nitration of poly(phenylene oxide) and polysulfone. Structural characterization and gas permeability.* Journal of Membrane Science, 1992. **72**(1): p. 91-97.

126. Ghosal, K., Chern, R.T., Freeman, B.D., Daly, W.H., and Negulescu, I.I., *Effect of basic substituents on gas sorption and permeation in polysulfone.* Macromolecules, 1996. **29**(12): p. 4360-4369.

127. Paul, D.R. and Yampol'skii, Y.P., eds. *Polymeric Gas Separation Membranes*. 1994, CRC Press, Inc.: Boca Raton, FL. 100-126.

128. McHattie, J.S., Koros, W.J., and Paul, D.R., *Gas-Transport Properties of Polysulfones .3. Comparison of Tetramethyl-Substituted Bisphenols.* Polymer, 1992. **33**(8): p. 1701-1711.

129. McHattie, J.S., Koros, W.J., and Paul, D.R., *Gas-Transport Properties of Polysulfones .1. Role of Symmetry of Methyl-Group Placement on Bisphenol Rings.* Polymer, 1991. **32**(5): p. 840-850.

130. Haggin, J., *New generation of membranes developed for industrial separations.* Chemical and Engineering News, 1988. **3**: p. 7-16.

131. Schell, W.J., Wensley, C.G., Chen, M.S.K., Venugopal, K.G., Miller, B.D., and Stuart, J.A., *Recent advances in cellulosic membranes for gas separation and pervaporation.* Gas Separation & Purification, 1989. **3**(4): p. 162-169.

132. White, L.S., *Evolution of natural gas treatment with membrane systems*, in *Membrane gas separation*, Y. Yampolskii and B.D. Freeman, Editors. 2010, John Wiley & Sons Ltd.: Chichester.

133. Loeb, S. and Sourirajan, S., eds. In saline water conversion II-Advances in chemistry series Vol. 38. 1963, American Chemical Society: Washington, DC. 117-132.

134. Spillman, R.W., *Economics of gas separation membranes.* Chemical Engineering Progress, 1989. **85**(1): p. 41–62.

135. Heinze, T. and Liebert, T., *Chemical characteristics of cellulose acetate.* Macromolecular Symposia, 2004. **208**: p. 167-237.

136. Kesting, R.E., *Synthetic polymer membranes: A structural perspective*. 1985, New York: Wiley-Interscience.

137. Saka, S. and Matsumura, H., *The raw materials of CA.* Macromolecular Symposia, 2004. **208**: p. 7-48.

138. Edgar, K.J., Buchanan, C.M., Debenham, J.S., Rundquist, P.A., Seiler, B.D., Shelton, M.C., and Tindall, D., *Advances in cellulose ester performance and application.* Progress in Polymer Science, 2001. **26**: p. 1605-1688.

139. Lee, S.Y. and Minhas, B.S., *Effect of gas composition and pressure on permeation through cellulose acetate membranes.* AIChE Symposium Series, 1988. **84**(264): p. 93-101.

140. Robeson, L.M., Farnham, A.G., and McGrath, J.E., eds. *Molecular Basis for Transitions and Relaxations*. Vol. 4. 1978, Gordon and Breach Midland Macromolecular Institute Monographs. 405.

141. Aycock, D., *Poly(phenylene ether),* in *Encyclopedia of polymer science and technology*1974, Interscience Publishers, NY.

142. Hay, A.S., Blanchard, H.S., Endres, G.F., and Eustance, J.W., *Polymerization by oxidative coupling.* Journal of the American Chemical Society, 1959. **81**(23): p. 6335.

143. Hay, A.S., Oxidation of phenols and resulting products US Pat. 3,306,875. 1967.

144. van Dort, H.M., Process for the formation of high molecular weight polyarylene ethers. CA Patent 798422. 1968.

145. Toi, K., Morel, G., and Paul, D.R., *Gas Sorption and Transport in Poly(Phenylene Oxide) and Comparisons with Other Glassy-Polymers.* Journal of Applied Polymer Science, 1982. **27**(8): p. 2997-3005.

146. Aguilar-Vega, M. and Paul, D.R., *Gas-Transport Properties of Polyphenylene Ethers.* Journal of Polymer Science Part B-Polymer Physics, 1993. **31**(11): p. 1577-1589.

147. S. Percec and G. Li, *Chemical modification of poly(2,6-dimethyl-1,4-phenylene oxide) and properties of the resulting polymers*, in *ACS Symposium Series*1988, American Chemical Society, Washington, DC.

148. Hamad, F., Khulbe, K.C., and Matsuura, T., *Characterization of gas separation membranes prepared from brominated poly (phenylene oxide) by infrared spectroscopy.* Desalination, 2002. **148**(1-3): p. 369-375.

149. Sridhar, S., Smitha, B., Ramakrishna, M., and Aminabhavi, T.M., *Modified poly(phenylene oxide) membranes for the separation of carbon dioxide from methane.* Journal of Membrane Science, 2006. **280**(1-2): p. 202-209.

150. Story, B.J. and Koros, W.J., *Sorption of CO_2/CH_4 mixtures in poly(phenylene oxide) and a carboxylated derivative.* Journal of Applied Polymer Science, 1991. **42**(9): p. 2613-2626.

151. Story, B.J. and Koros, W.J., *Sorption and transport of CO_2 and CH_4 in chemically modified poly(phenylene oxide).* Journal of Membrane Science, 1992. **67**(2-3): p. 191-210.

152. Zampini, A. and Malon, R.F., Proc. ACS Div. Polym. Mat., Sci. & Eng., 1985. **52**: p. 345.

153. Chern, R.T., Sheu, F.R., Jia, L., Stannett, V.T., and Hopfenberg, H.B., *Transport of gases in unmodified and aryl-brominated 2,6-dimethyl-1,4-poly(phenylene oxide).* Journal of Membrane Science, 1987. **35**(1): p. 103-115.

154. Chern, R.T., Jia, L., Shimoda, S., and Hopfenberg, H.B., *A note on the effects of mono- and dibromination on the transport properties of poly(2,6-dimethylphenylene oxide).* Journal of Membrane Science, 1990. **48**(2-3): p. 333-341.

155. Henis, J.M.S. and Tripodi, M.K., US Patent 4230426. 1980.

156. Ekiner, O.M. and Vassilatos, G., *Polyaramide hollow fibers for H_2/CH_4 separation II. Spinning and properties.* Journal of Membrane Science, 2001. **186**: p. 71-84.

157. Gaymans, R.J., *Polyamides*, in *Synthetic methods in step-growth polymers*, M.E. Rogers and T.E. Long, Editors. 2003, John Wiley & Sons: Hoboken.

158. Yang, H.H., *Aromatic high-strength fibers*, in *High-performance aromatic polyamides*2010, Wiley: New York.

159. García, J.M., García, F.C., Serna, F., and de la Peña, J.L., *High-performance aromatic polyamides.* Progress in Polymer Science, 2010. **35**: p. 623-686.

160. Preston, J., *Aromatic polyamides*, in *Encyclopedia of polymer science and engineering*, B.N. Mark HF, Overberger CG, Menges G, Editor 1988, John Wiley & Sons, Inc.: New York. p. 381-9.

161. Cadotte, J., Interfacially synthesized reverse osmosis membrane. US Patent 4,277,344. 1981.

162. Geise, G.M., Lee, H.S., Miller, D.J., Freeman, B.D., McGrath, J.E., and Paul, D.R., *Water purification by membranes: The role of polymer science.* Journal of Polymer Science Part B-Polymer Physics, 2010. **48**(15): p. 1685-1718.

163. Tien, C.F., Surnamer, A.D., and Langsam, M., Membranes formed from rigid aromatic polyamides. US Patent 5,034,027. 1991.

164. Espeso, J.F., Ferrero, E., De La Campa, J.G., Lozano, A.E., and De Abajo, J., *Synthesis and characterization of new soluble aromatic polyamides derived from 1,4-Bis(4-carboxyphenoxy)-2, 5-di-tert-butylbenzene.* Journal of Polymer Science Part A: Polymer Chemistry, 2001. **39**(4): p. 475-485.

165. Carrera-Figueiras, C. and Aguilar-Vega, M., *Gas permeability and selectivity of hexafluoroisopropylidene aromatic isophthalic copolyamides.* J Polym Sci B: Polym Phys, 2005. **43**: p. 2625-38.

166. López-Nava R, Vázquez-Moreno FS, Palí-Casanova R, and M., A.-V., *Gas permeability coefficients of isomeric aromatic polyamides obtained from 4,4 -(9-fluorenylidene) diamine and aromatic diacid chlorides.* Polym Bull, 2002. **49**: p. 165-72.

167. Ding Y and Bikson, B., *Soluble aromatic polyamides containing the phenylindane group and their gas transport characteristics.* Polymer, 2002. **43**: p. 4709-14.

168. Ekiner, O.M. and Vassilatos, G., Polymeric Membranes. 1992.

169. Freitag, D., *Polycarbonates*, in *Encyclopedia of polymer science and engineering*, J. Kroschwitz, Editor 1988, John Wiley & Sons. p. 648-718.

170. King Jr., J.A., *Synthesis of polycarbonates*, in *Handbook of Polycarbonate Science and Technology*, D.G. LeGrand and J.T. Bendler, Editors. 2000, Marcel Dekker Inc. p. 7-27.

171. Puri, P.S., *Commercial applications of membranes in gas separations*, in *Membrane engineering for the treatment of gases Vol 1: Gas separation problems with membranes*, E. Drioli and G. Barbieri, Editors. 2011, Royal Society of Chemistry: Cambridge.

172. Sanders Jr., E.S. and Overman III, D.C., Process for separating hydrogen from as mixtures using a semi-permeable membrane consisting predominantly of polycarbonates derived from tetrahalobisphenols. 1991.

173. Anand, J.N., Bales, S.E., Feay, D.C., and Jeanes, T.O., Tetrabromo bisphenol based polyestercarbonate membranes and method of using. US. Patent 4,840,646. 1989.

174. Ohya, H., Kudryavtsev, V.V., and Semenova, S.I., *Polyimide membranes - applications, fabrications, and properties*. 1996: Gordon and Breach.

175. Bateman, J. and Gordon, D.A., Soluble polyimides derived from phenylindane diamines and dianhydrides. U.S. Patent 3,856,752. 1974.

176. Falcigno, P., Masola, M., Williams, D., and Jasne, S., eds. *Comparison of properties of polyimides containing DAPI isomers and various dianhydrides*. Polyimides: Materials, chemistry and characterization, Proceedings of the 3rd International Conference on Polyimides, ed. C. Feger, M.M. Khohasteh, and J.E. McGrath 1989, Elsevier: Ellenville, NY. 497-512.

177. Farr, I.V., Kratzner, D., Glass, T.E., Dunson, D., Ji, Q., and McGrath, J.E., *The synthesis and characterization of polyimide homopolymers based on 5(6)-amino-1-(4-aminophenyl)1,3,3-trimethylindane.* Journal of Polymer Science Part A-Polymer Chemistry, 2000. **38**(15): p. 2840-2854.

178. Bateman, J.H., Geresy, W., and Neiditch, D.S., *Soluble polyimides derived from phenylindane diamine: a new approach to heat resistant protective coatings.* American Chemical Society, Division of Organic Coatings and Plastics Chemistry, 1975. **35**(2): p. 77-82.

179. Ekiner, O.M., Hayes, R.A., and Va, W., Phenylindane-containing polyimide gas separation membranes. US Patent 5015270. 1991.

180. Clausi, D.T. and Koros, W.J., *Formation of defect-free polyimide hollow fiber membranes for gas separations.* Journal of Membrane Science, 2000. **167**(1): p. 79-89.

181. Farr, I.V., Glass, T.E., Ji, Q., and McGrath, J.E., *Synthesis and characterization of diaminophenylindane based polyimides via ester-acid solution imidization.* High Performance Polymers, 1997. **9**(3): p. 345-352.

182. Lee, J.S., Madden, W., and Koros, W.J., *Antiplasticization and plasticization of Matrimid (R) asymmetric hollow fiber membranes-Part A. Experimental.* Journal of Membrane Science, 2010. **350**(1-2): p. 232-241.

183. Duthie, X., Kentish, S., Pas, S.J., Hill, A.J., Powell, C., Nagai, K., Stevens, G., and Qiao, G., *Thermal treatment of dense polyimide membranes.* Journal of Polymer Science Part B-Polymer Physics, 2008. **46**(18): p. 1879-1890.

184. Tin, P.S., Chung, T.S., Liu, Y., Wang, R., Liu, S.L., and Pramoda, K.P., *Effects of cross-linking modification on gas separation performance of Matrimid membranes.* Journal of Membrane Science, 2003. **225**(1-2): p. 77-90.

185. Zhao, H.-Y., Cao, Y.-M., Ding, X.-L., Zhou, M.-Q., Liu, J.-H., and Yuan, Q., *Poly(ethylene oxide) induced cross-linking modification of Matrimid membranes for selective separation of CO2.* Journal of Membrane Science, 2008. **320**(1-2): p. 179-184.

186. Ekiner, O.M., Hayes, R.A., and Manos, P., Novel multicomponent fluid separation membranes. 1992.

187. Sasaki, Y., Inoue, H., Itatani, H., and Kashima, M., Process for preparing polyimide solution US Pat. 4,290,936. 1981.

188. Itatani, H. and Yoshimoto, H., The Journal of Organic Chemistry, 1973. **38**: p. 76-79.

189. Kashima, M., Yoshimoto, H., and Itatani, H., *Isotope effect of aromatic coupling reaction catalyzed by palladium acetate.* Journal of Catalysis, 1973. **29**(1): p. 92-98.

190. Yamane, H. in *Proceedings of second International Conference on Polyimides, Society of Plastics Engineers*. Oct. 1985. Ellenville, NY.

191. Semenova, S.I., *Introduction: Trends in polyimide membrane development*. Polyimide membranes: Applications, fabrications, and properties, ed. H. Ohya, V.V. Kudryavstev, and S.I. Semenova1996, Amstertam, The Netherland: Gordon and Breach Science Publisher.

192. Sada, E., Kumazawa, H., and Xu, P., *Sorption and diffusion of carbon dioxide in polyimide films.* Journal of Applied Polymer Science, 1988. **35**(6): p. 1497-1509.

193. Okamoto, K.I., Tanihara, N., Watanabe, H., Tanaka, K., Kita, H., Nakamura, A., Kusuki, Y., and Nakagawa, K., *Sorption and diffusion of water-vapor in polyimide films.* Journal of Polymer Science Part B-Polymer Physics, 1992. **30**(11): p. 1223-1231.

194. Yates, S., Zaki, R., Arzadon, A., Liu, C., and Choiu, J., Thin film gas separation membranes. 2010.

195. Zimmerman, C.M., Singh, A., and Koros, W.J., *Tailoring mixed matrix composite membranes for gas separations.* Journal of Membrane Science, 1997. **137**: p. 145-154.

196. Chung, T.S., Jiang, L.Y., Li, Y., and Kulprathipanja, S., *Mixed matrix membranes (MMMs) comprising organic polymers with dispersed inorganic fillers for gas separation.* Progress in Polymer Science, 2007. **32**: p. 483-507.

197. Kim, S., Han, S.H., and Lee, Y.M., *Thermally rearranged (TR) polybenzoxazole hollow fiber membranes for CO_2 capture.* Journal of Membrane Science, 2012. **403-404**: p. 169-178.

198. Sanders, D.F., Smith, Z.P., Ribeiro, C.P., Guo, R., McGrath, J.E., Paul, D.R., and Freeman, B.D., *Permeability, diffusivity, and free volume of thermally rearranged polymers based on 3,3'-dihydroxy-4,4'-diamino-biphenyl (HAB) and 2,2'-bis-(3,4-dicarboxyphenyl) hexafluoropropane dianhydride (6FDA).* Journal of Membrane Science, 2012. **409-410**: p. 232-241.

199. Smith, Z.P., Sanders, D.F., Ribeiro, C.P., Guo, R., Freeman, B.D., Paul, D.R., McGrath, J.E., and Swinnea, S., *Gas sorption and characterization of thermally rearranged polyimides based on 3,3'-dihydroxy-4,4'-diamino-biphenyl (HAB) and 2,2'-bis-(3,4-dicarboxyphenyl) hexafluoropropane dianhydride (6FDA).* Journal of Membrane Science, 2012. **415-416**: p. 558-567.

200. Park, H.B., Han, S.H., Jung, C.H., Lee, Y.M., and Hill, A.J., *Thermally rearranged (TR) polymer membranes for CO_2 separation.* Journal of Membrane Science, 2010. **359**(1-2): p. 11-24.

201. Jung, C.H., Lee, J.E., Han, S.H., Park, H.B., and Lee, Y.M., *Highly permeable and selective poly(benzoxazole-co-imide) membranes for gas separation.* Journal of Membrane Science, 2010. **350**(1-2): p. 301-309.

202. Choi, J.I., Jung, C.H., Han, S.H., Park, H.B., and Lee, Y.M., *Thermally rearranged (TR) poly(benzoxazole-co-pyrrolone) membranes tuned for high gas permeability and selectivity.* Journal of Membrane Science, 2010. **349**(1-2): p. 358-368.

203. Han, S.H., Misdan, N., Kim, S., Doherty, C.M., Hill, A.J., and Lee, Y.M., *Thermally rearranged (TR) polybenzoxazole: Effects of diverse imidization routes on physical properties and gas transport behaviors.* Macromolecules, 2010. **43**(18): p. 7657-7667.

204. Kardash, I.Y. and Pravednikov, A.N., *Aromatic polyimides containing hydroxy- and methoxy-groups.* Vysokomol. soyed., 1967. **B9**: p. 873-876.

205. Tullos, G.L. and Mathias, L.J., *Unexpected thermal conversion of hydroxy-containing polyimides to polybenzoxazoles.* Polymer, 1999. **40**(12): p. 3463-3468.

206. Tullos, G.L., Powers, J.M., Jeskey, S.J., and Mathias, L.J., *Thermal conversion of hydroxy-containing imides to benzoxazoles: Polymer and model compound study.* Macromolecules, 1999. **32**(11): p. 3598-3612.

207. Guo, R., Sanders, D.F., Smith, Z.P., Freeman, B.D., Paul, D.R., and McGrath, J.E., *Synthesis and Characterization of Thermally Rearranged (TR) Polymers: Influence of ortho-positioned functional groups of polyimide precursors on TR process and gas transport properties.* Journal of Materials Chemistry A, 2013. **1**: p. 262-272.

208. Budd, P.M., Msayib, K.J., Tattershall, C.E., Ghanem, B.S., Reynolds, K.J., McKeown, N.B., and Fritsch, D., *Gas separation membranes from polymers of intrinsic microporosity.* Journal of Membrane Science, 2005. **251**: p. 263-269.

209. Ghanem, B.S., McKeown, N.B., Budd, P.M., Al-Haribi, N.M., Fritsch, D., Heinrich, K., Starannikova, L., Tokarev, A., and Yampolskii, Y., *Synthesis, characterization, and gas permeation properties of a novel group of polymers with intrinsic microporosity: PIM-Polyimides.* Macromolecules, 2009. **42**(20): p. 7881-7888.

210. Ma, X., Swaidan, R., Belmabkhout, Y., Zhu, Y., Litwiller, E., Jouiad, M., Pinnau, I., and Han, Y., *Synthesis and gas transport properties of hydroxyl-functionalized polyimides with intrinsic microporosity.* Macromolecules, 2012. **45**: p. 3841-3849.

211. Alentiev, A.Y., Shantarovich, V.P., Merkel, T.C., Bondar, V.I., Freeman, B.D., and Yampolskii, Y.P., *Gas and vapor sorption, permeation, and diffusion in glassy amorphous Teflon AF1600.* Macromolecules, 2002. **35**: p. 9513-9522.

212. Merkel, T.C., Bondar, V., Nagai, K., Freeman, B.D., and Yampolskii, Y.P., *Gas sorption, diffusion, and permeation in poly(2,2-bis(trifluoromehtyl)-4,5-difluoro-1,3-dioxole-co-tetrafluoroethylene).* Macromolecules, 1999. **32**: p. 8427-8440.

213. Merkel, T.C., Pinnau, I., Prabhakar, R., and Freeman, B.D., eds. *Gas and Vapor Transport Properties of Perfluoropolymers.* Materials science of membranes for gas and vapor separation, ed. Y. Yampolskii, Pinnau, I., Freeman B. D. 2006, Wiley: Chichester, UK. 251-270.

214. Kim, J.H., Koros, W.J., and Paul, D.R., *Effects of CO_2 exposure and physical aging on the gas permeability of thin 6FDA-based polyimide membranes - Part 2. with crosslinking.* Journal of Membrane Science, 2006. **282**(1-2): p. 32-43.

215. Lin, W.H. and Chung, T.S., *Gas permeability, diffusivity, solubility and aging characteristics of 6FDA-durene polyimide membranes.* Journal of Membrane Science, 2001. **186**: p. 183-193.

216. Stern, S.A., *Structure/permeability relationships of polyimide membranes: applications to the separation of gas mixtures.* Journal of Polymer Science, Part B: Polymer Physics, 1989. **27**(9): p. 1887-1909.

217. Wang, L., Cao, Y., Zhou, M., Zhou, S.J., and Yuan, Q., *Novel copolyimide membranes for gas separation.* Journal of Membrane Science, 2007. **305**: p. 338-346.

218. Bara, J.E., Gin, D.L., and Noble, R.D., *Effect of anion on gas separation performance of polymer-room-temperature ionic liquid composite membranes.* Industrial & Engineering Chemistry Research, 2008. **47**: p. 9919-9924.

219. Bara, J.E., Hatakeyama, E.S., Gin, D.L., and Noble, R.D., *Improving CO_2 permeability in polymerized room-temperature ionic liquid gas separation membranes through the formation of a solid composite with a room temperature ionic liquid.* Polymers for Advanced Technologies, 2008. **19**: p. 1415-1420.

220. Bara, J.E., Lessmann, S., Gabriel, C.J., Hatakeyama, E.S., Noble, R.D., and Gin, D.L., *Synthesis and performance of polymerizable room-temperature ionic liquids as*

gas separation membranes. Industrial & Engineering Chemistry Research, 2007. **46**: p. 5397-5404.

221. Guo, R., Sanders, D.F., Smith, Z.P., Freeman, B.D., and McGrath, J.E., *Synthesis and characterization of thermally rearranged (TR) polymer membranes: The effects of ortho-positioned functional group of polyimide precursors.* submitted, 2012.

222. Guo, R., Sanders, D.F., Smith, Z.P., Freeman, B.D., and McGrath, J.E., *Synthesis and characterization of thermally rearranged (TR) polymer membranes: Effect of glass transition temperature of poly(hydroxyimide) precursors.* Journal of Materials Chemistry A, 2013. **1**: p. 262-272.

223. Smith, Z.P., Sanders, D.F., Ribeiro, C.P., Guo, R., Freeman, B.D., Paul, D.R., McGrath, J.E., and Swinnea, S., *Gas sorption and characterization of thermally rearranged polyimides based on 3,3'-dihydroxy-4,4'-diamino-biphenyl (HAB) and 2,2'-bis-(3,4 dicarboxyphenyl) hexafluoropropane dianhydride (6FDA).* Journal of Membrane Science, 2011. **415-416**: p. 558-567.

224. Budd, P.M., Ghanem, B.S., Makhseed, S., McKeown, N.B., Msayib, K.J., and Tattershall, C.E., *Polymers of intrinsic microporosity (PIMs): robust, solution-processable, organic nanoporous materials.* Chemical Communications, 2004(2): p. 230-231.

225. Budd, P.M., Elabas, E.S., Ghanem, B.S., Makhseed, S., McKeown, N.B., Msayib, K.J., Tattershall, C.E., and Wang, D., *Solution-processed, organophilic membrane derived from a polymer of intrinsic microporosity.* Advanced Materials, 2004. **16**(5): p. 456-459.

226. McKeown, N.B. and Budd, P.M., *Polymers of intrinsic microporosity (PIMs): organic materials for membrane separations, heterogeneous catalysis and hydrogen storage.* Chemical Society Reviews, 2006. **35**(8): p. 675-683.

227. McKeown, N.B., Budd, P.M., Msayib, K.J., Ghanem, B.S., Kingston, H.J., Tattershall, C.E., Makhseed, S., Reynolds, K.J., and Fritsch, D., *Polymers of intrinsic microporosity (PIMs): Bridging the void between microporous and polymeric materials.* Chemistry-a European Journal, 2005. **11**(9): p. 2610-2620.

228. Ghanem, B.S., McKeown, N.B., Budd, P.M., Selbie, J.D., and Fritsch, D., *High-performance membranes from polyimides with intrinsic microporosity.* Advanced Materials, 2008. **20**(14): p. 2766-2771.

229. Emmler, T., Heinrich, K., Fritsch, D., Budd, P.M., Chaukura, N., Ehlers, D., Ratzke, K., and Faupel, F., *Free volume investigation of polymers of intrinsic*

microporosity (PIMs): PIM-1 and PIM1 copolymers incorporating ethanoanthracene units. Macromolecules, 2010. **43**(14): p. 6075-6084.

230. Scheirs, J., *High performance polymer for diverse applications*. 1997, Chichester: John Wiley & Sons.

231. Arcella, V., Colaianna, P., Maccone, P., Sanguineti, A., Gordano, A., Clarizia, G., and Drioli, E., *A study on a perfluoropolymer purification and its application to membrane formation.* Journal of Membrane Science, 1999. **163**(2): p. 203-209.

232. Arcella, V., Ghielmi, A., and Tommasi, G., *High performance perfluoropolymer films and membranes.* Annals of the New York Academy of Sciences, 2003. **984**(1): p. 226-244.

233. Squire, E.N., Amorphous copolymers of perfluoro-2,2-dimethyl-1,3-dioxole. US Patent 4,754,009. 1988.

234. Squire, E.N., Amorphous copolymers of perfluoro-2,2-dimethyl-1,3-dioxole US Patent 4,935,477. 1990.

235. Colaianna, P., Brinati, G., and Arcekka, V., Amorphous perfluoropolymers. 1999.

236. Nakamura, M., Kaneko, I., Oharu, K., Kojima, G., Matsuo, M., Sameijima, S., and Kamba, M., Cyclic Polymerization. U.S. Patent 4,910,276. 1990.

237. Nakamura, M., Sugiyama, N., Etoh, Y., and Endo, J., Nippon Kagaku Kaishi, 2001. **12**: p. 659-668.

238. Sasakura, H., Kobunshi Ronbunshu, 2003. **60**: p. 312-317.

239. Alentiev, A.Y., Yampolskii, Y.P., Shantarovich, V.P., Nemser, S.M., and Plate, N.A., *High transport parameters and free volume of perfluorodioxole copolymers.* Journal of Membrane Science, 1997. **126**(1): p. 123-132.

240. Bondar, V.I., Freeman, B.D., and Yampolskii, Y.P., *Sorption of gases and vapors in an amorphous glassy perfluorodioxole copolymer.* Macromolecules, 1999. **32**(19): p. 6163-6171.

241. Prabhakar, R.S., Freeman, B.D., and Roman, I., *Gas and vapor sorption and permeation in poly(2,2,4-trifluoro-5-trifluoromethoxy-1,3-dioxole-co-tetrafluoroethylene).* Macromolecules, 2004. **37**(20): p. 7688-7697.

242. Tokarev, A., Friess, K., Machkova, J., Sipek, M., and Yampolskii, Y., *Sorption and diffusion of organic vapors in amorphous Teflon AF2400.* Journal of Polymer Science Part B-Polymer Physics, 2006. **44**(5): p. 832-844.

243. Jansen, J.C., Macchione, M., and Drioli, E., *On the unusual solvent retention and the effect on the gas transport in perfluorinated Hyflon AD (R) membranes.* Journal of Membrane Science, 2007. **287**(1): p. 132-137.

244. Pinnau, I. and Toy, L.G., *Gas and vapor transport properties of amorphous perfluorinated copolymer membranes based on 2,2-bistrifluoromethyl-4,5-difluoro-1,3-dioxole/tetrafluoroethylene.* Journal of Membrane Science, 1996. **109**(1): p. 125-133.

245. Prabhakar, R.S., Grazia de Angelis, M., Sarti, G.C., Freeman, B.D., and Coughlin, M.C., *Gas and vapor sorption, permeation, and diffusion in poly(tetrafluoroethylene-co-perfluoromethyl vinyl ether).* Macromolecules, 2005. **38**: p. 7043-7055.

246. Pastermak, R.A., Burns, G.L., and Heller, J., *Diffusion and solubility of simple gases through a copolymer of hexafluoropropylene and tetafluroethylene.* Macromolecules, 1971. **4**(4): p. 470-475.

247. Bernardo, P., Drioli, E., and Golemme, G., *Membrane gas separation: A review/state of the art.* Industrial & Engineering Chemistry Research, 2009. **48**: p. 4638-4663.

248. Xiao, Y., Low, B.T., Hosseini, S.S., Chung, T.S., and Paul, D.R., *The strategies of molecular architecture and modification of polyimide-based membranes for CO2 removal from natural gas鈥 review.* Progress in Polymer Science, 2009. **34**(6): p. 561-580.

249. Staudt-Bickel, C. and Koros, W.J., *Improvement of CO_2/CH_4 separation characteristics of polyimide by chemical crosslinking.* Journal of Membrane Science, 1999. **155**: p. 145-154.

250. Hu, L., Xu, X.L., and Coleman, M.R., *Impact of H+ ion beam irradiation on Matrimid (R). II. Evolution in gas transport properties.* Journal of Applied Polymer Science, 2007. **103**(3): p. 1670-1680.

251. Kita, H., Inada, T., Tanaka, K., and Okamoto, K., *Effect of photo-cross-linking on permeability and permselectivity of gases through benzophenone-containing polyimide.* Journal of Membrane Science, 1994. **87**(1-2): p. 139-147.

252. Won, J., Kim, M.H., Kang, Y.S., Park, H.C., Kim, U.Y., Choi, S.C., and Koh, S.K., *Surface modification of polyimide and polysulfone membranes by ion beam for gas separation.* Journal of Applied Polymer Science, 2000. **75**(12): p. 1554-1560.

253. Xiao, Y.C., Chung, T.S., Guan, H.M., and Guiver, M.D., *Synthesis, cross-linking and carbonization of co-polyimides containing internal acetylene units for gas separation.* Journal of Membrane Science, 2007. **302**(1-2): p. 254-264.

254. Hillock, A.M.W. and Koros, W.J., *Cross-linkable polyimide membrane for natural gas purification and carbon dioxide plasticization reduction.* Macromolecules, 2007. **40**(3): p. 583-587.

255. Kim, H.S., Kim, Y.H., Ahn, S.K., and Kwon, S.K., *Synthesis and characterization of highly soluble and oxygen permeable new polyimides bearing a noncoplanar twisted biphenyl unit containing tert-butylphenyl or trimethylsilyl phenyl groups.* Macromolecules, 2003. **36**(7): p. 2327-2332.

256. Calle, M., Lozano, A.E., de La Campa, J.G., and de Abajo, J., *Novel Aromatic Polyimides Derived from 5 '-t-Butyl-2 '-pivaloylimino-3,4,3 '',4 ''-m-terphenyltetracarboxylic Dianhydride with Potential Application on Gas Separation Processes.* Macromolecules. **43**(5): p. 2268-2275.

257. Kim, Y.H., Kim, H.S., and Kwon, S.K., *Synthesis and characterization of highly soluble and oxygen permeable new polyimides based on twisted biphenyl dianhydride and spirobifluorene diamine.* Macromolecules, 2005. **38**(19): p. 7950-7956.

258. Noble, R.D. and Gin, D.L., *Persepective on ionic liquids and ionic liquid membranes.* Journal of Membrane Science, 2011. **369**: p. 1-4.

259. Mecerreyes, D., *Polymeric ionic liquids: Broadening the properties and applications of polyelectrolytes.* Progress in Polymer Science, 2011. **36**(12): p. 1629-1648.

260. Blanchard, L.A., Hancu, D., Beckman, E.J., and Brennecke, J.F., *Green processing using ionic liquids and CO2.* Nature, 1999. **399**(6731): p. 28-29.

261. Scovazzo, P., Kieft, J., Finan, D.A., Koval, C., DuBois, D., and Noble, R., *Gas separations using non-hexafluorophosphate [PF6](-) anion supported ionic liquid membranes.* Journal of Membrane Science, 2004. **238**(1-2): p. 57-63.

262. Fortunato, R., Afonso, C.A.M., Reis, M.A.M., and Crespo, J.G., *Supported liquid membranes using ionic liquids: study of stability and transport mechanisms.* Journal of Membrane Science, 2004. **242**(1-2): p. 197-209.

263. Li, P., Paul, D.R., and Chung, T.S., *High performance membranes based on ionic liquid polymers for CO_2 separation from the flue gas.* Green Chemistry, 2012. **14**: p. 1052-1063.

264. Scovazzo, P., *Determination of the upper limits, benchmarks, and critical properties for gas separations using stabilized romo temperature ionic liquid membranes (SILMs) for the purpose of guiding future research.* Journal of Membrane Science, 2009. **343**: p. 199-211.

265. Cadena, C., Anthony, J.L., Shah, J.K., Morrow, T.I., Brennecke, J.F., and Maginn, E.J., *Why is CO2 so soluble in imidazolium-based ionic liquids?* Journal of the American Chemical Society, 2004. **126**(16): p. 5300-5308.

266. Tang, J.B., Sun, W.L., Tang, H.D., Radosz, M., and Shen, Y.Q., *Enhanced CO2 absorption of poly(ionic liquid)s.* Macromolecules, 2005. **38**(6): p. 2037-2039.

267. Tang, J.B., Tang, H.D., Sun, W.L., Plancher, H., Radosz, M., and Shen, Y.Q., *Poly(ionic liquid)s: a new material with enhanced and fast CO2 absorption.* Chemical Communications, 2005(26): p. 3325-3327.

268. Tang, J.B., Tang, H.D., Sun, W.L., Radosz, M., and Shen, Y.Q., *Low-pressure CO2 sorption in ammonium-based poly(ionic liquid)s.* Polymer, 2005. **46**(26): p. 12460-12467.

269. Tang, J.B., Tang, H.D., Sun, W.L., Radosz, M., and Shen, Y.Q., *Poly(ionic liquid)s as new materials for CO_2 absorption.* Journal of Polymer Science Part a-Polymer Chemistry, 2005. **43**(22): p. 5477-5489.

270. Bara, J.E., Gabriel, C.J., Hatakeyama, E.S., Carlisle, T.K., Lessmann, S., Noble, R.D., and Gin, D.L., *Improving CO2 selectivity in polymerized room-temperature ionic liquid gas separation membranes through incorporation of polar substituents.* Journal of Membrane Science, 2008. **321**(1): p. 3-7.

271. Bara, J.E., Gabriel, C.J., Lessmann, S., Carlisle, T.K., Finotello, A., Gin, D.L., and Noble, R.D., *Enhanced CO2 separation selectivity in oligo(ethylene glycol) functionalized room-temperature ionic liquids.* Industrial & Engineering Chemistry Research, 2007. **46**(16): p. 5380-5386.

272. Bara, J.E., Noble, R.D., and Gin, D.L., *Effect of "free" cation substituent on gas separation performance of polymer-room-temperature ionic liquid composite membranes.* Industrial & Engineering Chemistry Research, 2009. **48**: p. 4607-4610.

273. Bara, J.E., Hatakeyama, E.S., Gabriel, C.J., Zeng, X., Lessmann, S., Gin, D.L., and Noble, R.D., *Synthesis and light gas separations in cross-linked gemini room temperature ionic liquid polymer membranes.* Journal of Membrane Science, 2008. **316**: p. 186-191.

274. Carlisle, T.K., Bara, J.E., Lafrate, A.L., Gin, D.L., and Noble, R.D., *Main-chain imidazolium polymer membranes for CO_2 separations: An initial study of a new ionic liquid-inspired platform.* Journal of Membrane Science, 2010. **359**: p. 37-43.

275. Wilson, D., Stenzenberger, H.D., and Hergenrother, P.M., *Polyimides*. 1990, New York: Chapman and Hall.

276. Ghosh, M.K. and Mittal, K.L., *Polyimides*. 1996, New York: Marcel Dekker Inc.

277. Xu, P. and Matsumoto, K., *Gas permeation properties of hexafluoro aromatic polyimides.* Journal of Applied Polymer Science, 1993. **47**: p. 1961-1972.

278. Xu, W., Synthesized polyimide membrnaes for pervaporation separations of toluene/iso-octane mixtures. Ph. D. Thesis from The University of Texas at Austin, 2005.

279. Martinez-Richa, A. and Vera-Graziano, R., *A solid-state NMR study of aromatic polyimides based on 4,4 '-diaminotriphenylmethane.* Journal of Applied Polymer Science, 1998. **70**(6): p. 1053-1064.

280. Xie, K., Liu, J.G., Zhou, H.W., Zhang, S.Y., He, M.H., and Yang, S.Y., *Soluble fluoro-polyimides derived from 1,3-bis(4-amino-2-trifluoromethyl- phenoxy) benzene and dianhydrides.* Polymer, 2001. **42**(17): p. 7267-7274.

Chapter 3: Materials and Experimental Methods

This section outlines the materials and experimental techniques used in this research. For synthesis methods, a typical example is given.

3.1 POLYIMIDES AND TR POLYMERS[3]

The majority of the research in this dissertation focuses on the HAB-6FDA polymer (formed by the reaction of 3,3'-dihydroxy-4,4'-diamino-biphenyl (HAB) and 2,2'-bis-(3,4-dicarboxyphenyl) hexafluoropropane dianhydride (6FDA)). The chemical structures of the monomers are shown in Figure 3.1. This structure was chosen due to the relatively high reactivity of HAB compared to other commercially available diamines. The high reactivity of HAB ensures a comparable molecular weight despite the varying synthesis route to give a better comparison of the effect of synthesis route on transport properties. The 6FDA dianhydride was chosen to increase polyimide solubility, but also due to its favorable performance in other polymeric gas separation membrane studies, including previous TR studies [1-3].

[3] Portions adapted with permission from Sanders, D.F., Guo, R., Smith, Z.P., Liu, Q., Stevens, K.A., McGrath, J.E., Paul, D.R., and Freeman, B.D., Influence of polyimide precursor synthesis route and ortho-position functional group on thermally rearranged polymers: Thermal properties and free volume. In preparation. D. F. Sanders performed the majority of experiments and wrote and edited the manuscript. Z. P. Smith, R. Guo, Q. Liu, and K. A. Stevens provided experimental assistance. B. D. Freeman, J. E. McGrath, and D. R. Paul supervised this project and provided technical expertise.

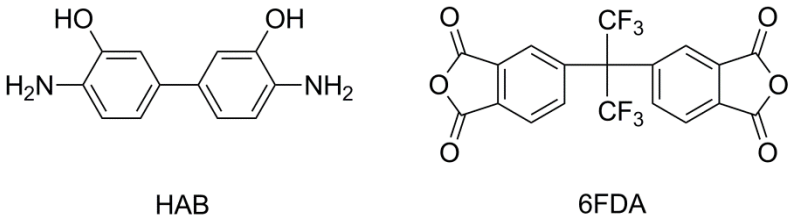

Figure 3.1 Chemical structure of HAB diamine and 6FDA dianhydride used to synthesize HAB-6FDA polyimide.

Five variations of the HAB-6FDA polyimide were prepared as precursors for TR polymers in this study to study the effects of synthesis route and *ortho*-position functional group. Figure 3.2 shows these structures and the general mechanism for the thermal rearrangement reaction.

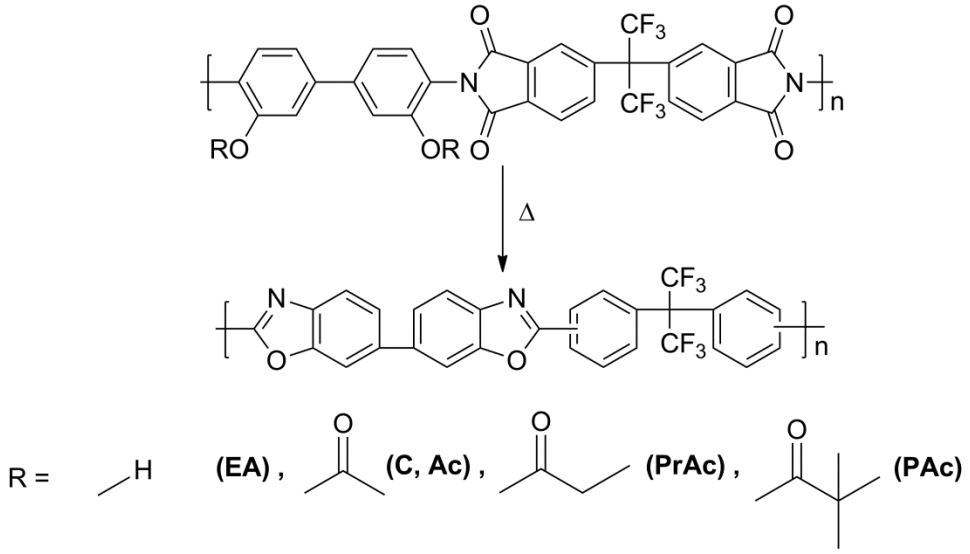

Figure 3.2 General mechanism of thermal rearrangement for structures including various ortho-position functional groups.

The five structures in Figure 3.2 include four different *ortho*-position functional groups and two different synthesis routes. HAB-6FDA polyimides containing hydroxyl (EA), acetate (Ac), propanoate (PrAc), and pivalate (PAc) *ortho*-position groups were synthesized using a thermal method with an ester-acid intermediate, which will be

described in more detail later. The Ac, PrAc, and PAc polymers were produced by a post-imidization modification of the EA polymer [4]. These groups are lost during thermal rearrangement, and the polymers form the same polybenzoxazoles (PBO) structure despite varying *ortho*-position groups (c.f. Figure 3.2). These materials were chosen to determine the effect of increasing leaving group size on the transport properties of this TR polymer.

Chemical imidization was also used to prepare an HAB-6FDA polyimide (HAB-6FDA-C). Chemical imidization is a common method for preparing polyimides, and it carried out using acetic anhydride and pyridine [5, 6]. The presence of acetic anhydride causes the conversion of *ortho*-position hydroxyl groups into acetate groups. Therefore, it is not possible to produce an HAB-6FDA polymer with hydroxyl functionality using conventional chemical imidization. This polymer, along with the EA and Ac polymers, was used to compare the effect of synthesis route on TR polymer transport properties. Both the C and Ac polymers have identical chemical structures, but they were produced through different synthesis routes. Therefore, these two polymers were used decouple the effects of synthesis route and *ortho*-position functional group on transport properties. The relationship between these two polymers and the EA polymer is shown in Figure 3.3.

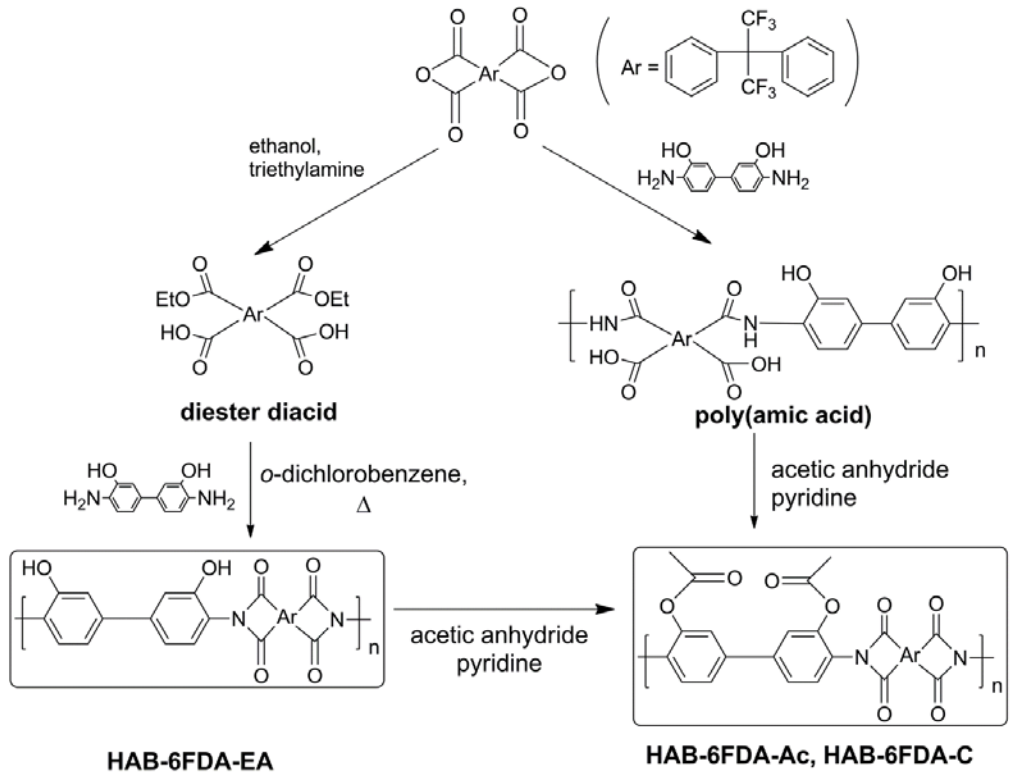

Figure 3.3 Synthesis route relationships for HAB-6FDA-EA, HAB-6FDA-Ac, and HAB-6FDA-C.

The acetate groups, or other non-hydroxyl *ortho*-position groups, are lost during thermal rearrangement, as shown in Figure 3.2, which can influence the transport properties of the resulting TR polymer [4]. The loss of these groups is believed to increase free volume and alter the free volume distribution of the resulting TR polymer. For example, TR polymers formed from acetate-containing polyimides have CO_2 permeabilities roughly three times higher than those formed from hydroxyl-containing polyimides after rearrangement at 400 ºC [4].

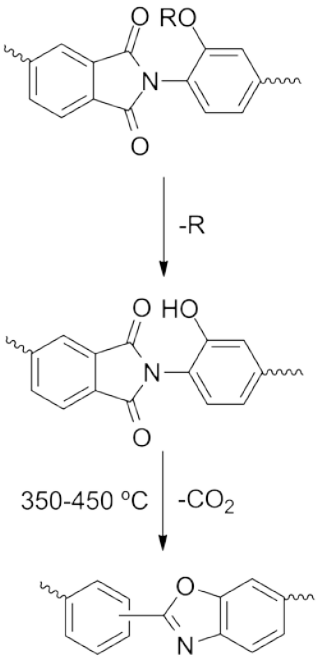

Figure 3.4 Conversion of an *ortho*-functional polyimide to a PBO via thermal rearrangement where R represents the *ortho*-position group. [7]. The conversion of the *ortho*-position group to a hydroxyl group requires H_2O, which is believed to be available in trace amounts in the polymer [8, 9].

The relative size of these *ortho*-position groups (i.e., -OR in Figure 3.2) is given by the van der Waals volumes in Table 3.1. The van der Waals volume increases from the acetate to propanoate and is largest for the pivalate group. All of these *ortho*-position groups are significantly larger than the hydroxyl group, and their varying sizes are used to determine the effect of *ortho*-position group size on the transport properties of TR polymers.

Table 3.1 van der Waals volumes of the *ortho*-position groups studied.

ortho-Position Group	van der Waals Volume (cm^3/mol)
EA	8.00
Ac	28.87
PrAc	39.10
PAc	59.55

3.1.1 Synthesis of *ortho*-Functional Polyimides

Chemical imidization was performed at the University of Texas at Austin, while ester-acid imidization was performed via collaboration with Dr. James McGrath at Virginia Tech. The following sections describe typical synthesis of the polymers used in this study.

Both HAB and 6FDA monomers and NMP (1-methyl-2-pyrrolidone) solvent were purified before use. HAB and 6FDA monomers were purchased from Chriskev (Lenexa, KS). The HAB monomer was heated in the absence of light at 50 ºC at -30 inHg overnight. The 6FDA monomer was held at 30 ºC under vacuum for 30 minutes before dehydrated air was reintroduced, and the sample was heated at 200 ºC at -10 inHg and then 120 ºC under -30 inHg vacuum overnight to restore any anhydride rings that may have been hydrolyzed. NMP (>99%) was purchased from Sigma Aldrich and distilled before use. Other reagents including *o*-dichlorobenzene (*o*-DCB), triethylamine (TEA), ethanol, methanol, various anhydrides, and pyridine were purchased from Sigma Aldrich and used as received.

3.1.1.1 Chemical Imidization

HAB-6FDA-C was synthesized via conventional chemical imidization [7, 9]. Under a UHP nitrogen atmosphere, 20 mmol of purified HAB and 44 ml of distilled

NMP were added to a three neck flask and dissolved with a mechanical stirrer. After complete dissolution, 20 mmol of purified 6FDA was added along with another 44 ml of NMP. The reaction mixture was then placed in an ice bath overnight to form a poly(amic acid). The poly(amic acid) intermediate was chemically imidized by adding 8 mol of acetic anhydride and 8 mol of pyridine per mol of HAB, stirred overnight, and then heated to 60ºC 1 hour to complete imidization.

The resulting polyimide was precipitated in methanol, vacuum filtered, and stirred in methanol for one day to extract any remaining solvent. Following extraction, the polymer was heated at 100ºC and 120ºC for one day each and 200ºC for two days to remove any remaining solvent.

3.1.1.2 Thermal Imidization via Ester-Acid Intermediate

Hydroxyl-functional polyimides (HAB-6FDA-EA) were synthesized using the ester-acid method [4, 10]. A three neck flask was equipped with a condenser, dean stark trap, mechanical stirrer, and a nitrogen purge. 6FDA monomer (6.75 mmol), 225 ml of ethanol (7-10 mol per gram 6FDA), and 4 ml of TEA catalyst were added to the three neck flask, and a Dean-Stark trap was filled with ethanol. This solution was refluxed for approximately 1 hour until the Dean-Stark trap was drained, and a viscous ester-acid solution was formed.

HAB (6.75 mmol) was dissolved in a 12% (w/v) solution of NMP and *o*-DCB (4/1 v/v), and the Dean-Stark trap was drained and filled with *o*-DCB as an azeotroping agent. This solution was heated in an oil bath to 180ºC under a nitrogen atmosphere for 24 hours to form the polyimide. The resulting polyimide was precipitated in the same manner as the chemically imidized polymer in Section 3.1.1.1.

3.1.1.3 Synthesis of Various ortho-Functional Polyimides by Chemical Modification of Hydroxyl-Functional Polyimides

Polyimides with larger *ortho*-position groups (Ac, PrAc, and PAc) were synthesized via chemical modification of the ester-acid imidized polymer (EA) using reagents similar to those that cause the *ortho*-position acetate group to form during chemical imidization [4]. In a typical synthesis, a 7% (w/v) solution of HAB-6FDA-EA in NMP with 6 mol excess anhydride per repeat unit was added to a three-neck flask equipped with an N_2 purge, condenser, and mechanical stirrer. This mixture was stirred at 110ºC for 24 hours to accelerate the modification.

3.1.2 Thermal Rearrangement of ortho-Functional Polyimides[4]

The EA, Ac, C, PrAc, and PAc samples were thermally rearranged at 350, 400, and 450ºC to study the effect of thermal rearrangement. Thermal rearrangement of film samples was performed at ambient pressure in a Carbolite Split-Tube Furnace (Carbolite, Watertown, WI, USA). A film sample, approximately 13 cm^2 in area, was placed between two ceramic plates separated by a stainless steel washer to allow the films to contract, but not curl, during thermal rearrangement. A nitrogen purge of 900 ml/min was used to maintain an inert atmosphere around the sample during thermal rearrangement. All thermal rearrangements in this study were performed by heating a sample, initially at ambient conditions, at a ramp rate of 5ºC/min to 300ºC, where the sample was held isothermally for one hour to ensure complete imidization [11]. As will be discussed later, some loss of *ortho*-position functionality can also occur during this hold. The temperature was then increased at 5ºC/min to the target thermal rearrangement

[4] Adapted from Sanders DF, Smith ZP, Ribeiro CP, Guo R, McGrath JE, Paul DR, and Freeman BD. Journal of Membrane Science 2012;409-410:232-241; Copyright Elsevier. D. F. Sanders performed the majority of experiments and wrote and edited the manuscript. Z. P. Smith, R. Guo, and C. P. Ribeiro provided experimental assistance. B. D. Freeman, J. E. McGrath, and D. R. Paul supervised this project and provided technical expertise.

temperature (350, 400, or 450ºC), where the sample was held for the desired amount of time (typically 30 minutes or one hour). The furnace was then cooled to ambient conditions at a rate no greater than 10ºC/min. This protocol was used to expose the samples to thermal histories similar to those reported in previous studies of TR polymers [2, 3]. Thermal rearrangement, and the substantial accompanying mass loss, resulted in some shrinkage of the polymer film, but the resulting films were not cracked or curled and were suitable for subsequent transport and physical property characterization.

3.1.3 Film Casting[5]

Polymer films having thicknesses between 30 and 50 μm were cast from solutions of approximately 3 wt% solids. Solutions were filtered through a 5 μm polytetrafluoroethylene filter and cast onto a flat glass plate with a glass ring attached. Film thickness was controlled by the concentration of the solution and the amount of solution added to the casting ring. Solvent and drying temperature varied between polyimides due to solubility and solvent removal temperature.

HAB-6FDA-C films were cast from DMAc (N-N-dimethylacetamide), while Ac and PAc films were cast from NMP. These films dried at 80ºC overnight in ambient atmosphere to remove the bulk of the solvent and then at 200ºC overnight under full vacuum to remove any residual solvent. EA samples were also cast from NMP, but the second drying step was increased to 260ºC under full vacuum to completely remove solvent. The mass loss from thermogravimetric analysis (TGA) due to solvent loss and thermal rearrangement could not be decoupled for the PrAc sample when using NMP and

[5] Adapted from Sanders DF, Smith ZP, Ribeiro CP, Guo R, McGrath JE, Paul DR, and Freeman BD. Journal of Membrane Science 2012;409-410:232-241; Copyright Elsevier. Copyright Elsevier. D. F. Sanders performed the majority of experiments and wrote and edited the manuscript. Z. P. Smith, R. Guo, and C. P. Ribeiro provided experimental assistance. B. D. Freeman, J. E. McGrath, and D. R. Paul supervised this project and provided technical expertise.

DMAc as a solvent, so this polymer was cast from methylene chloride and dried at 80ºC overnight in ambient and then at 200ºC under full vacuum overnight. Solvent removal was confirmed using thermogravimetric analysis. When the mass loss peak prior to thermal rearrangement was no longer visible, it was determined that there was a negligible amount of solvent remaining in the film.

3.2 EXPERIMENTAL METHODS[6]

3.2.1 Pure Gas Permeability

Gas permeability coefficients of H_2, CO_2, O_2, N_2, and CH_4 were measured using a constant volume, variable pressure method [12]. The gases were tested in the order listed to prevent conditioning of the polymer by CO_2. The upstream pressure in the system was measured using a STJE 1000 psig pressure transducer (Honeywell Sensotec, Columbus, Ohio). The film to be studied was mounted in a 47mm HP Filter Holder (Millipore, Billerica, MA). Membranes were masked with aluminum tape or a brass sheet and sealed with epoxy (Devcon, No. 145250, Danvers, MA) to provide a well-defined area. The sample area was measured by scanning the film and calculating the area using ImageJ (http://rsb.info.nih.gov/ij/index.html). Film thickness was measured using a Mitutoyo Depth Gauge. The downstream pressure was kept below 10 torr using a vacuum pump, and it was measured using a Baratron 626A 10 torr capacitance manometer (MKS, Andover, MA, USA). All data were recorded using National Instruments LabVIEW Software. Pure gas permeability coefficients were measured at feed pressures ranging

[6]Sections adapted from Sanders DF, Smith ZP, Ribeiro CP, Guo R, McGrath JE, Paul DR, and Freeman BD. Journal of Membrane Science 2012;409-410:232-241; Copyright Elsevier and Smith ZP, Sanders DF, Ribeiro CP, Guo R, Freeman BD, Paul DR, McGrath JE, and Swinnea S. Journal of Membrane Science 2012;415-416:558-567; Copyright Elsevier. Copyright Elsevier. D. F. Sanders performed the majority of experiments and wrote and edited the manuscript. Z. P. Smith, R. Guo, and C. P. Ribeiro, S. Swinnea provided experimental assistance and technical expertise. B. D. Freeman, J. E. McGrath, and D. R. Paul supervised this project and provided technical expertise.

from approximately 3 to 16 atm. All measurements were made at 35ºC with UHP grade gases from Airgas (Radnor, PA, USA).

3.2.2 Density Measurement

Density was measured using an Ametek Two Column Density Gradient Column (Ametek TCI Division, Largo, Florida). Columns were prepared from solutions of water and calcium nitrate, and experiments were performed according to ASTM D1505-10 [13]. Three small pieces (approximately 1 cm^2) of each film were introduced into the column and allowed to equilibrate for 24 hours before measurement. Density was also measured using a Mettler Toledo benchtop density gradient kit (for AX/AT/AG balances, Mettler Toledo, Greifensee, Switzerland) with *n*-heptane as the reference fluid. This fluid was chosen because all four samples considered in this study exhibited very low *n*-heptane uptakes over the time scale of the density measurement.

3.2.3 Thermogravimetric Analysis and Mass Spectrometry

Thermogravimetric Analysis (TGA) was performed using a TA Instruments Q500 (Newcastle, DE, USA). A UHP nitrogen purge (40 ml/min balance, 60 ml/min sample) was used to maintain an inert atmosphere during the TGA experiments. A 30 minute isothermal hold was used before experiments to ensure stability and remove any water that may be present. All samples were run under a nitrogen atmosphere with a heating rate of 5ºC/min unless otherwise noted.

The evolved gas from the TGA was analyzed with a Pfeiffer Thermostar GSD-320 mass spectrometer with a capillary temperature of 200 ºC to prevent any condensation. TGA-MS analysis was typically performed in two steps. The first step was a “bargraph” scan where masses of 10 to 100 amu were analyzed. This step was used to determine which masses were present due to thermal rearrangement. Once these masses

were identified, an “MID” scan was used to look specifically at these masses and provide a higher resolution scan.

3.3 REFERENCES

1. Koros, W.J. and Fleming, G.K., *Membrane-based gas separation.* Journal of Membrane Science, 1993. **83**(1): p. 1-80.

2. Park, H.B., Han, S.H., Jung, C.H., Lee, Y.M., and Hill, A.J., *Thermally rearranged (TR) polymer membranes for CO_2 separation.* Journal of Membrane Science, 2010. **359**(1-2): p. 11-24.

3. Park, H.B., Jung, C.H., Lee, Y.M., Hill, A.J., Pas, S.J., Mudie, S.T., Van Wagner, E., Freeman, B.D., and Cookson, D.J., *Polymers with cavities tuned for fast selective transport of small molecules and ions.* Science, 2007. **318**(5848): p. 254-258.

4. Guo, R., Sanders, D.F., Smith, Z.P., Freeman, B.D., Paul, D.R., and McGrath, J.E., *Synthesis and Characterization of Thermally Rearranged (TR) Polymers: Influence of ortho-positioned functional groups of polyimide precursors on TR process and gas transport properties.* Journal of Materials Chemistry A, 2013. **1**: p. 262-272.

5. Ghosh, M.K. and Mittal, K.L., *Polyimides*. 1996, New York: Marcel Dekker Inc.

6. Wilson, D., Stenzenberger, H.D., and Hergenrother, P.M., *Polyimides*. 1990, New York: Chapman and Hall.

7. Sanders, D.F., Smith, Z.P., Ribeiro, C.P., Guo, R., McGrath, J.E., Paul, D.R., and Freeman, B.D., *Permeability, diffusivity, and free volume of thermally rearranged polymers based on 3,3'-dihydroxy-4,4'-diamino-biphenyl (HAB) and 2,2'-bis-(3,4-dicarboxyphenyl) hexafluoropropane dianhydride (6FDA).* Journal of Membrane Science, 2012. **409-410**: p. 232-241.

8. Guo, R., Sanders, D.F., Smith, Z.P., Freeman, B.D., and McGrath, J.E., *Synthesis and characterization of thermally rearranged (TR) polymer membranes: The effects of ortho-positioned functional group of polyimide precursors.* submitted, 2012.

9. Smith, Z.P., Sanders, D.F., Ribeiro, C.P., Guo, R., Freeman, B.D., Paul, D.R., McGrath, J.E., and Swinnea, S., *Gas sorption and characterization of thermally*

rearranged polyimides based on 3,3'-dihydroxy-4,4'-diamino-biphenyl (HAB) and 2,2'-bis-(3,4-dicarboxyphenyl) hexafluoropropane dianhydride (6FDA). Journal of Membrane Science, 2012. **415-416**: p. 558-567.

10. Moy, T.M., DePorter, C.D., and McGrath, J.E., *Synthesis of soluble polyimides and functionalized imide oligomers via solution imidization of aromatic diester-diacids and aromatic diamines.* Polymer, 1993. **34**(4): p. 819-824.

11. Ohya, H., Kudryavtsev, V.V., and Semenova, S.I., *Polyimide membranes - applications, fabrications, and properties*. 1996: Gordon and Breach.

12. Lin, H.Q. and Freeman, B.D., *Permeation and diffusion* in *Springer handbook for materials measurement methods*, H. Czichos, T. Saito, and L. Smith, Editors. 2011, Springer: Berlin. p. 426-444.

13. *ASTM D1505-10. Standard Test Method for Density of Plastics by the Density-Gradient Technique*, 2010.

Chapter 4: Permeability, Diffusivity, and Solubility of Chemically Imidized HAB-6FDA[7]

4.1 INTRODUCTION

Pure gas permeability, diffusivity, and solubility in chemically imidized HAB-6FDA (HAB-6FDA-C) were studied to determine the fundamental causes of permeability increases in TR polymers due to thermal rearrangement. The permeability, solubility, and free volume were measured as a function of thermal conversion, and the diffusivity was calculated using the solution-diffusion model to determine how the material and its transport properties changed as thermal rearrangement occurred.

4.2 THERMAL REARRANGEMENT

The thermal treatment conditions for samples used in gas permeability and density studies were established by first characterizing the thermal rearrangement process via TGA. The thermal profile used in the TGA studies and results for several samples are presented in Figure 4.1a. To mimic the thermal history applied to samples in the split tube furnace, samples in the TGA were heated from ambient conditions to 300ºC at a ramp rate of 5°C/min, and then the sample was held at 300ºC for one hour. This procedure ensures complete imidization of the sample before rearrangement [1]. Afterwards, temperature was increased to the desired thermal rearrangement temperature, T_2, (350, 400, 425, or 450ºC) at a ramp rate of 5°C/min. Then, the sample was held isothermally at the desired thermal rearrangement temperature, T_2, for ten hours (i.e., t_2=10 hours in Figure 4.1(a)).

[7] Adapted from Sanders, D.F., Smith, Z.P., Ribeiro, C.P., Guo, R., McGrath, J.E., Paul, D.R., and Freeman, B.D., Permeability, diffusivity, and free volume of thermally rearranged polymers based on 3,3'-dihydroxy-4,4'-diamino-biphenyl (HAB) and 2,2'-bis-(3,4-dicarboxyphenyl) hexafluoropropane dianhydride (6FDA). Journal of Membrane Science, 2012. 409-410: p. 232-241.; copyright Elsevier. D. F. Sanders performed the majority of experiments and wrote and edited the manuscript. Z. P. Smith, R. Guo, and C. P. Ribeiro provided experimental assistance. B. D. Freeman, J. E. McGrath, and D. R. Paul supervised this project and provided technical expertise.

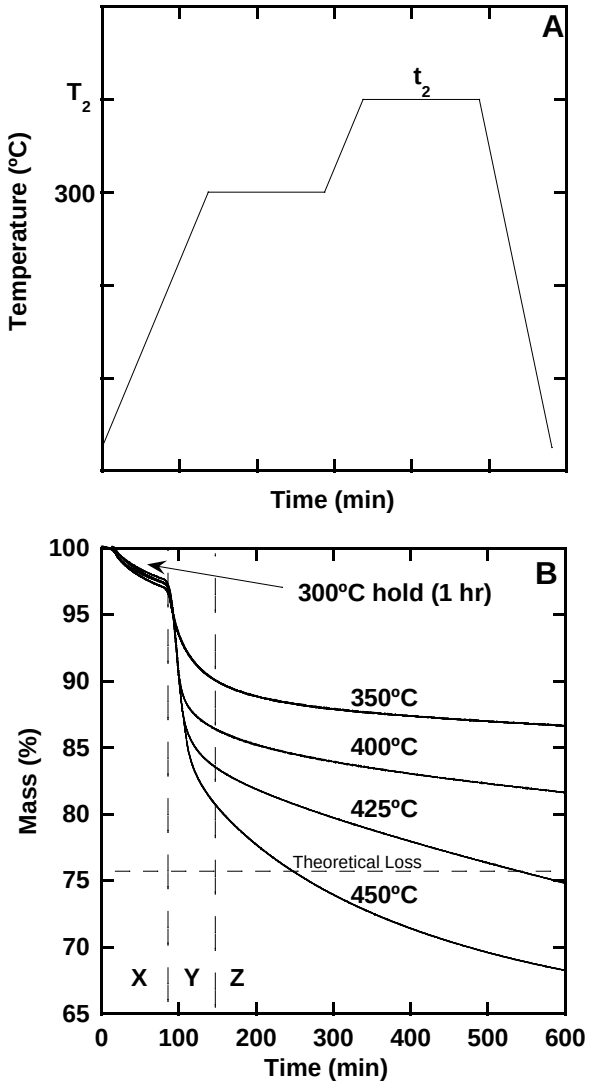

Figure 4.1 (a) Heating protocol for thermal rearrangement. (b) Mass loss during the thermal rearrangement protocol for HAB-6FDA polymers using the TGA where t_2 = 10 hours and T_2 is labeled on the corresponding curve. Time=0 is selected to be when T=200ºC. Vertical lines separate regions of acetate loss (X), thermal rearrangement (Y), and thermal degradation (Z). The dashed line labeled "Theoretical Mass Loss" corresponds to the mass loss expected if the thermal rearrangement occurs as indicated in the Materials and Methods section.

Three features in Figure 4.1(b) provide information regarding the thermal rearrangement of HAB-6FDA. The first region, below approximately 95 minutes (labeled "X" in Figure 4.1(b)), shows a slight mass loss during the 300ºC hold. This mass loss is attributed to conversion of some of the ortho-position acetate groups to hydroxyl functionality, as shown in Figure 4.1, which is believed to be the precursor to the ultimate conversion of the ortho-position hydroxyl groups to the final PBO structure discussed in the materials and methods section [2]. This acetate conversion is believed to take place due to the presence of trace amounts of water in the polymer. The acetic acid byproduct has been observed via ^{1}H-NMR, and further details regarding this mechanism are reported elsewhere [3]. The second region (labeled "Y" in Figure 4.1(b)), at times longer than approximately 95 minutes, contains a substantial mass loss ascribed to thermal rearrangement of the ortho-functional polyimide to the associated PBO (cf., Figure 3.1) [4-6]. The magnitude of this mass loss depends on rearrangement temperature. The third region (labeled "Z" in Figure 4.1(b)), at times beyond approximately 150 minutes, shows a continuous, approximately linear mass loss that is more rapid at higher temperatures. This mass loss is believed to mark, at least in part, the onset of thermal degradation of the polymer when held for long periods of time at high temperatures. At treatment temperatures of 425 and 450ºC, the mass loss increases beyond the value expected if thermal rearrangement were the only mechanism for mass loss, so we assume that thermal degradation must occur either following or alongside thermal rearrangement at these temperatures. The resulting films were brittle after 10 hours, which we have taken as an indication that the polymer was undergoing thermal degradation. The maximum mass loss labeled in Figure 4.1(b) ("Theoretical Mass Loss"), which is 24.3%, corresponds to the mass loss associated with complete conversion of the starting polymer to the final polybenzoxazole structure. Long heat treatment times, even at lower thermal

treatment temperatures of 350 and 400°C, which do not result in mass losses beyond that expected for complete thermal rearrangement (i.e., towards the right hand side of region "Z" in Figure 4.1(b)), also result in brittle films, which we speculate further supports the hypothesis that at least some thermal degradation is occurring. However, we cannot rule out the possibility that further rearrangement at these temperatures may also be contributing to the decrease in mechanical properties in these films.

Based upon this TGA screening study, thermal treatment protocols were selected to ensure that samples used for permeation and density studies experienced minimal thermal degradation. In these cases, samples large enough for permeation and density measurements were thermally rearranged in a split-tube furnace. The time that the samples were held at the desired rearrangement temperature was selected to be shortly after the rapid mass loss associated with thermal rearrangement, between approximately 100 and 150 minutes in Figure 4.1(b), to minimize thermal degradation. The filled circles in Figure 4.2 denote the times chosen for thermal treatment at the desired rearrangement temperature for rearrangement temperatures of 350 (1 hr), 400 (1 hr), and 450°C (30 min). These protocols were selected so that transport property changes would be due principally to thermal rearrangement and not due to polymer degradation. The mass loss results were used to estimate the conversion of the polyimide precursor to the final PBO TR structure because, if there is no significant thermal degradation, all mass loss should be due to thermal rearrangement. In this regard, Equation 4.1 was used to estimate the percent conversion of the polyimide precursor to TR polymer:

$$\%\,\text{Conversion} = \frac{\text{Actual Mass Loss}}{\text{Theoretical Mass Loss}} x100 \tag{4.1}$$

Using Equation 4.1 and the TGA results, conversion was estimated for polymer films after undergoing the thermal treatments selected from TGA experiments, and the

resulting values are recorded in Table 4.1. Conversions range from 39% to 76% and were consistent when measured in both the TGA and the furnace. Conversions higher than 76% were not pursued to minimize thermal degradation.

Table 4.1 Percent conversion of samples used to characterize HAB-6FDA TR polymer transport properties.

Treatment Temperature (ºC)	Treatment Time (min)	Conversion (%)
-	-	0
350	60	39
400	60	60
450	30	76

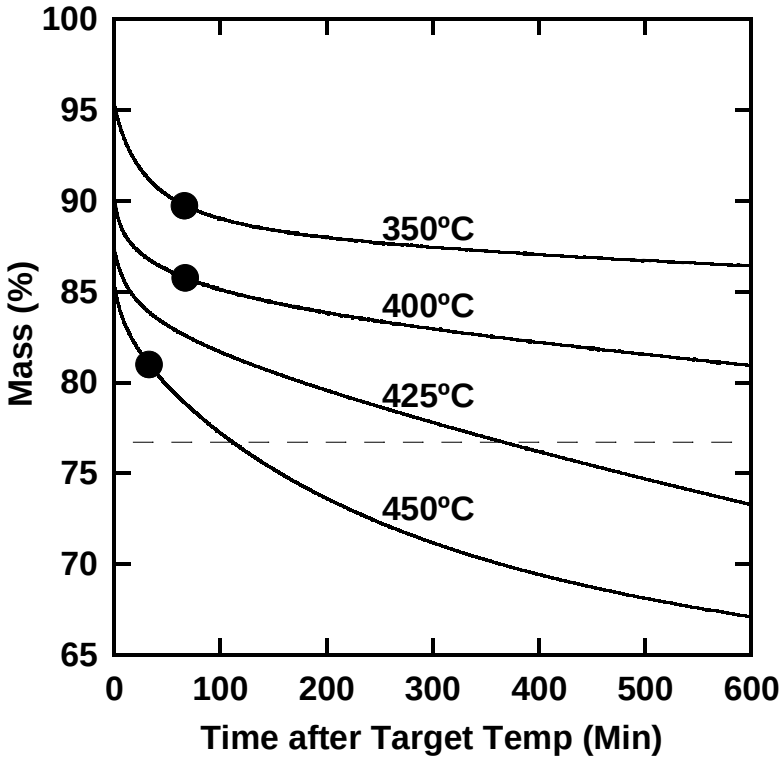

Figure 4.2 TGA thermograms showing mass loss as a function of time that the sample was held at the rearrangement target temperature, T2. Values of T2 are given in the figure. Samples prepared at the conditions indicated by the filled circles were used for transport property characterization.

The loss of the acetate group, leaving a hydroxyl group in its place, likely occurs before the resulting hydroxyl groups undergo thermal rearrangement to reach the final benzoxazole structure. This conversion can be observed by the appearance of hydroxyl peaks in FT-IR measurements after thermal conversion [2]. This measure of conversion does not distinguish between loss of the acetate group and conversion of the resulting hydroxyl groups to benzoxazole structures.

4.3 Pure Gas Permeability and Selectivity

Pure gas permeabilities of CH_4, N_2, O_2, CO_2, and H_2 were measured at pressures ranging from 3-16 atm at 35ºC. Table 4.2 presents pure gas permeability coefficients of HAB-6FDA polyimide and its partially converted TR analogs at a feed pressure of 10 atm. Uncertainties were calculated using propagation of error. As conversion increases, permeability increases. For example, CO_2 permeability increases by nearly a factor of three after treatment at 350ºC for one hour, which corresponds to 39% conversion. After thermal rearrangement at 450ºC for 30 minutes, CO_2 permeability increases by more than a factor of 30. The relative increase in gas permeability is highest for methane and lowest for hydrogen. Thus, the extent of permeability increase with conversion is greater in molecules with larger kinetic diameters [7]. If a central feature of the TR conversion process is to increase average free volume, this trend is reasonable and consistent with previous reports on TR polymers [4].

For many separations, pure gas selectivity in TR polymers decreases as conversion increases, as reported previously by Park et al. for polymers imidized in the solid state from poly(amic acids) [8]. As shown in Table 4.3, the TR350 sample shows only a slight loss in gas selectivity compared to the polyimide precursor, except for

CO_2/CH_4, which shows an increase in selectivity. This result may be due to a more favorable free volume distribution, which improves the separation performance of the polymer.

Table 4.2 Pure gas permeability (Barrer) of HAB-6FDA polyimide and TR polymers at 10 atm and 35ºC. Uncertainties were estimated using the propagation of errors method [9].

Sample	Conversion (%)	CH_4	N_2	O_2	CO_2	H_2
HAB-6FDA	0	0.313 ± 0.007	0.56 ± 0.01	3.18 ± 0.07	12.0 ± 0.3	37.8 ± 0.9
TR350	39	0.77 ± 0.01	1.62 ± 0.03	8.9 ± 0.2	35.3 ± 0.6	95 ± 2
TR400	60	5.6 ± 0.4	8.7 ± 0.6	39 ± 3	160 ± 10	290 ± 20
TR450	76	18.2 ± 0.4	25.3 ± 0.6	100 ± 2	410 ± 10	530 ± 10

Table 4.3 Pure gas selectivity of HAB-6FDA polyimide and TR polymers at 10 atm and 35ºC. Uncertainties were estimated using the propagation of errors method [9].

Sample	CO_2/CH_4	O_2/N_2	CO_2/N_2	H_2/N_2
Polyimide	38 ± 1	5.7 ± 0.2	21.6 ± 0.7	68 ± 2
TR350	46 ± 1	5.5 ± 0.2	21.7 ± 0.5	58 ± 2
TR400	28 ± 3	4.5 ± 0.5	18.2 ± 0.2	33 ± 3
TR450	22.4 ± 0.7	3.9 ± 0.1	16.1 ± 0.5	21.0 ± 0.6

Figures 4.3 and 4.4 present permeability and pure gas CO_2/CH_4 selectivity as a function of conversion of the API to its PBO. From these results, permeability becomes increasingly sensitive to conversion as conversion increases. Selectivity seems to become less sensitive to conversion at higher conversions; for example, the selectivity decreases by 35% as conversion increases from 39 to 60%, while selectivity only decreases by 17% as conversion increases from 60 to 76%. Based on this result, to

achieve high permeability/selectivity combinations, it may be of interest to consider polymers that rearrange to high conversion without significant thermal degradation.

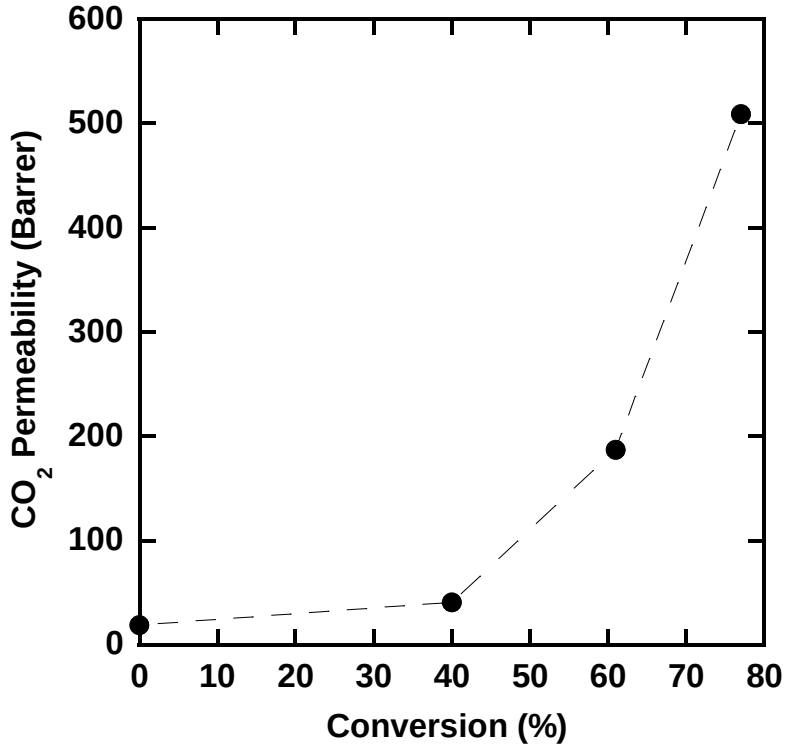

Figure 4.3 CO_2 permeability as a function of TR conversion.

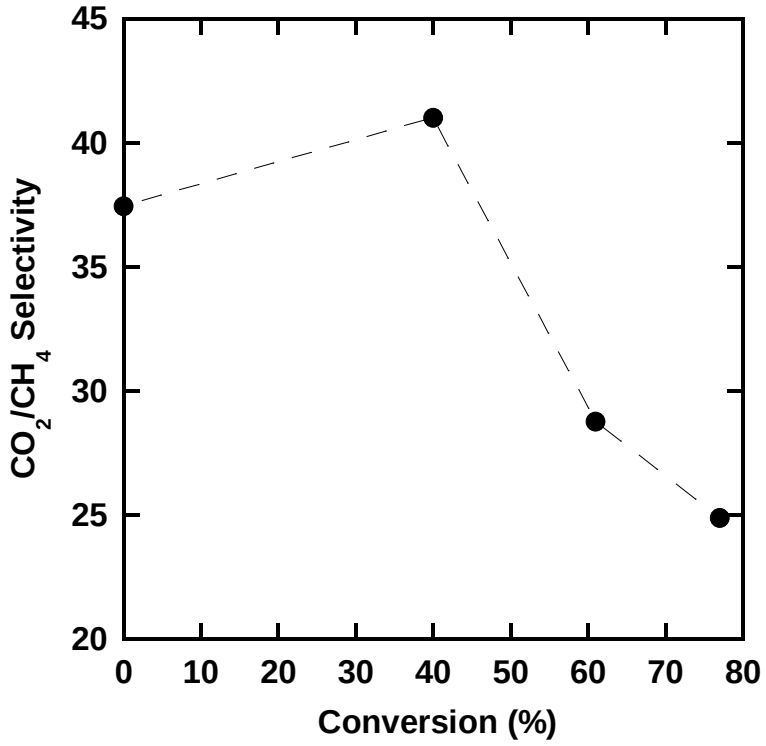

Figure 4.4 CO_2/CH_4 pure gas selectivity as a function of TR conversion.

One way to determine whether permeability is simply being exchanged for selectivity in the TR conversion process is to compare the permeability and selectivity values on an upper bound plot. Figure 4.5 presents Robeson's 1991 and 2008 upper bounds for CO_2/CH_4 separation [10, 11]. Comparing the changes in permeability and selectivity with the upper bound lines, thermal rearrangement moves gas transport properties of the HAB-6FDA polymers across the 1991 upper bound and closer to the 2008 upper bound, so thermal rearrangement improves the permeability/selectivity combinations of these materials.

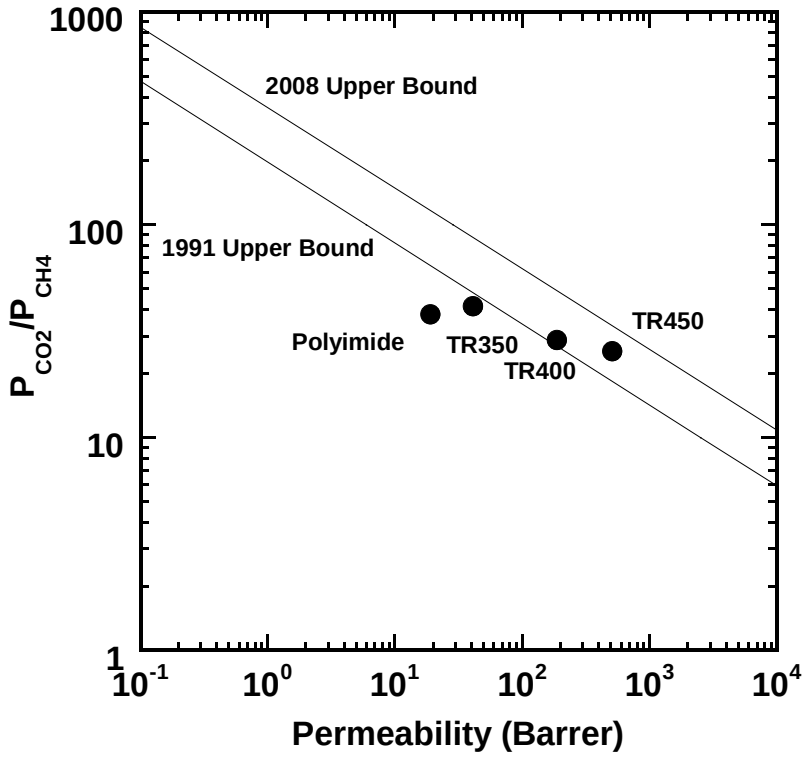

Figure 4.5 Permeability/selectivity properties of HAB-6FDA polyimide and TR polymers compared with 1991 and 2008 upper bounds [10, 11].

As shown in Figures 4.6-4.8, permeability was also measured at feed pressures ranging from approximately 3 to 16 atm. Permeability decreases with increasing pressure, most notably for more condensable gases such as CO_2 and CH_4. This behavior is typical for glassy polymers [12]. No plasticization behavior was observed for CO_2 up to 16 atm in these pure gas studies, and permeability decreased or was constant with increasing pressure, suggesting that no defects were introduced into the films during thermal rearrangement.

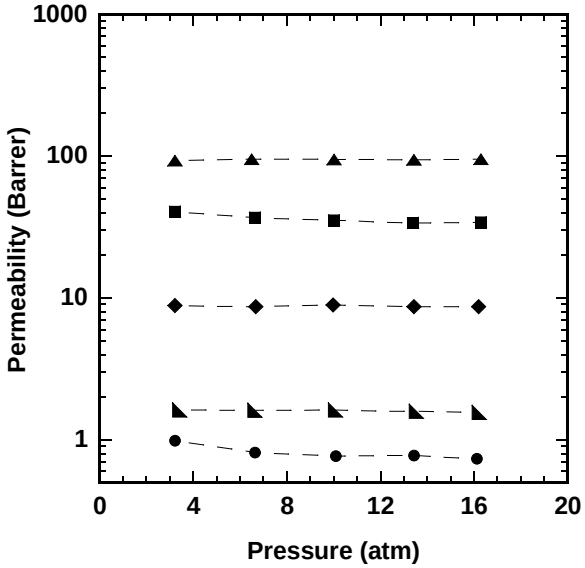

Figure 4.6 Permeability as a function of feed pressure for HAB-6FDA-TR350 at 35ºC.

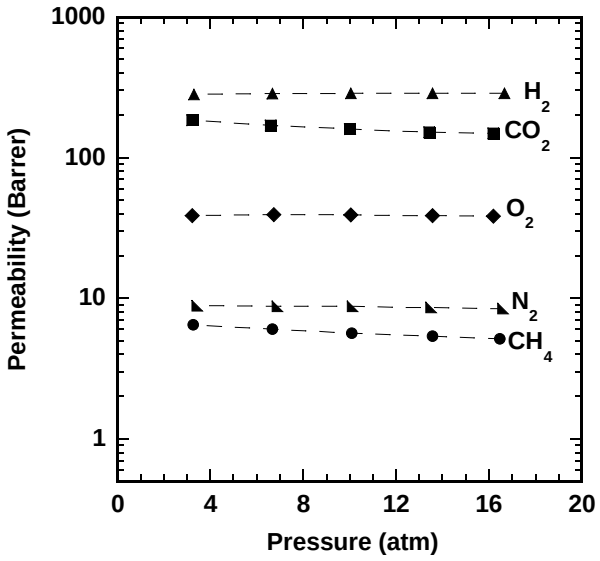

Figure 4.7 Permeability as a function of feed pressure for HAB-6FDA-TR400 at 35ºC.

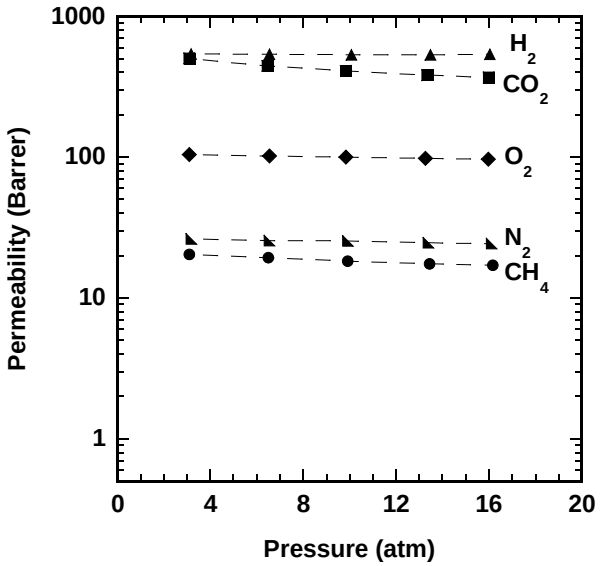

Figure 4.8 Permeability as a function of feed pressure for HAB-6FDA-TR450 at 35ºC.

The permeabilities of HAB-6FDA TR polymers reported in this study were nearly an order of magnitude lower than those of the APAF-6FDA based TR polymers reported by Han et al., which were also synthesized using chemical imdization [13]. Polymers containing many 6F linkages typically exhibit higher gas permeabilities than other polymers, such as those containing HAB [8, 14]. TR polymers explored by Han et al. were thermally rearranged at 450ºC for one hour, which would result in some thermal degradation in the HAB-6FDA polymers used in this study; therefore, identical heat treatment protocols were not pursued. The extent of conversion to the TR polymer was not reported by Han et al., so comparison of changes in permeability at fixed conversion is also not possible. Han et al. also measured permeability at a lower upstream pressure and temperature than used in our studies. Lower pressure increases permeability due to dual-mode effects while lower temperature commonly decreases permeability in polymers due to restricted chain motion. These differences in measurement conditions also make a quantitative comparison of permeabilities difficult.

4.4 PERMEABILITY, DIFFUSIVITY, AND SOLUBILITY

Permeability in dense polymer films can be described by the solution-diffusion model as shown in Equation 4.2 [15]:

$$P = D \text{ x } S \tag{4.2}$$

where P is the gas permeability, D is the diffusion coefficient, S is the solubility coefficient, and all are typically dependent on pressure in glassy polymer such as those considered in this study [2].

The permeability of HAB-6FDA polyimide and its corresponding TR polymers was measured, and, using solubility coefficients reported elsewhere [2], diffusivity values were calculated using Equation 4.2. Table 4.4 presents representative P, D and S values for CH_4, N_2, O_2, CO_2, and H_2 at 10 atm and 35ºC. These results indicated that the increase in diffusivity with conversion is the dominant contribution to the observed increase in gas permeability. Solubility also increases as conversion increases, but not to the same extent as diffusion coefficients. For example, diffusivity for all gases increases by approximately an order of magnitude, while solubility typically increases by approximately a factor of approximately two as conversion increases from 0 to 76%.

Table 4.4 Permeability, Diffusivity, and Solubility for HAB-6FDA polyimide and TR polymers at 10 atm at 35ºC. Uncertainties were estimated using the propagation of errors method [9].

Gas	Sample	Permeability (Barrer)	Solubility (cm^3(STP)/ (cm^3 polymer atm)[2]	Diffusivity $\times 10^9$ (cm^2/s)
CH_4	Polyimide	0.313 ± 0.007	1.07 ± 0.08	2.2 ± 0.2
	TR 350	0.77 ± 0.01	1.65 ± 0.09	3.5 ± 0.2
	TR 400	5.6 ± 0.4	2.6 ± 0.1	17 ± 1
	TR 450	18.2 ± 0.4	2.8 ± 0.1	50 ± 2
N_2	Polyimide	0.56 ± 0.01	0.44 ± 0.08	10 ± 2
	TR 350	1.62 ± 0.03	0.69 ± 0.08	18± 2
	TR 400	8.7 ± 0.6	1.11 ± 0.09	60 ± 6
	TR 450	25.3 ± 0.6	1.18 ± 0.09	160 ± 10
O_2	Polyimide	3.18 ± 0.07	0.60 ± 0.08	40 ± 5
	TR 350	8.9 ± 0.2	0.94 ± 0.08	72 ± 6
	TR 400	39 ± 3	1.42 ± 0.09	210 ± 20
	TR 450	100 ± 2	1.52 ± 0.09	500 ± 30
CO_2	Polyimide	12.0 ± 0.3	4.04 ± 0.09	22.6 ± 0.8
	TR 350	35.3 ± 0.6	5.18 ± 0.09	52 ± 1
	TR 400	160 ± 10	6.7 ± 0.1	180 ± 10
	TR 450	410 ± 10	7.0 ± 0.1	440 ± 10
H_2	Polyimide	37.8 ± 0.9	0.21 ± 0.07	1400 ± 400
	TR 350	95 ± 2	0.25 ± 0.07	2800 ± 900
	TR 400	290 ± 20	0.35 ± 0.09	6000 ± 2000
	TR 450	530 ± 10	0.35 ± 0.08	11000 ± 3000

Table 4.5 compares P, D, and S values for CO_2 of the HAB-6FDA series of polymers with values from Matrimid® and cellulose acetate, materials similar to those used commercially for natural gas separation [16-19]. HAB-6FDA exhibits much higher CO_2 permeabilities after thermal rearrangement while maintaining good CO_2/CH_4 selectivity values. For example, the HAB-6FDA-TR400 sample has a CO_2 permeability of 160 Barrer compared to 10 and 4.8 Barrer for Matrimid® and cellulose acetate, respectively. The CO_2/CH_4 selectivity is comparable for all samples, with the Matrimid® polyimide having the highest selectivity at 35, cellulose acetate following at 32, and the

HAB-6FDA-TR400 sample having a selectivity of 29. The permeability and selectivity values of TR polymer are tunable by thermal treatment temperature and time. The TR350 sample has a selectivity of 45, higher than that of either Matrimid® or cellulose acetate polymers, and it has a CO_2 permeability of approximately 35.3 Barrer, more than three times higher than that of Matrimid® polyimide and approximately 6 times higher than that of cellulose acetate.

Table 4.5 Permeability, diffusivity, and solubility coefficients of HAB-6FDA polyimide and TR polymers compared to common polymers used in natural gas separations. Data are reported at 10 atm and 35ºC unless otherwise noted. [a] P from Vu, Koros, and Miller[19]; S from Moore and Koros[17] at 3 atm.[b] Data from Puleo, Paul, and Kelley[18] at 1 atm.

Sample	**P_{CO_2} [Barrer]**	**P_{CO_2}/P_{CH_4}**	**$D_{CO_2}\times10^9$ (cm^2/s)**	**S (cm^3gas(STP)/ (cm^3polymer(atm))[2]**
Matrimid® polyimide[a]	10	36	42	1.8
Cellulose acetate[b]	4.8	32	77	0.46
Polyimide	12	40	23	4.05
TR350	35.3	45	52	5.18
TR400	160	29	180	6.7
TR450	410	24	440	7.0

The changes in selectivity as conversion increases can also be interpreted within the framework of the solution-diffusion model. Because permeability depends upon solubility and diffusivity, permeability selectivity can be separated into solubility selectivity and diffusivity selectivity. Table 4.6 presents pure gas diffusivity and solubility selectivity for CO_2/CH_4 at 35ºC and 10 atm. From these results, solubility selectivity decreases as thermal treatment temperature increases, but diffusivity selectivity reaches a maximum at a treatment temperature of 350ºC. This maximum in selectivity may reflect a more favorable cavity size and free volume distribution for this

gas pair. Table 4.6 also shows the solubility and diffusivity selectivities of Matrimid® and cellulose acetate polymers. In general, the HAB-6FDA-TR polymers show lower solubility selectivities and higher diffusivity selectivities than Matrimid® and cellulose acetate polymers, so these TR polymers are more effective at separating gases based on size, but less effective at separating based on solubility differences.

Table 4.6 CO_2/CH_4 diffusivity and solubility selectivity of HAB-6FDA polyimide and TR polymers. Data are reported at 10 atm and 35ºC unless otherwise noted. [a]P from Vu, Koros, and Miller [19], S from Moore and Koros [17] at 3 atm. [b]Data from Puleo, Paul, and Kelley [18] at 1 atm.

Sample	P_{CO_2}/P_{CH_4}	D_{CO_2}/D_{CH_4}	S_{CO_2}/S_{CH_4}
Matrimid® Polyimide[a]	36	2	15.3
Cellulose Acetate[b]	32	4	8.2
Polyimide	38	12	3.8
TR350	46	14	3.1
TR400	28	11	2.6
TR450	22	9	2.5

Table 4.7 shows that a maximum in CO_2/CH_4 selectivity occurs for the TR350 sample. This maximum also occurs for all gas pairs containing methane, but for gas pairs not including methane, no maximum is observed. These data suggest that the cavity size and free volume distribution in these TR polymers are favorable for separations involving methane. As expected, the selectivities shown in Table 4.7 are also highest for gas pairs with the largest difference in kinetic diameter. For higher treatment temperatures, such as 450ºC, both diffusivity and solubility selectivities are approximately 25% lower than in HAB-6FDA polyimide, so decreases in permeability selectivity are due to diffusivity and solubility increasing more for CH_4 as a function of conversion than for CO_2.

Table 4.7 Pure gas methane permeability selectivities for HAB-6FDA polyimide and TR polymers at 10 atm and 35ºC. Uncertainties were estimated using the propagation of errors method [9].

Sample	**N_2/CH_4**	**O_2/CH_4**	**CO_2/CH_4**	**H_2/CH_4**
Polyimide	1.77 ± 0.05	10.1 ± 0.3	38 ± 1	120 ± 4
TR350	2.11 ± 0.04	11.6 ± 0.3	46 ± 1	123 ± 3
TR400	1.6 ± 0.2	6.9 ± 0.7	28 ± 3	51 ± 5
TR450	1.39 ± 0.04	5.5 ± 0.2	22.4 ± 0.7	29.3 ± 0.8

4.5 FRACTIONAL FREE VOLUME

Fractional free volume was estimated using Equation 4.3 [20]:

$$FFV = \frac{V - V_O}{V} \tag{4.3}$$

where V_o is the so-called occupied volume of the polymer chains [21, 22]. V is the specific volume, which is the inverse of the density of the polymer. V_o is determined using a group contribution method as follows:

$$V_O = 1.3\sum V_W \tag{4.4}$$

where V_w is the van der Waal's volume of molecular groups comprising the polymer backbone [21, 22].

Previously, density of TR polymers was measured using a density determination kit for an analytical balance [8]. In this method, based on Archimedes' principle, the polymer sample was weighed in air and in water, and the density of the polymer was inferred from the difference of the sample weight in air and in water [8]. In this study, density was measured using: (1) a density gradient column and (2) a density determination kit and an analytical balance. However, for the analytical balance method, *n*-heptane was used as the auxiliary liquid to minimize any artifacts that might arise due to water uptake by the sample. This hydrocarbon, a much larger molecule than water, was not sorbed to a measurable extent in the samples during the measurements.

Table 4.8 presents density values obtained using the density gradient column method. These results may be influenced by any water sorbed by the samples during the measurement, as water uptake could potentially alter the overall density of a sample. Density determination using the density kit and an analytical balance provides more flexibility in the choice of the liquid used for the measurement, and a fluid that does not interact with the polymer can be more easily chosen. However, this method is generally

less precise than the density gradient column method, yielding density values accurate to approximately ±0.01 g/cm^3 rather than approximately ±0.0003 g/cm^3 in the case of the density gradient column.

Table 4.8 Density of HAB-6FDA polyimide and TR polymer density using density gradient column without corrections for water uptake. Uncertainties were calculated as the standard deviation of at least three repeat measurements.

Sample	Density (g/cm^3)
Polyimide	1.4255 ± 0.0004
TR350	1.4404 ± 0.0002
TR400	1.4010 ± 0.0003
TR450	1.3586 ± 0.0002

The density of the TR350 sample, as measured by the density gradient column, is higher than that of the polyimide, while densities of TR polymers rearranged at higher temperatures are lower than that of the initial polyimide. This higher density measured in the column is attributed to an increased presence of hydroxyl groups from monomers that lost ortho-position acetate groups, but did not go undergo thermal rearrangement to form the final benzoxazole. The presence of these hydroxyl groups may influence the water uptake by the polymer and alter the measured density.

The equilibrium water uptake of HAB-6FDA polyimide and its TR polymers are recorded in Table 4.9. Both the polyimide and TR400 sample show relatively low water uptake values of 0.5%, while the TR350 and TR450 samples show much higher water uptakes of 2.9% and 2.1% respectively. The increased water uptake in the TR350 sample is consistent with an increased number of hydroxyl groups present from the conversion of ortho-position acetate groups to ortho-position hydroxyl groups. These hydroxyl groups would make the polymer more hydrophilic and increase water uptake. As TR conversion increases further, a decrease in hydroxyl group concentration is observed by FT-IR as

these groups are converted to benzoxazole structures, and free volume increases [2]. The increased free volume of the structure could assist in increasing water uptake [23].

Table 4.9 Equilibrium water uptake in HAB-6FDA polyimide and TR polymers. Uncertainties were calculated as the standard deviation of at least three repeat measurements.

Sample	Water Uptake (% mass)
Polyimide	0.5% ± 0.2%
TR350	2.9% ± 0.4%
TR400	0.5% ± 0.4%
TR450	2.1% ± 0.8%

Two limits on the effect of water uptake on density are provided by the so-called additive volume uptake and constant volume uptake models [24]. In the additive volume uptake model, water and polymer mix according to the principle of volume additivity, with the partial molar volume of water being equal to that of pure water. In the constant volume water uptake model, water sorbs into a polymer with no change in volume. As reported by Rowe et al., polysulfone and Matrimid® polyimide each showed approximately 70% additive volume water uptake and 30% constant volume water uptake over a range of relative humidities [24]. Therefore, in this study, these proportions of additive volume and constant volume water uptake were used to correct density measurements from the density gradient column for water uptake. Using this approximation, corrected densities from the density gradient column are listed in Table 4.10 and shown alongside measurements made using a benchtop density measurement kit with *n*-heptane as the reference liquid. Table 4.10 shows that there is relatively good agreement between the two techniques after corrections are made for water uptake. Density values from the two measurement techniques are plotted against each other in Figure 4.9 to give a visual comparison. This agreement suggests that the water uptake

during density gradient column measurements is significant, especially in the TR350 sample, and should be accounted for in density values obtained using this method.

Table 4.10 Densities using the density gradient column with corrections for water uptake and the density determination kit using *n*-heptane as a reference liquid. Uncertainties were calculated as the standard deviation of at least three repeat measurements.

Sample	Method	Density (g/cm^3)
Polyimide	Column	1.4211
TR350	Column	1.4176
TR400	Column	1.3968
TR450	Column	1.3422
Polyimide	Density Kit	1.407 ± 0.009
TR350	Density Kit	1.398 ± 0.009
TR400	Density Kit	1.400 ± 0.009
TR450	Density Kit	1.34 ± 0.01

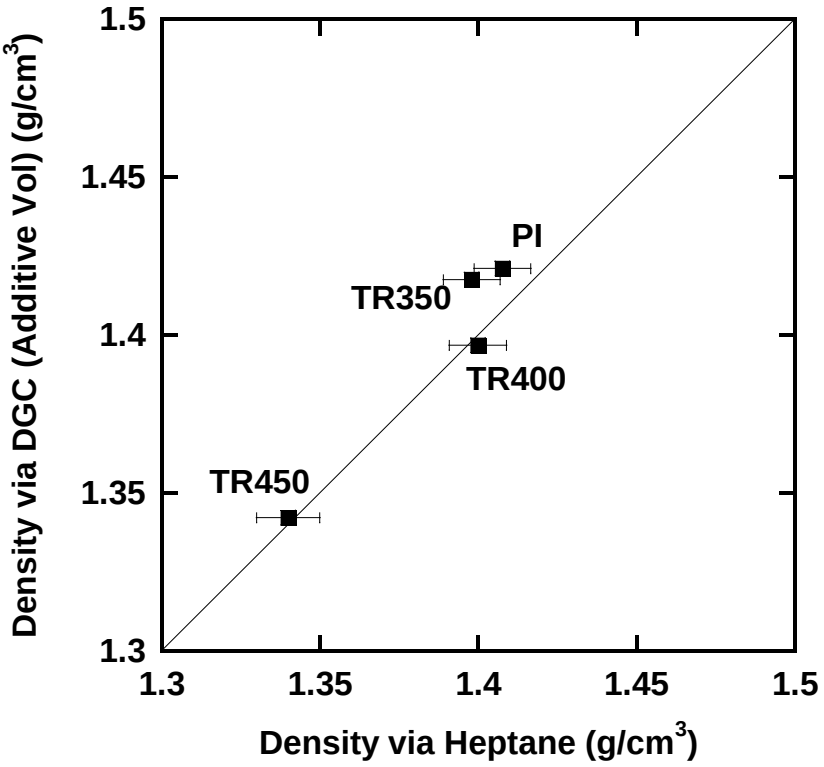

Figure 4.9 Comparison of densities from the density gradient column (DGC) and density determination kit using *n*-heptane. Density values obtained using the DGC were corrected for water uptake by the method described in Rowe et al., assuming that 70% of the water uptake resulted in swelling of the polymer film via an additive mixing model and 30% of the water uptake sorbed into the polymer without changing the volume of the polymer sample [24].

The occupied volume of each polymer sample was estimated using the group contribution method [21, 22], modified as shown in Equation 4.5 to account for partial conversion of the polyimide to the TR polymer:

$$V_O = cV_{O,TR} + (1-c)V_{O,PI} \tag{4.5}$$

where $V_{O,TR}$ is the occupied volume of TR polymer chains (cm^3/g), $V_{O,PI}$ is the occupied volume of polyimide chains (cm^3/g), and c is the fractional mass conversion, calculated as the actual mass loss measured by TGA divided by the theoretical mass loss needed to

achieve 100% conversion of the polyimide precursor to the TR polymer. The relevant van der Waal's volumes were obtained from the literature [21, 22, 25, 26]. This approach requires the structure of the remaining polyimide to be known. Based on previous discussion in this work and elsewhere, the *ortho*-position acetate groups can be converted to hydroxyl groups prior to final conversion to benzoxazole structures [2]. However, we do not have a quantitative estimate of the number of acetate and hydroxyl groups in partially converted samples because they become insoluble, making quantitative determination difficult. Fortuitously, the occupied volume of the acetate and hydroxyl containing polymers differ by less than 2%, so this lack of complete information regarding the structure has a negligible impact on free volume calculations. In the calculations described below, any unconverted functional groups are assumed to be acetate groups.

The calculated fractional free volume values are presented in Table 4.11. Qualitatively consistent with the trends observed in transport properties, fractional free volume increases from 15% in the polyimide to nearly 20% in the TR450 sample. However, the transport properties would suggest a larger increase in free volume. Figure 4.10 presents CO_2 permeability coefficients as a function of fractional free volume for the HAB-6FDA polyimide and its TR polymers, several other polyimides, and a general trend for a wide range of polymers [7].

Table 4.11 Fractional Free Volume (FFV) of HAB-6FDA polyimide and TR polymers.

Sample	Conversion (%)	FFV (%)
HAB-6FDA	0	15.0%
TR350	39	15.1%
TR400	60	16.3%
TR450	76	19.6%

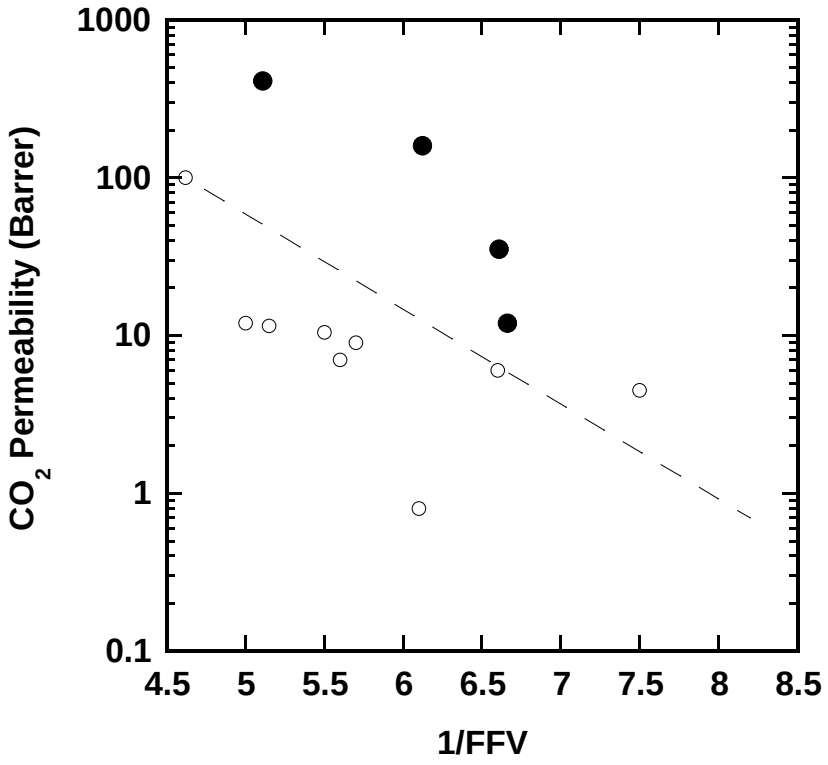

Figure 4.10 CO_2 permeability at 35°C and 10 atm feed pressure as a function of free volume for HAB-6FDA polyimide and TR polymers (filled circles) and various polyimides (open circles) [7]. The dashed line is the best fit slope for a wide range of polymers [7].

CO_2 permeability in the HAB-6FDA polyimide and its related TR polymers is more sensitive to changes in FFV, brought about by thermal rearrangement, than expected based on results for other polymers. This result qualitatively supports the finding by Park et al. that, in addition to increasing fractional free volume, thermal rearrangement changed the free volume distribution, resulting in large cavities separated by narrow necks [4]. This free volume distribution appears to be favorable for higher gas permeabilities than other families of polymers with similar fractional free volumes.

4.6 REFERENCES

1. Ohya, H., Kudryavtsev, V.V., and Semenova, S.I., *Polyimide membranes - applications, fabrications, and properties*. 1996: Gordon and Breach.

2. Smith, Z.P., Sanders, D.F., Ribeiro, C.P., Guo, R., Freeman, B.D., Paul, D.R., McGrath, J.E., and Swinnea, S., *Gas sorption and characterization of thermally rearranged polyimides based on 3,3'-dihydroxy-4,4'-diamino-biphenyl (HAB) and 2,2'-bis-(3,4-dicarboxyphenyl) hexafluoropropane dianhydride (6FDA).* Journal of Membrane Science, 2012. **415-416**: p. 558-567.

3. Guo, R., Sanders, D.F., Smith, Z.P., Freeman, B.D., Paul, D.R., and McGrath, J.E., *Synthesis and Characterization of Thermally Rearranged (TR) Polymers: Influence of ortho-positioned functional groups of polyimide precursors on TR process and gas transport properties.* Journal of Materials Chemistry A, 2013. **1**: p. 262-272.

4. Park, H.B., Jung, C.H., Lee, Y.M., Hill, A.J., Pas, S.J., Mudie, S.T., Van Wagner, E., Freeman, B.D., and Cookson, D.J., *Polymers with cavities tuned for fast selective transport of small molecules and ions.* Science, 2007. **318**(5848): p. 254-258.

5. Tullos, G.L. and Mathias, L.J., *Unexpected thermal conversion of hydroxy-containing polyimides to polybenzoxazoles.* Polymer, 1999. **40**(12): p. 3463-3468.

6. Tullos, G.L., Powers, J.M., Jeskey, S.J., and Mathias, L.J., *Thermal conversion of hydroxy-containing imides to benzoxazoles: Polymer and model compound study.* Macromolecules, 1999. **32**(11): p. 3598-3612.

7. Matteucci, S., Yampolskii, Y., Pinnau, I., and Freeman, B.D., *Transport of gases and vapors in glassy and rubbery polymers*, in *Materials science of membranes for gas and vapor separation*, Y. Yampolskii, I. Pinnau, and B.D. Freeman, Editors. 2006, John Wiley & Sons: Chichester. p. 2-46.

8. Park, H.B., Han, S.H., Jung, C.H., Lee, Y.M., and Hill, A.J., *Thermally rearranged (TR) polymer membranes for CO_2 separation.* Journal of Membrane Science, 2010. **359**(1-2): p. 11-24.

9. Bevington, P.R. and Robinson, K.D., *Data Reduction and Error Analysis for the Physical Sciences*. 2003, Boston: McGraw Hill. 320.

10. Robeson, L.M., *Correlation of separation factor versus permeability for polymeric membranes.* Journal of Membrane Science, 1991. **62**(2): p. 165-185.

11. Robeson, L.M., *The upper bound revisited.* Journal of Membrane Science, 2008. **320**(1-2): p. 390-400.

12. Koros, W.J., Chan, A.H., and Paul, D.R., *Sorption and transport of various gases In polycarbonate.* Journal of Membrane Science, 1977. **2**(2): p. 165-190.

13. Han, S.H., Misdan, N., Kim, S., Doherty, C.M., Hill, A.J., and Lee, Y.M., *Thermally rearranged (TR) polybenzoxazole: Effects of diverse imidization routes on physical properties and gas transport behaviors.* Macromolecules, 2010. **43**(18): p. 7657-7667.

14. Hirayama, Y., Yoshinaga, T., Kusuki, Y., Ninomiya, K., Sakakibara, T., and Tamari, T., *Relation of gas permeability with structure of aromatic polyimides I.* Journal of Membrane Science, 1996. **111**: p. 169-182.

15. Wijmans, J.G. and Baker, R.W., *The solution-diffusion model - a review.* Journal of Membrane Science, 1995. **107**(1-2): p. 1-21.

16. Baker, R.W. and Lokhandwala, K., *Natural gas processing with membranes: An overview.* Industrial & Engineering Chemistry Research, 2008. **47**(7): p. 2109-2121.

17. Moore, T.T. and Koros, W.J., *Gas sorption in polymers, molecular sieves, and mixed matrix membranes.* Journal of Applied Polymer Science, 2007. **104**(6): p. 4053-4059.

18. Puleo, A.C., Paul, D.R., and Kelley, S.S., *The effect of degree of acetylation on gas sorption and transport behavior in cellulose-acetate.* Journal of Membrane Science, 1989. **47**(3): p. 301-332.

19. Vu, D.Q., Koros, W.J., and Miller, S.J., *Mixed matrix membranes using carbon molecular sieves - I. Preparation and experimental results.* Journal of Membrane Science, 2003. **211**(2): p. 311-334.

20. Baker, R.W., *Membrane technology and applications*. 2004, Chichester: John Wiley & Sons.

21. Bondi, A., *van der Waals volumes and radii.* The Journal of Physical Chemistry, 1964. **68**(3): p. 441-451.

22. Bondi, A., *Physical properties of molecular crystals, liquids, and glasses*. 1968: Wiley.

23. Xie, W., Ju, H., Geise, G., Freeman, B.D., Mardel, J.I., Hill, A.J., and McGrath, J.E., *Effect of free volume on water and salt transport properties in directly copolymerized disulfonated poly(arylene ether sulfone) random copolymers.* Macromolecules, 2011. **44**: p. 4428-4430.

24. Rowe, B.W., Freeman, B.D., and Paul, D.R., *Effect of sorbed water and temperature on the optical properties and density of thin glassy polymer films on a silicon substrate.* Macromolecules, 2007. **40**(8): p. 2806-2813.

25. van Krevelen, D.W., *Properties of polymers*. 1972, Amsterdam: Elsevier.

26. Park, J.Y. and Paul, D.R., *Correlation and prediction of gas permeability in glassy polymer membrane materials via modified free volume based group contribution method.* Journal of Membrane Science, 1997. **125**(1): p. 23-39.

Chapter 5: Influence of Polyimide Precursor Synthesis Route and ortho-Position Functional Group on Thermally Rearranged (TR) Polymer Properties: Thermal Rearrangement and Free Volume[8]

5.1 INTRODUCTION

This chapter presents fundamental characterization of the effects of differences in synthesis routes and *ortho*-position groups on TR polymer properties. This characterization is achieved by studying a thermally imidized polymer, a chemically imidized polymer, and a thermally imidized polymer that was subsequently reacted with various dianhydrides to have acetate, propanoate, and pivalate *ortho*-position groups. These materials are discussed in chapter 3 and are illustrated in Figures 3.2 and 3.3.

In this chapter, TGA with mass spectrometry (MS) will be used to examine the thermal properties and byproducts of thermal rearrangement. A heating rate of 5 ºC/min is used for the hydroxyl, acetate, propanoate and pivalate-containing HAB-6FDA polymers. The propanoate group provides an additional chemical structure to help elucidate the effects of *ortho*-position group size on the properties of TR polymers. Comparisons of thermal rearrangement and degradation are also analyzed by isothermal holds at temperatures where thermal rearrangement occurs.

In chapter 4, the percent conversion of the polyimide precursor to the thermally rearranged PBO was estimated by assuming that the final structure of partially converted TR polymers consisted of only the original *ortho*-functional polyimide and its corresponding PBO [1]. In this chapter, the influence of various assumptions regarding the structure of partially converted TR polymers on the calculated percent conversion is

[8] Adapted from Sanders, D.F., Guo, R., Smith, Z.P., Liu, Q., Stevens, K.A., McGrath, J.E., Paul, D.R., and Freeman, B.D., Influence of polyimide precursor synthesis route and ortho-position functional group on thermally rearranged polymers: Thermal properties and free volume. In Preparation. D. F. Sanders performed the majority of experiments and wrote and edited the manuscript. Z. P. Smith, R. Guo, Q. Liu and K. A. Stevens provided experimental assistance. B. D. Freeman, J. E. McGrath, and D. R. Paul supervised this project and provided technical expertise.

also reported. Using this percent conversion, the free volume of these polymers was analyzed to determine whether the size of the *ortho*-position functional group can be related to the free volume of the resulting TR polymer. Pure gas transport properties as a function of conversion will be reported separately to examine the effect of *ortho*-position group on gas transport properties at various conversion conditions [2].

5.2 Thermal Rearrangement of TR Polymers with Varying Synthesis Route and *ortho*-Position Group

The thermal behavior of HAB-6FDA based polymers with varying *ortho*-position groups and synthesis routes was studied to determine the influence of these variables on thermal rearrangement. Mass spectrometry (MS) has been used in previous studies to determine the thermal rearrangement products of hydroxyl and acetate-functional polyimides [3, 4]. The major byproducts of this rearrangement are CO_2 and products related to *ortho*-position group loss (cf., Figure 3.2). Representative TGA-MS results are shown in Figure 5.1. The results for HAB-6FDA-C are very similar to those of the HAB-6FDA-Ac sample and have been reported previously [4]. The PrAc figure has been omitted, as many of the same trends are seen in the Ac sample. Rearrangement products for this sample will be discussed in the text.

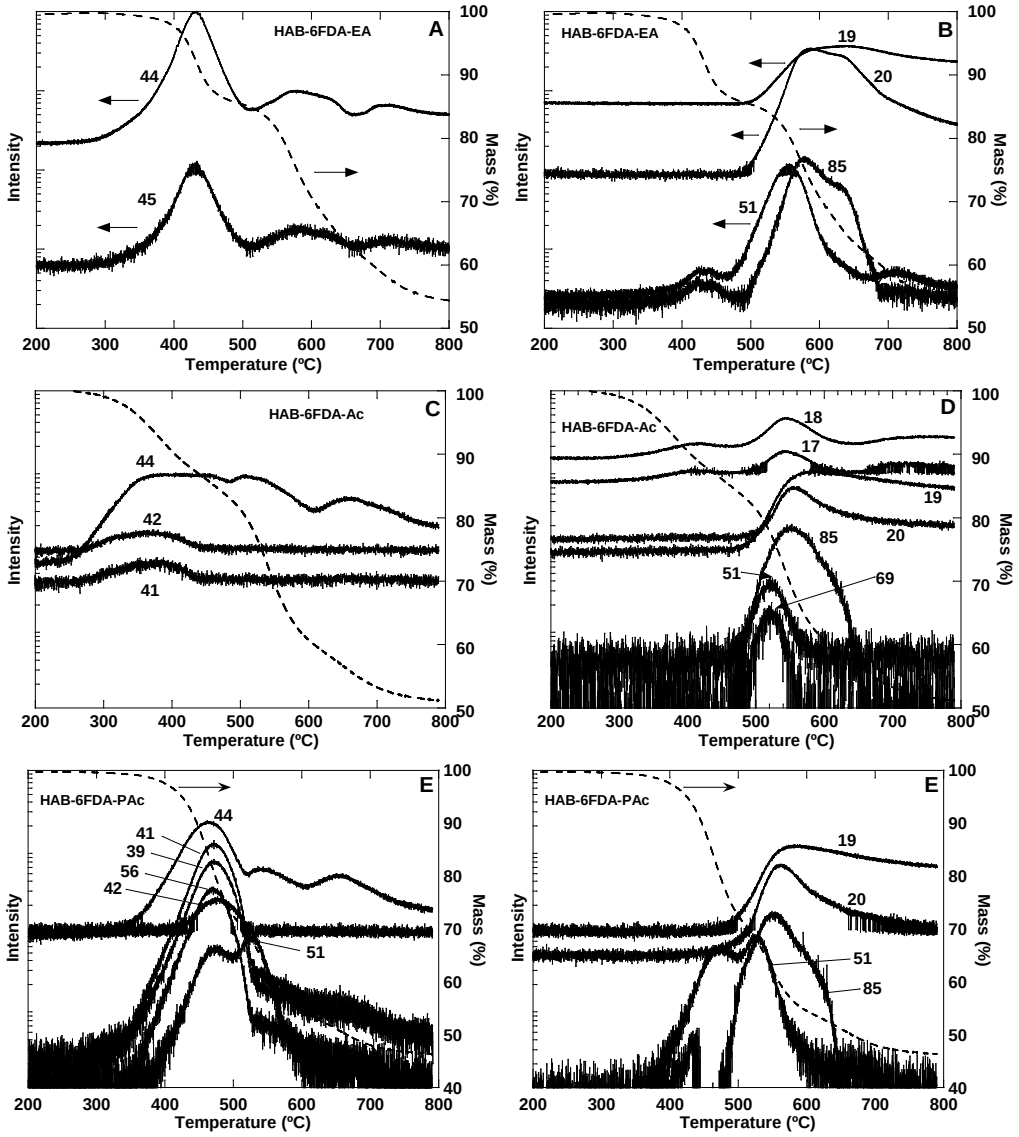

Figure 5.1 TGA-MS plots for HAB-6FDA EA, Ac, and PAc samples. Parts A, C, and E are for species that evolve during rearrangement and, in some cases, during thermal degradation as well. Parts B, D, and F are for species that evolve mainly during thermal degradation. Dotted lines represent the mass loss of the sample. Scans were performed at 5 ºC/min under a nitrogen atmosphere.

All TGA-MS results show thermal rearrangement occurring at temperatures between 300 and 450 ºC. CO_2 (*i.e.* 44 amu) is the major byproduct, which is consistent with previous reports on TR polymers and Figure 5.1 [3]. The Ac plymer also shows an

additional loss, at mass number 41/42, corresponding to ketene (cf., Figure 5.1C). Ketene is present from the thermal degradation of acetic acid, which is formed by conversion of *ortho*-position acetate groups io *ortho*-position hydroxyl groups prior to thermal rearrangement [4, 5]. Despite being synthesized via different routes, the TGA/MS results for the Ac sample are identical in fragments detected and curve shape to those previously reported for HAB-6FDA-C, so these two polymers appear to thermally rearrange via a similar mechanism [4]. That is, the route used to synthesize the ester-containing polyimide precursor does not appear to influence the thermal rearrangement and degradation of the material in samples having the same *ortho*-postion group, which is acetate in this case.

As shown in Figure 5.1E, the PAc sample has additional peaks at 39, 41, 42, and 58 amu during thermal rearrangement. These peaks are consistent with isobutylene, which could be formed by high temperature degradation of pivalic acid [6]. Additional rearrangement peaks at 41 and 51-57 amu were identified for the PrAc sample (data not shown), and these fragments likely correspond to thermal degradation products of the propanoate group as it is converted to hydroxyl functionality. Peaks other than CO_2 are not seen in the EA sample (Figure 5.1A) because the *ortho*-position group is already in the hydroxyl form. As shown in Figure 5.1B, mass numbers 19, 20, 51, and 85 correspond to thermal degradation products coming from the degradation of CF_3 groups and the polymer backbone [4]. These degradation products were observed in all of the HAB-6FDA samples considered in this study.

As explained above, thermal rearrangement fragments other than CO_2 (44 amu) are present only in HAB-6FDA polymers with non-hydroxyl *ortho*-position groups and can be directly related to reasonable thermal degradation products of these groups for the PAc and Ac samples. This evidence supports the hypothesized *ortho*-position group loss

and thermal rearrangement shown in Figure 3.2 and our previous studies [1]. The common degradation products also suggest thermal rearrangement of these various *ortho*-functional polyimides results in the formation of the same PBO.

The CO_2 peak in the TGA-MS for the EA and PAc samples are also much sharper than the CO_2 peak in the Ac and PrAc sample. The sharp peak in the EA polymer is believed to result from more rapid conversion, which results in decreasing CO_2 intensity before degradation. In the PAc polymer, the pivalate group is more thermally stable than the acetate or propanoate groups. The higher temperature at which the pivalate groups are lost may allow thermal rearrangement to occur more rapidly, resulting in a narrower temperature range over which rearrangement occurs. The broad peak in the TGA-MS for the acetate-containing polymers is due to the concurrent conversion of acetate functional groups to hydroxyl groups and thermal rearrangement to PBO [1, 4], and similar behavior is seen in the PrAc polymer. This similarity is reasonable due to the similarities between the Ac and PrAc structures.

TGA ramps of TR polymers typically show a two-stage mass loss [3, 4, 7-12]. As shown by TGA-MS, the first stage is associated with thermal rearrangement, and the second stage is attributed to thermal degradation. In cases where the polyimide does not undergo thermal rearrangement, only the degradation region is seen [13, 14]. As shown in Figure 5.1, the first stage mass loss begins between 275 and 350 ºC depending on the sample. This mass loss is ascribed predominantly to thermal rearrangement. The second stage of mass loss began at temperatures in the range of 450-500 ºC for samples in this study. Thus, the TGA/MS results in this study are consistent with literature reports for similar materials.

As shown in Figure 5.2, TGA results show identical thermal behavior with roughly 1% variation over the entire temperature range studied for the C and Ac

polymers, so the synthesis route used to obtain the acetate-containing polymer structure does not markedly influence the mass loss of these polymers. Compared to the PAc and EA polymers, both the C and Ac polymers undergo a relatively gradual mass loss once temperature increases past 300 ºC. This result agrees well with previous studies on chemically imidized HAB-6FDA, where this gradual mass loss is largely due to the conversion of acetate groups to hydroxyl groups, and this process overlaps the onset of thermal rearrangement [4]. Similar behavior is seen for the propanoate-containing polymer, HAB-6FDA-PrAc, but a larger overall mass loss is observed due to the larger *ortho*-position group lost during thermal rearrangement.

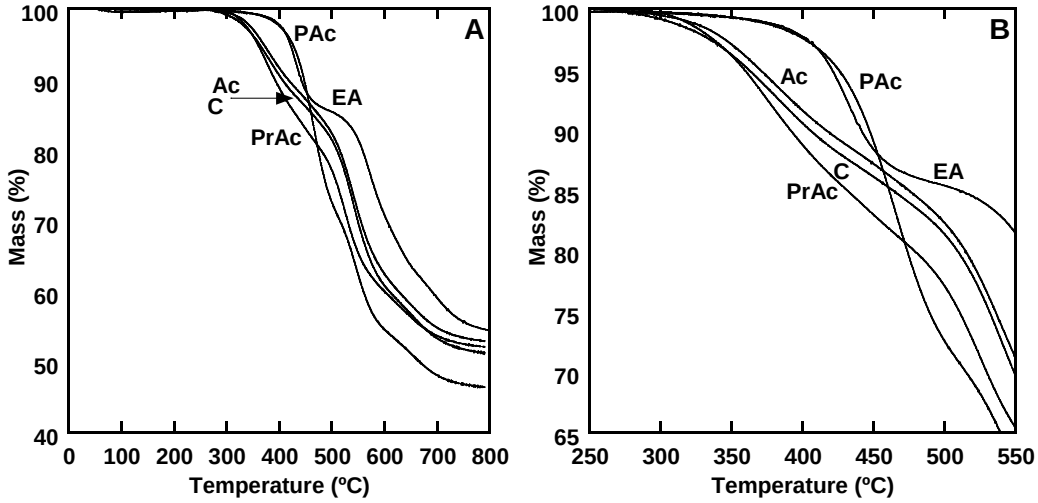

Figure 5.2 TGA scans at 5 ºC/min under N_2 atmosphere for HAB-6FDA with various functional groups. A) complete scan up to 800 ºC. B) Scan focusing on the region between 250 and 550 º C.

Both the Ac and PrAc polyimides show a significantly larger mass loss than PAc and EA polyimides at 400 ºC (e.g., approximately 10-15% mass loss for Ac and PrAc and 2% mass loss for EA and PAc), which signifies a lower thermal rearrangement temperature and less thermally stable *ortho*-position groups in the Ac and PrAc samples.

The *ortho*-position group is lost before thermal rearrangement occurs, which contributes to the early mass loss, and polyimides with a lower T_g rearrange at lower temperatures [1, 7, 11, 15].

The T_g values for the polymers in this study are shown in Table 5.1. The EA sample has the highest T_g, at roughly 314ºC, most likely due to hydrogen bonding from the *ortho*-position hydroxyl groups. The Ac, PrAc, and PAc samples all lack the hydroxyl functionality and have lower T_g values than the EA sample. The PAc sample has the bulkiest *ortho*-position group, which likely is a barrier to rotation and gives it the highest T_g among these larger *ortho*-position groups. The Ac and PrAc polymers have similar sized *ortho*-position groups, but the longer side chain in the PrAc polymer results in a slightly lower T_g. This behavior is typical for polymers with long or bulky side chains [16].

Table 5.1 T_g of HAB-6FDA based polyimides. [a] Data from reference [1]. [b] Data from reference [4].

Synthesis Route	*o*-Position Group	T_g (ºC)
EA[a]	-OH	314
Ac[a]	$-OCOCH_3$	280
C[b]	$-OCOCH_3$	267
PrAc	$-OCOCH_2CH_3$	262
PAc[a]	$-OCOC(CH_3)_3$	288

In contrast to the Ac and PrAc samples, the EA and PAc samples exhibited less than 1% loss at 350 ºC, but mass loss increased substantially above 400 ºC where the bulk of the thermal rearrangement occurred. The higher rearrangement temperature of EA is attributed to the relatively high T_g shown in Table 5.1. Thermal rearrangement begins only when the sample reaches its T_g. Above its T_g, the chains have sufficient mobility to

undergo the molecular motion to bring about rearrangement [15]. The more substantial mass loss above 400 ºC in the EA sample is likely caused by the absence of a bulky *ortho*-position group. Without such a group, the polyimide can directly convert to the TR polymer, and the broad mass loss region observed in the Ac and PrAc polymers is not present. A well-defined plateau is also present between thermal rearrangement and degradation in the EA polymer (cf., Figure 5.2B), which suggests more complete rearrangement.

The pivalate *ortho*-position group (i.e., sample PAc) is more stable than the acetate or propanoate group, as shown by the lack of mass loss in the PAc sample until the temperature exceeded 400 ºC (cf., Figure 5.2B). When this group is lost and the corresponding hydroxyimide is formed, the elevated temperature may allow for more rapid rearrangement. This rapid rearrangement results in a steep mass loss, similar to that of the EA polymer but with a much larger magnitude due to the bulky pivalate *ortho*-position group. For example, the mass loss at the shoulder of these curves (roughly 450 ºC for EA and 475 ºC for PAc) is approximately 13% for EA and 25% for PAc. No clear plateau region is present in the PAc polymer, but a shoulder can be seen at roughly 475 ºC. Significant mass loss occurs between 450-475 ºC for PAc, where thermal degradation is also beginning. Thus, full rearrangement in the Pac sample likely does not occur before degradation, especially at a 5 ºC/min ramp rate. The substantial differences in thermal behavior between the polymers synthesized via the ester acid route (EA, Ac, PrAc, PAc) and the similarities in thermal behavior between both acetate-containing polyimides (Ac and C) imply that the *ortho*-position group is the dominant influence on thermal rearrangement, rather than the imidization route used.

While these TGA and TGA/MS ramps provide information about the thermal rearrangement and byproducts of these polymers, they provide no information about how

thermal rearrangement occurs when a sample is held at a prescribed temperature over a longer period of time. Information on the rate of mass loss during the thermal rearrangement protocol used to prepare samples for free volume and other studies was collected by using the TGA to study samples at the same thermal history that they are exposed to in the furnace (i.e., a hold at 300 ºC hold and subsequent heating to the final target temperature for rearrangement). Once the rearrangement temperature was reached in the TGA, the sample was held isothermally for 10 hours. Results from these experiments are shown in Figure 5.3.

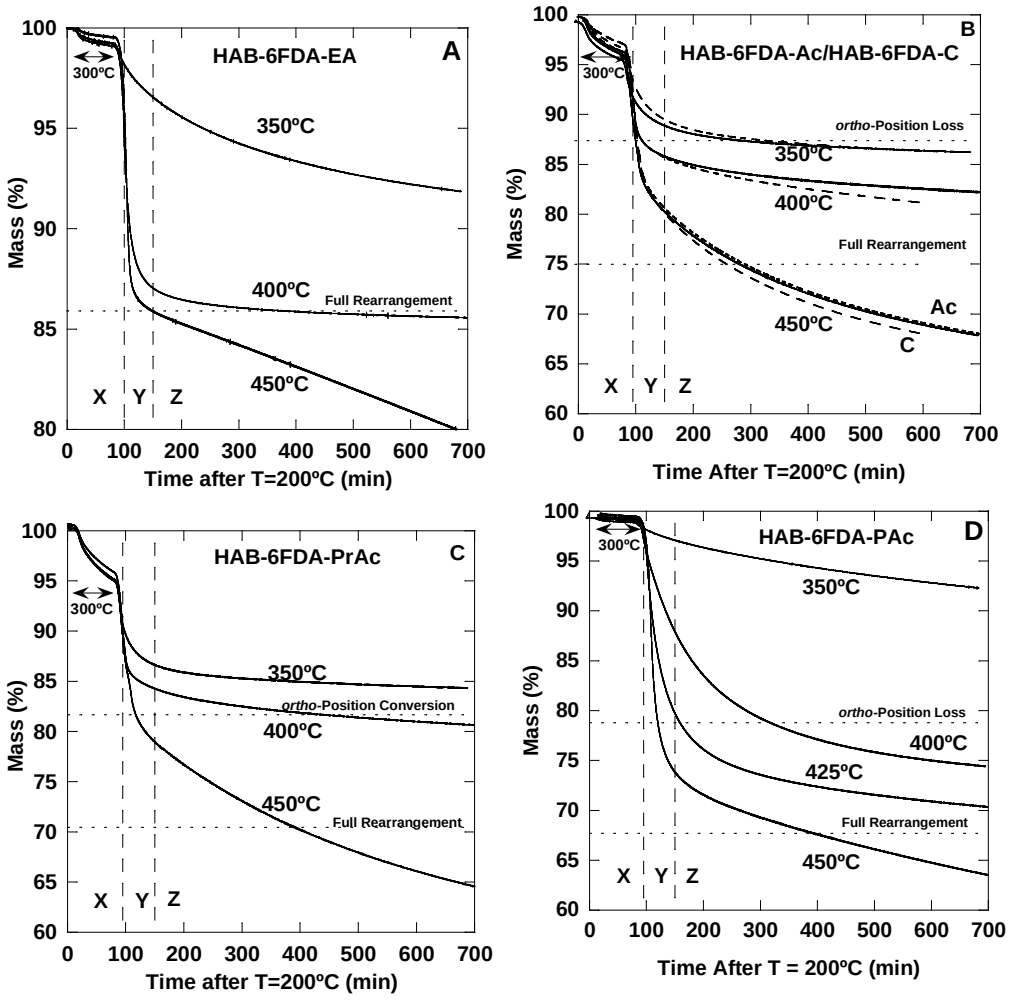

Figure 5.3 TGA scan of HAB-6FDA-EA, Ac, C, PrAc, and PAc. Samples were heated to 300 ºC at 5 ºC/min and held for 1 hour before being heated at 5 ºC to the desired temperature (given in the figure) and held for 10 hours. The dashed lines show the mass loss expected if the *ortho*-position group converted to a hydroxyl group ("*ortho*-position conversion") and if the polyimide precursor fully converted to the TR polymer shown in Figure 1 ("full rearrangement"). In Figure 6B, the dotted lines represent the chemically imidized sample (C), and the solid lines represent the acetate-containing sample modified from the ester-acid route (Ac).

The curves in Figure 5.3 show the same time and temperature regions discussed previously [11]. For each material, there is a first region during the isothermal hold at 300 ºC, labeled "X", where a relatively gradual mass loss occurs, except in the case of PAc

(cf., Figure 6D), in which case there is very little mass loss. The mass loss in this region is most noticeable for the PrAc and Ac samples (cf., Figures 5.3B and 5.3C) and likely corresponds to some *ortho*-position loss and perhaps a small amount of TR conversion. These results provide additional evidence that acetate and propanoate *ortho*-position groups are less thermally stable than pivalate groups, and the lower T_g values lead to lower rearrangement temperatures. The EA sample (cf., Figure 5.3A) has only a hydroxyl *ortho* position group and is held slightly below its T_g, which results in minimal mass loss in this region. The PAc sample, which has a more thermally stable pivalate *ortho*-position group, shows almost no mass loss during the 300 ºC hold.

The second region, labeled "Y" and occurring between roughly 100 and 200 minutes in Figure 5.3, is associated mainly with thermal rearrangement. The Ac and PrAc samples show an abrupt mass loss at approximately 100 min followed by a slower, broader mass loss, which is attributed to the concurrent loss of *ortho*-position acetate or propanoate groups and conversion to PBO [1, 11].

In region Y of Figure 5.3D, the PAc sample exhibits only a broad mass loss at 350 ºC between 100 and 200 minutes, with no sharp mass loss. Therefore, the pivalate *ortho*-position group is likely still relatively stable at this temperature and prevents widespread thermal rearrangement. As the heat treatment temperature reaches 400, where mass loss for the PAc sample begins in Figure 5.2B, more mass loss in region Y of Figure 5.3D is observed. When the temperature reaches 450ºC, a sharp mass loss region appears, so the pivalate group can be rapidly lost, and the PBO can be formed at this temperature.

The EA sample (cf., Figure 5.3A) has only a broad mass loss in region Y at 350 ºC, which supports the observation from Figure 5.2 and chapter 4 that only a small amount of thermal rearrangement can occur at this temperature [1]. However, between 100 and 200 min in Figure 5.3A at 400 and 450 ºC, a rapid mass loss occurs. This mass

loss approaches theoretical conversion, so the thermal rearrangement apparently occurs nearly quantitatively in the hydroxyl-containing EA sample, most likely because there is no *ortho*-position group to be lost before conversion.

The mass loss in the third region of the plots in Figure 5.3, labeled "Z", at times above roughly 150 minutes, has been attributed mainly to slow thermal degradation over long times [11]. At higher temperatures, this degradation is more apparent for all samples because the mass loss decreases below levels expected for full conversion of the polyimide precursor to the PBO. The mass loss is less apparent at lower temperatures, but samples were noticeably more brittle when removed from the TGA, potentially consistent with some thermal degradation [11]. However, continued rearrangement at these temperatures may also result in more brittle films.

Figure 5.3B also shows a comparison between the thermal behavior of HAB-6FDA-C and HAB-6FDA-Ac, two polymers with the same chemical structure synthesized via different routes. The dashed lines represent the chemically imidized sample (C), and the solid lines represent the acetate-containing sample obtained by modifying the ester-acid route polyimide as shown in Figure 3.3 (Ac). These two polymers show essentially identical thermal rearrangement behavior. Thus, the *ortho*-position group apparently has a larger impact on thermal rearrangement behavior than the polyimide synthesis route.

Samples for density and free volume characterization were rearranged in the tube furnace at 350 or 400 ºC for 1 hour or 450 ºC for 30 minutes, and they are referred to by sample name and rearrangement temperature. For example, EA-350 is an EA sample rearranged at 350ºC for 1 hour, and EA-PI is the unconverted EA polyimide. Heat treatment times were chosen to minimize thermal degradation in the chemically imidized samples [11]. The mass loss of a sample, relative to the mass loss expected if the TR

process proceeds as shown in Figure 3.2, has been used in previous literature reports to approximate the percent conversion of polyimide to the resultant PBO [4, 11]. Other techniques to measure conversion, such as NMR or other solution-based analytical methods, were not possible on the partially rearranged samples because they were insoluble after rearrangement [1, 11]. However, there is some uncertainty when calculating the percent conversion based on mass loss because the exact chemical structure of the partially converted TR polymer is not well characterized. For example, when the *ortho*-position group is lost, hydroxyimide moieties are formed before conversion to the final PBO [1]. Therefore, the partially converted TR structure may contain a combination of the original *ortho*-position polyimide, the hydroxyimide, and the PBO.

Several methods were explored in an effort to determine the amount of the original *ortho*-position polyimide, hydroxyl polyimide, and TR polymer in partially converted samples, but none of them were able to accurately determine the relative amounts of these structures. Solid-state NMR has been used previously, but the broad peaks did not allow a quantitative determination of the concentrations of these functional groups [3]. Titration with acetic anhydride, which could potentially be used to determine the fraction of hydroxyl groups [17], was not possible due to steric effects in the insoluble sample. Quantitative FT-IR could not be used to determine the structure due to the overlapping and shifting peaks during thermal rearrangement. Elemental analysis was also used to determine the ratio of carbon to nitrogen atoms, but the accuracy of the technique was not within the bounds necessary to accurately determine the composition of a partially converted TR polymer.

Due to these experimental constraints, two boundaries, representing the extremes of what might occur, are discussed regarding the extent of TR conversion and the

resulting values of fractional free volume. In the first limit, which is referred to as the *o*-pos assumption, any *ortho*-position group undergoing thermal rearrangement is assumed to convert completely to the PBO. Therefore, only the original *ortho*-position polyimide and PBO structures remain in partially converted samples. In the second limit, which is referred to as the OH assumption, each *ortho*-position group undergoing reaction is presumed to convert to a hydroxyl group (i.e., with loss of the acetate, pivalate, etc. linkages). Then, if the sample mass loss is above and beyond that which could be explained by conversion of *ortho*-position groups exclusively to hydroxyl groups, any further mass loss is ascribed to hydroxyimides undergoing thermal rearrangement to form PBO structures. In this case, only the original *ortho*-position polyimide and hydroxyimide structures, or hydroxyimide and PBO structures remain. Equations 5.1-5.6 below will further clarify these assumptions. These assumptions do not impact the EA polymer because it is already in the hydroxyimide form. In the calculations of conversion to be described below, an implicit assumption is that only original polyimide, hydroxyimide, and PBO exist in the final structure, so no thermal degradation reactions (i.e., chemical reactions that lead to structures other than hydroxyimide or PBO) are presumed to occur.

From a quantitative perspective, if all polyimides with *ortho*-position groups that underwent reaction were converted to PBO units (i.e., the *o*-pos assumption), the fractional conversion of *ortho*-position groups (c_{PBO}), on a mass basis, would be:

$$c_{PBO} = \frac{\Delta m_{\exp}}{\Delta m_{\max,o-pos\rightarrow PBO}} \tag{5.1}$$

where Δm_{exp} is the experimental mass loss in the film, and $\Delta m_{max,o\text{-}pos\rightarrow PBO}$ is the hypothetical maximum mass loss from the original sample if all *ortho*-position groups

were converted to PBO units. The hypothetical maximum mass loss is calculated as follows:

$$\Delta m_{\max,o-pos\rightarrow PBO} = m_o\left(\frac{M_{o-pos} - M_{PBO}}{M_{o-pos}}\right) \tag{5.2}$$

where m_o is the original sample mass, $M_{o\text{-}pos}$ is the repeat unit molecular weight of the polyimide with original *ortho*-position functionality, and M_{PBO} is the repeat unit molecular weight of the polybenzoxazole. The calculation of c_{PBO} according to Equation 5.1, when multiplied by 100 to put it on a percentage basis, is equivalent to percent conversion previously reported for TR polymers [4, 11]. This method of estimating the extent of the thermal rearrangement correlated well with gas transport properties [1, 11]. Table 5.2 records relevant values of repeat unit molecular weight and percent mass loss (the parenthetical expression in Equation 5.2) for each structure considered in this study.

Table 5.2 Molecular weight of each repeat unit and percent mass loss associated with the formation of various products.

Sample	***o*-position Group**	**MW (g/mol)**	**%Mass Loss**		
			***o*-pos→PBO**	***o*-pos→OH**	**OH→PBO**
EA	-OH	624.4	-	-	14.1
Ac	$-OCOCH_3$	708.5	24.3	11.9	14.1
PrAc	$-OCOCH_2CH_3$	736.5	27.2	15.2	14.1
PAc	$-OCOC(CH_3)_3$	792.5	32.2	21.2	14.1
PBO	-	536.4	-	-	-

Note: x→y represents the conversion of a polyimide with x type *ortho*-position groups (where x is either original *ortho*-position groups (*o*-pos) or hydroxyl groups (OH)) to y (PBO units or hydroxyl groups).

Two subcases are considered where the *ortho*-position groups are converted to hydroxyl groups (OH assumption). If there is insufficient mass loss to convert all of the *ortho*-position groups to hydroxyl groups, then no PBO structures would be formed.

Thus, the sample would have a mixture of *ortho*-position groups and hydroxyl groups. In this case, the mass fraction of *ortho*-position groups converted to hydroxyimide (c_{OH}) can be calculated using Equation 5.3.

$$c_{OH} = \frac{\Delta m_{\exp}}{\Delta m_{\max,o-pos\rightarrow OH}} \tag{5.3}$$

In this case, the hypothetical maximum mass loss is calculated as follows:

$$\Delta m_{\max,o-pos\rightarrow OH} = m_o\left(\frac{M_{o-pos} - M_{OH}}{M_{o-pos}}\right) \tag{5.4}$$

where m_o is the original sample mass, $M_{o\text{-}pos}$ is the repeat unit molecular weight of the polyimide with original *ortho*-position functionality, and M_{OH} is the repeat unit molecular weight of the polyimide with hydroxyl functional groups.

In a related subcase, if there is enough mass loss to convert all of the ortho-position groups to hydroxyl groups and to further convert some (or all) of the hydroxyl groups to PBO linkages, then Equation 5.4 is used to estimate the fraction of PBO units formed:

$$c_{PBO} = \frac{(\Delta m_{\exp} - \Delta m_{\max,o-pos\rightarrow OH})}{\Delta m_{\max,OH\rightarrow PBO}} \tag{5.5}$$

In this case, the hypothetical maximum mass loss in the numerator is calculated using Equation 5.4 and the hypothetical maximum mass loss in the denominator is calculated as follows:

$$\Delta m_{\max,OH\rightarrow PBO} = m_o\left(\frac{M_{OH} - M_{PBO}}{M_{OH}}\right) \tag{5.6}$$

where m_o is the original sample mass, $M_{o\text{-}pos}$ is the repeat unit molecular weight of the polyimide with original *ortho*-position functionality, M_{OH} is the repeat unit molecular weight of the polyimide with hydroxyl functional groups, and M_{PBO} is the repeat unit

molecular weight of the polybenzoxazole. The numerator in Equation 5.5 represents the amount of mass loss beyond that required to fully convert the *ortho*-position groups to hydroxyl groups, and the denominator is the hypothetical maximum mass loss to convert the hydroxyimides to PBO linkages.

Table 5.3 presents the percent conversions for the EA, Ac, C, PrAc, and PAc samples under each of these scenarios. As seen in Table 5.3, there can be a considerable difference in the estimated chemical structure of these partially converted TR polymers based on the assumptions made concerning the conversion chemistry. These assumptions are more important when the *ortho*-position group is larger, as seen in the PAc sample, which must lose 21% of its mass to convert all pivalate *ortho*-position groups to hydroxyl groups. For example, the PAc-TR400 sample can have either a 58% PBO conversion or a 0% PBO conversion and 88% conversion of *ortho*-position groups to hydroxyl groups depending on the assumption made. The difference in conversion based on each assumption is also significant for the acetate-containing Ac polymer. At a TR temperature of 350 ºC, the Ac polymer could have either a 39% PBO conversion or a 0% PBO conversion and 80% conversion of acetate to hydroxyl functionality. These differences based on structural assumptions highlight the uncertainty in calculating percent conversion for TR polymers from polyimides with non-hydroxyl *ortho*-position groups. This structural uncertainty is not present in the EA sample because there is no *ortho*-position group lost before conversion to the PBO. The uncertainties also point out the desirability of using additional information, such as FTIR analysis, when available to identify the species present following a given thermal history.

Table 5.3 Conversion of EA, Ac, C, PrAc, and PAc samples calculated assuming all remaining polyimides maintain their original *ortho*-position functionality and assuming all polyimides are converted to hydroxyimides before rearrangement.

Sample	*o*-pos Assumption		OH Assumption		
	%*o*-pos	%PBO	%*o*-pos	%OH	%PBO
EA-PI	-	-	-	100	
EA-350	-	-	-	55	45
EA-400	-	-	-	24	76
EA-450	-	-	-	0	118
Ac-PI	100	-	100	-	-
Ac-350	61	39	20	80	0
Ac-400	40	60	0	78	22
Ac-450	32	68	0	63	37
C-PI	100	-	100	-	-
C-350	62	38	22	78	0
C-400	40	60	0	78	22
C-450	24	76	0	47	53
PrAc-PI	100	-	100	-	-
PrAc-350	61	39	30	70	0
PrAc-400	44	56	0	88	12
PrAc-450	22	78	0	48	52
PAc-PI	100	-	100	-	-
PAc-350	86	14	79	21	0
PAc-400	42	58	12	88	0
PAc-450	19	81	0	55	45

NOTE: Conversion values were calculated using Equations 5.1-5.6. *o*-pos refers to the original *ortho*-position group. The assumption labeled *o*-pos assumes that any remaining polyimide structures have original *ortho*-position functionality, and the OH assumption assumes that any remaining polyimide structures have been converted to the hydroxyimide.

The actual PBO conversion most likely lies between the limiting values set forth in Table 5.3. Polymers with *ortho*-position acetate groups convert to hydroxyl groups as

they undergo thermal rearrangement, but these samples also exhibit a considerable increase in gas permeability associated with the formation of PBO [11]. For example, the C-350 sample shown in Table 5.3 has a PBO conversion between 0 and 38% depending on the *ortho*-position assumptions made. This sample has a CO_2 permeability three times higher than its polyimide precursor and is insoluble, so there is likely some PBO formation [11]. While there is evidence of conversion of *ortho*-position groups to hydroxyl functionality and PBO formation, there is currently no clear way to quantitatively distinguish the amount of each structure present in a sample following a given thermal protocol.

Based on the mass loss data, the HAB-6FDA-C and HAB-6FDA-Ac polymers have similar thermal rearrangement behavior. The only discrepancy between these two samples is the conversion difference between samples rearranged at 450 ºC for 30 minutes, as seen in Table 5.3. Conversions in these samples typically have an uncertainty of approximately ±4%, so it is not unreasonable to think variations in film and furnace conditions could extend this range beyond what is seen between these two samples, especially at higher rearrangement temperatures [4].

The 118% conversion calculated from mass loss in the film for EA-450 indicates a higher observed mass loss than expected based on complete conversion of the polyimide to PBO [18]. Therefore, some thermal degradation may be occurring in the EA sample when heated at 450ºC, which was not observed in the acetate-containing polymers.

5.3 Density and Fractional Free Volume of TR Polymers with Varying Synthesis Route and *ortho*-Position Group

The density and fractional free volume of these polymers as a function of thermal rearrangement were also studied. Table 5.4 presents the density of the polyimide and TR

polymers for the EA, Ac, PrAc, and PAc polymers. Among the unconverted polyimide precursors, larger *ortho*-position groups disrupt chain packing and decrease density. The PAc sample, which contained the largest *ortho*-position group, had the lowest density (1.29 g/cm^3), while the EA sample, with the smallest *ortho*-position groups (i.e., hydroxyl groups) and likely influenced most by hydrogen bonding, had the highest density (1.48 g/cm^3). Among the EA, Ac, and PrAc materials, density decreased as extent of thermal rearrangement increased. This trend is attributed to the formation of the very rigid PBO structure, which has been shown to increase fractional free volume in other TR studies [9-11]. The densities of the Ac sample agree with those previously reported for the HAB-6FDA-C sample [11], so the synthesis route used does not appear to influence the properties of these TR polymers as much as the *ortho*-position group of the polyimide precursor.

Table 5.4 Density of HAB-6FDA TR polymers with various *ortho*-position functional groups. Uncertainties are the standard deviation of density measurements for at least 4 samples. [a] Data from reference [11].

Thermal Treatment	Density (g/cm^3)				
	EA	Ac	C[a]	PrAc	PAc
None	1.48 ± 0.02	1.428 ± 0.007	1.421 ± 0.009	1.39 ± 0.01	1.29 ± 0.01
350	1.45 ± 0.01	1.41 ± 0.01	1.418 ± 0.009	1.38 ± 0.01	1.27 ± 0.01
400	1.36 ± 0.01	1.38 ± 0.01	1.397 ± 0.009	1.368 ± 0.006	1.293 ± 0.005
450	1.34 ± 0.01	1.335 ± 0.009	1.34 ± 0.01	1.309 ± 0.008	1.286 ± 0.008

Note: Samples labeled with a thermal treatment of "None" correspond to the polyimides that were only dried and not subjected to thermal treatments designed to bring about thermal rearrangement. As described in the experimental section, those labeled "350" and "400"were heated to 350°C or 400°C for 1 hour, and those labeled "450" were heated to 450°C for 30 minutes.

The PAc structure did not show the same decrease in density with thermal rearrangement as the EA, Ac, C and PrAc sample. The PAc samples treated at various temperatures, within the uncertainty of the density measurements, have very similar densities, suggesting there may be competing effects on density as pivalate groups are lost and PBO is formed [1]. In this structure, the conversion of pivalate groups to hydroxyl groups reintroduces smaller *ortho*-position groups and likely hydrogen bonding, promoting the formation of a more dense structure. However, the formation of PBO typically results in a higher free volume. Both of these conversions happening concurrently could result in similar density values in the PAc samples. While these competing processes are likely also occurring in the

Ac and PrAc samples, the acetate and propanoate groups are much smaller than the pivalate groups, so the decrease in density brought about by formation of PBO structures is the dominant effect.

The density values in Table 5.4 were used to estimate the fractional free volume of these polymers using Equation 5.7:

$$FFV = \frac{V - V_o}{V} \tag{5.7}$$

where V is the specific volume, which is the reciprocal of the density values shown in Table 5.4. V_o is the occupied volume of the polymer chains. These volumes were calculated using the group contribution method of van Krevelen and the van der Waals volumes from Bondi, where V_o is approximated as 1.3 times the cumulative van der Waals volume of the structure [19-22]. Table 5.5 shows the occupied volumes calculated using this method.

Table 5.5 Occupied volumes for each of the HAB-6FDA polyimides and PBO.

Sample	**V_o (cm^3/g)**
EA-PI	0.5898
Ac-PI	0.598
PrAc-PI	0.6114
PAc-PI	0.6352
PBO-PI	0.5996

The occupied volumes for partially converted samples were calculated using Equation 5.8:

$$V_o = x_{PBO}V_{o,PBO} + x_{o-pos}V_{o,o-pos} + x_{OH}V_{o,EA} \tag{5.8}$$

where $V_{o,PBO}$ is the occupied volume of the PBO, $V_{o,o\text{-pos}}$ is the occupied volume of the polyimide having the original *ortho*-position functionality, and $V_{o,EA}$ is the occupied

volume of the poly(hydroxyimide). The mass fractions of PBO, residual ortho-position polyimide groups, and residual hydroxyimides are given by x_{PBO}, $x_{o\text{-}pos}$, and x_{OH}, respectively. These occupied volumes are weighted by the mass fractions reported in Table 5.3, based on the two limiting assumptions previously discussed.

As seen in Table 5.5, the occupied volumes for the poly(hydroxyimide) (EA), the acetate-containing polymer (Ac), and the PBO have similar values. Thus, for these materials, variations in assumptions regarding the structure of partially converted samples do not influence free volume calculations as much as they do for samples with larger *ortho*-position groups, such as the pivalate-containing PAc sample. V_o for the PAc sample is considerably different from that of the poly(hydroxyimide) and the PBO.

Using Equations 5.5 and 5.6, the fractional free volume of each sample was calculated under both of the limiting assumptions regarding the structure of partially converted samples, and the resulting values are reported in Table 5.6. Uncertainties in fractional free volume values were estimated from uncertainties in density measurements of at least 4 samples according to the method of propagation of errors [12]. EA-PI has the lowest free volume, likely due to combination of a small ortho-position group (i.e., hydroxyl) and potentially more hydrogen bonding present in the poly(hydroxyimide) than in the other polyimides. For all samples, fractional free volume increases as thermal rearrangement temperature and conversion increase, and the total increase in free volume after thermal treatment is roughly 4-6%. The exact value of free volume for each sample differs depending on structural assumptions except in the EA sample. In the EA sample, there *ortho*position group begins as a hydroxyl group. Therefore all chains are either hydroxyimide or PBO.

For TR polymers from polyimdies with non-hydroxyl *ortho*-position groups, the FFV is greater for the OH assumption than the *o*-pos assumption. The simplest reason for

this higher free volume is the presence of hydroxyimides in the partially converted TR polymer. The hydroxyimide, labeled EA-PI in Table 5.5, has the lowest occupied volume of any possible structure that could be present in the partially converted sample by these assumptions. Therefore, if the density is constant and the free volume is calculated, there will be less occupied volume if hydroxyimides are present. Less occupied volume and a constant density results in a higher fractional free volume (cf., Equation 5.5).

Table 5.6 Fractional free volume of HAB-6FDA polymers with various *ortho*-position functional groups and their TR polymers.

Thermal Treatment	Free Volume (%)			
	EA		Ac	
	o-pos	OH	*o*-pos	OH
None	13 ± 1	13 ± 1	14.6 ± 0.5	14.6 ± 0.5
350	13.8 ± 0.7	13.8 ± 0.7	15.6 ± 0.7	16.6 ± 0.7
400	18.7 ± 0.7	18.7 ± 0.7	17.3 ± 0.7	18.3 ± 0.7
450	19.6 ± 0.8	19.6 ± 0.8	20.0 ± 0.7	20.7 ± 0.7
Thermal Treatment	Free Volume (%)			
	PrAc		PAc	
	o-pos	OH	*o*-pos	OH
None	15.0 ± 0.7	15.0 ± 0.7	18.1 ± 0.8	18.1 ± 0.8
350	16.2 ± 0.7	17.7 ± 0.7	20.1 ± 0.8	20.5 ± 0.8
400	17.3 ± 0.4	19.2 ± 0.4	20.7 ± 0.4	23.0 ± 0.4
450	21.2 ± 0.6	22.1 ± 0.6	22.0 ± 0.6	23.5 ± 0.6

Note: Thermal treatments are the same as those discussed in Table 5.4 and the experimental section. The fractional free volume values recorded in this table were calculated using the two limiting assumptions regarding the structure of partially converted TR polymers as presented in Table 5.3 and discussed above.

The similarities in thermal properties, density, and free volume between the acetate-containing polymers prepared via chemical and thermal imidization (Ac and C)

and their differences relative to the thermally imidized hydroxyimide sample (EA) suggest that the *ortho*-position group has a larger influence on TR polymer properties than synthesis route. The strong influence of the *ortho*-position group on density and free volume may be due to the concurrent loss of these groups and the formation of the rigid, glassy PBO structure. After thermal rearrangement, these polymers have no measurable T_g before degradation [4]. Therefore, these partially converted TR polymers are in the glassy state and have limited mobility [4]. The free volume and free volume distribution may be influenced if these *ortho*-position groups are lost, and the polymer chains do not have sufficient mobility to pack efficiently in the vacated space. This change in free volume and free volume distribution, which has also been observed for acetate-containing TR polymers with a fluorinated diamine [3], could significantly influence transport properties.

5.4 REFERENCES

1. Guo, R., Sanders, D.F., Smith, Z.P., Freeman, B.D., Paul, D.R., and McGrath, J.E., *Synthesis and Characterization of Thermally Rearranged (TR) Polymers: Influence of ortho-positioned functional groups of polyimide precursors on TR process and gas transport properties.* Journal of Materials Chemistry A, 2013. **1**: p. 262-272.

2. Sanders, D.F., Guo, R., Smith, Z.P., Liu, Q., Stevens, K.A., McGrath, J.E., Paul, D.R., and Freeman, B.D., *Influence of polyimide precursor synthesis route and ortho-position functional group on thermally rearranged polymers: Pure gas permeability and selectivity.* In Preparation.

3. Han, S.H., Misdan, N., Kim, S., Doherty, C.M., Hill, A.J., and Lee, Y.M., *Thermally rearranged (TR) polybenzoxazole: Effects of diverse imidization routes on physical properties and gas transport behaviors.* Macromolecules, 2010. **43**(18): p. 7657-7667.

4. Smith, Z.P., Sanders, D.F., Ribeiro, C.P., Guo, R., Freeman, B.D., Paul, D.R., McGrath, J.E., and Swinnea, S., *Gas sorption and characterization of thermally rearranged polyimides based on 3,3'-dihydroxy-4,4'-diamino-biphenyl (HAB) and 2,2'-bis-(3,4-dicarboxyphenyl) hexafluoropropane dianhydride (6FDA).* Journal of Membrane Science, 2012. **415-416**: p. 558-567.

5. Waters, T., O'Hair, R.A.J., and Wedd, A.G., *Catalytic gas phase dehydration of acetic acid to ketene.* International Journal of Mass Spectrometry, 2003. **228**(2-3): p. 599-611.

6. *Mass Spectra* in *NIST Chemistry WebBook, NIST Standard Reference Database Number 69,* S.E. Stein, Editor 2013, National Institute of Standards and Technology: Gaithersburg MD, 20899.

7. Calle, M., Chan, Y., Hye, J.J., and Lee, Y.M., *The relationship between the chemical structure and thermal conversion temperatures of thermally rearranged (TR) polymers.* Polymer, 2012. **53**: p. 2783-2791.

8. Calle, M. and Lee, Y.M., *Thermally rearranged (TR) poly(ether-benzoxazole) membranes for gas separation.* Macromolecules, 2011. **44**: p. 1156-1165.

9. Park, H.B., Han, S.H., Jung, C.H., Lee, Y.M., and Hill, A.J., *Thermally rearranged (TR) polymer membranes for CO_2 separation.* Journal of Membrane Science, 2010. **359**(1-2): p. 11-24.

10. Park, H.B., Jung, C.H., Lee, Y.M., Hill, A.J., Pas, S.J., Mudie, S.T., Van Wagner, E., Freeman, B.D., and Cookson, D.J., *Polymers with cavities tuned for fast selective transport of small molecules and ions.* Science, 2007. **318**(5848): p. 254-258.

11. Sanders, D.F., Smith, Z.P., Ribeiro, C.P., Guo, R., McGrath, J.E., Paul, D.R., and Freeman, B.D., *Permeability, diffusivity, and free volume of thermally rearranged polymers based on 3,3'-dihydroxy-4,4'-diamino-biphenyl (HAB) and 2,2'-bis-(3,4-dicarboxyphenyl) hexafluoropropane dianhydride (6FDA).* Journal of Membrane Science, 2012. **409-410**: p. 232-241.

12. Bevington, P.R. and Robinson, K.D., *Data reduction and error analysis for the physical sciences*. 2003, Boston: McGraw Hill.

13. Kothawade, S.S., Kulkarni, M.P., Kharul, U.K., Patil, A.S., and Vernekar, S.P., *Synthesis, characterization, and gas permeability of aromatic polyimides containing pendant phenoxy group.* Journal of Applied Polymer Science, 2007. **108**: p. 3881-3889.

14. Schab-Balcerzak, E., Mitsutoshi, J., and Kakimoto, M., *Thermal rearrangement of poly(o-hydroxyimide)s synthesized from 4,6-diaminoresorcinol dihydrochloride.* Polymer Journal, 2003. **35**: p. 208-212.

15. Guo, R., Sanders, D.F., Smith, Z.P., Freeman, B.D., Paul, D.R., and McGrath, J.E., *Synthesis and characterization of thermally rearranted (TR) polymers: Effect of glass transition temperature of aromatic poly(hydroxyimide) precursors on TR process and gas permeation properties.* Journal of Materials Chemistry A, 2013. **In Press**.

16. Hiemenz, P.C. and Lodge, T.P., *Polymer Chemistry*. 2nd ed. 2007, Boca Raton: CRC Press.

17. Siggia, S., *Quantitative organic analysis via functional groups*. 3rd ed. 1963, New York: John Wiley and Sons, Inc.

18. Sanders, D.F., Guo, R., Smith, Z.P., Liu, Q., Stevens, K.A., McGrath, J.E., Paul, D.R., and Freeman, B.D., *Influence of polyimide precursor synthesis route and ortho-position functional group on thermally rearranged polymers: Thermal properties and free volume*. In Preparation.

19. Bondi, A., *van der Waals volumes and radii.* The Journal of Physical Chemistry, 1964. **68**(3): p. 441-451.

20. Bondi, A., *Physical properties of molecular crystals, liquids, and glasses*. 1968: Wiley.

21. van Krevelen, D.W., *Properties of polymers*. 1972, Amsterdam: Elsevier.

22. Park, J.Y. and Paul, D.R., *Correlation and prediction of gas permeability in glassy polymer membrane materials via modified free volume based group contribution method.* Journal of Membrane Science, 1997. **125**(1): p. 23-39.

Chapter 6: Influence of Polyimide Precursor Synthesis Route and *ortho*-Position Functional Group on Thermally Rearranged (TR) Polymer Properties: Pure Gas Permeability and Selectivity[9]

6.1 INTRODUCTION

Polyimides are commonly synthesized using chemical or thermal imidization [1]. In chemical imidization, a poly(amic acid) intermediate is formed, and it is then imidized using pyridine and acetic anhydride [1, 2]. Thermal imidization is typically achieved by imidizing a poly(amic acid) precursor by heating it to roughly 180 ºC in solution with *o*-dichlorobenzene as an azeotroping agent [1, 2]. An alternative route to thermal imidization involves the formation of an ester-acid intermediate, which can then be converted back to the poly(amic acid) at 180 ºC and simultaneously imidized [3]. The ester-acid intermediate is more hydrolytically stable and can yield higher molecular weight polyimides than the traditional thermal imidization [3].

The polyimide synthesis route can affect the transport properties of the resulting polymer [4, 5]. For example, Matsumoto and Xu reported a chemically imidized fluorinated polyimide having 2 times higher CO_2 permeability and 1.5 times higher CO_2/CH_4 selectivity than the same polymer synthesized via thermal imidization. Xu, Koros, and Paul have reported no difference in toluene flux from pervaporation measurements of a fluorinated polyimide synthesized via thermal and chemical imidization, but different fluxes were obtained depending on the synthesis route used to prepare copolymers [5]. Differences in transport properties from polymers synthesized via thermal and chemical imidization have been attributed to differences in molecular

[9] Adapted from Sanders, D.F., Guo, R., Smith, Z.P., Liu, Q., Stevens, K.A., McGrath, J.E., Paul, D.R., and Freeman, B.D., Influence of polyimide precursor synthesis route and ortho-position functional group on thermally rearranged polymers: Pure gas permeability and selectivity. In Preparation. D. F. Sanders performed the majority of experiments and wrote and edited the manuscript. Z. P. Smith, R. Guo, Q. Liu and K. A. Stevens provided experimental assistance. B. D. Freeman, J. E. McGrath, and D. R. Paul supervised this project and provided technical expertise.

weight depending on the synthesis method and the formation of isoimide structures during chemical imidization [1, 4, 5]. In addition to different molecular weight and isoimide content, the *ortho*-position functional group present in polyimide precursors to TR polymers can also be modified. For example, as discussed in chapter 3, chemical imidization results in the conversion of *ortho*-position hydroxyl groups to acetate groups.

Due to the potential impact of synthesis route on polyimide properties, the influence of precursor synthesis route on TR polymer transport properties has been investigated [2, 6]. Varying the precursor synthesis route can result in permeabilities that differ by roughly a factor of 3 after thermal rearrangement at 400 ºC. However, these differences in transport properties were primarily due to changes in the *ortho*-position group as a result of using various synthesis routes [2, 6].

One reason for our interest in *ortho*-position groups other than hydroxyl groups is that polyimide precursors to TR polymers synthesized via chemical rather than thermal imidization typically have higher permeability values; this difference is believed to be due, in part, to differences in the *ortho*-position groups present as a result of the synthesis route [2, 6]. For example, chemical imidization, while converting the amic acid units to imide linkages, also naturally converts *ortho*-position hydroxyl groups to more bulky and less polar *ortho*-position acetate groups, which may disrupt chain packing, resulting in higher permeability coefficients [6, 7].

This chapter reports gas transport properties of the series of HAB-6FDA-based polyimides with hydroxyl, acetate, propanoate, and pivalate groups as shown in Figure 3.2 and synthesized as shown in Figure 3.3. Additionally, the influence of TR conversion on transport properties in these polymers is also reported. Pure gas permeability and selectivity values are reported as a function of conversion for CH_4, N_2, O_2, CO_2, and H_2 to

further elucidate the influence of ortho-position group and synthesis route on gas transport properties in such materials.

6.2 Pure Gas Permeability and Selectivity of TR Polymers with Varying Synthesis Route and *ortho*-Position Group

Representative permeability data are presented in Figure 6.1. Pure gas permeability measurements showed typical dual-mode behavior over the pressure range of 3-15 atm [8-10]. No evidence of plasticization was observed. Figures 6.1A and 6.1B show the permeation behavior for CO_2 and H_2 in the HAB-6FDA-PAc-TR450 sample. This behavior is typical of all of the samples considered in this study. Because H_2 sorption is relatively low in polymers, including TR polymers [11], dual-mode effects are not apparent. As a result, H_2 permeability does not decrease significantly as pressure increases. CO_2 shows the characteristic dual mode decrease in permeability as pressure increases [8-10, 12, 13]. These effects can be significant, as seen in Figure 6.1A, where CO_2 permeability decreases by roughly 25% from 3-15 atm. For the purposes of comparing overall permeation properties in the various materials studied, we focus on permeability coefficients measured at an upstream pressure of roughly 10 atm. Actual upstream pressure varied from approximately 9.8 – 10.2 atm based on experimental variation, but it is assumed that permeability coefficients vary little with pressure over such a narrow range, so the permeability values appearing in subsequent figures and tables will be referred to as the permeability coefficients at an upstream pressure of 10 atm.

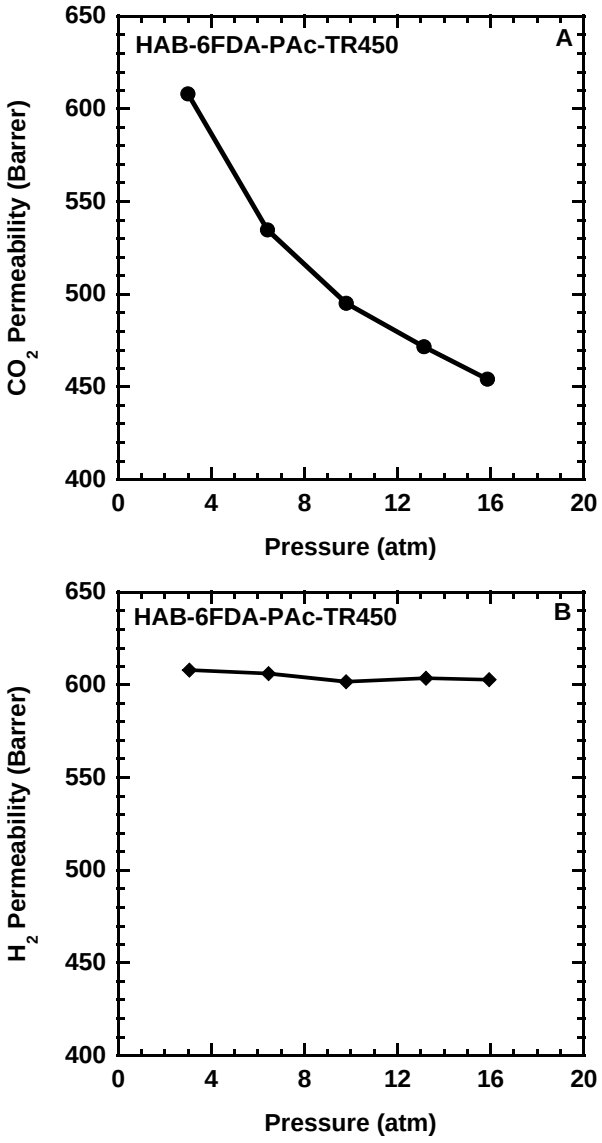

Figure 6.1 Influence of upstream pressure on CO_2 and H_2 permeability coefficients at 35°C for HAB-6FDA-PAc-TR450.

6.3 Effect of Synthesis Route on TR Polymer Transport Properties

Table 6.1 presents pure gas permeability coefficients in the EA, Ac, C, PrAc, and PAc polymers. For all samples studied, the permeability of all gases increases as conversion increased. As in previous studies on other TR polymers, chemically imidized

polymers show significantly higher permeability than those synthesized through thermal routes, such as the EA polymer studied here [2, 6]. The chemically imidized polyimide precursor (i.e., sample C in Table 6.1) has a CO_2 permeability of 12.6 Barrer, which is approximately 4 times higher than the untreated thermally imidized polymer (i.e., sample EA in Table 6.1), which has a CO_2 permeability of 3.1 Barrer. This difference in CO_2 permeability is reduced following heat treatment at 350 ºC, but then increases as heat treatment temperature increases. For example, HAB-6FDA-C has CO_2 permeability coefficients approximately 2, 3, and 5 times higher than HAB-6FDA-EA after rearrangement at 350, 400, and 450 ºC respectively. This general trend is observed for each gas considered, which suggests that the gas permeability increases more rapidly as more acetate *ortho*-position groups are lost during thermal rearrangement at higher temperatures. This rapid increase is likely due to the loss of these bulky acetate groups, which causes changes in free volume and/or free volume distribution of the resulting partially converted TR polymers [2, 6].

Table 6.1 Pure gas permeability coefficients at 10 atm and 35 ºC for HAB-6FDA polyimides with various *ortho*-position functional groups and their TR polymers.

			Permeability (Barrer)				
***ortho*-Position Group**	**Thermal Treatment**	**PBO Conversion (%)**	**CH_4**	**N_2**	**O_2**	**CO_2**	**H_2**
EA**	-	-	0.06	0.1	0.65	3.1	11
EA	350	45	0.24	0.6	3.8	17	56
EA**	400	76	1.4	2.6	13	54	115
EA	450	118	2.9	4.4	20	80	150
C*	-	-	0.31	0.56	3.2	12.6	38
C*	350	39	0.78	1.6	9	35	94
C*	400	60	5.7	8.8	39	167	280
C*	450	76	18	25	100	427	550
Ac**	-	-	0.26	0.46	2.6	11	32
Ac	350	39	0.75	1.58	8.9	37	98.4
Ac**	400	60	5.1	8.6	39	170	290
Ac	450	68	12	17	73	320	445
PrAc	-	-	0.68	0.94	4.6	17	41
PrAc	350	39	1.48	2.6	12.8	46	112
PrAc	400	56	4.8	6.9	30.3	118	215
PrAc	450	78	28	34	135	530	690
PAc**	-	-	3.1	3.3	15.7	57	108
PAc	350	14	4.4	4.9	21.5	76	136
PAc	400	58	63	14	15	61	230
PAc	450	81	26	32	127	500	600

NOTE: An asterisk (*) denotes data from reference [14], and two asterisks denote CO_2 and CH_4 data from reference [2]. The information in the "Thermal Treatment" column refers to the time/temperature combinations used to prepare TR polymers. A dash (-) represents data for the precursor polyimide; entries of 350, 400, and 450 represent polyimide precursors treated, as described in the Experimental section, in a tube furnace at 350°C or 400°C for 1 hour or 450°C for 30 minutes. PBO conversion was estimated as described in the text, with the details of the estimation method reported in chapter 5 [15].

The PBO conversions listed in Table 6.1 are derived from the change in sample mass as a result of the thermal treatment, and they are based on the assumption that any *ortho*-position acetate group lost during thermal rearrangement converts to a PBO structure, which we call the *o*-pos assumption [15]. This assumption has been previously used in the chapter 4 due to its systematic correlation with gas transport properties [14]. In this case, only acetate-containing polyimide and PBO structures would be present in the polymer after thermal rearrangement. However, some hydroxyimides could also be present, as shown in Figure 3.4. Thus, another limit for the structure of polyimides partially converted to their corresponding TR polymers is that all acetate groups are first converted to hydroxyl groups before any PBO units are formed, which we call the OH assumption [15]. Because thermally treated polyimide precursors often become insoluble at low extents of conversion to TR polymers, exact analysis of the chemical structure following thermal rearrangement becomes difficult (since solution state NMR can no longer be used) and leads to some uncertainty in the chemical structure of the resulting TR polymers. These assumptions and their ramifications are described in detail in chapter 5 [15]. For reasons discussed in more detail below, the assumption embodied in the conversion values reported in Table 6.1, where all unconverted polyimides retain their original *ortho*-position group, provides a more logical correlation with measured transport properties than the so-called OH assumption. Consequently, conversion values

reported in this study will be based on the *o*-pos assumption, which is introduced to provide additional support for the decision to base conversion on the *o*-pos assumption. Obviously, the conversion values reported for EA samples, where the polyimide precursor has only hydroxyl *ortho*-position groups, are not affected by this issue.

As seen in Table 6.1, the permeability of the thermally imidized sample (i.e., EA) is lower than the acetate-containing samples (i.e., C and Ac) for all gases at each thermal treatment condition. This difference has been ascribed to the lack of a leaving group in the EA material and the possibility of more extensive hydrogen bonding in the hydroxyl-bearing EA material [2]. Both factors would tend to improve chain packing, resulting in lower free volume in the hydroxyl containing material relative to the acetate containing polymer [7].

Because the synthesis route and *ortho*-position group both differ between the EA and C samples, it is desirable to compare two samples with the same chemical structure synthesized via different routes. As shown in Figure 3.4, the hydroxyl *ortho*-position group of HAB-6FDA-EA may be converted to an acetate group by contacting HAB-6FDA-EA with acetic acid and pyridine to yield a polymer referred to as HAB-6FDA-Ac. Thus, a polyimide having the same acetate-containing *ortho*-position structure as HAB-6FDA-C can be prepared via a different synthesis route. As shown in Table 6.1 for HAB-6FDA-C and HAB-6FDA-Ac, the pure gas permeability coefficients of the polyimides and samples rearranged at 350 and 400 ºC are very similar for all gases. The thermal properties and free volume of these samples are also very similar, which suggests that that the synthesis route used to form these polymers does not strongly influence their properties [2, 15]. There is a larger variation in gas permeation properties between the Ac and C samples rearranged at 450 ºC. For example, the CO_2 permeability of HAB-6FDA-Ac is 25% lower than the CO_2 permeability of HAB-6FDA-C. A similar trend is

observed for all gases. However, HAB-6FDA-C has a PBO conversion of 76% while Ac was only 68% converted to PBO [15]. Lower conversion typically results in lower gas permeability in TR polymers [14, 16]. The CO_2 permeability of the Ac and C samples is especially sensitive to conversion at higher conversion values independent of structural assumptions used in the conversion calculation. Therefore, the difference in conversion between the Ac and C samples rearranged at 450 ºC may play a role in their different transport properties.

Figures 6.2A and 6.2B present CO_2 permeability of the EA, C, and AC samples at 10 atm as a function of conversion to benzoxazole units calculated two ways, corresponding to the o-pos assumption (Figure 6.2A) and the OH assumption (Figure 6.2B). As indicated earlier, conversion is assessed based upon the mass loss of a sample relative to what would be expected if that sample underwent the TR conversion reactions shown in Figure 3 (that is, no allowance is made for other reactions, such as thermal degradation). The conversion data are taken from results in chapter 5 [15]. In Figure 6.2A, a value of zero percent conversion corresponds to the precursor polyimide before any thermal treatment to bring about TR conversion. In Figure 6.2B, zero percent conversion would include the precursor polyimide and any thermally rearranged polymers which have not lost enough mass to account for the complete conversion of ortho-position groups to hydroxyl groups. That is, at low levels of thermal treatment (e.g., 350°C for one hour), some samples will not lose enough mass to have begun to form benzoxazole units according to the OH assumption. As indicated earlier, these two limiting cases do not affect conversion calculations for the EA sample, since its precursor polyimide contains only hydroxyl groups that are presumed to rearrange directly to benzoxazole units. In both figures, the EA-450 sample has over 100% conversion,

suggesting that this sample has undergone at least some thermal degradation in addition to thermal rearrangement.

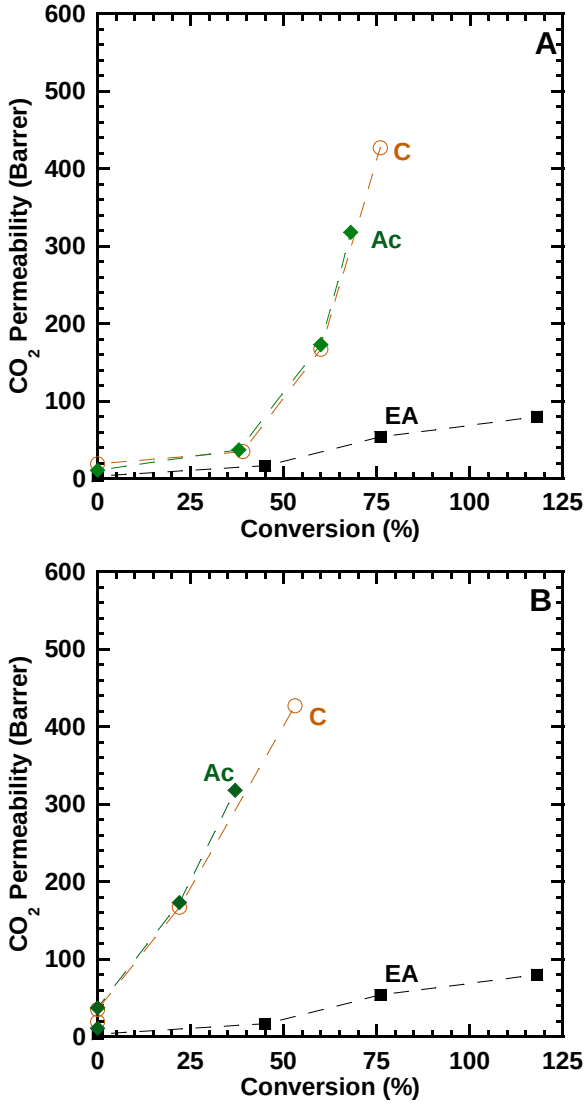

Figure 6.2 CO_2 permeability as a function of conversion for cases where A) all polyimides are converted to PBO or retain their original *ortho*-position group (*o*-pos assumption) and B) all *ortho*-position groups are converted to hydroxyl groups before any PBO is formed (OH assumption). Permeabilities were measured at 10 atm and 35 ºC for EA (■), C (○), and Ac (♦).

Both the Ac and C samples, which should have the same nominal chemical structure but were prepared via different synthesis routes, exhibit increasing permeability with increasing conversion, as shown in Figure 6.2. The permeability of the precursor

polyimides is quite similar. Additionally, the C-350 and Ac-350 samples have quite similar permeability coefficients and conversion values, and the same trend is observed with the C-400 and Ac-400 samples. The C-450 sample, however, exhibits substantially higher permeabilities than the Ac-450 sample. Interestingly, the conversion of the C-450 sample (76%) is also higher than that in the Ac-450 sample (68%). Therefore, the differences in permeability between the TR450 samples are likely due to conversion differences. The difference in conversion between these samples may have been a result of small variations in the temperature/time protocol used to prepare the samples. At high rearrangement temperatures (e.g., 450C), sample-to-sample variations in mass loss are common and can result in roughly ± 4% variations in the degree of conversion. Therefore, the observed differences in conversion and permeability may well be the result of slightly different furnace conditions when the two samples were thermally treated.

As shown in Table 1 and Figures 6.2A and 6.2B, TR polymers prepared from polyimides with acetate *ortho*-position groups (i.e., the C and Ac samples) have a much larger increase in CO_2 permeability with conversion than the hydroxyl-containing EA sample. This larger increase is independent of synthesis route, so the *ortho*-position functional group must have a stronger influence on the transport properties than the synthesis route of the polyimide precursor.

Based on trends in Figure 6.2, the structural assumptions in Figure 6.2A (i.e., the *o*-pos assumption) may be more representative of the actual structure of partially converted TR polymers at low rearrangement temperatures such as 350 ºC. For example, Figure 6.2B assumes all *ortho*-position groups are converted to hydroxyl groups before any rearrangement occurs. The result is 80% conversion of *ortho*-position acetate groups into hydroxyl groups and 0% conversion to PBO for the C-350 sample. Increasing potential hydrogen bonding due to a larger number of hydroxyl groups and a

simultaneous decrease in the number of bulky acetate groups would likely decrease permeability. However, after thermal treatment at 350 ºC, gas permeability in the chemically imidized sample increased for all gases studied. For example, CO_2 permeability was roughly 3 times higher in the C-350 sample than in the chemically imidized polyimide. Thus, some PBO formation is likely to be occurring in the C and Ac samples [14, 17]. The assumption in Figure 6.2A, where all unconverted polyimides maintain their original *ortho*-position group provides a more logical correlation with measured transport properties. The trends in permeability are not significantly affected by this assumption at higher conversions. Therefore, this assumption will be used for analysis of these polymers in the remainder of what follows. In reality, the actual structure of these partially converted polymers most likely lies between the values given by these two assumptions.

6.4 Influence of *ortho*-Position Group on TR Polymer Permeability

The *ortho*-position group was varied using the same synthesis route to explore the effect of leaving group structure on gas transport properties. In addition to the polyimides with hydroxyl and acetate groups discussed in the previous section, polymers with propanoate and pivalate *ortho*-position groups were prepared by modification of the hydroxyimide (i.e., the EA polyimide precursor). As shown in Table 6.1, the permeability coefficients of the polyimide precursors increase with increasing *ortho*-position group size, presumably due to increased free volume in polymers with more bulky and less polar *ortho*-position groups [15, 18]. For example, the CO_2 permeability increases from 3.1 Barrer for the EA sample, which has a hydroxyl *ortho*-position group, to 11 Barrer for the acetate-containing polyimide (Ac), to 17 Barrer for the propanoate-containing polyimide (PrAc), and to 57 Barrer for the pivalate-containing polyimide (PAc). Similar

increases in permeability are observed for all gases measured. These larger groups effectively inhibit chain packing and likely undergo less hydrogen bonding than the hydroxyl samples. Both of these characteristics should increase the free volume of the polymer and, in turn, the transport properties [15].

While pure gas permeability increases for all samples as thermal rearrangement progresses, the permeability at a given conversion is dependent on the polyimide precursor *ortho*-position group. For example, Figure 6.3 presents CO_2 permeability as a function of conversion for the EA, Ac, PrAc, and PAc polymers. This figure shows large increases in CO_2 permeability for all TR polymers made from polyimides with non-hydroxyl *ortho*-position groups compared to the hydroxyl-containing EA sample. Assuming all unconverted chains in the PrAc and PAc samples retain their original *ortho*-position groups, the EA-400, PrAc-450, and PAc-450 samples all have between 76 and 81% PBO units by mass. However, the CO_2 permeability of the PrAc and PAc samples is roughly 500 Barrer, while that of the EA sample is 80 Barrer, despite similar PBO conversion. Comparing results at the same thermal treatment protocols instead of conversion, the PrAc-450 sample and PAc-450 samples exhibit a CO_2 permeability approximately 4 times higher than the EA-450 sample (cf., Table 1). Therefore, this difference is not an artifact of the structural assumptions that enter the PBO conversion calculation.

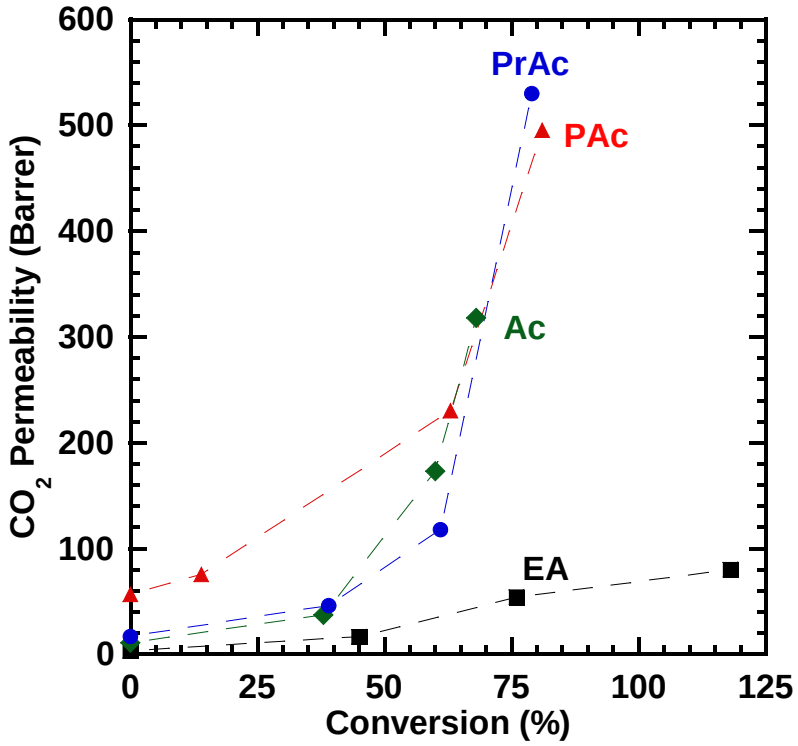

Figure 6.3 CO_2 permeability at 10 atm and 35 ºC as a function of TR conversion assuming all unconverted polyimides retain original *ortho*-position functionality (*o*-pos assumption) for EA (■), Ac (♦), PrAc (●), and PAc (▲).

As illustrated in Figure 3.2, all of the polyimides considered here are expected to rearrange to form the same PBO structure, but the *ortho*-position groups lost during thermal rearrangement have a large effect on the transport properties of the final TR polymer (cf., Table 6.1 and Figure 6.3). This effect may be caused by the simultaneous loss of *ortho*-position groups and thermal rearrangement in these polymers. Rearrangement forms a highly rigid, possibly-crosslinked structure [15]. These partially converted TR polymers also exhibit no measurable T_g before thermal degradation, indicating little chain mobility. Therefore, if bulky *ortho*-position groups are lost and chains lack sufficient mobility to reorganize so as to efficiently occupy the space vacated

by the leaving group, the free volume and its distribution could potentially be altered, which would be expected to influence gas transport properties [18].

As shown in Figure 6.3 and Table 6.1, the size of the *ortho*-position group also influences the evolution of permeability with conversion. This trend is most noticeable when the PBO conversion is below roughly 60%. The CO_2 permeability of the PAc sample is roughly 1.5 times the CO_2 permeability of the Ac sample in this conversion range (cf., Table 6.1). Similar trends are seen for all gases. At the same *ortho*-position conversion, any remaining bulky groups (e.g., pivalate) would likely increase permeability more than any remaining acetate groups, as they do in the polyimide precursors.

The PrAc samples exhibit higher permeabilities for all gases than Ac samples for conversions less than 60% except for the sample rearranged at 400 ºC. For the PrAc-400 sample, all gas permeabilities in this study are lower than the Ac-400 sample. The most dramatic case is a 30% lower CO_2 permeability. This lower permeability is unexpected, since the Ac-400 and PAc-400 samples have the same fractional free volume [15]. Fractional free volume was calculated assuming that all units that were not converted to PBO units retained their original *ortho*-position group (i.e., the *o*-pos assumption) [15]. The difference in permeability of all gases at 400 ºC for the PrAc and Ac samples may be caused by differing amounts of *ortho*-position conversion. For example, if acetate groups were lost more readily than propanoate groups at 400 ºC, the polyimide units present after thermal rearrangement may contain more hydroxyl groups (c.f., Figure 3.4). At a given density value, a larger fraction of hydroxyl groups would result in a higher calculated fractional free volume and could explain the differences in permeability seen between these two polymers after rearrangement at 400 ºC.

Above 60% conversion to PBO units, the resulting TR polymers formed from non-hydroxyl *ortho*-position polyimides (i.e., Ac, PrAc, PAc) fall onto the same line of CO_2 permeability as a function of conversion in Figure 6.3. Similar trends are seen for all gases. The Ac sample has a lower CO_2 permeability than the PrAc and PAc samples, but falls on the same trend line. As previously discussed, the Ac sample had a relatively low conversion at 450 ºC, and permeability is very sensitive to conversion at these rearrangement temperatures, as shown in Figure 6.2A. Therefore, the *ortho*-position group becomes less important as more of these groups are lost and a larger fraction of PBO units is formed. The CO_2 permeability of these materials at all conversions is much higher than the CO_2 permeability of the hydroxyl-containing EA sample. The higher permeability for all gases of the Ac, PrAc, and PAc samples compared to the EA samples at all conversions suggest that bulkier *ortho*-position groups or a lack of hydrogen bonding may lead to increased TR polymer permeability. However, the similar permeabilities for all gases at higher conversions for the Ac, PrAc, and PAc samples suggests that the size of the *ortho*-position group may not play as large of a role as hydrogen bonding at higher conversions.

Pure gas selectivities are listed in Table 6.2 and are shown graphically for CO_2/CH_4 in Figure 6.4. In general, selectivity decreases as thermal rearrangement progresses. In fact, it decreases monotonically with conversion for the O_2/N_2 and CO_2/N_2 gas pairs. However, a maximum in selectivity for gas pairs containing CH_4 is observed after thermal rearrangement at 350 ºC for all samples, except the one designated as PAc, as reported previously for HAB-6FDA-C [14]. This selectivity maximum may arise from a more favorable free volume distribution in samples at the maximum in selectivity for CO_2/CH_4 separation. Such a distribution may exist if an average free volume element size that inhibits CH_4 diffusion was formed after rearrangement at 350 ºC. Table 6.2 shows a

similar maximum in N_2/CH_4 selectivity for all samples except PAc, and no maximums are seen for gas pairs not containing CH_4, further supporting this hypothesis. The lack of a maximum in the PAc sample may be due to a higher initial free volume element size arising from these bulky pivalate *ortho*-position groups [15].

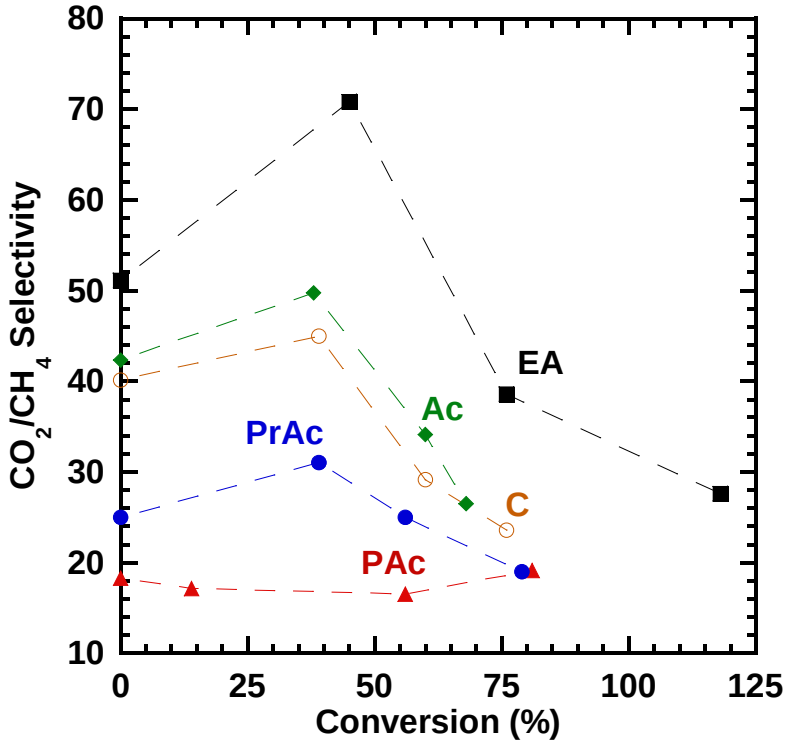

Figure 6.4 CO_2/CH_4 pure gas selectivity at 10 atm and 35 ºC as a function of TR conversion (*o*-pos assumption) for EA (■), C (○), Ac (♦), PrAc (●), and PAc (▲).

As seen in Figure 6.4, the CO_2/CH_4 selectivity is roughly 25% higher in the EA sample than in the Ac or C samples over the range of 0 to 75% conversion. This result suggests a permeability/selectivity tradeoff in these polymers. For polymers with non-hydroxyl *ortho*-position groups, selectivity decreases as the *ortho*-position group size increases at conversions less than roughly 60%. However, like the permeability, CO_2/CH_4

selectivity values converge to a similar value of around 20 as conversion increases to higher levels in these samples. The hydroxyl-containing EA sample maintains higher selectivity and lower permeability at all conversions than the TR polymers from polyimides with non-hydroxyl *ortho*-position groups. These trends are true for all gas pairs listed in Table 6.2. Therefore, hydrogen bonding in the precursor polyimide and/or the small nature of the leaving group may strongly influence the free volume and its distribution in these polymers.

Table 6.2 Pure gas selectivity at 10 atm and 35 ºC for HAB-6FDA polyimides and TR polymers with various *ortho*-position functional groups

		Selectivity			
***ortho*-Position Group**	**Treatment**	**CO_2/CH_4**	**CO_2/N_2**	**O_2/N_2**	**N_2/CH_4**
EA	-	51	32	6.6	1.6
EA	350	71	28	6.3	2.5
EA	400	39	21	5	1.9
EA	450	28	18	4.5	1.5
C*	-	40	23	5.7	1.8
C*	350	45	22	5.5	2.1
C*	400	29	19	4.5	1.5
C*	450	24	17	4.0	1.4
Ac	-	42	24	5.7	1.8
Ac	350	50	24	5.6	2.1
Ac	400	34	20	4.5	1.7
Ac	450	27	19	4.3	1.4
PrAc	-	25	18	4.9	1.4
PrAc	350	31	18	4.9	1.8
PrAc	400	25	17	4.4	1.4
PrAc	450	19	16	4.0	1.2
PAc	-	18	17	4.8	1.1
PAc	350	17	15	4.4	1.1
PAc	400	16	15	4.1	1.1
PAc	450	19	15	3.9	1.2

NOTE: An asterisk (*) denotes data from reference [5].

The permeability/selectivity trade-off from adding these non-hydroxyl *ortho*-position groups can be visualized using the Robeson upper bound shown in Figure 6.5 [19]. For a given sample, the conversion increases from left to right in this figure. All of the HAB-6FDA polyimides are well below the 1991 upper bound but move towards the upper bound as rearrangement occurs. The EA hydroxyimide shows improvements in permeability and selectivity that place it on the 1991 upper bound after rearrangement at

350 ºC. However, additional rearrangement for this polymer shows a permeability-selectivity trade off similar to that expected by the upper bound, and no further overall improvement in transport properties is observed. In contrast, thermal rearrangement of the non-hydroxyl Ac, PrAc, and PAc samples results in selectivity decreases that are less than those anticipated by the upper bound. Therefore, these samples traverse the 1991 upper bound as TR conversion increases. Because of this overall increase in transport properties, it may be advantageous to use non-hydroxyl *ortho*-position groups, especially for applications where high permeability is desired.

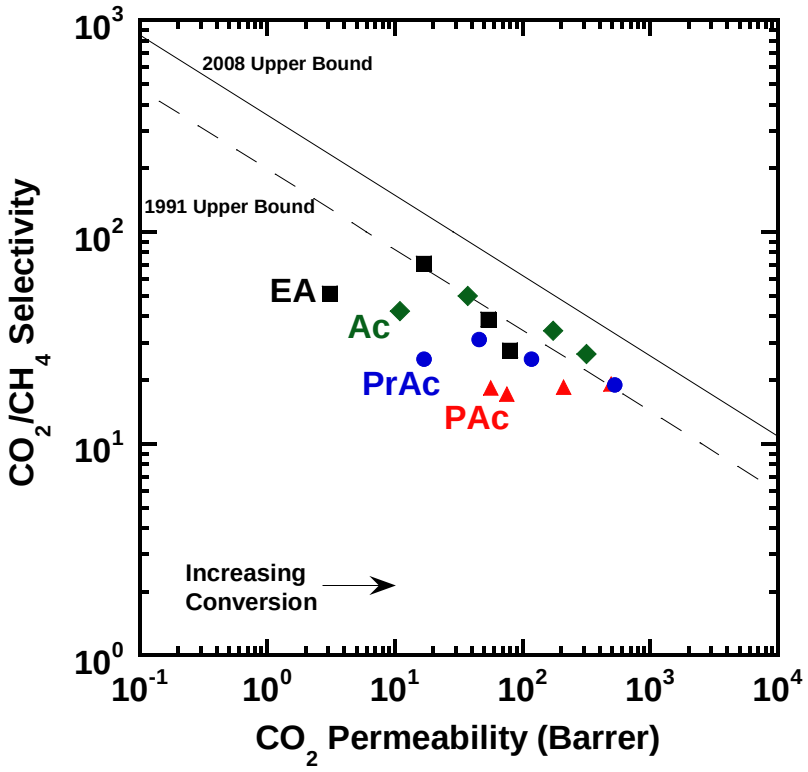

Figure 6.5 Upper bound plot for EA (■), Ac (♦), PrAc (●), and PAc (▲) [19, 20]. Conversion increases within samples from left to right.

While the upper bound methodology provides a convenient means to assess membrane performance, fractional free volume analysis can provide a fundamental

interpretation of permeability changes from sample to sample. Figure 6.6 presents CO_2 permeability as a function of the calculated fractional free volume of each polymer using the *o*-pos assumption. CO_2 is again used as a representative gas, and all other gases show similar trends. The detailed calculation of fractional free volume is reported elsewhere [15]. In general, higher free volume results in higher permeability for all samples prepared from the same polyimide precursor. However, this trend is not always obeyed when comparing samples from different polyimide precursors. The largest difference can be seen between the hydroxyl-containing EA samples and the other samples in this study. For example, the EA-450 and Ac-450 sample have roughly the same free volume (1/FFV = 5 in Figure 6.6) [15], but the CO_2 permeability of the Ac-450 sample is 4 times higher than that in EA-450. The significant difference in permeability of these samples, despite their similar free volume, may be due to differences in free volume distribution.

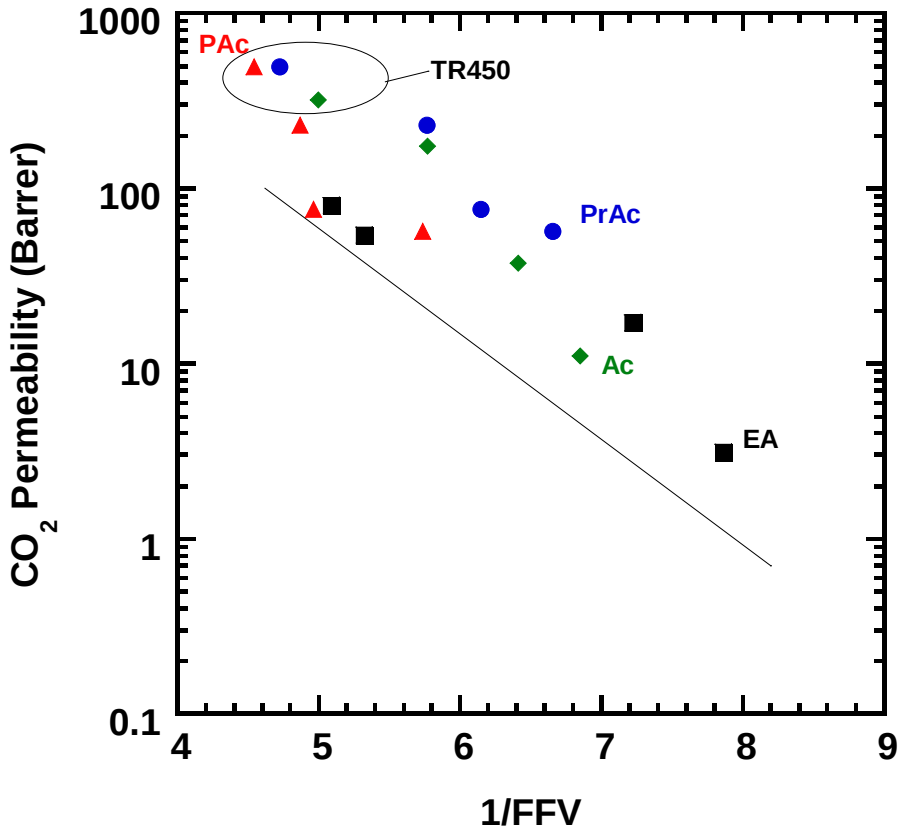

Figure 6.6 CO_2 permeability at 10 atm and 35 ºC as a function of 1/FFV for EA (■), Ac (♦), PrAc (●), and PAc (▲). The dashed line represents a trend averaged for many families of polymers [18].

The PAc, PrAc, and PrAc samples that were thermally rearranged at 450 ºC, shown in the top left corner of Figure 6.6, have similar FFV and CO_2 permeability values [15]. Therefore, TR polymers from polyimides with non-hydroxyl *ortho*-position groups may form similar structures as TR conversion increases towards higher amounts of PBO units.

6.5 REFERENCES

1. Ohya, H., Kudryavtsev, V.V., and Semenova, S.I., *Polyimide membranes - applications, fabrications, and properties*. 1996: Gordon and Breach.

2. Guo, R., Sanders, D.F., Smith, Z.P., Freeman, B.D., Paul, D.R., and McGrath, J.E., *Synthesis and Characterization of Thermally Rearranged (TR) Polymers: Influence of ortho-positioned functional groups of polyimide precursors on TR process and gas transport properties.* Journal of Materials Chemistry A, 2013. **1**: p. 262-272.

3. Farr, I.V., Glass, T.E., Ji, Q., and McGrath, J.E., *Synthesis and characterization of diaminophenylindane based polyimides via ester-acid solution imidization.* High Performance Polymers, 1997. **9**(3): p. 345-352.

4. Matsumoto, K. and Xu, P., *Gas permeation properties of hexafluoro aromatic polymers.* Journal of Applied Polymer Science, 1993. **47**: p. 1961-1972.

5. Xu, W., Synthesized polyimide membranes for pervaporation separations of toluene/iso-octane mixtures. Ph.D. Thesis from The University of Texas at Austin, 2005.

6. Han, S.H., Misdan, N., Kim, S., Doherty, C.M., Hill, A.J., and Lee, Y.M., *Thermally rearranged (TR) polybenzoxazole: Effects of diverse imidization routes on physical properties and gas transport behaviors.* Macromolecules, 2010. **43**(18): p. 7657-7667.

7. Muruganandam, N., Koros, W.J., and Paul, D.R., *Gas Sorption and Transport in Substituted Polycarbonates.* Journal of Polymer Science Part B-Polymer Physics, 1987. **25**(9): p. 1999-2026.

8. Chan, A.H., Koros, W.J., and Paul, D.R., *Analysis of hydrocarbon gas sorption and transaport in ethyl cellulose using the dual sorption/partial immobilization methods.* Journal of Membrane Science, 1978. **3**: p. 117-130.

9. Paul, D.R., *Gas sorption and transport in glassy polymers.* Berichte der Bunsengesellschaft für physikalische Chemie, 1979. **83**: p. 294-302.

10. Paul, D.R. and Koros, W.J., *Effect of partially immobilizing sorption on permeability and the diffusion time lag.* Journal of Polymer Science: Part B: Polymer Physics, 1976. **14**: p. 675-685.

11. Smith, Z.P., Sanders, D.F., Ribeiro, C.P., Guo, R., Freeman, B.D., Paul, D.R., McGrath, J.E., and Swinnea, S., *Gas sorption and characterization of thermally rearranged polyimides based on 3,3'-dihydroxy-4,4'-diamino-biphenyl (HAB) and 2,2'-bis-(3,4-dicarboxyphenyl) hexafluoropropane dianhydride (6FDA).* Journal of Membrane Science, 2012. **415-416**: p. 558-567.

12. Koros, W.J., Sorption and transport of gases in glassy polymers. Ph.D. Thesis from The University of Texas at Austin, 1977.

13. Koros, W.J., Paul, D.R., and Rocha, A.A., *Carbon dioxide sorption and transport in polycarbonate.* Journal of Polymer Science: Part B: Polymer Physics, 1976. **14**: p. 687-702.

14. Sanders, D.F., Smith, Z.P., Ribeiro, C.P., Guo, R., McGrath, J.E., Paul, D.R., and Freeman, B.D., *Permeability, diffusivity, and free volume of thermally rearranged polymers based on 3,3'-dihydroxy-4,4'-diamino-biphenyl (HAB) and 2,2'-bis-(3,4-dicarboxyphenyl) hexafluoropropane dianhydride (6FDA).* Journal of Membrane Science, 2012. **409-410**: p. 232-241.

15. Sanders, D.F., Guo, R., Smith, Z.P., Liu, Q., Stevens, K.A., McGrath, J.E., Paul, D.R., and Freeman, B.D., *Influence of polyimide precursor synthesis route and ortho-position functional group on thermally rearranged polymers: Thermal properties and free volume.* In Preparation.

16. Park, H.B., Jung, C.H., Lee, Y.M., Hill, A.J., Pas, S.J., Mudie, S.T., Van Wagner, E., Freeman, B.D., and Cookson, D.J., *Polymers with cavities tuned for fast selective transport of small molecules and ions.* Science, 2007. **318**(5848): p. 254-258.

17. Park, H.B., Han, S.H., Jung, C.H., Lee, Y.M., and Hill, A.J., *Thermally rearranged (TR) polymer membranes for CO_2 separation.* Journal of Membrane Science, 2010. **359**(1-2): p. 11-24.

18. Matteucci, S.T., Yampolskii, Y.P., Freeman, B.D., and Pinnau, I., *Transport of gases and vapors in glassy and rubbery polymers*, in *Materials science of membranes for gas and vapor separation*, Y. Yampolskii, I. Pinnau, and B.D. Freeman, Editors. 2006, John Wiley & Sons: Chichester. p. 1-47.

19. Robeson, L.M., *The upper bound revisited.* Journal of Membrane Science, 2008. **320**(1-2): p. 390-400.

20. Robeson, L.M., *Correlation of separation factor versus permeability for polymeric membranes.* Journal of Membrane Science, 1991. **62**(2): p. 165-185.

Chapter 7: Conclusions and Recommendations

7.1 CONCLUSIONS

7.1.1 Permeability, Diffusivity, and Solubility of Chemically Imidized HAB-6FDA[10]

HAB-6FDA polyimide was synthesized using chemical imidization and was successfully thermally rearranged to give various fractions of PBO units by heat treatment at 350 and 400ºC for 1 hour and 450ºC for 0.5 hours. These temperatures gave conversions of the polyimide precursor towards its TR polymer analog ranging from 39% to 76% as estimated from mass loss. Thermally rearranged polymers from HAB-6FDA have a CO_2 permeability more than 30 times higher, at 10 atm and 35ºC, than the precursor polyimide after thermal rearrangement at 450ºC for 0.5 hours. Significant increases in permeability were also observed for H_2, CH_4, N_2, and O_2; these changes are due to increases in both solubility and diffusivity. However, the increase in diffusivity was greater than the increase in solubility. In one example, the diffusivity of the gas considered typically increased by approximately an order of magnitude after thermal rearrangement while the solubility increased by roughly a factor of two.

Low degrees of thermal rearrangement increased CO_2 permeability and CO_2/CH_4 selectivity. However, thermal rearrangement at temperatures higher than 350 ºC began to decrease selectivity as permeability increased. These thermally rearranged polymers were found to traverse Robeson's 1991 upper bound and move closer to the 2008 upper bound. Thus, thermal rearrangement to form PBO units improved the transport properties of

[10] Adapted from Sanders, D.F., Smith, Z.P., Ribeiro, C.P., Guo, R., McGrath, J.E., Paul, D.R., and Freeman, B.D., Permeability, diffusivity, and free volume of thermally rearranged polymers based on 3,3'-dihydroxy-4,4'-diamino-biphenyl (HAB) and 2,2'-bis-(3,4-dicarboxyphenyl) hexafluoropropane dianhydride (6FDA). Journal of Membrane Science,2012. 409-410: p. 232-241.; copyright Elsevier. D. F. Sanders performed the majority of experiments and wrote and edited the manuscript. Z. P. Smith, R. Guo, and C. P. Ribeiro. B. D. Freeman, J. E. McGrath, and D. R. Paul supervised this project and provided technical expertise.

these polymers and did not simply trade permeability for selectivity as might be expected for changes among a family of polymers that simply increased (or decreased) average free volume. Decreases in CO_2/CH_4 permeability selectivity were due to a decrease in both solubility and diffusivity selectivity. For example, the conversion of this chemically imidized HAB-6FDA polyimide to the C-TR450 sample caused the CO_2/CH_4 selectivity to decrease by 42%. This decrease was due to a 25% decrease in diffusivity selectivity and a 34% decrease in solubility selectivity.

7.1.2 Effect of Synthesis Route and *ortho*-Position Functional Group on TR Polymer Thermal Rearrangement and Free Volume[11]

The properties of HAB-6FDA-based TR polymers vary depending on the *ortho*-position groups attached to polyimide precursors. Acetate and propanoate *ortho*-position groups have lower thermal stability than pivalate groups, and polymers with these groups begin thermal rearrangement at lower temperatures than those with pivalate or hydroxyl groups. Thermal rearrangement largely occurs before the onset of thermal degradation, since thermal rearrangement occurs between about 300-450 ºC while degradation begins at around 450-500 ºC. By-products from the loss of the *ortho*-position groups evolve as thermal rearrangement occurs, and the observed mass fragments agree with likely *ortho*-position degradation products. Density decreases and fractional free volume increases as a function of thermal rearrangement in all samples. Free volume increased by approximately 4-6% from the PI to the TR450, but exact values could not be determined due to uncertainties in the exact structure of partially converted TR polymers. The HAB-

[11] Adapted from Sanders, D.F., Guo, R., Smith, Z.P., Liu, Q., Stevens, K.A., McGrath, J.E., Paul, D.R., and Freeman, B.D., *Influence of polyimide precursor synthesis route and ortho-position functional group on thermally rearranged polymers: Thermal properties and free volume.* In Preparation. D. F. Sanders performed the majority of experiments and wrote and edited the manuscript. Z. P. Smith, R. Guo, Q. Liu and K. A. Stevens provided experimental assistance. B. D. Freeman, J. E. McGrath, and D. R. Paul supervised this project and provided technical expertise.

6FDA-Ac and HAB-6FDA-C samples have very similar free volume and thermal properties, despite being synthesized by different routes. The synthesis routes used to form these materials should, in principle, lead to the same polyimide chemical structure, so the chemical structure of the *ortho*-position functional group apparently has a much larger effect on TR polymer properties than the synthesis route used to prepare the polyimide precursor.

7.1.3 Effect of Synthesis Route and *ortho*-Position Functional Group on TR Polymer Pure Gas Permeability and Selectivity[12]

A comparison of permeability as a function of conversion for acetate-functionalized HAB-6FDA polymers synthesized by two different routes showed no significant differences in transport properties. Both polymers exhibited significantly higher permeabilities than the HAB-6FDA polymer synthesized via thermal imidization. Therefore, the polyimide precursor *ortho*-position group has a larger effect on transport properties than the precursor synthesis route. The impact of the *ortho*-position group is consistent with concurrent loss of the group and formation of a rigid, glassy PBO structure. The permeability and selectivity of TR polymers formed from precursors with various *ortho*-position groups were also studied. TR polymers with non-hydroxyl *ortho*-position functional groups showed higher permeability and lower selectivity as a function of conversion than those from hydroxyl-containing polyimides. Decreases in selectivity for these non-hydroxyl TR polymers were less than expected based on the trade-off relationship of the upper bound line. Non-hydroxyl *ortho*-position functional groups

[12] Adapted from Sanders, D.F., Guo, R., Smith, Z.P., Liu, Q., Stevens, K.A., McGrath, J.E., Paul, D.R., and Freeman, B.D., *Influence of polyimide precursor synthesis route and ortho-position functional group on thermally rearranged polymers: Pure gas permeability and selectivity.* In Preparation. D. F. Sanders performed the majority of experiments and wrote and edited the manuscript. Z. P. Smith, R. Guo, Q. Liu and K. A. Stevens provided experimental assistance. B. D. Freeman, J. E. McGrath, and D. R. Paul supervised this project and provided technical expertise.

enable a polymer with relatively common transport properties to traverse the 1991 upper bound and move towards performance at the current state of the art in membrane technology. TR polymers from polyimides with non-hydroxyl *ortho*-position groups also had relatively similar free volumes to those from hydroxyl-containing precursors despite having a significantly higher permeability. Therefore, the free volume distribution is likely affected by these *ortho*-position groups.

7.2 Recommendations for Future Work

7.2.1 Effect of *ortho*-Position Group on TR Polymer Mixed Gas Transport Properties

The results in this dissertation focused on pure gas transport properties of HAB-6FDA TR polymers with varying *ortho*-position group and synthesis route. Based on these results, HAB-6FDA polymers with non-hydroxyl *ortho*-position groups may be of interest for applications where high permeability is desired. However, the plasticization behavior of these polymers when exposed to highly soluble gases like CO_2 has not been studied.

TR polymers with hydroxyl *ortho*-position groups have shown no indications of plasticization in pure gas measurements up to 15 atm CO_2 [1]. Under these same conditions, the polyimide precursors to TR polymers exhibit significant plasticization. For example, the CO_2/CH_4 mixed gas selectivity of a fluorine-containing polyimide decreased from 85 to 58 as CO_2 partial pressure increased from 0 to 5 atm [1]. There is currently no study, in this dissertation or in the literature that shows the plasticization resistance of these TR polymers as a function of conversion. A study of mixed gas permeation including components like CO_2 would be especially important for polyimides

with non-hydroxyl *ortho*-position groups because complete conversion is typically not achieved during thermal rearrangement. Incomplete conversion would result in residual imide linkages that may be susceptible to plasticization by CO_2 [2-4].

Determination of the CO_2 plasticization resistance for TR polymers with hydroxyl and acetate *ortho*-position groups as a function of conversion could help to resolve whether plasticization resistance comes from PBO formation or chemical crosslinking. Thermal rearrangement converts polyimides into PBOs, but this reaction could also occur inter-molecularly [5-8]. If plasticization resistance is due to these inter-molecular reactions, selectivity may remain fairly stable at low conversions. This stability would be essential for the commercial use of TR polymers from polyimides with non-hydroxyl *ortho*-position groups for natural gas purification because full conversion is not achieved during rearrangement.

7.2.2 Effect of *ortho*-Position Group on TR Polymer Mechanical Properties

The mechanical properties of TR polymers from polyimides with non-hydroxyl *ortho*-position groups are currently poorly understood. Since this thermal rearrangement occurs in the solid state, a significant amount of mass loss occurs in these films. For example, roughly 32% of the initial mass would be lost to complete conversion of the HAB-6FDA-PAc sample to PBO [5]. In this study, the flexibility of TR polymers from hydroxyl, acetate, propanoate, and pivalate groups were qualitatively different, but quantitative measurements have not been performed.

Because the transport properties of TR polymers with non-hydroxyl *ortho*-position groups become similar at higher degrees of conversion, an understanding of the mechanical properties of these materials may indicate the most promising candidates for further study. Elongation at break and tensile strength are the commonly measured

mechanical properties for membrane materials and are used as indicators of their ability to be handled, fabricated into modules, and for subsequent use [9]. A study of these properties as a function of conversion for the *ortho*-position groups in this dissertation could determine if there is a connection between mass loss in the solid state and the mechanical properties of the TR polymer.

7.2.3 Positron Annihilation Lifetime Spectroscopy Study on HAB-6FDA TR Polymers with varying *ortho*-Position Groups

Chapter 6 presented the effect of non-hydroxyl *ortho*-position groups on the transport properties of partially converted TR polymers. TR polymers formed from polyimides containing these groups showed higher permeability and lower selectivity than those formed from hydroxyimides [6]. However, the fractional free volume calculated from density measurements was not significantly different. This similar free volume may indicate a difference in free volume distribution, which can be influenced by thermal rearrangement [1, 10].

Positron Annihilation Lifetime Spectroscopy (PALS) has been used to determine the free volume distribution in a variety of polymers [1, 10-14]. Using this technique, the lifetime of *o*-positronium can be correlated with the size of free volume elements within the polymer. The annihilation of *o*-positronium is tracked using a detector, and the free volume distribution within the polymer can be approximated by use of models [14]. Using this technique, the average size of free volume elements within the polymer and a free volume distribution can be determined. A comparison of the free volume distribution between TR polymers from polyimides hydroxyl and non-hydroxyl *ortho*-position groups may help explain the significant differences in permeability despite their similar average free volumes [6].

7.2.4 Gas Transport in HAB-6FDA TR Polymers with Bulky, Polar *ortho*-Position Groups

TR polymers from polyimides with non-hydroxyl *ortho*-position groups, regardless of their size, show similar permeabilities at high conversions to PBO. In contrast, TR polymers from hydroxyimides show significantly lower permeability than TR polymers with these larger groups. Therefore, the hydrogen bonding in these hydroxyimide samples may lead to less permeable TR polymers.

The study of a polyimide with a non-hydroxyl *ortho*-position group that can still undergo hydrogen bonding would provide additional information on the influence of *ortho*-position group on TR polymer transport properties. Figure 7.1 shows one possible *ortho*-position group with a structure similar to the acetate groups studied in this dissertation. The group in Figure 7.1 also includes a hydroxyl group which could allow for hydrogen bonding.

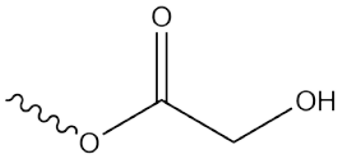

Figure 7.1. Possible ortho-position groups to probe effects of larger groups that promote hydrogen bonding

7.2.5 Gas Transport in Acetate-containing TR Polymers with Varying Backbone T_g

The rigid, glassy nature of the PBO formed may be a contributing factor in the significantly higher permeabilities observed in TR polymers from polyimides with non-hydroxyl *ortho*-position groups [5, 6]. If the *ortho*-position group is lost and the chains do not have sufficient mobility to pack efficiently, the free volume distribution could be affected. This hypothesis could be verified by adding acetate *ortho*-position groups to TR polymers having significantly lower T_g values than those considered in this study.

TR polymers from polyimides with T_gs spanning more than 120 ºC have been prepared [15, 16]. Particularly, polyimides with ether linkages have quite low T_gs and low thermal rearrangement temperatures. Typically TR polymers from these polyimides show permeabilities up to 100 times less than the most permeable TR polymers reported [17]. However, no study of these polyimides with non-hydroxyl *ortho*-position groups has been reported in the literature.

A study of TR polymers from polyimides with relatively low T_g would help to determine if the effect of the non-hydroxyl *ortho*-position groups is diminished by having a more mobile, less rigid chain structure. The T_g of the PBO is very likely correlated with the T_g of the initial polyimide. If the PBO can undergo some degree of rearrangement in the rubbery state, increases in permeability from *ortho*-position acetate groups may be diminished. A range of T_gs should be studied with acetate and hydroxyl functionality to determine if the relative increase in permeability from acetate *ortho*-position group is affected by the T_g of the polyimide and PBO.

7.3 REFERENCES

1. Park, H.B., Jung, C.H., Lee, Y.M., Hill, A.J., Pas, S.J., Mudie, S.T., Van Wagner, E., Freeman, B.D., and Cookson, D.J., *Polymers with cavities tuned for fast selective transport of small molecules and ions.* Science, 2007. **318**(5848): p. 254-258.

2. Bos, A., Pünt, I.G.M., Wessling, M., and Strathmann, H., *Plasticization-resistant glassy polyimide membranes for CO_2/CO_4 separations.* Separation and Purification Technology, 1998. **14**(1-3): p. 27-39.

3. Wind, J.D., Sirard, S.M., Paul, D.R., Green, P.F., Johnston, K.P., and Koros, W.J., *Carbon dioxide-induced plasticization of polyimide membranes: Pseudo-equilibrium relationships of diffusion, sorption, and swelling.* Macromolecules, 2003. **36**: p. 6433-6441.

4. Wind, J.D., Staudt-Bickel, C., Paul, D.R., and Koros, W.J., *The effects of crosslinking chemistry on CO_2 plasticization of polyimide gas separation membranes.* Industrial & Engineering Chemistry Research, 2002. **41**: p. 6139-6148.

5. Sanders, D.F., Guo, R., Smith, Z.P., Liu, Q., Stevens, K.A., McGrath, J.E., Paul, D.R., and Freeman, B.D., *Influence of polyimide precursor synthesis route and ortho-position functional group on thermally rearranged polymers: Thermal properties and free volume.* In Preparation.

6. Sanders, D.F., Guo, R., Smith, Z.P., Liu, Q., Stevens, K.A., McGrath, J.E., Paul, D.R., and Freeman, B.D., *Influence of polyimide precursor synthesis route and ortho-position functional group on thermally rearranged polymers: Pure gas permeability and selectivity.* In Preparation.

7. Sanders, D.F., Smith, Z.P., Ribeiro, C.P., Guo, R., McGrath, J.E., Paul, D.R., and Freeman, B.D., *Permeability, diffusivity, and free volume of thermally rearranged polymers based on 3,3'-dihydroxy-4,4'-diamino-biphenyl (HAB) and 2,2'-bis-(3,4-dicarboxyphenyl) hexafluoropropane dianhydride (6FDA).* Journal of Membrane Science, 2012. **409-410**: p. 232-241.

8. Smith, Z.P., Sanders, D.F., Ribeiro, C.P., Guo, R., Freeman, B.D., Paul, D.R., McGrath, J.E., and Swinnea, S., *Gas sorption and characterization of thermally rearranged polyimides based on 3,3'-dihydroxy-4,4'-diamino-biphenyl (HAB) and 2,2'-bis-(3,4-dicarboxyphenyl) hexafluoropropane dianhydride (6FDA).* Journal of Membrane Science, 2012. **415-416**: p. 558-567.

9. Park, J.Y. and Paul, D.R., *Correlation and prediction of gas permeability in glassy polymer membrane materials via modified free volume based group contribution method.* Journal of Membrane Science, 1997. **125**(1): p. 23-39.

10. Han, S.H., Misdan, N., Kim, S., Doherty, C.M., Hill, A.J., and Lee, Y.M., *Thermally rearranged (TR) polybenzoxazole: Effects of diverse imidization routes on physical properties and gas transport behaviors.* Macromolecules, 2010. **43**(18): p. 7657-7667.

11. Han, S.H., Kwon, H.J., Kim, K.Y., Seong, J.G., Park, C.H., Kim, S., Doherty, C.M., Thornton, A.W., Hill, A.J., Lozano, A.E., Berchtold, K.A., and Lee, Y.M., *Tuning microcavities in thermally rearranged polymer membranes for CO_2 capture.* Physical Chemistry Chemical Physics, 2012. **14**: p. 4365-4373.

12. Merkel, T.C., Freeman, B.D., Spontak, R.J., Pinnau, I., He, Z., Meakin, P., and Hill, A.J., *Sorption, transport, and structural evidence for enhanced free volume in poly(4-methyl-2-pentyne)/fumed silica nanocomposite membranes.* Chemistry of Materials, 2003. **15**: p. 109-123.

13. Nagai, K., Freeman, B.D., and Hill, A.J., *Effect of pysical aging of poly(1-trimethylsilyl-1-propyne) films synthesized with $TaCl_5$ and $NbCl_5$ on gas permeability, fractional free volume, and positron annihilation lifetime spectroscopy parameters.* Journal of Polymer Science, Part B: Polymer Physics, 2000. **38**: p. 1222-1239.

14. Rowe, B.W., Pas, S.J., Hill, A.J., Suzuki, R., Freeman, B.D., and Paul, D.R., *A variable energy positron annihilation life spectroscopy study of physical aging in thin glassy polymer films.* Polymer, 2009. **50**: p. 6149-6156.

15. Calle, M. and Lee, Y.M., *Thermally rearranged (TR) poly(ether-benzoxazole) membranes for gas separation.* Macromolecules, 2011. **44**: p. 1156-1165.

16. Guo, R., Sanders, D.F., Smith, Z.P., Freeman, B.D., Paul, D.R., and McGrath, J.E., *Synthesis and characterization of thermally rearranted (TR) polymers: Effect of glass transition temperature of aromatic poly(hydroxyimide) precursors on TR process and gas permeation properties.* Journal of Materials Chemistry A, 2013. **Accepted**.

17. Calle, M., Lozano, A.E., and Lee, Y.M., *Formation of thermally rearranged (TR) polybenzoxazoles: Effect of synthesis routes and polymer form.* European Polymer Journal, 2012. **48**: p. 1313-1322.

Appendix A: Pure gas permeability as a function of Pressure

This appendix reports the pure gas permeability as a function of pressure for each polymer studied in this dissertation. The trends in these plots are discussed in detail in Chapter 6.

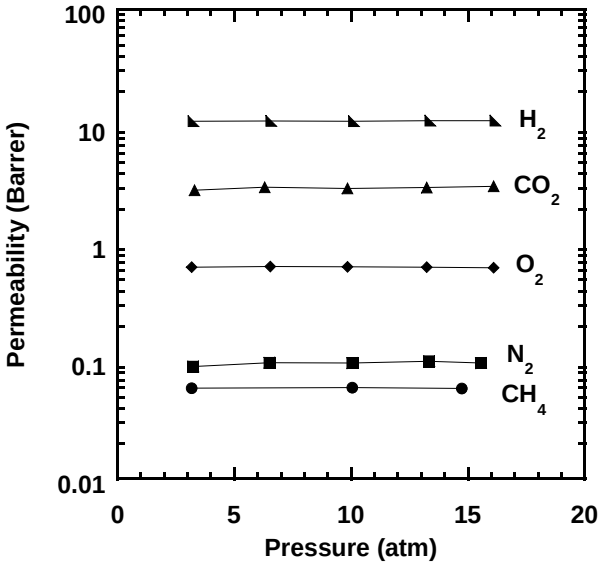

Figure A.1 Pure gas permeability of the HAB-6FDA-EA polyimide as a function of pressure.

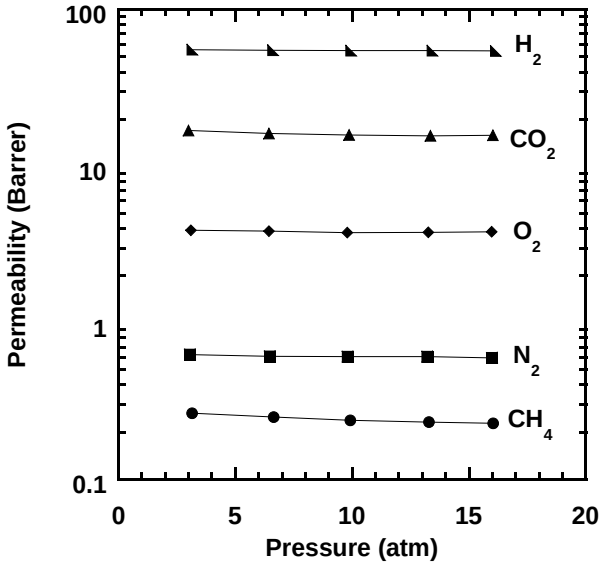

Figure A.2 Pure gas permeability of HAB-6FDA-EA-TR350 as a function of pressure.

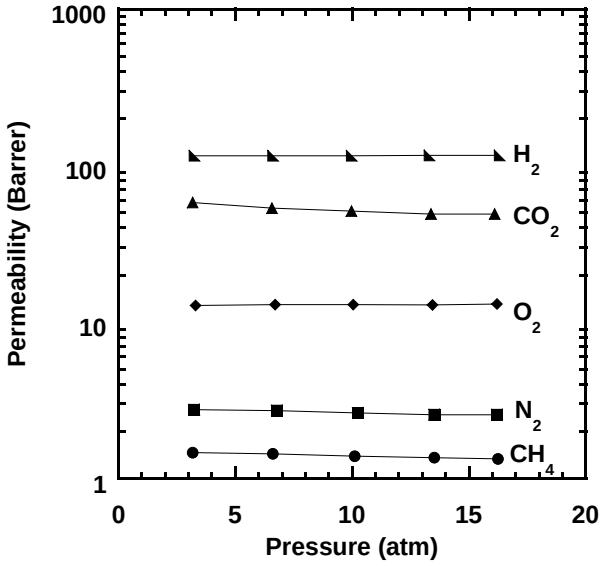

Figure A.3 Pure gas permeability of HAB-6FDA-EA-TR400 as a function of pressure.

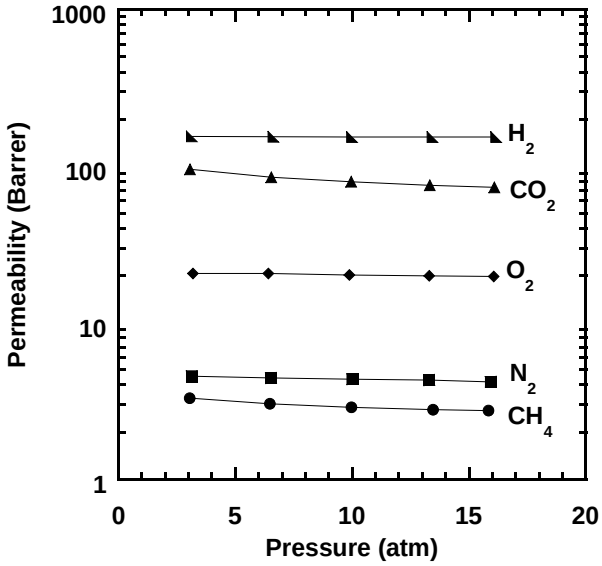

Figure A.4 Pure gas permeability of HAB-6FDA-EA-TR450 as a function of pressure.

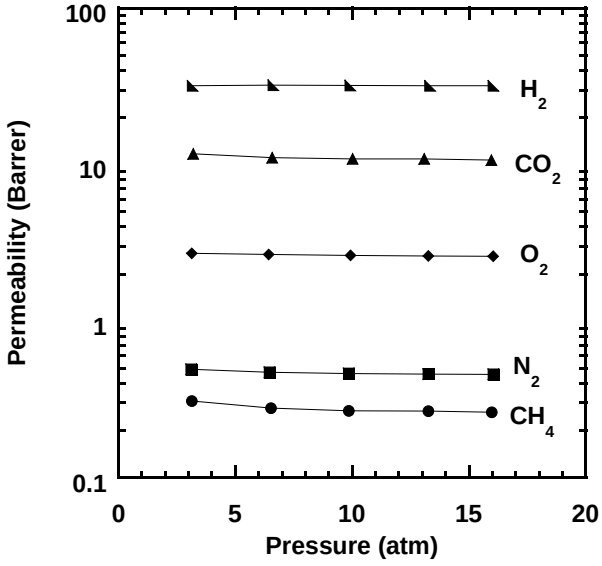

Figure A.5 Pure gas permeability of the HAB-6FDA-Ac polyimide as a function of pressure.

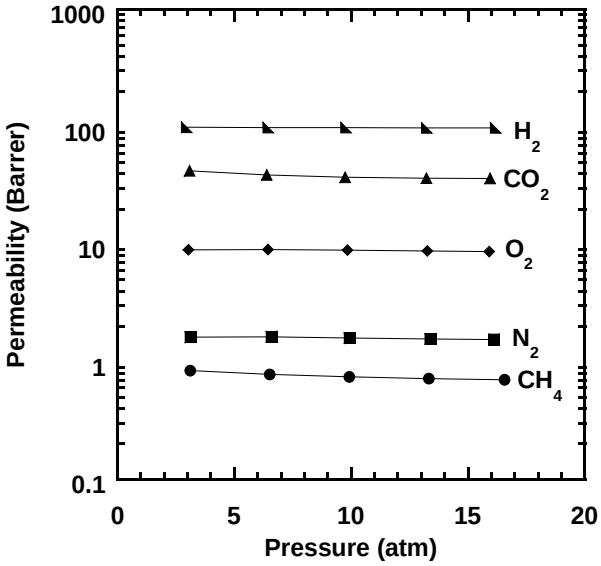

Figure A.6 Pure gas permeability of HAB-6FDA-Ac-TR350 as a function of pressure .

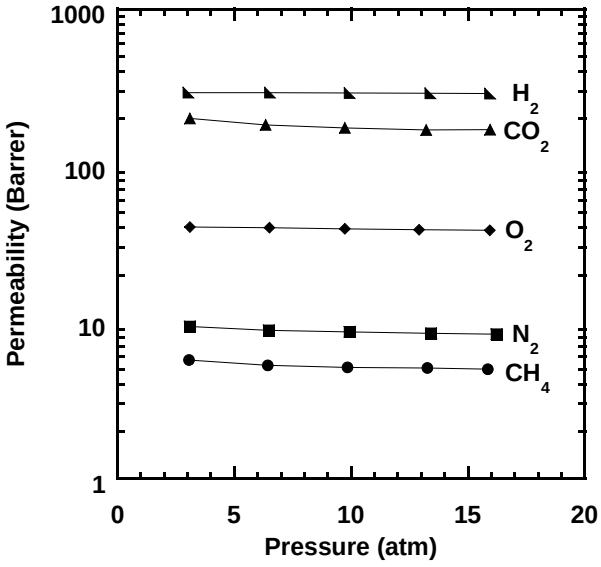

Figure A.7 Pure gas permeability of HAB-6FDA-Ac-TR400 as a function of pressure.

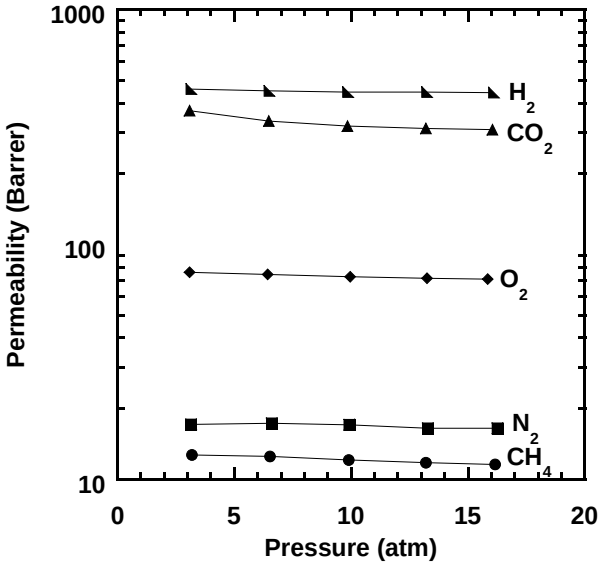

Figure A.8 Pure gas permeability of HAB-6FDA-Ac-TR450 as a function of pressure.

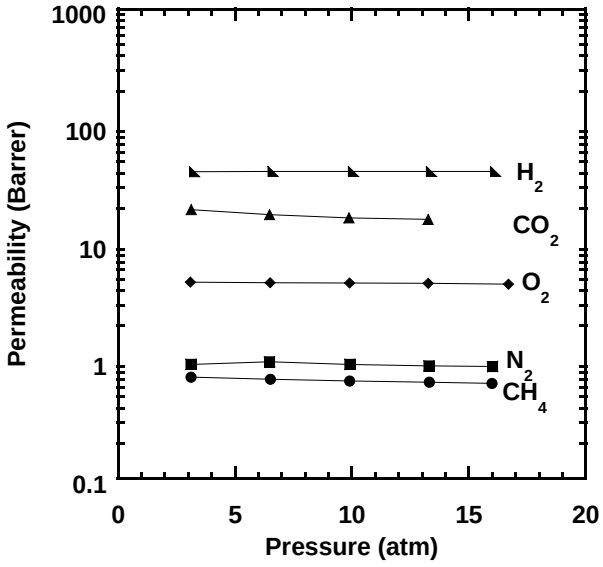

Figure A.9 Pure gas permeability of the HAB-6FDA-PrAc polyimide as a function of pressure.

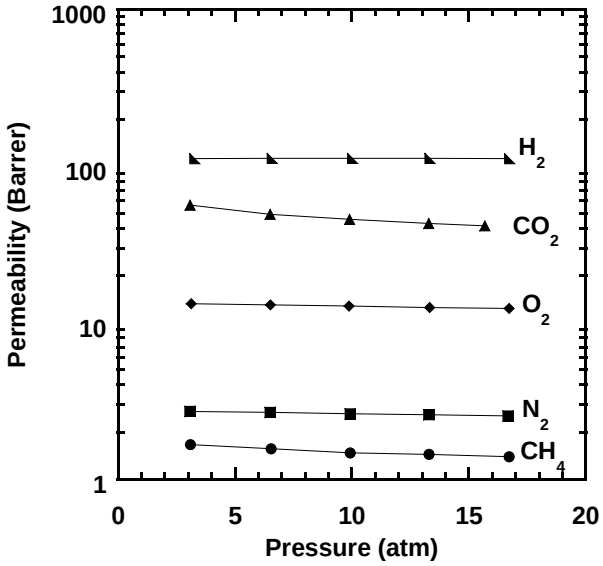

Figure A.10 Pure gas permeability of HAB-6FDA-PrAc-TR350 as a function of pressure.

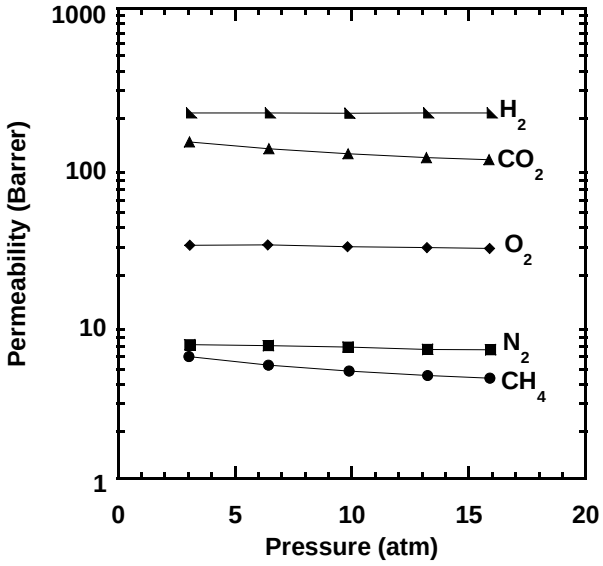

Figure A.11 Pure gas permeability of HAB-6FDA-PrAc-TR400 as a function of pressure.

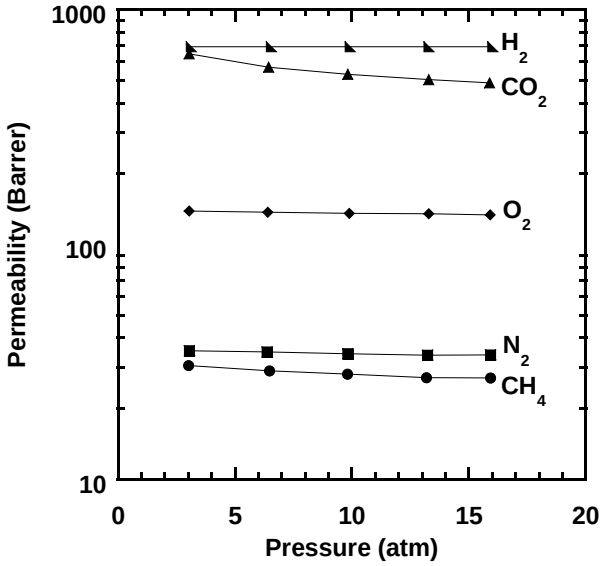

Figure A.12 Pure gas permeability of HAB-6FDA-PrAc-TR450 as a function of pressure.

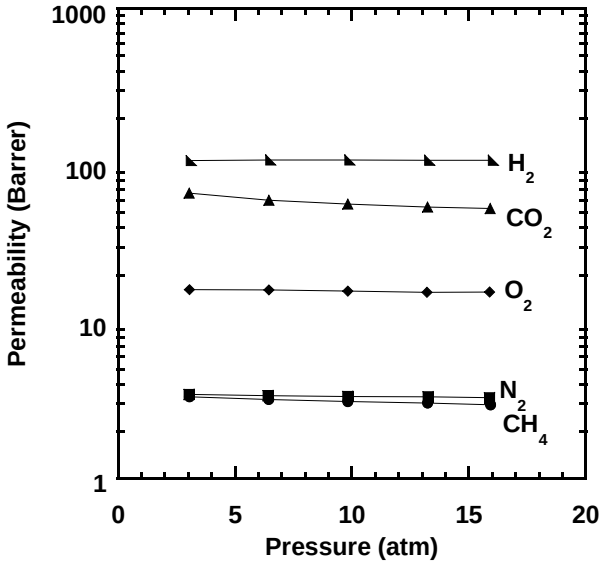

Figure A.13 Pure gas permeability of HAB-6FDA-PAc polyimide as a function of pressure.

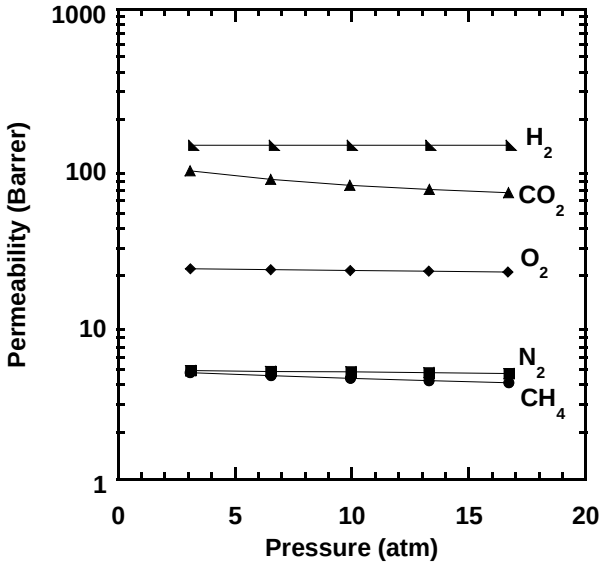

Figure A.14 Pure gas permeability of HAB-6FDA-PAc-TR350 as a function of pressure.

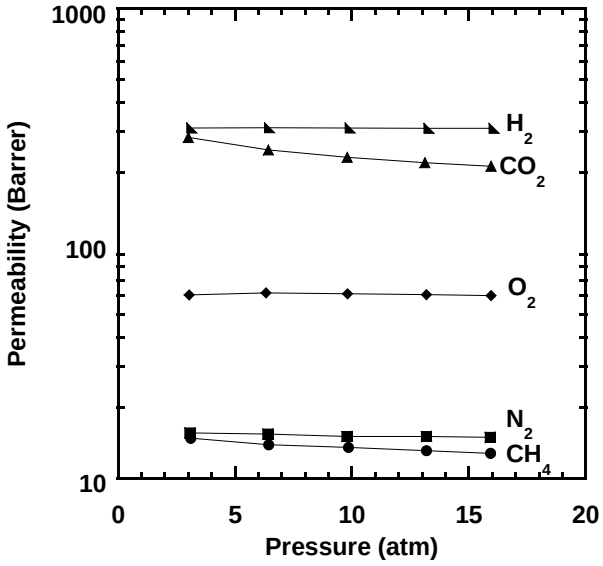

Figure A.15 Pure gas permeability of HAB-6FDA-PAc-TR400 as a function of pressure.

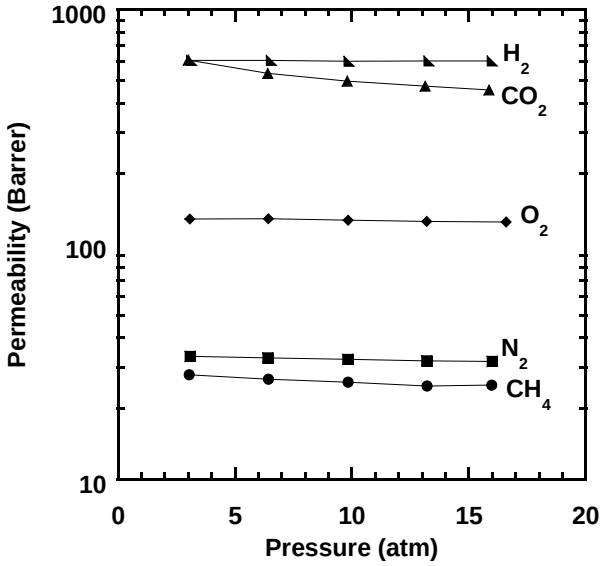

Figure A.16 Pure gas permeability of HAB-6FDA-PAc-TR450 as a function of pressure.

References

ASTM D1505-10. Standard Test Method for Density of Plastics by the Density-Gradient Technique, 2010.

Mass Spectra in *NIST Chemistry WebBook, NIST Standard Reference Database Number 69,* S.E. Stein, Editor 2013, National Institute of Standards and Technology: Gaithersburg MD, 20899.

Aguilar-Vega, M. and Paul, D.R., *Gas-Transport Properties of Polyphenylene Ethers.* Journal of Polymer Science Part B-Polymer Physics, 1993. **31**(11): p. 1577-1589.

Aitken, C.L., Koros, W.J., and Paul, D.R., *Effect of Structural Symmetry on Gas-Transport Properties of Polysulfones.* Macromolecules, 1992. **25**(13): p. 3424-3434.

Aitken, C.L., Koros, W.J., and Paul, D.R., *Gas-Transport Properties of Biphenol Polysulfones.* Macromolecules, 1992. **25**(14): p. 3651-3658.

Alentiev, A.Y., Shantarovich, V.P., Merkel, T.C., Bondar, V.I., Freeman, B.D., and Yampolskii, Y.P., *Gas and vapor sorption, permeation, and diffusion in glassy amorphous Teflon AF1600.* Macromolecules, 2002. **35**: p. 9513-9522.

Alentiev, A.Y. and Yampolskii, Y.P., *Free volume model and tradeoff relations of gas permeability and selectivity in glassy polymers.* Journal of Membrane Science, 2000. **165**(2): p. 201-216.

Alentiev, A.Y., Yampolskii, Y.P., Shantarovich, V.P., Nemser, S.M., and Plate, N.A., *High transport parameters and free volume of perfluorodioxole copolymers.* Journal of Membrane Science, 1997. **126**(1): p. 123-132.

Allen, S.M., Fujii, M., Stannett, V., Hopfenberg, H.B., and Williams, J.L., *The barrier properties of polyacrolonitrile.* Journal of Membrane Science, 1977. **2**(2): p. 153-163.

Anand, J.N., Bales, S.E., Feay, D.C., and Jeanes, T.O., Tetrabromo bisphenol based polyestercarbonate membranes and method of using. US. Patent 4,840,646. 1989.

Arcella, V., Colaianna, P., Maccone, P., Sanguineti, A., Gordano, A., Clarizia, G., and Drioli, E., *A study on a perfluoropolymer purification and its application to membrane formation.* Journal of Membrane Science, 1999. **163**(2): p. 203-209.

Arcella, V., Ghielmi, A., and Tommasi, G., *High performance perfluoropolymer films and membranes.* Annals of the New York Academy of Sciences, 2003. **984**(1): p. 226-244.

Aycock, D., *Poly(phenylene ether),* in *Encyclopedia of polymer science and technology*1974, Interscience Publishers, NY.

Baker, R.W., *Future directions of membrane gas separation technology.* Industrial & Engineering Chemistry Research, 2002. **41**(6): p. 1393-1411.

Baker, R.W., *Membrane technology and applications*. 3rd ed. 2004, Chichester: John Wiley & Sons.

Baker, R.W. and Lokhandwala, K., *Natural gas processing with membranes: An overview.* Industrial & Engineering Chemistry Research, 2008. **47**(7): p. 2109-2121.

Bara, J.E., Gabriel, C.J., Hatakeyama, E.S., Carlisle, T.K., Lessmann, S., Noble, R.D., and Gin, D.L., *Improving CO2 selectivity in polymerized room-temperature ionic liquid gas separation membranes through incorporation of polar substituents.* Journal of Membrane Science, 2008. **321**(1): p. 3-7.

Bara, J.E., Gabriel, C.J., Lessmann, S., Carlisle, T.K., Finotello, A., Gin, D.L., and Noble, R.D., *Enhanced CO2 separation selectivity in oligo(ethylene glycol) functionalized room-temperature ionic liquids.* Industrial & Engineering Chemistry Research, 2007. **46**(16): p. 5380-5386.

Bara, J.E., Gin, D.L., and Noble, R.D., *Effect of anion on gas separation performance of polymer-room-temperature ionic liquid composite membranes.* Industrial & Engineering Chemistry Research, 2008. **47**: p. 9919-9924.

Bara, J.E., Hatakeyama, E.S., Gabriel, C.J., Zeng, X., Lessmann, S., Gin, D.L., and Noble, R.D., *Synthesis and light gas separations in cross-linked gemini room temperature ionic liquid polymer membranes.* Journal of Membrane Science, 2008. **316**: p. 186-191.

Bara, J.E., Hatakeyama, E.S., Gin, D.L., and Noble, R.D., *Improving CO_2 permeability in polymerized room-temperature ionic liquid gas separation membranes through the formation of a solid composite with a room temperature ionic liquid.* Polymers for Advanced Technologies, 2008. **19**: p. 1415-1420.

Bara, J.E., Lessmann, S., Gabriel, C.J., Hatakeyama, E.S., Noble, R.D., and Gin, D.L., *Synthesis and performance of polymerizable room-temperature ionic liquids as*

gas separation membranes. Industrial & Engineering Chemistry Research, 2007. **46**: p. 5397-5404.

Bara, J.E., Noble, R.D., and Gin, D.L., *Effect of "free" cation substituent on gas separation performance of polymer-room-temperature ionic liquid composite membranes.* Industrial & Engineering Chemistry Research, 2009. **48**: p. 4607-4610.

Barbari, T.A., Koros, W.J., and Paul, D.R., *Polymeric membranes based on bisphenol A for gas separations.* Journal of Membrane Science, 1989. **42**(1-2): p. 69-86.

Barrer, R.M., *Permeability in relation to viscosity and structure of rubber.* Transactions of the Faraday Society, 1942. **38**: p. 322-330.

Bateman, J. and Gordon, D.A., Soluble polyimides derived from phenylindane diamines and dianhydrides. U.S. Patent 3,856,752. 1974.

Bateman, J.H., Geresy, W., and Neiditch, D.S., *Soluble polyimides derived from phenylindane diamine: a new approach to heat resistant protective coatings.* American Chemical Society, Division of Organic Coatings and Plastics Chemistry, 1975. **35**(2): p. 77-82.

Bernardo, P., Drioli, E., and Golemme, G., *Membrane gas separation: A review/state of the art.* Industrial & Engineering Chemistry Research, 2009. **48**: p. 4638-4663.

Bevington, P.R. and Robinson, K.D., *Data reduction and error analysis for the physical sciences*. 2003, Boston: McGraw Hill.

Bevington, P.R. and Robinson, K.D., *Data Reduction and Error Analysis for the Physical Sciences*. 2003, Boston: McGraw Hill. 320.

Blanchard, L.A., Hancu, D., Beckman, E.J., and Brennecke, J.F., *Green processing using ionic liquids and CO2.* Nature, 1999. **399**(6731): p. 28-29.

Böddeker, K.W., *Commentary: Tracing membrane science.* Journal of Membrane Science, 1995. **100**: p. 65-68.

Bondar, V.I., Freeman, B.D., and Yampolskii, Y.P., *Sorption of gases and vapors in an amorphous glassy perfluorodioxole copolymer.* Macromolecules, 1999. **32**(19): p. 6163-6171.

Bondi, A., *Physical properties of molecular crystals, liquids, and glasses*. 1968: Wiley.

Bondi, A., *van der Waals volumes and radii.* The Journal of Physical Chemistry, 1964. **68**(3): p. 441-451.

Bos, A., Pünt, I.G.M., Wessling, M., and Strathmann, H., *CO_2-induced plasticization phenomenon in glassy polymers.* Journal of Membrane Science, 1999. **155**: p. 67-78.

Bos, A., Pünt, I.G.M., Wessling, M., and Strathmann, H., *Plasticization-resistant glassy polyimide membranes for CO_2/CH_4 separations.* Separation and Purification Technology, 1998. **14**: p. 27-39.

Bos, A., Pünt, I.G.M., Wessling, M., and Strathmann, H., *Plasticization-resistant glassy polyimide membranes for CO_2/CO_4 separations.* Separation and Purification Technology, 1998. **14**(1-3): p. 27-39.

Bos, A., Pünt, I.G.M., Wessling, M., and Strathmann, H., *Suppression of CO2-plasticization by semiinterpenetrating polymer network formation.* Journal of Polymer Science Part B-Polymer Physics, 1998. **36**(9): p. 1547-1556.

Bottoms, R.R., Process for separating acidic gases. US Patent 1,834,016. 1931.

Breck, D.W., *Zeolite molecular sieves.* 1974, New York, NY.

Budd, P.M., Elabas, E.S., Ghanem, B.S., Makhseed, S., McKeown, N.B., Msayib, K.J., Tattershall, C.E., and Wang, D., *Solution-processed, organophilic membrane derived from a polymer of intrinsic microporosity.* Advanced Materials, 2004. **16**(5): p. 456-459.

Budd, P.M., Ghanem, B.S., Makhseed, S., McKeown, N.B., Msayib, K.J., and Tattershall, C.E., *Polymers of intrinsic microporosity (PIMs): robust, solution-processable, organic nanoporous materials.* Chemical Communications, 2004(2): p. 230-231.

Budd, P.M., Msayib, K.J., Tattershall, C.E., Ghanem, B.S., Reynolds, K.J., McKeown, N.B., and Fritsch, D., *Gas separation membranes from polymers of intrinsic microporosity.* Journal of Membrane Science, 2005. **251**: p. 263-269.

Cadena, C., Anthony, J.L., Shah, J.K., Morrow, T.I., Brennecke, J.F., and Maginn, E.J., *Why is CO2 so soluble in imidazolium-based ionic liquids?* Journal of the American Chemical Society, 2004. **126**(16): p. 5300-5308.

Cadotte, J., Interfacially synthesized reverse osmosis membrane. US Patent 4,277,344. 1981.

Calle, M., Chan, Y., Hye, J.J., and Lee, Y.M., *The relationship between the chemical structure and thermal conversion temperatures of thermally rearranged (TR) polymers.* Polymer, 2012. **53**: p. 2783-2791.

Calle, M. and Lee, Y.M., *Thermally rearranged (TR) poly(ether-benzoxazole) membranes for gas separation.* Macromolecules, 2011. **44**: p. 1156-1165.

Calle, M., Lozano, A.E., de La Campa, J.G., and de Abajo, J., *Novel Aromatic Polyimides Derived from 5 '-t-Butyl-2 '-pivaloylimino-3,4,3 '',4 ''-m-terphenyltetracarboxylic Dianhydride with Potential Application on Gas Separation Processes.* Macromolecules. **43**(5): p. 2268-2275.

Calle, M., Lozano, A.E., and Lee, Y.M., *Formation of thermally rearranged (TR) polybenzoxazoles: Effect of synthesis routes and polymer form.* European Polymer Journal, 2012. **48**: p. 1313-1322.

Carlisle, T.K., Bara, J.E., Lafrate, A.L., Gin, D.L., and Noble, R.D., *Main-chain imidazolium polymer membranes for CO_2 separations: An initial study of a new ionic liquid-inspired platform.* Journal of Membrane Science, 2010. **359**: p. 37-43.

Carrera-Figueiras, C. and Aguilar-Vega, M., *Gas permeability and selectivity of hexafluoroisopropylidene aromatic isophthalic copolyamides.* J Polym Sci B: Polym Phys, 2005. **43**: p. 2625-38.

Chan, A.H., Koros, W.J., and Paul, D.R., *Analysis of hydrocarbon gas sorption and transaport in ethyl cellulose using the dual sorption/partial immobilization methods.* Journal of Membrane Science, 1978. **3**: p. 117-130.

Chen, C., Qiu, W., Miller, S.J., and Koros, W.J., *Plasticization-resistant hollow fiber membranes for CO_2/CH_4 separation based on a thermally crosslinkable polyimide.* Journal of Membrane Science, 2011. **382**: p. 212-221.

Chern, R.T., Jia, L., Shimoda, S., and Hopfenberg, H.B., *A note on the effects of mono- and dibromination on the transport properties of poly(2,6-dimethylphenylene oxide).* Journal of Membrane Science, 1990. **48**(2-3): p. 333-341.

Chern, R.T. and Provan, C.N., *Gas-induced plasticization and the permselectivity of poly(tetrabromophenolphthalein terephthalate) to a mixture of carbon dioxide and methane.* Macromolecules, 1991. **24**: p. 2203-2207.

Chern, R.T., Sheu, F.R., Jia, L., Stannett, V.T., and Hopfenberg, H.B., *Transport of gases in unmodified and aryl-brominated 2,6-dimethyl-1,4-poly(phenylene oxide).* Journal of Membrane Science, 1987. **35**(1): p. 103-115.

Chiou, J.S. and Paul, D.R., *Effects of CO_2 exposure on gas transport properties of glassy polymers.* Journal of Membrane Science, 1987. **32**: p. 195-205.

Choi, J.I., Jung, C.H., Han, S.H., Park, H.B., and Lee, Y.M., *Thermally rearranged (TR) poly(benzoxazole-co-pyrrolone) membranes tuned for high gas permeability and selectivity.* Journal of Membrane Science, 2010. **349**(1-2): p. 358-368.

Chung, T.S., Jiang, L.Y., Li, Y., and Kulprathipanja, S., *Mixed matrix membranes (MMMs) comprising organic polymers with dispersed inorganic fillers for gas separation.* Progress in Polymer Science, 2007. **32**: p. 483-507.

Clausi, D.T. and Koros, W.J., *Formation of defect-free polyimide hollow fiber membranes for gas separations.* Journal of Membrane Science, 2000. **167**(1): p. 79-89.

Cohen, M.H. and Turnbull, D., *Molecular transport in liquids and glasses.* The Journal of Physical Chemistry, 1959. **31**(5): p. 1164-1169.

Colaianna, P., Brinati, G., and Arcekka, V., Amorphous perfluoropolymers. 1999.

Cooley, T.E. and Coady, A.B., Removal of H_2S and/or CO_2 from a light hydrocarbon stream by use of gas permeable membrane. US Patent 4,130,403. 1978.

Cui, L., Qiu, W., Paul, D.R., and Koros, W.J., *Physical aging of 6FDA-based polyimide membranes monitored by gas permeability.* Polymer, 2011. **52**: p. 3374-3380.

Dhoot, S.N., Freeman, B.D., and Stewart, M.E., *Barrier polymers*, in *Encyclopedia of polymer science and technology*, J. Kroschweitz, Editor 2003, John Wiley & Sons: New York. p. 198-263.

Ding Y and Bikson, B., *Soluble aromatic polyamides containing the phenylindane group and their gas transport characteristics.* Polymer, 2002. **43**: p. 4709-14.

Donohue, M.D., Minhas, B.S., and Lee, S.Y., *Permeation behavior of carbon dioxide-methane mixtures in cellulose acetate membranes.* Journal of Membrane Science, 1989. **42**: p. 197-214.

Dorkenoo, K.D. and Pfromm, P.H., *Accelerated physical aging of thin poly[1-(trimethylsilyl)-1-propyne] films.* Macromolecules, 2000. **33**: p. 3747-3751.

Duthie, X., Kentish, S., Pas, S.J., Hill, A.J., Powell, C., Nagai, K., Stevens, G., and Qiao, G., *Thermal treatment of dense polyimide membranes.* Journal of Polymer Science Part B-Polymer Physics, 2008. **46**(18): p. 1879-1890.

Edgar, K.J., Buchanan, C.M., Debenham, J.S., Rundquist, P.A., Seiler, B.D., Shelton, M.C., and Tindall, D., *Advances in cellulose ester performance and application.* Progress in Polymer Science, 2001. **26**: p. 1605-1688.

Ekiner, O.M., Hayes, R.A., and Manos, P., Novel multicomponent fluid separation membranes. 1992.

Ekiner, O.M., Hayes, R.A., and Va, W., Phenylindane-containing polyimide gas separation membranes. US Patent 5015270. 1991.

Ekiner, O.M. and Vassilatos, G., *Polyaramide hollow fibers for H_2/CH_4 separation II. Spinning and properties.* Journal of Membrane Science, 2001. **186**: p. 71-84.

Ekiner, O.M. and Vassilatos, G., *Polyaramide hollow fibers for hydrogen/methane separation - spinning and properties.* Journal of Membrane Science, 1990. **53**: p. 259-273.

Ekiner, O.M. and Vassilatos, G., Polymeric Membranes. 1992.

Emmler, T., Heinrich, K., Fritsch, D., Budd, P.M., Chaukura, N., Ehlers, D., Ratzke, K., and Faupel, F., *Free volume investigation of polymers of intrinsic microporosity (PIMs): PIM-1 and PIM1 copolymers incorporating ethanoanthracene units.* Macromolecules, 2010. **43**(14): p. 6075-6084.

Erb, A.J. and Paul, D.R., *Gas Sorption and Transport in Polysulfone.* Journal of Membrane Science, 1981. **8**(1): p. 11-22.

Espeso, J.F., Ferrero, E., De La Campa, J.G., Lozano, A.E., and De Abajo, J., *Synthesis and characterization of new soluble aromatic polyamides derived from 1,4-Bis(4-carboxyphenoxy)-2, 5-di-tert-butylbenzene.* Journal of Polymer Science Part A: Polymer Chemistry, 2001. **39**(4): p. 475-485.

Falcigno, P., Masola, M., Williams, D., and Jasne, S., eds. *Comparison of properties of polyimides containing DAPI isomers and various dianhydrides*. Polyimides: Materials, chemistry and characterization, Proceedings of the 3rd International Conference on Polyimides, ed. C. Feger, M.M. Khohasteh, and J.E. McGrath 1989, Elsevier: Ellenville, NY. 497-512.

Farr, I.V., Glass, T.E., Ji, Q., and McGrath, J.E., *Synthesis and characterization of diaminophenylindane based polyimides via ester-acid solution imidization.* High Performance Polymers, 1997. **9**(3): p. 345-352.

Farr, I.V., Kratzner, D., Glass, T.E., Dunson, D., Ji, Q., and McGrath, J.E., *The synthesis and characterization of polyimide homopolymers based on 5(6)-amino-1-(4-aminophenyl)1,3,3-trimethylindane.* Journal of Polymer Science Part A-Polymer Chemistry, 2000. **38**(15): p. 2840-2854.

Fick, A., *On liquid diffusion.* Journal of Membrane Science, 1995. **100**: p. 33-38.

Fleming, G.K. and Koros, W.J., *Carbon dioxide conditioning effects on sorption and volume dilation behavior for bisphenol A-polycarbonate.* Macromolecules, 1990. **23**: p. 1353-1360.

Fleming, G.K. and Koros, W.J., *Dilation of polymers by sorption of carbon dioxide at elevated pressures. 1. Silicone rubber and unoconditioned polycarbonate.* Macromolecules, 1986. **19**: p. 2285-2291.

Fleming, G.K. and Koros, W.J., *Dilation of substituted polycarbonates caused by high-pressure carbon dioxide sorption.* Journal of Polymer Science Part B: Polymer Physics, 2003. **28**(7): p. 1137-1152.

Fortunato, R., Afonso, C.A.M., Reis, M.A.M., and Crespo, J.G., *Supported liquid membranes using ionic liquids: study of stability and transport mechanisms.* Journal of Membrane Science, 2004. **242**(1-2): p. 197-209.

Freeman, B.D., *Basis of permeability/selectivity tradeoff relations in polymeric gas separation membranes.* Macromolecules, 1999. **32**(2): p. 375-380.

Freitag, D., *Polycarbonates*, in *Encyclopedia of polymer science and engineering*, J. Kroschwitz, Editor 1988, John Wiley & Sons. p. 648-718.

García, J.M., García, F.C., Serna, F., and de la Peña, J.L., *High-performance aromatic polyamides.* Progress in Polymer Science, 2010. **35**: p. 623-686.

Gaymans, R.J., *Polyamides*, in *Synthetic methods in step-growth polymers*, M.E. Rogers and T.E. Long, Editors. 2003, John Wiley & Sons: Hoboken.

Geise, G.M., Lee, H.S., Miller, D.J., Freeman, B.D., McGrath, J.E., and Paul, D.R., *Water purification by membranes: The role of polymer science.* Journal of Polymer Science Part B-Polymer Physics, 2010. **48**(15): p. 1685-1718.

Geise, G.M., Park, H.B., Sagle, A.C., Freeman, B.D., and McGrath, J.E., *Water permeability and water/salt selectivity tradeoff in polymers for desalination.* Journal of Membrane Science, 2011. **369**(1-2): p. 130-138.

Ghanem, B.S., McKeown, N.B., Budd, P.M., Al-Haribi, N.M., Fritsch, D., Heinrich, K., Starannikova, L., Tokarev, A., and Yampolskii, Y., *Synthesis, characterization, and gas permeation properties of a novel group of polymers with intrinsic microporosity: PIM-Polyimides.* Macromolecules, 2009. **42**(20): p. 7881-7888.

Ghanem, B.S., McKeown, N.B., Budd, P.M., Selbie, J.D., and Fritsch, D., *High-performance membranes from polyimides with intrinsic microporosity.* Advanced Materials, 2008. **20**(14): p. 2766-2771.

Ghosal, K. and Chern, R.T., *Aryl nitration of poly(phenylene oxide) and polysulfone. Structural characterization and gas permeability.* Journal of Membrane Science, 1992. **72**(1): p. 91-97.

Ghosal, K., Chern, R.T., and Freeman, B.D., *Gas-Permeability of Radel-a Polysulfone.* Journal of Polymer Science Part B-Polymer Physics, 1993. **31**(7): p. 891-893.

Ghosal, K., Chern, R.T., Freeman, B.D., Daly, W.H., and Negulescu, I.I., *Effect of basic substituents on gas sorption and permeation in polysulfone.* Macromolecules, 1996. **29**(12): p. 4360-4369.

Ghosal, K. and Freeman, B.D., *Gas separation using polymer membranes: An overview.* Polymers for Advanced Technologies, 1994. **5**: p. 673-697.

Ghosh, M.K. and Mittal, K.L., *Polyimides*. 1996, New York: Marcel Dekker Inc.

Graham, T., *On the absorption and dialytic separation of gases by colloid septa Part I. - Action of a septum of caoutchouc.* Journal of Membrane Science, 1995. **100**: p. 27-31.

Guo, R. and McGrath, J.E., *Aromatic polyethers, polyetherketones, polysulfides, and polysulfones*, in *Polymer science: A comprehensive reference*, K. Matyjaszewski and M. Möller, Editors. 2012, Elsevier BV: Amsterdam. p. 377-430.

Guo, R., Sanders, D.F., Smith, Z.P., Freeman, B.D., and McGrath, J.E., *Synthesis and characterization of thermally rearranged (TR) polymer membranes: Effect of glass transition temperature of poly(hydroxyimide) precursors.* Journal of Materials Chemistry A, 2013. **1**: p. 262-272.

Guo, R., Sanders, D.F., Smith, Z.P., Freeman, B.D., and McGrath, J.E., *Synthesis and characterization of thermally rearranged (TR) polymer membranes: The effects of ortho-positioned functional group of polyimide precursors.* submitted, 2012.

Guo, R., Sanders, D.F., Smith, Z.P., Freeman, B.D., Paul, D.R., and McGrath, J.E., *Synthesis and Characterization of Thermally Rearranged (TR) Polymers: Influence of ortho-positioned functional groups of polyimide precursors on TR process and gas transport properties.* Journal of Materials Chemistry A, 2013. **1**: p. 262-272.

Guo, R., Sanders, D.F., Smith, Z.P., Freeman, B.D., Paul, D.R., and McGrath, J.E., *Synthesis and characterization of thermally rearranted (TR) polymers: Effect of glass transition temperature of aromatic poly(hydroxyimide) precursors on TR process and gas permeation properties.* Journal of Materials Chemistry A, 2013. **In Press**.

Haggin, J., *New generation of membranes developed for industrial separations.* Chemical and Engineering News, 1988. **3**: p. 7-16.

Hamad, F., Khulbe, K.C., and Matsuura, T., *Characterization of gas separation membranes prepared from brominated poly (phenylene oxide) by infrared spectroscopy.* Desalination, 2002. **148**(1-3): p. 369-375.

Han, S.H., Kwon, H.J., Kim, K.Y., Seong, J.G., Park, C.H., Kim, S., Doherty, C.M., Thornton, A.W., Hill, A.J., Lozano, A.E., Berchtold, K.A., and Lee, Y.M., *Tuning microcavities in thermally rearranged polymer membranes for CO_2 capture.* Physical Chemistry Chemical Physics, 2012. **14**: p. 4365-4373.

Han, S.H., Misdan, N., Kim, S., Doherty, C.M., Hill, A.J., and Lee, Y.M., *Thermally rearranged (TR) polybenzoxazole: Effects of diverse imidization routes on physical properties and gas transport behaviors.* Macromolecules, 2010. **43**(18): p. 7657-7667.

Hay, A.S., Oxidation of phenols and resulting products US Pat. 3,306,875. 1967.

Hay, A.S., Blanchard, H.S., Endres, G.F., and Eustance, J.W., *Polymerization by oxidative coupling.* Journal of the American Chemical Society, 1959. **81**(23): p. 6335.

Heinze, T. and Liebert, T., *Chemical characteristics of cellulose acetate.* Macromolecular Symposia, 2004. **208**: p. 167-237.

Henis, J.M.S. and Tripodi, M.K., US Patent 4230426. 1980.

Henis, J.S. and Tripodi, M.K., Multicomponent membranes for gas separations. US. Patent 4,230,463. 1977.

Hiemenz, P.C. and Lodge, T.P., *Polymer Chemistry*. 2nd ed. 2007, Boca Raton: CRC Press.

Hill, A.J., Tant, M.R., McGill, R.L., Shang, R.R., Stockl, D.L., Murray, D.L., and Cloyd, J.D., *Free volume distribution during consolidation and coalescence of latex films.* Journal of Coatings Technology, 2001. **73**(913): p. 115-124.

Hillock, A.M.W. and Koros, W.J., *Cross-linkable polyimide membrane for natural gas purification and carbon dioxide plasticization reduction.* Macromolecules, 2007. **40**(3): p. 583-587.

Hirayama, Y., Yoshinaga, T., Kusuki, Y., Ninomiya, K., Sakakibara, T., and Tamari, T., *Relation of gas permeability with structure of aromatic polyimides I.* Journal of Membrane Science, 1996. **111**: p. 169-182.

Horn, N.R. and Paul, D.R., *Carbon dioxide plasticization and conditioning effects in thick vs. thin glassy polymer films.* Polymer, 2011. **52**: p. 1619-1627.

Horn, N.R. and Paul, D.R., *Carbon dioxide plasticization of thin glassy polymer films.* Polymer, 2011. **52**: p. 5587-5594.

Hu, L., Xu, X.L., and Coleman, M.R., *Impact of H+ ion beam irradiation on Matrimid (R). II. Evolution in gas transport properties.* Journal of Applied Polymer Science, 2007. **103**(3): p. 1670-1680.

Hu, Y., Shiotsuki, M., Sanda, F., Freeman, B.D., and Masuda, T., *Synthesis and properties of indan-based polyacetylenes that feature the highest gas permeability among all the existing polymers.* Macromolecules, 2007. **41**: p. 8525-8532.

Huang, Y. and Paul, D.R., *Effect of film thickness on the gas-permeation characteristics of glassy polymer membranes.* Industrial & Engineering Chemistry Research, 2007. **46**: p. 2343-2347.

Huang, Y. and Paul, D.R., *Effect of molecular weight and temperature on physical aging of thin glassy poly(2,6-dimethyl-1,4-phenylene oxide) films.* Journal of Polymer Science, Part B: Polymer Physics, 2007. **45**: p. 1390-1398.

Huang, Y. and Paul, D.R., *Experimental methods for tracking physical aging of thin glassy polymer films by gas permeation.* Journal of Membrane Science, 2004. **244**: p. 167-178.

Huang, Y. and Paul, D.R., *Physical aging of thin glassy polymer films monitored by gas permeability.* Polymer, 2004. **45**: p. 8377-8393.

Huang, Y. and Paul, D.R., *Physical aging of thin glassy polymer films monitored by optical properties.* Macromolecules, 2006. **39**(1554-1559).

Huang, Y., Wang, X., and Paul, D.R., *Physical aging of thin glassy polymer films: Free volume interpretation.* Journal of Membrane Science, 2006. **277**: p. 219-229.

Hutchinson, J.M., *Physical aging of polymers.* Progress in Polymer Science, 1995. **20**(4): p. 703-760.

Itatani, H. and Yoshimoto, H., The Journal of Organic Chemistry, 1973. **38**: p. 76-79.

Jansen, J.C., Macchione, M., and Drioli, E., *On the unusual solvent retention and the effect on the gas transport in perfluorinated Hyflon AD (R) membranes.* Journal of Membrane Science, 2007. **287**(1): p. 132-137.

Jordan, S.M., Fleming, G.K., and Koros, W.J., *Permeability of carbon dioxide at elevated pressures in substituted polycarbonates.* Journal of Polymer Science Part B: Polymer Physics, 2003. **28**(12): p. 2305-2327.

Jung, C.H., Lee, J.E., Han, S.H., Park, H.B., and Lee, Y.M., *Highly permeable and selective poly(benzoxazole-co-imide) membranes for gas separation.* Journal of Membrane Science, 2010. **350**(1-2): p. 301-309.

Kanehashi, S., Nakagawa, T., Nagai, K., Duthie, X., Kentish, S., and Stevens, G., *Effects of carbon dioxide-induced plasticization on the gas transport properties of glassy polyimide membranes.* Journal of Membrane Science, 2007. **298**: p. 147-155.

Kardash, I.Y. and Pravednikov, A.N., *Aromatic polyimides containing hydroxy- and methoxy-groups.* Vysokomol. soyed., 1967. **B9**: p. 873-876.

Kashima, M., Yoshimoto, H., and Itatani, H., *Isotope effect of aromatic coupling reaction catalyzed by palladium acetate.* Journal of Catalysis, 1973. **29**(1): p. 92-98.

Kelman, S.D., Rowe, B.W., Bielawski, C.W., Pas, S.J., Hill, A.J., Paul, D.R., and Freeman, B.D., *Crosslinking of poly[1-(trimethylsilyl)-1-propyne] and its effect on physical stability.* Journal of Membrane Science, 2008. **320**: p. 123-134.

Kesting, R.E., *Synthetic polymer membranes: A structural perspective*. 1985, New York: Wiley-Interscience.

Kesting, R.E. and Fritzsche, A.K., *Polymeric gas separation membranes*. 1993, New York, NY, USA: John Wiley & Sons.

Kim, H.S., Kim, Y.H., Ahn, S.K., and Kwon, S.K., *Synthesis and characterization of highly soluble and oxygen permeable new polyimides bearing a noncoplanar twisted biphenyl unit containing tert-butylphenyl or trimethylsilyl phenyl groups.* Macromolecules, 2003. **36**(7): p. 2327-2332.

Kim, J.H., Koros, W.J., and Paul, D.R., *Effects of CO_2 exposure and physical aging on the gas permeability of thin 6FDA-based polyimide membranes - Part 1. without crosslinking.* Journal of Membrane Science, 2006. **282**: p. 21-31.

Kim, J.H., Koros, W.J., and Paul, D.R., *Effects of CO_2 exposure and physical aging on the gas permeability of thin 6FDA-based polyimide membranes - Part 2. with crosslinking.* Journal of Membrane Science, 2006. **282**(1-2): p. 32-43.

Kim, J.H., Koros, W.J., and Paul, D.R., *Effects of CO_2 exposure and physical aging on the gas permeability of thin 6FDA-based polyimide membranes. Part 2. with crosslinking.* Journal of Membrane Science, 2006. **282**: p. 32-43.

Kim, J.H., Koros, W.J., and Paul, D.R., *Physical aging of thin 6FDA-based polyimide membranes containing carboxyl acid groups. Part I. Transport properties.* Polymer, 2006. **47**: p. 3094-3103.

Kim, S., Han, S.H., and Lee, Y.M., *Thermally rearranged (TR) polybenzoxazole hollow fiber membranes for CO_2 capture.* Journal of Membrane Science, 2012. **403-404**: p. 169-178.

Kim, T.H., Koros, W.J., Husk, G.R., and O'Brien, K.C., *Relationship between gas separation properties and chemical structure in a series of aromatic polyimides.* Journal of Membrane Science, 1988. **37**(1): p. 45-62.

Kim, Y.H., Kim, H.S., and Kwon, S.K., *Synthesis and characterization of highly soluble and oxygen permeable new polyimides based on twisted biphenyl dianhydride and spirobifluorene diamine.* Macromolecules, 2005. **38**(19): p. 7950-7956.

King Jr., J.A., *Synthesis of polycarbonates*, in *Handbook of Polycarbonate Science and Technology*, D.G. LeGrand and J.T. Bendler, Editors. 2000, Marcel Dekker Inc. p. 7-27.

Kita, H., Inada, T., Tanaka, K., and Okamoto, K., *Effect of photo-cross-linking on permeability and permselectivity of gases through benzophenone-containing polyimide.* Journal of Membrane Science, 1994. **87**(1-2): p. 139-147.

Kohl, A. and Nielsen, R., *Gas purification*. 5th ed. 1997, Houston, TX: Gulf Publishing Company.

Koros, W.J., Sorption and transport of gases in glassy polymers. Ph.D. Thesis from The University of Texas at Austin, 1977.

Koros, W.J., Chan, A.H., and Paul, D.R., *Sorption and transport of various gases In polycarbonate.* Journal of Membrane Science, 1977. **2**(2): p. 165-190.

Koros, W.J. and Fleming, G.K., *Membrane-based gas separation.* Journal of Membrane Science, 1993. **83**(1): p. 1-80.

Koros, W.J., Fleming, G.K., Jordan, S.M., Kim, T.H., and Hoehn, H.H., *Polymeric membrane materials for solution-diffusion based permeation separations.* Progress in Polymer Science, 1988. **13**(4): p. 339-401.

Koros, W.J., Paul, D.R., and Rocha, A.A., *Carbon dioxide sorption and transport in polycarbonate.* Journal of Polymer Science: Part B: Polymer Physics, 1976. **14**: p. 687-702.

Kothawade, S.S., Kulkarni, M.P., Kharul, U.K., Patil, A.S., and Vernekar, S.P., *Synthesis, characterization, and gas permeability of aromatic polyimides containing pendant phenoxy group.* Journal of Applied Polymer Science, 2007. **108**: p. 3881-3889.

Laciak, D.V., Robeson, L.M., and Smith, C.D., *Group contribution modeling of gas transport inpolymeric membranes*, in *Polymer membranes for gas and vapor separation, ACS symposium series 733*, B.D. Freeman and I. Pinnau, Editors. 1999, American Chemical Society: Washington D.C.

Langsam, M. and Robeson, L.M., *Substituted propyne polymers - Part II. Effects of agining on the gas permeability properties of poly[1-(trimethylsilyl)propyne] for gas separation membranes.* Polymer Engineering and Science, 1989. **29**(1): p. 44-54.

Lee, J.S., Madden, W., and Koros, W.J., *Antiplasticization and plasticization of Matrimid (R) asymmetric hollow fiber membranes-Part A. Experimental.* Journal of Membrane Science, 2010. **350**(1-2): p. 232-241.

Lee, S.Y. and Minhas, B.S., *Effect of gas composition and pressure on permeation through cellulose acetate membranes.* AIChE Symposium Series, 1988. **84**(264): p. 93-101.

Lee, W.M., *Selection of barrier materials from molecular structure.* Polymer Engineering and Science, 1980. **20**(1): p. 65-69.

Li, P., Paul, D.R., and Chung, T.S., *High performance membranes based on ionic liquid polymers for CO_2 separation from the flue gas.* Green Chemistry, 2012. **14**: p. 1052-1063.

Lin, H.Q. and Freeman, B.D., *Permeation and diffusion* in *Springer handbook for materials measurement methods*, H. Czichos, T. Saito, and L. Smith, Editors. 2011, Springer: Berlin. p. 426-444.

Lin, H.Q., Freeman, B.D., Kalakkunnath, S., and Kalika, D.S., *Effect of copolymer composition, temperature, and carbon dioxide fugacity on pure- and mixed-gas permeability in poly(ethylene glycol)-based materials: Free volume interpretation.* Journal of Membrane Science, 2007. **291**: p. 131-139.

Lin, W.H. and Chung, T.S., *Gas permeability, diffusivity, solubility and aging characteristics of 6FDA-durene polyimide membranes.* Journal of Membrane Science, 2001. **186**: p. 183-193.

Loeb, S. and Sourirajan, S., eds. In saline water conversion II-Advances in chemistry series Vol. 38. 1963, American Chemical Society: Washington, DC. 117-132.

Lonsdale, H.K., *The growth of membrane technology.* Journal of Membrane Science, 1982. **10**(2-3): p. 81-181.

López-Nava R, Vázquez-Moreno FS, Palí-Casanova R, and M., A.-V., *Gas permeability coefficients of isomeric aromatic polyamides obtained from 4,4 -(9-fluorenylidene) diamine and aromatic diacid chlorides.* Polym Bull, 2002. **49**: p. 165-72.

Ma, X., Swaidan, R., Belmabkhout, Y., Zhu, Y., Litwiller, E., Jouiad, M., Pinnau, I., and Han, Y., *Synthesis and gas transport properties of hydroxyl-functionalized polyimides with intrinsic microporosity.* Macromolecules, 2012. **45**: p. 3841-3849.

Maeda, Y. and Paul, D.R., *Effect of antiplasticization on selectivity and productivity of gas separation membranes.* Journal of Membrane Science, 1987. **30**(1): p. 1-9.

Martinez-Richa, A. and Vera-Graziano, R., *A solid-state NMR study of aromatic polyimides based on 4,4 '-diaminotriphenylmethane.* Journal of Applied Polymer Science, 1998. **70**(6): p. 1053-1064.

Mason, E.A., *From pig bladders and cracked jars to polysulfones: an historical perspective on membrane transport.* Journal of Membrane Science, 1991. **60**: p. 125-145.

Matsumoto, K. and Xu, P., *Gas permeation properties of hexafluoro aromatic polymers.* Journal of Applied Polymer Science, 1993. **47**: p. 1961-1972.

Matteucci, S., Yampolskii, Y., Pinnau, I., and Freeman, B.D., *Transport of gases and vapors in glassy and rubbery polymers*, in *Materials science of membranes for gas and vapor separation*, Y. Yampolskii, I. Pinnau, and B.D. Freeman, Editors. 2006, John Wiley & Sons: Chichester. p. 2-46.

Matteucci, S.T., Yampolskii, Y.P., Freeman, B.D., and Pinnau, I., *Transport of gases and vapors in glassy and rubbery polymers*, in *Materials science of membranes for gas and vapor separation*, Y. Yampolskii, I. Pinnau, and B.D. Freeman, Editors. 2006, John Wiley & Sons: Chichester. p. 1-47.

McCaig, M.S. and Paul, D.R., *Effect of film thickness on the changes in gas permeability of a glassy polyarylate due to physical aging. Part I. Experimental Observations.* Polymer, 2000. **41**: p. 629-637.

McCaig, M.S. and Paul, D.R., *Effect of UV crosslinking and physical aging on the gas permeability of thin glassy polyarylate films.* Polymer, 1999. **40**: p. 7209-7225.

McCaig, M.S., Paul, D.R., and Barlow, J.W., *Effect of film thickness on the changes in gas permeability of a glassy polyarylate due to physical aging. Part II. Mathematical Model.* Polymer, 2000. **41**: p. 639-648.

McGrail, P.T., *Polyaromatics.* Polymer International, 1996. **41**(2): p. 103-121.

McHattie, J.S., Koros, W.J., and Paul, D.R., *Gas-Transport Properties of Polysulfones .1. Role of Symmetry of Methyl-Group Placement on Bisphenol Rings.* Polymer, 1991. **32**(5): p. 840-850.

McHattie, J.S., Koros, W.J., and Paul, D.R., *Gas-Transport Properties of Polysulfones .2. Effect of Bisphenol Connector Groups.* Polymer, 1991. **32**(14): p. 2618-2625.

McHattie, J.S., Koros, W.J., and Paul, D.R., *Gas-Transport Properties of Polysulfones .3. Comparison of Tetramethyl-Substituted Bisphenols.* Polymer, 1992. **33**(8): p. 1701-1711.

McKeown, N.B. and Budd, P.M., *Polymers of intrinsic microporosity (PIMs): organic materials for membrane separations, heterogeneous catalysis and hydrogen storage.* Chemical Society Reviews, 2006. **35**(8): p. 675-683.

McKeown, N.B., Budd, P.M., Msayib, K.J., Ghanem, B.S., Kingston, H.J., Tattershall, C.E., Makhseed, S., Reynolds, K.J., and Fritsch, D., *Polymers of intrinsic microporosity (PIMs): Bridging the void between microporous and polymeric materials.* Chemistry-a European Journal, 2005. **11**(9): p. 2610-2620.

Meares, P., *The diffusion of gases through polyvinyl acetate.* Journal of the American Chemical Society, 1954. **76**: p. 3415-3422.

Mecerreyes, D., *Polymeric ionic liquids: Broadening the properties and applications of polyelectrolytes.* Progress in Polymer Science, 2011. **36**(12): p. 1629-1648.

Mehta, A. and Zydney, A.L., *Permeability and selectivity analysis for ultrafiltration membranes.* Journal of Membrane Science, 2005. **249**: p. 245-249.

Merkel, T.C., Bondar, V., Nagai, K., Freeman, B.D., and Yampolskii, Y.P., *Gas sorption, diffusion, and permeation in poly(2,2-bis(trifluoromehtyl)-4,5-difluoro-1,3-dioxole-co-tetrafluoroethylene).* Macromolecules, 1999. **32**: p. 8427-8440.

Merkel, T.C., Freeman, B.D., Spontak, R.J., Pinnau, I., He, Z., Meakin, P., and Hill, A.J., *Sorption, transport, and structural evidence for enhanced free volume in poly(4-methyl-2-pentyne)/fumed silica nanocomposite membranes.* Chemistry of Materials, 2003. **15**: p. 109-123.

Merkel, T.C., Pinnau, I., Prabhakar, R., and Freeman, B.D., *Gas and vapor transport properties of perfluoropolymers*, in *Materials science of membranes for gas and vapor separations*, Y. Yampolskii, I. Pinnau, and B.D. Freeman, Editors. 2006, John Wiley & Sons Ltd. p. 251-267.

Merkel, T.C., Pinnau, I., Prabhakar, R., and Freeman, B.D., eds. *Gas and Vapor Transport Properties of Perfluoropolymers*. Materials science of membranes for gas and vapor separation, ed. Y. Yampolskii, Pinnau, I., Freeman B. D. 2006, Wiley: Chichester, UK. 251-270.

Michaels, A.S. and Bixler, H.J., *Solubility of gases in polyethylene [and rubbery polymers]*. Journal of Polymer Science, 1961. **50**: p. 393-412.

Michaels, A.S. and Parker Jr., R.B., *Sorption and flow of gases in polyethylene.* Journal of Polymer Science, 1959. **41**: p. 53-71.

Michaels, A.S., Vieth, W.R., and Barrie, J.A., *Solution of gases in poly(ethylene terephthalate).* Journal of Applied Physics, 1963. **34**: p. 1-13.

Mitchell, J.K., *On the penetrativeness of fluids.* Journal of Membrane Science, 1995. **100**: p. 11-16.

Moore, T.T. and Koros, W.J., *Gas sorption in polymers, molecular sieves, and mixed matrix membranes.* Journal of Applied Polymer Science, 2007. **104**(6): p. 4053-4059.

Moy, T.M., DePorter, C.D., and McGrath, J.E., *Synthesis of soluble polyimides and functionalized imide oligomers via solution imidization of aromatic diester-diacids and aromatic diamines.* Polymer, 1993. **34**(4): p. 819-824.

Murphy, T.M., Langhe, D.S., Ponting, M., Baer, E., Freeman, B.D., and Paul, D.R., *Physical aging of layered glassy polymer films via gas permeability tracking.* Polymer, 2011. **52**: p. 6117-6125.

Murphy, T.M., Offord, G.T., and Paul, D.R., *Fundamentals of membrane gas separation*, in *Membrane opperations. Innovative separations and transformations.*, E. Drioli and L. Giorno, Editors. 2009, Wiley-VCH: Weinheim, Germany. p. 63-82.

Muruganandam, N., Koros, W.J., and Paul, D.R., *Gas Sorption and Transport in Substituted Polycarbonates.* Journal of Polymer Science Part B-Polymer Physics, 1987. **25**(9): p. 1999-2026.

Muruganandam, N. and Paul, D.R., *Evaluation of substituted polycarbonates and a blend with polystyrene as gas separation membranes.* Journal of Membrane Science, 1987. **34**: p. 1987.

Nagai, K., Freeman, B.D., and Hill, A.J., *Effect of pysical aging of poly(1-trimethylsilyl-1-propyne) films synthesized with $TaCl_5$ and $NbCl_5$ on gas permeability, fractional free volume, and positron annihilation lifetime spectroscopy parameters.* Journal of Polymer Science, Part B: Polymer Physics, 2000. **38**: p. 1222-1239.

Nagai, K., Higuchi, A., and Nakagawa, T., *Gas permeability and stability of poly(1-trimethylsilyl-1-propyne-co-1-phenyl-1-propyne).* Journal of Polymer Science, Part B: Polymer Physics, 1995. **33**(2): p. 289-298.

Nagai, K. and Nakagawa, T., *Effects of aging on the gas permeability and solubility in poly(1-trimethylsilyl-1-propyne) membranes synthesized with various catalysts.* Journal of Membrane Science, 1995. **105**: p. 261-272.

Nakamura, M., Kaneko, I., Oharu, K., Kojima, G., Matsuo, M., Sameijima, S., and Kamba, M., Cyclic Polymerization. U.S. Patent 4,910,276. 1990.

Nakamura, M., Sugiyama, N., Etoh, Y., and Endo, J., Nippon Kagaku Kaishi, 2001. **12**: p. 659-668.

Noble, R.D. and Gin, D.L., *Persepective on ionic liquids and ionic liquid membranes.* Journal of Membrane Science, 2011. **369**: p. 1-4.

Nollet, J.A., *Investigations on the causes for the ebullition of liquids.* Journal of Membrane Science, 1995. **100**: p. 1-3.

Ohya, H., Kudryavtsev, V.V., and Semenova, S.I., *Polyimide membranes - applications, fabrications, and properties*. 1996: Gordon and Breach.

Okamoto, K.I., Tanihara, N., Watanabe, H., Tanaka, K., Kita, H., Nakamura, A., Kusuki, Y., and Nakagawa, K., *Sorption and diffusion of water-vapor in polyimide films.* Journal of Polymer Science Part B-Polymer Physics, 1992. **30**(11): p. 1223-1231.

Park, H.B., Han, S.H., Jung, C.H., Lee, Y.M., and Hill, A.J., *Thermally rearranged (TR) polymer membranes for CO_2 separation.* Journal of Membrane Science, 2010. **359**(1-2): p. 11-24.

Park, H.B., Jung, C.H., Lee, Y.M., Hill, A.J., Pas, S.J., Mudie, S.T., Van Wagner, E., Freeman, B.D., and Cookson, D.J., *Polymers with cavities tuned for fast selective transport of small molecules and ions.* Science, 2007. **318**(5848): p. 254-258.

Park, J.Y. and Paul, D.R., *Correlation and prediction of gas permeability in glassy polymer membrane materials via modified free volume based group contribution method.* Journal of Membrane Science, 1997. **125**(1): p. 23-39.

Pastermak, R.A., Burns, G.L., and Heller, J., *Diffusion and solubility of simple gases through a copolymer of hexafluoropropylene and tetafluroethylene.* Macromolecules, 1971. **4**(4): p. 470-475.

Paul, D.R., *Gas sorption and transport in glassy polymers.* Berichte der Bunsengesellschaft für physikalische Chemie, 1979. **83**: p. 294-302.

Paul, D.R. and Koros, W.J., *Effect of partially immobilizing sorption on permeability and the diffusion time lag.* Journal of Polymer Science: Part B: Polymer Physics, 1976. **14**: p. 675-685.

Paul, D.R. and Yampol'skii, Y.P., eds. *Polymeric Gas Separation Membranes*. 1994, CRC Press, Inc.: Boca Raton, FL. 100-126.

Petropoulos, J.H., *Mechanisms and theories for sorption and diffusion of gases in polymers*, in *Polymeric gas separation membranes*, D.R. Paul and Y. Yampolskii, Editors. 1994, CRC Press: Boca Raton, Florida, USA. p. 17-82.

Pinnau, I. and Toy, L.G., *Gas and vapor transport properties of amorphous perfluorinated copolymer membranes based on 2,2-bistrifluoromethyl-4,5-difluoro-1,3-dioxole/tetrafluoroethylene.* Journal of Membrane Science, 1996. **109**(1): p. 125-133.

Pixton, M.R. and Paul, D.R., *Relationships between structure and transport properties for polymers with aromatic backbones*, in *Polymeric gas separation membranes*, D.R. Paul and Y. Yampolskii, Editors. 1994, CRC Press: Boca Raton. p. 83-154.

Prabhakar, R.S., Freeman, B.D., and Roman, I., *Gas and vapor sorption and permeation in poly(2,2,4-trifluoro-5-trifluoromethoxy-1,3-dioxole-co-tetrafluoroethylene).* Macromolecules, 2004. **37**(20): p. 7688-7697.

Prabhakar, R.S., Grazia de Angelis, M., Sarti, G.C., Freeman, B.D., and Coughlin, M.C., *Gas and vapor sorption, permeation, and diffusion in poly(tetrafluoroethylene-co-perfluoromethyl vinyl ether).* Macromolecules, 2005. **38**: p. 7043-7055.

Preston, J., *Aromatic polyamides*, in *Encyclopedia of polymer science and engineering*, B.N. Mark HF, Overberger CG, Menges G, Editor 1988, John Wiley & Sons, Inc.: New York. p. 381-9.

Puleo, A.C., Paul, D.R., and Kelley, S.S., *The effect of degree of acetylation on gas sorption and transport behavior in cellulose-acetate.* Journal of Membrane Science, 1989. **47**(3): p. 301-332.

Puri, P.S., *Commercial applications of membranes in gas separations*, in *Membrane engineering for the treatment of gases Vol 1: Gas separation problems with membranes*, E. Drioli and G. Barbieri, Editors. 2011, Royal Society of Chemistry: Cambridge.

Ribeiro, C.P., Freeman, B.D., Kalika, D.S., and Kalakkunnath, S., *Aromatic polyimide and polybenzoxazole membranes for the fractionation of aromatic/aliphatic*

hydrocarbons by pervaporation. Journal of Membrane Science, 2012. **390-391**: p. 182-193.

Ribeiro, C.P., Freeman, B.D., and Paul, D.R., *Modeling of multicomponent mass transfer across polymer films using a thermodynamically consistent formulation of the Maxwell-Stefan equations in terms of volume fractions.* Polymer, 2011. **52**: p. 3970-3983.

Robeson, L.M., *Correlation of separation factor versus permeability for polymeric membranes.* Journal of Membrane Science, 1991. **62**(2): p. 165-185.

Robeson, L.M., *Polymer blends in membrane transport processes.* Industrial & Engineering Chemistry Research, 2010. **49**(23): p. 11859-11865.

Robeson, L.M., *The upper bound revisited.* Journal of Membrane Science, 2008. **320**(1-2): p. 390-400.

Robeson, L.M., Burgoyne, W.F., Langsam, M., Savoca, A.C., and Tien, C.F., *High performance polymers for membrane separation.* Polymer, 1994. **35**(23): p. 4970-4978.

Robeson, L.M., Farnham, A.G., and McGrath, J.E., eds. *Molecular Basis for Transitions and Relaxations*. Vol. 4. 1978, Gordon and Breach Midland Macromolecular Institute Monographs. 405.

Robeson, L.M., Freeman, B.D., Paul, D.R., and Rowe, B.W., *An empirical correlation of gas permeability and permselectivity in polymers and its theoretical basis.* Journal of Membrane Science, 2009. **341**(1-2): p. 178-185.

Robeson, L.M., Hwu, H.H., and McGrath, J.E., *Upper bound relationship for proton exchange membranes: Empirical relationship and relevance of phase separated blends.* Journal of Membrane Science, 2007. **302**(1-2): p. 70-77.

Robeson, L.M., Smith, C.D., and Langsam, M., *A group contribution approach to predict permeability and permselectivity of aromatic polymers.* Journal of Membrane Science, 1997. **132**(1): p. 33-54.

Rowe, B.W., Freeman, B.D., and Paul, D.R., *Effect of sorbed water and temperature on the optical properties and density of thin glassy polymer films on a silicon substrate.* Macromolecules, 2007. **40**(8): p. 2806-2813.

Rowe, B.W., Freeman, B.D., and Paul, D.R., *Influence of previous history on physical aging in thin glassy polymer films as gas separation membranes.* Polymer, 2010. **51**: p. 3784-3792.

Rowe, B.W., Freeman, B.D., and Paul, D.R., *Physical aging of membranes for gas separations*, in *Membrane engineering for the treatment of gases, volume 1: Gas-separation problems with membranes*, E. Drioli and G. Barbieri, Editors. 2011, Royal Society of Chemistry.

Rowe, B.W., Freeman, B.D., and Paul, D.R., *Physical aging of ultrathin glassy polymer films tracked by gas permeability.* Polymer, 2009. **50**: p. 5565-5575.

Rowe, B.W., Pas, S.J., Hill, A.J., Suzuki, R., Freeman, B.D., and Paul, D.R., *A variable energy positron annihilation life spectroscopy study of physical aging in thin glassy polymer films.* Polymer, 2009. **50**: p. 6149-6156.

Rowe, B.W., Robeson, L.M., Freeman, B.D., and Paul, D.R., *Influence of temperature on the upper bound: Theoretical considerations and comparison with experimental results.* Journal of Membrane Science, 2010. **360**(1-2): p. 58-69.

S. Percec and G. Li, *Chemical modification of poly(2,6-dimethyl-1,4-phenylene oxide) and properties of the resulting polymers*, in *ACS Symposium Series*1988, American Chemical Society, Washington, DC.

Sada, E., Kumazawa, H., and Xu, P., *Sorption and diffusion of carbon dioxide in polyimide films.* Journal of Applied Polymer Science, 1988. **35**(6): p. 1497-1509.

Saka, S. and Matsumura, H., *The raw materials of CA.* Macromolecular Symposia, 2004. **208**: p. 7-48.

Sanders, D.F., Guo, R., Smith, Z.P., Liu, Q., Stevens, K.A., McGrath, J.E., Paul, D.R., and Freeman, B.D., *Influence of polyimide precursor synthesis route and ortho-position functional group on thermally rearranged polymers: Pure gas permeability and selectivity.* In Preparation.

Sanders, D.F., Guo, R., Smith, Z.P., Liu, Q., Stevens, K.A., McGrath, J.E., Paul, D.R., and Freeman, B.D., *Influence of polyimide precursor synthesis route and ortho-position functional group on thermally rearranged polymers: Thermal properties and free volume.* In Preparation.

Sanders, D.F., Smith, Z.P., Ribeiro, C.P., Guo, R., McGrath, J.E., Paul, D.R., and Freeman, B.D., *Permeability, diffusivity, and free volume of thermally rearranged polymers based on 3,3'-dihydroxy-4,4'-diamino-biphenyl (HAB) and 2,2'-bis-(3,4-*

dicarboxyphenyl) hexafluoropropane dianhydride (6FDA). Journal of Membrane Science, 2012. **409-410**: p. 232-241.

Sanders, E.S., *Penetrant-induced plasticization and gas permeation in glassy polymers.* Journal of Membrane Science, 1988. **37**: p. 63-80.

Sanders Jr., E.S. and Overman III, D.C., Process for separating hydrogen from as mixtures using a semi-permeable membrane consisting predominantly of polycarbonates derived from tetrahalobisphenols. 1991.

Sasaki, Y., Inoue, H., Itatani, H., and Kashima, M., Process for preparing polyimide solution US Pat. 4,290,936. 1981.

Sasakura, H., Kobunshi Ronbunshu, 2003. **60**: p. 312-317.

Schab-Balcerzak, E., Mitsutoshi, J., and Kakimoto, M., *Thermal rearrangement of poly(o-hydroxyimide)s synthesized from 4,6-diaminoresorcinol dihydrochloride.* Polymer Journal, 2003. **35**: p. 208-212.

Scheirs, J., *High performance polymer for diverse applications*. 1997, Chichester: John Wiley & Sons.

Schell, W.J., Wensley, C.G., Chen, M.S.K., Venugopal, K.G., Miller, B.D., and Stuart, J.A., *Recent advances in cellulosic membranes for gas separation and pervaporation.* Gas Separation & Purification, 1989. **3**(4): p. 162-169.

Scovazzo, P., *Determination of the upper limits, benchmarks, and critical properties for gas separations using stabilized romo temperature ionic liquid membranes (SILMs) for the purpose of guiding future research.* Journal of Membrane Science, 2009. **343**: p. 199-211.

Scovazzo, P., Kieft, J., Finan, D.A., Koval, C., DuBois, D., and Noble, R., *Gas separations using non-hexafluorophosphate [PF6](-) anion supported ionic liquid membranes.* Journal of Membrane Science, 2004. **238**(1-2): p. 57-63.

Semenova, S.I., *Introduction: Trends in polyimide membrane development*. Polyimide membranes: Applications, fabrications, and properties, ed. H. Ohya, V.V. Kudryavstev, and S.I. Semenova1996, Amstertam, The Netherland: Gordon and Breach Science Publisher.

Siggia, S., *Quantitative organic analysis via functional groups*. 3rd ed. 1963, New York: John Wiley and Sons, Inc.

Singh, A., Freeman, B.D., and Pinnau, I., *Pure and mixed gas acetone/nitrogen permeation properties of polydimethylsiloxane [PDMS]*. Journal of Polymer Science, Part B: Polymer Physics, 1998. **36**(2): p. 289-301.

Smith, Z.P., Sanders, D.F., Ribeiro, C.P., Guo, R., Freeman, B.D., Paul, D.R., McGrath, J.E., and Swinnea, S., *Gas sorption and characterization of thermally rearranged polyimides based on 3,3'-dihydroxy-4,4'-diamino-biphenyl (HAB) and 2,2'-bis-(3,4-dicarboxyphenyl) hexafluoropropane dianhydride (6FDA).* Journal of Membrane Science, 2012. **415-416**: p. 558-567.

Smith, Z.P., Sanders, D.F., Ribeiro, C.P., Guo, R., Freeman, B.D., Paul, D.R., McGrath, J.E., and Swinnea, S., *Gas sorption and characterization of thermally rearranged polyimides based on 3,3'-dihydroxy-4,4'-diamino-biphenyl (HAB) and 2,2'-bis-(3,4 dicarboxyphenyl) hexafluoropropane dianhydride (6FDA).* Journal of Membrane Science, 2011. **415-416**: p. 558-567.

Spillman, R.W., *Economics of gas separation membranes.* Chemical Engineering Progress, 1989. **85**(1): p. 41–62.

Squire, E.N., Amorphous copolymers of perfluoro-2,2-dimethyl-1,3-dioxole US Patent 4,935,477. 1990.

Squire, E.N., Amorphous copolymers of perfluoro-2,2-dimethyl-1,3-dioxole. US Patent 4,754,009. 1988.

Sridhar, S., Smitha, B., Ramakrishna, M., and Aminabhavi, T.M., *Modified poly(phenylene oxide) membranes for the separation of carbon dioxide from methane.* Journal of Membrane Science, 2006. **280**(1-2): p. 202-209.

Srinivasan, R., Auvil, S.R., and Burban, P.M., *Elucidating the mechanism(s) of gas transport in poly[1-(trimethylsilyl)-1-propyne] (PTMSP) membranes.* Journal of Membrane Science, 1994. **86**: p. 67-86.

Staudt-Bickel, C. and Koros, W.J., *Improvement of CO_2/CH_4 separation characteristics of polyimide by chemical crosslinking.* Journal of Membrane Science, 1999. **155**: p. 145-154.

Stern, S.A., *Polymers for gas separations: the next decade.* Journal of Membrane Science, 1994. **94**: p. 1-65.

Stern, S.A., *Structure/permeability relationships of polyimide membranes: applications to the separation of gas mixtures.* Journal of Polymer Science, Part B: Polymer Physics, 1989. **27**(9): p. 1887-1909.

Stern, S.A., Mi, Y., and Yamamoto, H., *Structure/permeability relationships of polyimide membranes. Applications to the separation of gas mixtures.* Journal of Polymer Science: Part B: Polymer Physics, 1989. **27**: p. 1887-1909.

Story, B.J. and Koros, W.J., *Sorption and transport of CO_2 and CH_4 in chemically modified poly(phenylene oxide).* Journal of Membrane Science, 1992. **67**(2-3): p. 191-210.

Story, B.J. and Koros, W.J., *Sorption of CO_2/CH_4 mixtures in poly(phenylene oxide) and a carboxylated derivative.* Journal of Applied Polymer Science, 1991. **42**(9): p. 2613-2626.

Struik, L.C.E., *Physical aging in amorphous polymers and other materials*. 1978, Amsterdam, The Netherlands: Elsevier.

Tanaka, K., Taguchi, A., Hao, J., Kita, H., and Okamoto, K., *Permeation and separation properties of polyimide membranes to olefins and paraffins.* Journal of Membrane Science, 1996. **121**: p. 197-207.

Tang, J.B., Sun, W.L., Tang, H.D., Radosz, M., and Shen, Y.Q., *Enhanced CO2 absorption of poly(ionic liquid)s.* Macromolecules, 2005. **38**(6): p. 2037-2039.

Tang, J.B., Tang, H.D., Sun, W.L., Plancher, H., Radosz, M., and Shen, Y.Q., *Poly(ionic liquid)s: a new material with enhanced and fast CO2 absorption.* Chemical Communications, 2005(26): p. 3325-3327.

Tang, J.B., Tang, H.D., Sun, W.L., Radosz, M., and Shen, Y.Q., *Low-pressure CO2 sorption in ammonium-based poly(ionic liquid)s.* Polymer, 2005. **46**(26): p. 12460-12467.

Tang, J.B., Tang, H.D., Sun, W.L., Radosz, M., and Shen, Y.Q., *Poly(ionic liquid)s as new materials for CO_2 absorption.* Journal of Polymer Science Part a-Polymer Chemistry, 2005. **43**(22): p. 5477-5489.

Thornton, A.W., Nairn, K.M., and Hill, A.J., *New relation between diffusion and free volume: 1. Predicting gas diffusion.* Journal of Membrane Science, 2009. **338**(1-2): p. 29-37.

Tien, C.F., Surnamer, A.D., and Langsam, M., Membranes formed from rigid aromatic polyamides. US Patent 5,034,027. 1991.

Tin, P.S., Chung, T.S., Liu, Y., Wang, R., Liu, S.L., and Pramoda, K.P., *Effects of cross-linking modification on gas separation performance of Matrimid membranes.* Journal of Membrane Science, 2003. **225**(1-2): p. 77-90.

Toi, K., Morel, G., and Paul, D.R., *Gas Sorption and Transport in Poly(Phenylene Oxide) and Comparisons with Other Glassy-Polymers.* Journal of Applied Polymer Science, 1982. **27**(8): p. 2997-3005.

Tokarev, A., Friess, K., Machkova, J., Sipek, M., and Yampolskii, Y., *Sorption and diffusion of organic vapors in amorphous Teflon AF2400.* Journal of Polymer Science Part B-Polymer Physics, 2006. **44**(5): p. 832-844.

Tullos, G.L. and Mathias, L.J., *Unexpected thermal conversion of hydroxy-containing polyimides to polybenzoxazoles.* Polymer, 1999. **40**(12): p. 3463-3468.

Tullos, G.L., Powers, J.M., Jeskey, S.J., and Mathias, L.J., *Thermal conversion of hydroxy-containing imides to benzoxazoles: Polymer and model compound study.* Macromolecules, 1999. **32**(11): p. 3598-3612.

Turnbull, D. and Cohen, M.H., *Free volume model of the amorphous phase: glass transition.* The Journal of Chemical Physics, 1961. **34**(1): p. 120-125.

van Dort, H.M., Process for the formation of high molecular weight polyarylene ethers. CA Patent 798422. 1968.

van Krevelen, D.W., *Properties of polymers*. 1972, Amsterdam: Elsevier.

Visser, T., Masetto, N., and Wessling, M., *Materials dependence of mixed gas plasticization behavior in asymmetric membranes.* Journal of Membrane Science, 2007. **306**: p. 16-28.

Vu, D.Q., Koros, W.J., and Miller, S.J., *Mixed matrix membranes using carbon molecular sieves - I. Preparation and experimental results.* Journal of Membrane Science, 2003. **211**(2): p. 311-334.

Wang, L., Cao, Y., Zhou, M., Zhou, S.J., and Yuan, Q., *Novel copolyimide membranes for gas separation.* Journal of Membrane Science, 2007. **305**: p. 338-346.

Waters, T., O'Hair, R.A.J., and Wedd, A.G., *Catalytic gas phase dehydration of acetic acid to ketene.* International Journal of Mass Spectrometry, 2003. **228**(2-3): p. 599-611.

Weinkauf, D.H. and Paul, D.R., *Effects of structural order on barrier properties.* ACS Symposium Series. Barrier Polymers and Structures, 1990: p. 60-91.

Weinkauf, D.H. and Paul, D.R., *Gas transport properties of thermotropic liquid-crystalline copolyesters. II. The effects of copolymer composition.* Journal of Polymer Science Part B-Polymer Physics, 1992. **30**: p. 837-849.

Wessling, M., Schoeman, S., van der Boomgaard, T., and Smolders, C.A., *Plasticization of gas separation membranes.* Gas Separation & Purification, 1991. **5**: p. 221-228.

White, L.S., *Evolution of natural gas treatment with membrane systems*, in *Membrane gas separation*, Y. Yampolskii and B.D. Freeman, Editors. 2010, John Wiley & Sons Ltd.: Chichester.

White, L.S., Blinka, T.A., Kloczewski, H.A., and Wang, I., *Properties of a polyimide gas separation membrane in natural gas streams.* Journal of Membrane Science, 1995. **103**: p. 73-82.

Wijmans, J.G. and Baker, R.W., *The solution-diffusion model - a review.* Journal of Membrane Science, 1995. **107**(1-2): p. 1-21.

Wilson, D., Stenzenberger, H.D., and Hergenrother, P.M., *Polyimides*. 1990, New York: Chapman and Hall.

Wind, J.D., Paul, D.R., and Koros, W.J., *Natural gas permeation in polyimide membranes.* Journal of Membrane Science, 2004. **228**(2): p. 227-236.

Wind, J.D., Sirard, S.M., Paul, D.R., Green, P.F., Johnston, K.P., and Koros, W.J., *Carbon dioxide-induced plasticization of polyimide membranes: Pseudo-equilibrium relationships of diffusion, sorption, and swelling.* Macromolecules, 2003. **36**: p. 6433-6441.

Wind, J.D., Staudt-Bickel, C., Paul, D.R., and Koros, W.J., *The effects of crosslinking chemistry on CO_2 plasticization of polyimide gas separation membranes.* Industrial & Engineering Chemistry Research, 2002. **41**: p. 6139-6148.

Wind, J.D., Staudt-Bickel, C., Paul, D.R., and Koros, W.J., *Solid-state covalent cross-linking of polyimide membranes for carbon dioxide plasticization reduction.* Macromolecules, 2003. **36**(6): p. 1882-1888.

Won, J., Kim, M.H., Kang, Y.S., Park, H.C., Kim, U.Y., Choi, S.C., and Koh, S.K., *Surface modification of polyimide and polysulfone membranes by ion beam for gas separation.* Journal of Applied Polymer Science, 2000. **75**(12): p. 1554-1560.

Xiao, Y., Low, B.T., Hosseini, S.S., Chung, T.S., and Paul, D.R., *The strategies of molecular architecture and modification of polyimide-based membranes for CO2 removal from natural gas鈥 review.* Progress in Polymer Science, 2009. **34**(6): p. 561-580.

Xiao, Y.C., Chung, T.S., Guan, H.M., and Guiver, M.D., *Synthesis, cross-linking and carbonization of co-polyimides containing internal acetylene units for gas separation.* Journal of Membrane Science, 2007. **302**(1-2): p. 254-264.

Xie, K., Liu, J.G., Zhou, H.W., Zhang, S.Y., He, M.H., and Yang, S.Y., *Soluble fluoro-polyimides derived from 1,3-bis(4-amino-2-trifluoromethyl- phenoxy) benzene and dianhydrides.* Polymer, 2001. **42**(17): p. 7267-7274.

Xie, W., Ju, H., Geise, G., Freeman, B.D., Mardel, J.I., Hill, A.J., and McGrath, J.E., *Effect of free volume on water and salt transport properties in directly copolymerized disulfonated poly(arylene ether sulfone) random copolymers.* Macromolecules, 2011. **44**: p. 4428-4430.

Xu, P. and Matsumoto, K., *Gas permeation properties of hexafluoro aromatic polyimides.* Journal of Applied Polymer Science, 1993. **47**: p. 1961-1972.

Xu, W., Synthesized polyimide membranes for pervaporation separations of toluene/iso-octane mixtures. Ph.D. Thesis from The University of Texas at Austin, 2005.

Xu, W., Synthesized polyimide membrnaes for pervaporation separations of toluene/iso-octane mixtures. Ph. D. Thesis from The University of Texas at Austin, 2005.

Yamane, H. in *Proceedings of second International Conference on Polyimides, Society of Plastics Engineers*. Oct. 1985. Ellenville, NY.

Yampolskii, Y., *Polymeric Gas Separation Membranes.* Macromolecules, 2012. **45**: p. 3298-3311.

Yang, H.H., *Aromatic high-strength fibers*, in *High-performance aromatic polyamides*2010, Wiley: New York.

Yates, S., Zaki, R., Arzadon, A., Liu, C., and Choiu, J., Thin film gas separation membranes. 2010.

Zampini, A. and Malon, R.F., Proc. ACS Div. Polym. Mat., Sci. & Eng., 1985. **52**: p. 345.

Zhang, Y., Musselman, I., Ferraris, J., and Balkus Jr., K.J., *Gas permeability properties of Matrimid® membranes containing metal-organic framework Cu-BPY-HFS.* Journal of Membrane Science, 2008. **313**: p. 170-181.

Zhao, H.-Y., Cao, Y.-M., Ding, X.-L., Zhou, M.-Q., Liu, J.-H., and Yuan, Q., *Poly(ethylene oxide) induced cross-linking modification of Matrimid membranes for selective separation of CO2.* Journal of Membrane Science, 2008. **320**(1-2): p. 179-184.

Zheng, J., Qiu, J., Madeira, L.M., and Mendes, A., *Polymer structure and the compensation effect of the diffusion pre-exponential factor and activation energy of a permeating solute.* Journal of Physical Chemistry B, 2007. **111**: p. 2828-2835.

Zimmerman, C.M., Singh, A., and Koros, W.J., *Tailoring mixed matrix composite membranes for gas separations.* Journal of Membrane Science, 1997. **137**: p. 145-154.

Vita

After graduating from Cypress Falls High School in Houston, Texas, David Finley Sanders attended The University of Texas at Austin where he earned a Bachelor of Science degree in Chemical Engineering in 2008. The next fall, David entered graduate school at the University of Texas at Austin under the guidance of Dr. Benny D. Freeman and Dr. Donald R. Paul. He earned his Ph.D. in Chemical Engineering in May of 2013.

Permanent email: davidsanders@utexas.edu

This dissertation was typed by David Sanders.